U.S. Department of Transportation

National Highway Traffic Safety Administration

DOT HS 812 737 July 2019

Front Seat Modeling in Rear Impact Crashes: Development of a Detailed Finite-Element Model for Seat Back Strength Requirements

DISCLAIMER

This report is furnished to the U.S. Department of Transportation, and under the terms of DOT contract DTNH22-15-D-00006 / DTNH22-17-F-00118 DOT and EDAG, Inc. This research was funded by the National Highway Traffic Safety Administration's Structures and Restraints Research Division. The views and conclusions contained in this document are those of the authors and should not be interpreted as representing the official policies, either expressed or implied, of the National Highway Traffic Safety Administration or the U.S. Government. The opinions, findings and conclusions expressed in this report are those of the authors and not necessarily those of EDAG, Inc. Publication of this report by EDAG, Inc. should not be considered an endorsement by EDAG, Inc., or the accuracy or validity of any opinions, findings, or conclusions expressed herein.

In publishing this report, EDAG, Inc. make no warranty or representation, expressed or implied, with respect to the accuracy, completeness, usefulness, or fitness for purpose of the information contained herein, or that the use of any information, method, process, or apparatus disclosed in this report may not infringe on privately owned rights. EDAG, Inc. assume no liability with respect to the use of, or for damages resulting from the use of, any information method, process, or apparatus described in this report.

Suggested APA Format Citation:

Bridges, W., Ganesan, V., Jayakumar, P., Davies, J., & Paramasuwom, M. (2019, July). *Front seat modeling in rear impact crashes: Development of a detailed finite-element model for seat back strength requirements* (Report No. DOT HS 812 737). Washington, DC: National Highway Traffic Safety Administration.

1. Report No. DOT HS 812 737	2. Government Accession No.	3. Recipient's Catalog No.

4. Title and Subtitle Front Seat Modeling in Rear Impact Crashes: Development of a Detailed Finite-Element Model for Seat Back Strength Requirements	5. Report Date July 2019 6. Performing Organization Code
7. Authors Wade Bridges, principal investigator; Velayudham Ganesan, Praneshkumar Jayakumar, James Davies, Mahendran Paramasuwom, all EDAG Inc.	8. Performing Organization Report No.
9. Performing Organization Name and Address EDAG, Inc. 1875 Research Drive Troy, MI 48083	10. Work Unit No. (TRAIS) 11. Contract or Grant No. DTNH22-15-D-00006/DTNH22-17-F-00118
12. Sponsoring Agency Name and Address National Highway Traffic Safety Administration 1200 New Jersey Avenue SE Washington, DC 20590	13. Type of Report and Period Covered Final Report 14. Sponsoring Agency Code

15. Supplementary Notes
Prepared for Sanjay Patel, NHTSA's Structures and Restraints Division (NSR-210), and Janella Davis, NHTSA's Office of Acquisition Management (NFO-300).

16. Abstract
NHTSA contracted EDAG, Inc., to re-examine feasibility of increasing seat back strength by developing a detailed finite-element (FE) model of a current vehicle front seat design that can be used with existing anthropomorphic test dummy (ATD) models of the Biofidelic rear impact dummy (Bio-RID) to study seat performance in rear impact crashes. The results from this task order are the finite-element models of a 2014 Honda Accord mid-size sedan representing typical front seats. There are two front seat models that have been developed using LS-DYNA simulation code. One is a manually operated seat and the other is a power operated seat , both capable of simulating occupant kinematics and injury performance measures in rear impact in a longitudinal direction, and capable of responding to incremental impulses spanning from 17 km/hr. up to 40 km/hr.

17. Key Words Quasi-static seat pull test, FMVSS301, Bio-RID II occupant dummy, front seat back rotation, low-speed whiplash test	18. Distribution Statement Document is available to the public from the National Technical Information Service, www.ntis.gov.

19. Security Classif. (of this report) Unclassified	20. Security Classif. (of this page) Unclassified	21. No. of Pages 136	22. Price

Form DOT F 1700.7 (8-72) Reproduction of completed page authorized

Contents

List of Figures

List of Tables

1 Executive Summary

The National Highway Traffic Safety Administration awarded a contract to EDAG, Inc., an automotive design and engineering company, to re-examine possibilities for increasing seat back strength by developing a detailed finite-element (FE) model of a current vehicle front seat design that can be used with existing anthropomorphic test dummy (ATD) models of the Biofidelic rear impact dummy (Bio-RID) to study seat performance in rear impact crashes. The results from this task order are the finite-element models of a model year (MY) 2014 Honda Accord mid-size sedan representing typical front seats. There are two front seat models that have been developed using LS-DYNA simulation code. One is a manually operated seat (manual seat) and the other is a power operated seat (power seat). These seat models are capable of simulating occupant kinematics and injury performance measures in rear impact in a longitudinal direction, and are capable of responding to incremental impulses spanning from 17 km/hr. up to 40 km/hr. This report documents the work done to fulfill the requirements of this task order. Specifically:

1. The FE seat models demonstrated acceptable correlation with quasi-static seat back pull test results. The kinematics of deformation and force versus displacement curves matched reasonably well.

2. The seat models developed using LS-DYNA simulation code incorporated detailed FE modeling of components and assembly, such as
    - Seat bottom and seat back frames;
    - Seat mechanisms; 4-way seat adjustment mechanism for manual seats and 6-way seat mechanism for power seats;
    - Recliner mechanism;
    - Seat bottom and seat back cushions; and
    - Representation of material properties of all seat components, using actual components of manual and power seats.

3. FE analysis (FEA) simulations of FMVSS 301 rear impacts demonstrated significant front seat back rotation and deformation to the rear seat passenger region. This simulation using 20G rear impact pulse revealed requirements for improvement in front seat back strength

4. FMVSS 301 rear impact modeling included the following.
    - Driver side sled model developed from 2014 Honda Accord full vehicle model
    - Rear seat assembly
    - Bio-RID II occupant dummy seated on front seat
    - Bio-RID II occupant dummy seated on rear seat
    - FE seatbelt for front seat occupant dummy

5. Improvement of the front seat back frames with upgraded gauge and material grade reduced the seat back rotation. It also needed validation for other rear impact protection requirements such as low-speed whiplash test.

6. The updated front seat performance was validated using Insurance Institute for Highway Safety (IIHS) whiplash (low-speed rear impact) simulation and recording no degradation of current vehicle injury measures.

2 Introduction and Scope of Work

2.1 Introduction

NHTSA seating systems standard, Federal Motor Vehicle Safety Standard (FMVSS) No. 207, has a rearward seat strength portion that is derived from the Society of Automotive Engineers (SAE) Recommended Practice J879 (1963). [Note: In 2006 the Society of Automotive Engineers changed its name to SAE International. Regulations adopted before the name change retain their old Society of Automotive Engineers name.] The procedures and requirements for the static strength of seat backs have not been significantly updated since it went into force in 1968. Over the years, NHTSA has been petitioned to revise the provision in the standard that dictates the strength of the seat back in the rearward direction. Through the 1990s and into the early 2000s, an upgrade to the seat back standard was considered by NHTSA. During this period NHTSA reviewed research on this topic with widely varying opinions on the desirability of increased seat back strength. In addition, NHTSA funded and performed its own research into the topic, most recently in a series of studies published in the early 2000s (Saunders, ESV 2001 and 2003; Kuppa, SAE 2003[1]; for other relevant reports, see docket folder NHTSA-1998-4064[2]). NHTSA considered options to revise the standard by raising the strength requirement in the rearward static test and introducing a dynamic requirement.

---

[1] Saunders, III, J. W., Molino, L. N., & Sun, E. (2001). Effects of seat back force-deflection properties on injuries for both front and rear seat occupants in rear impacts. In Proceedings of the 17th International Technical Conference on the Enhanced Safety of Vehicles, Amsterdam, The Netherlands, June 4 - 7, 2001;
Saunders, III, J. W., Molino, L. N., Kuppa, S., & McKoy, F. L. (2003). Performance of seating systems in a FMVSS No. 301 rear impact crash test. In Proceedings of the 18th International Technical Conference on the Enhanced Safety of Vehicles (ESV) Proceedings, Nagoya, Japan, May 19-22, 2003.https://www-nrd.nhtsa.dot.gov/departments/esv/17th/ https://one.nhtsa.gov/Research/Public-Meetings/SAE-2003-Government-Industry-Meeting
[2] Gupta, V., Menon, R., Gupta, S., Mani, A., & Shanmugavelu, I., Advanced integrated structural seat: Final Report - NHTSA Contract DTNH22-92-D07323, Task-11, DOT Docket Management System NHTSA-1998-4064, February, 1997; Sieveka, E., Kitis, L., & Pilkey, W. D: Simulation of occupant and seat responses in rear impacts, NHTSA Contract DTRS-57-93-C-00105, Task 4B, DOT Docket Management System NHTSA-1998-4064, March 18, 1996.

As a point of reference, NHTSA also has a separate standard for head restraints, FMVSS No. 202a, that mitigates whiplash injuries in rear end crashes. It was published in 2004 and was phased in over the 2010 and 2011 model years. The revised head restraint standard assures a minimum level of safety under a low-speed rear impulse (9 G, 17.3 km/hr.).

NHTSA has continued investigation in a possible upgrade to the seat back standard. Since 2004, NHTSA now has a better understanding of whiplash, a more mature physical test tool (Bio-RID II), better computational models than were available circa 2004, and seats designed specifically for compliance with 2004 head restraint upgrade.

2.2 Program Tasks Summary

The objective of this task order is twofold:

- To develop finite-element models to represent typical seat capable of simulating occupant kinematics and injury performance measures in rear impact in a longitudinal direction, and capable of responding to incremental impulses spanning from 17 km/hr. up to 40 km/hr.
- To have the finite-element models use the LS-DYNA simulation code, incorporate sufficient rear seat geometry to support evaluation of seat back rotation/deformation into the region occupied by a rear seat occupant, carry out static and dynamic testing of an actual seat to support validation of the resulting finite-element model, and make the model publicly available upon completion of this task order.

This report summarizes the work performed under contract DTNH22-15-D-00006/ DTNH22-17-F-00118 that includes the following tasks.

- Front seat model development for two seats
  - Front seat with manual adjuster
  - Front seat with power adjuster
- Validation of front seat models
  - Quasi-static seat back pull test correlation
  - FMVSS 301 rear impact high-speed sled test comparison
- FMVSS 301 sled simulation with rear seat passenger
- Front seat back strength analysis and design improvement
- Cost impact study on design improved seat

3 Baseline Seat Simulation

This section of report explains the baseline FEA seat model validation and test simulations. The objective of this seat simulation was to compare the FE simulations results to the physical test and determine the FE seat models are equivalent representation of the physical seats.

3.1 Baseline Seat Choice

The selected seats for this task order was from the MY 2014 Honda Accord mid-size sedan. This vehicle FE model was used for NHTSA Contract DTNH22-15-D-00006 Structural Countermeasure/Research Program, *Mass and Cost Increase due to Oblique Offset Moving Deformable Barrier Impact Test*. It was also used for NHTSA Contract DTNH22-15-D-00006/0002 Vehicle Interior and Restraint Modeling/Research Program, *Development of*

Full Vehicle Finite Element Model including Vehicle Interior and Occupant Restraints Systems for Occupant Safety Analysis using THOR Dummies. The vehicle model included the basic MY2012 seat models of minimum details without any validation for seat back strength.

For this task order the seat models were developed based on MY2014 seats available in the market by scanning the parts and modeling the additionally required details. The driver side of the full vehicle was used for FMVSS 301 rear impact simulation with Bio-RID II occupant dummy model.

EDAG purchased the following seat assemblies. Figure 1 shows the pictures of the seat assemblies purchased for testing and modeling purpose.

1. Front seat without cushions and plastic trims, manual adjustable
2. Front seat without cushions and plastic trims, power adjustable
3. Front seat fully trimmed, with cushions and standard cloth trim, manual adjustable
4. Front seat fully trimmed, with cushions and leather trim, power adjustable

Figure 1: Seat Assemblies

Seat assemblies 1 and 2 were used for seat back pull test. Seat assemblies 3 and 4 were used for FMVSS 301 rear impact sled test.

3.2 Baseline Seat Tests

In order to develop a detailed seat model, the seat model was validated with physical test results. The seat back strength was chosen as validation criteria to compare the FE seat model with physical test. The seat back strength was tested using seat back pull test. The test was conducted with a similar loading method to that stated in FMVSS 207 Rearward Moment ,[3] but the loads were applied until the seats collapsed. The load was applied at the uppermost seatback at -9 degree as shown in Figure 2: Schematic Diagram of the Seat Back

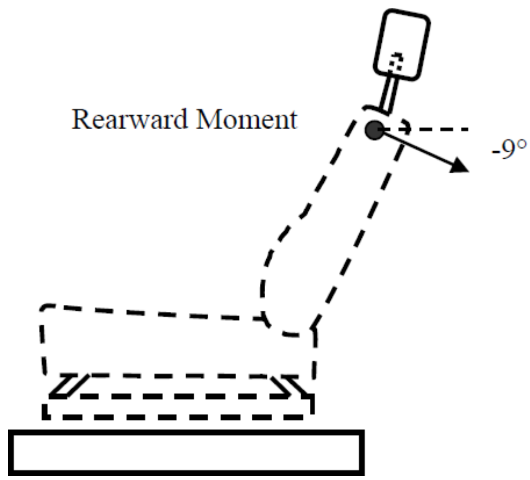

Figure 2: Schematic Diagram of the Seat Back

[3] 49 CFR 571.207 S4.2d, October 1, 2016

3.2.1 Seat Back Pull Test – Manual Seat

This test was conducted on the manual seat without cushions and plastic trim in a quasi-static loading condition. The following load profile shown in Table 1 was used to pull the seat back. The necessary seat fixtures were fabricated to mount the seat at four seat bolts at the four corners of the seat base. The load of 875N corresponds to the FMVSS207 moment requirement of 373Nm.

Load Profile		
Time(second)	Load (N)	Change in Seat Back angle(degree)
0	88	0
5	875	1.94
11	875	2.05
51.2	7,151	26.85
132	20,000	40.5

Table 1: Seat Back Pull Test Load Profile – Manual Seat

The seat back pull test setup of the manual seat is shown in Figure 3 and the test position of the seat is given in Table 2.

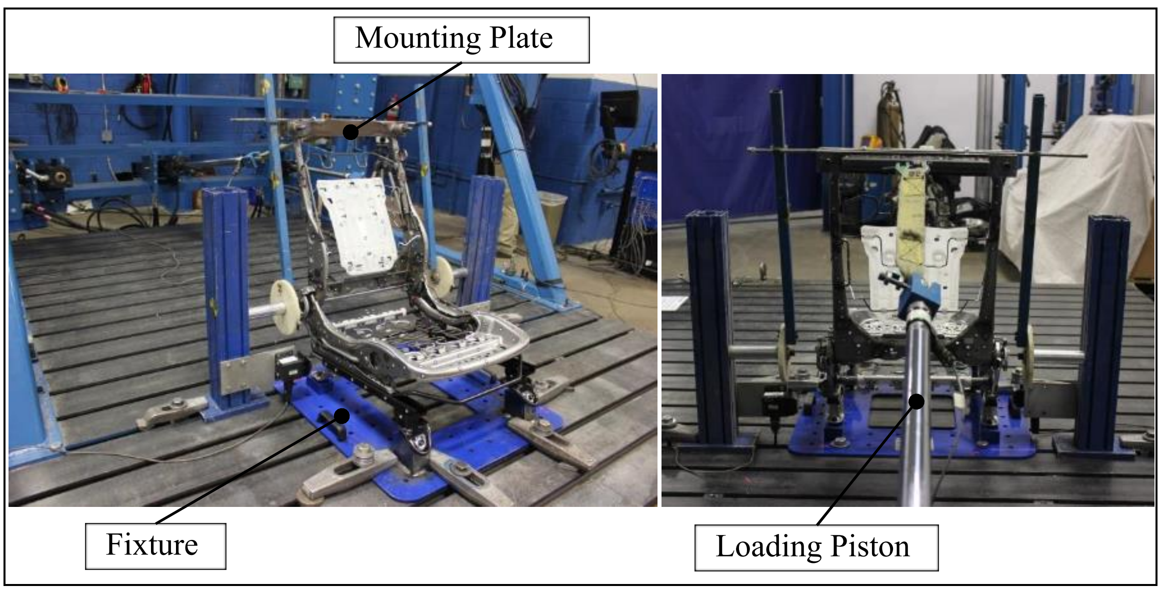

Figure 3: Seat Back Pull Test Seat Setup – Manual Seat

Seat Type: 1st Row 6 Way Manual Driver Seat	
Seat Function	**Test Position**
Track Position	Full Rearward
Vertical Position	Full Down
Seat Back Angle (Ref: See drawing)	18°
H-point (Ref: Rear lower cross tube)	159 mm Above
Moment Arm (Ref: H-Point)	426 mm Above
Load Angle	-9°
Temperature	72°F
Humidity	22%

Table 2: Seat Back Pull Test Seat Position – Manual Seat

The load was applied at mounting plate on the top of the seat back frame in the rearward direction. A pull load was applied in the rearward direction from 88 N (at 0 seconds) to 875 N (at 5 seconds), and then the load was maintained for the next 6 seconds (per the FMVSS 207 quasi static seat back strength test). The intent of this study is to observe the seat back strength for the maximum seat back rotation that might cause injury to the rear seat passenger by contact with the seat back. Therefore, after 11 seconds the pull load was increased further, until the seat back collapsed. It was found that the manual seat collapsed at 7,151N. Images of deformed seat frames after the seat back pull test are shown in Figure 4 and Figure 5.

Figure 4: Seat Back Pull Test, Post Test – Manual Seat

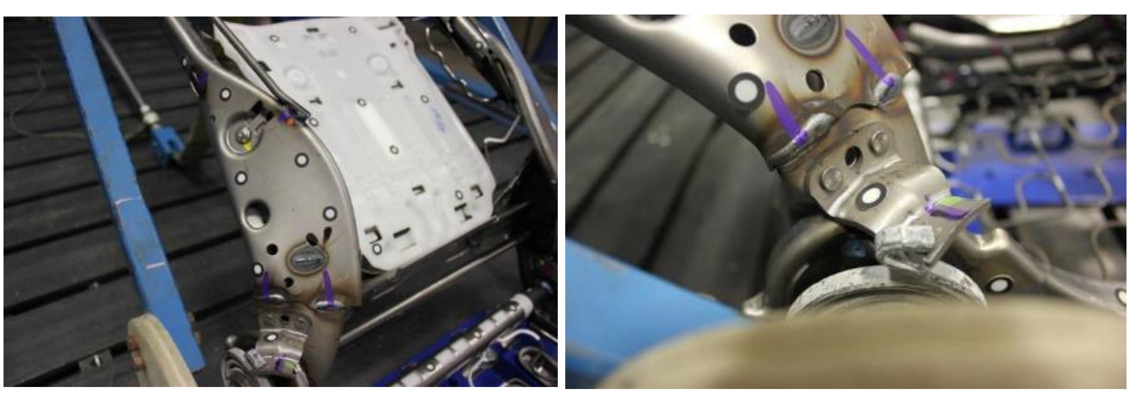

Figure 5: Seat Back Pull Test, Post Test, Seat Back Frame Deformation –Manual Seat

From the test results we can observe that until 11 sec there is no deformation or failure. The deformation is been observed on the seat bottom frame at the connecting flanges also we can see significant deformation occurred symmetrically at the seat back frame at weld joint location. There are no failures or deformation observed on the recliner mechanism. The collapse of the seat started when the seat back angle reached 50.1 degrees from the normal.

3.2.2 Seat Back Pull Test – Power Seat

Similar to the manual seat, the seat back pull test was conducted on the power seat without cushions and plastic trim in quasi-static loading condition. The following load profile shown in Table 3 was used to pull the seat back. The necessary seat fixtures were fabricated to mount the seat at four seat bolts, in the same way as was done for the manual seat.

Load Profile		
Time(second)	**Load (N)**	**Change in Seat Back angle(degree)**
0	86	0
5	861	2.14
11	861	2.26
46.6	6,246	20.96
132	20,000	28.55

Table 3: Seat Back Pull Test Load Profile – Power Seat

The power seat, seat back pull test setup is shown in Figure 6.

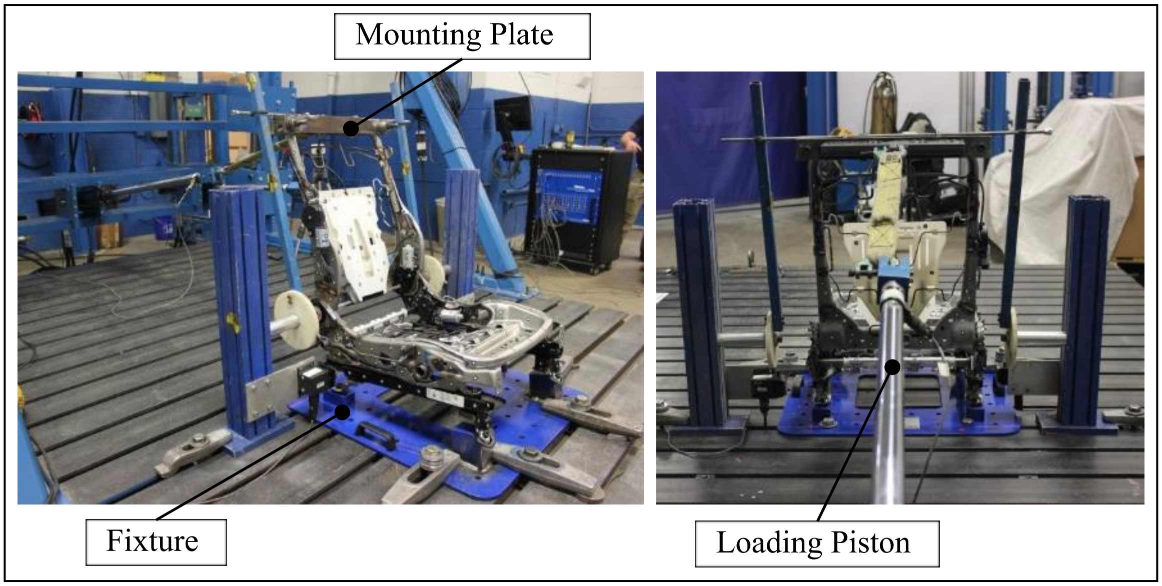

Figure 6: Seat Back Pull Test Seat up – Power Seat

The load was applied at mounting plate on the top of the seat back frame in the rearward direction. A pull load was applied in the rearward direction from 86 N (at 0 seconds) to 861 N (at 5 seconds), and then the load was maintained for the next 6 seconds (per the FMVSS 207 quasi static seat back strength test). Similar to the manual seat test, after 11 seconds the pull load was increased further until the seat back collapsed. It was found that the power seat collapsed at 6,246N. Images of deformed seat frames after the seat back pull test are shown in Figures 7 and Figure 8.

Figure 7: Seat Back Pull Test, Post Test – Power Seat

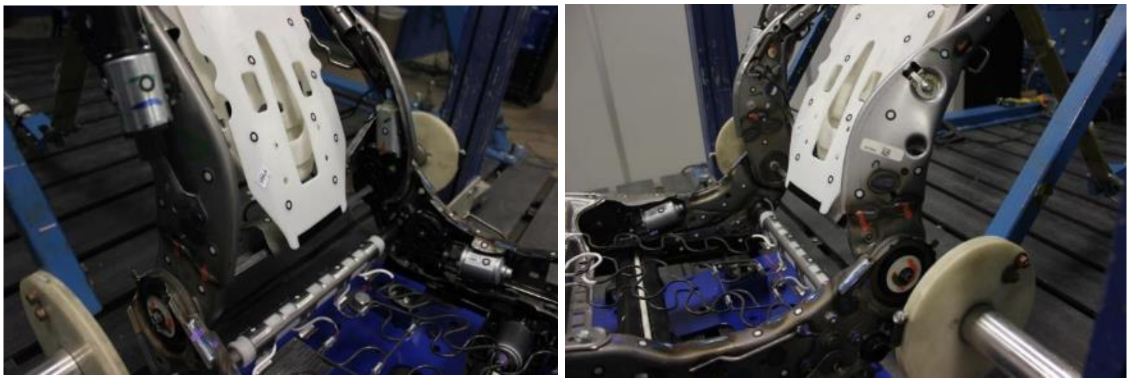

Figure 8: Seat Back Pull Test, Post Test, Seat Back Frame Deformation – Power Seat

Similar to the manual seat there is no deformation or failures seen until 11 sec. There are no failures or deformation observed on the recliner mechanism. Unlike the manual seat, the power seat frame deformation was not symmetric due to the varied motor and mechanisms attachment locations on the seat frames. The left hand side (LHS) seat frame deformed higher than the right hand side (RHS) seat frame. The (LHS) frame collapsed first at 37.1 degrees and (RHS) collapsed later at 20 degrees respectively.

The detailed test reports for both manual seat and power seat have been provided in **Appendix A.1**.

3.2.3 Seat FE Model Development

The Honda Accord MY2014 FE data in this study included the seat data from MY2012 vehicle. Therefore, it was decided to update the seat models with MY2014 seat structural components. The manual and power seat structural parts were compared to the MY2012 FE seat models. The parts that were new and significantly different from MY2012 seat models (in terms of design and assembling) were scanned and exported to stereolithographic (STL) digital format readable in computer-aided design tools. The thicknesses of the new parts were recorded. The material grades were estimated based on a hardness test. The scanned CAD data of the manual and power seats are shown in Figure 9.

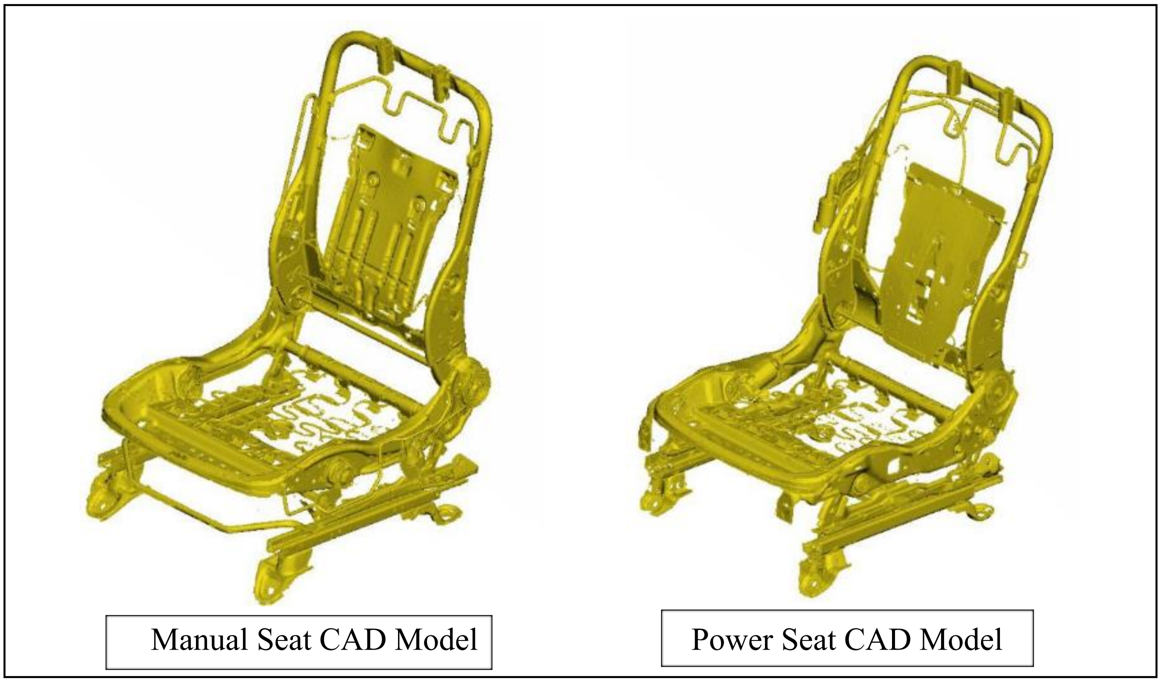

Figure 9: Scanned Seat Models

The new and significantly different parts CAD data were then meshed in commercially available FE modeling tools. The FE meshed parts were integrated to the respective manual and power seat FE models. The main differences between the MY2012 and MY2014 seat models are the seat back and seat rest frames (See **Appendix B**). The detailed MY2014 manual and power seat models are shown in Figure 10.

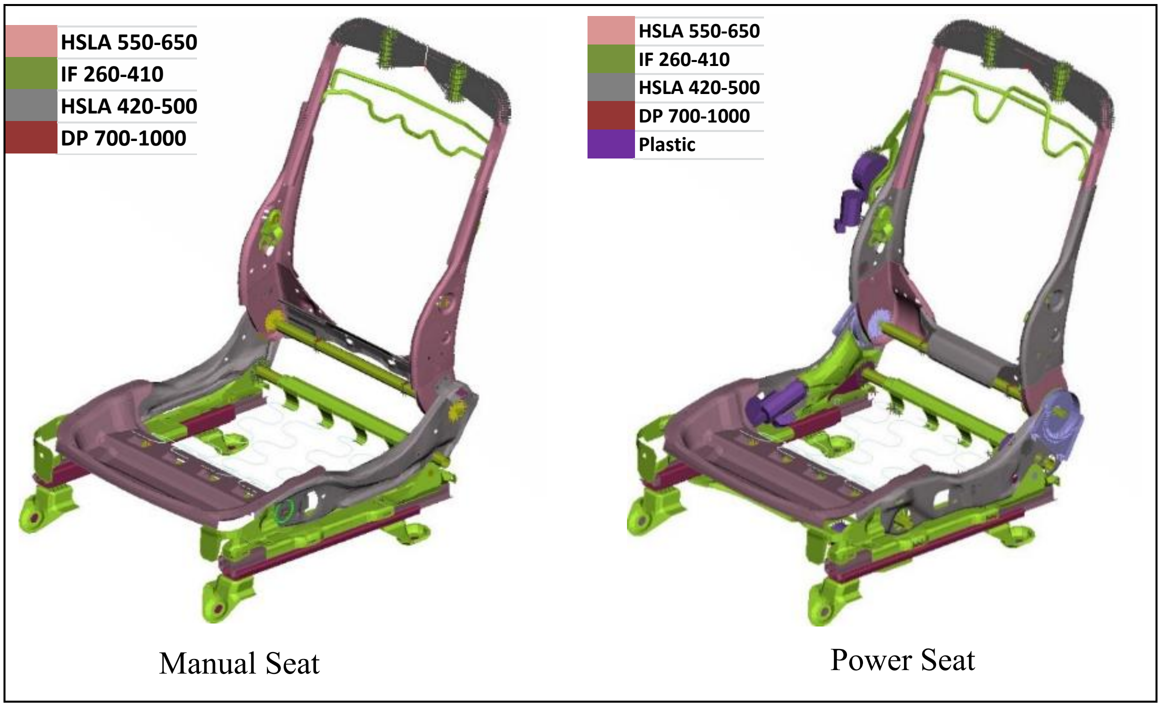

Figure 10: MY 2014 Detailed FE Models

3.2.4 Manual Seat – Seat Back Pull Test Correlation

The manual seat (MY2014) FE model was set up with positioning the seat to full down, full rear position by adjusting the seat position mechanism. The seat back was rotated to 18 degrees rearward with respect to vertical plane. A nodal rigid body (NRB) was created representing the rigid mounting plate welded on the uppermost member of the seat. The load profile in terms of load curve (force versus. time) was applied at the NRB at -9 degrees with respect to the horizontal plane. It was noted from the test that as the loading piston pulls the seat back rearward, the concentrated force rotates about global Y axis at the point of application of load. Therefore, the FE model was setup to represent this force rotation. The load was applied in the direction matching to the loading piston displacement from the test. A local coordinate system was included in the model, at the centroid of the NRB to measure the seat back displacement along the loading direction. The load application and boundary conditions are shown in Figures 11 and 12.

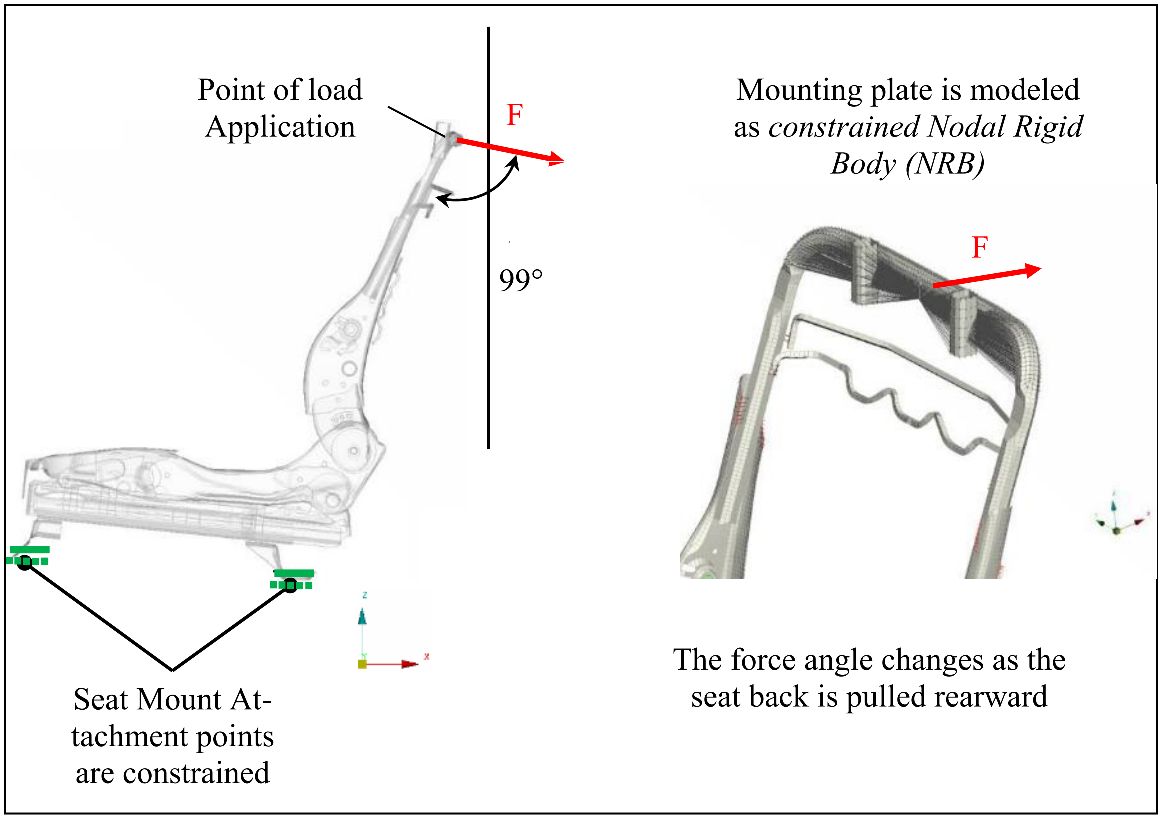

Figure 11: Manual Seat (MY2014) FE Model Setup, Loading, and Boundary Conditions

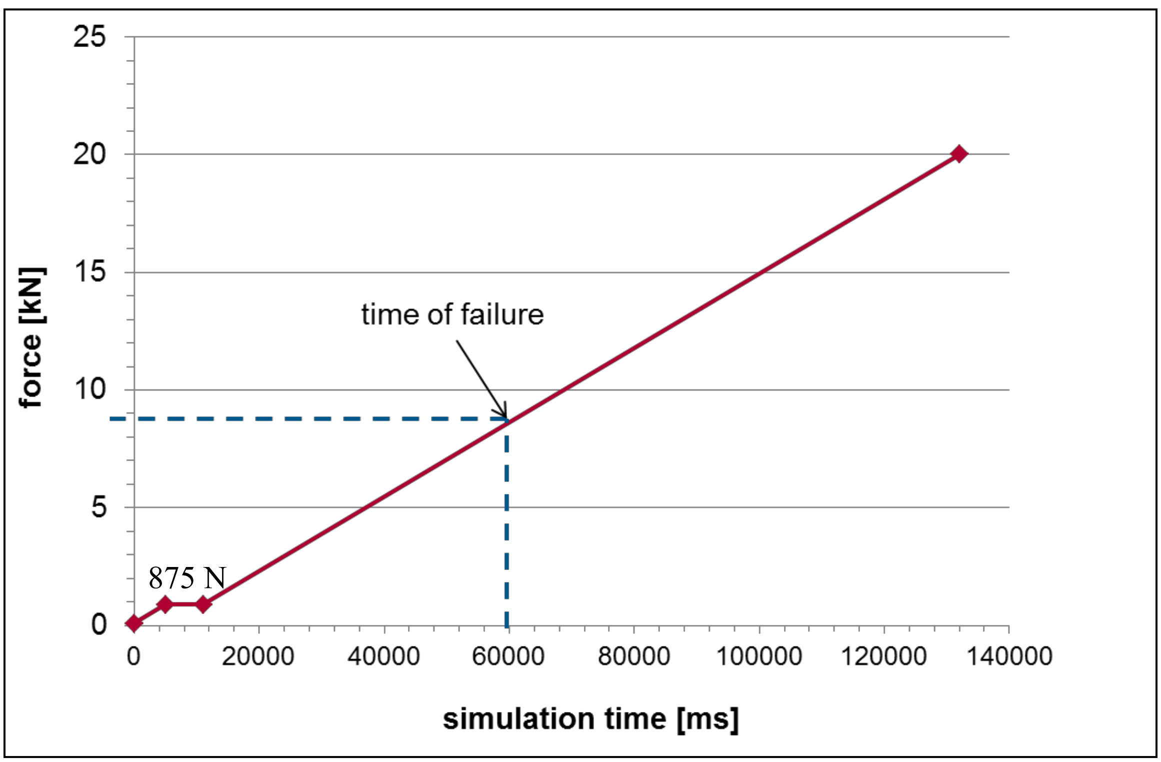

Figure 12: Loading Curve – Manual Seat

LS-DYNA simulation was run in implicit mode (LS-DYNA solver option to run quasi-static simulations) for 60 seconds. It should be noted that the material properties of FE parts were assumed with 0 strain rate stress-strain curve to run in quasi-static condition. FE simulation results of the manual seat back pull test were compared with the physical test. Figure 13 shows the comparison of the deformed shape of the seat. Figures 14, 15 and 16 show the deformation of the collapsed seat frames at the failed area.

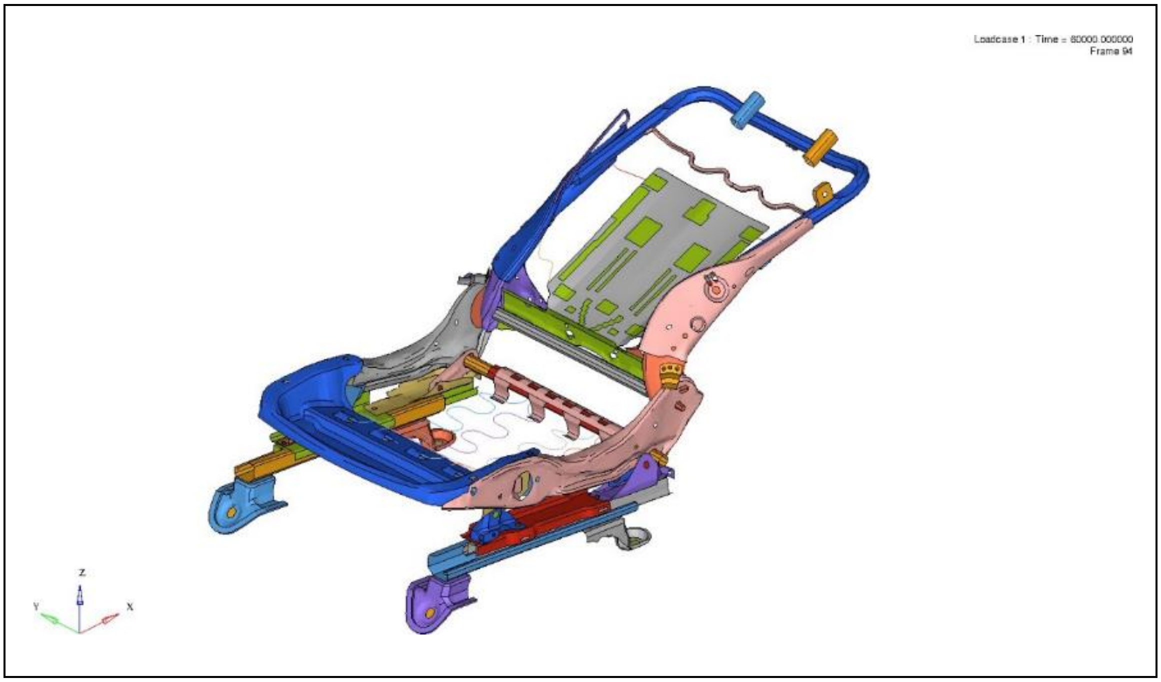

Figure 13: Global Deformation of the Seat Frame – Manual Seat

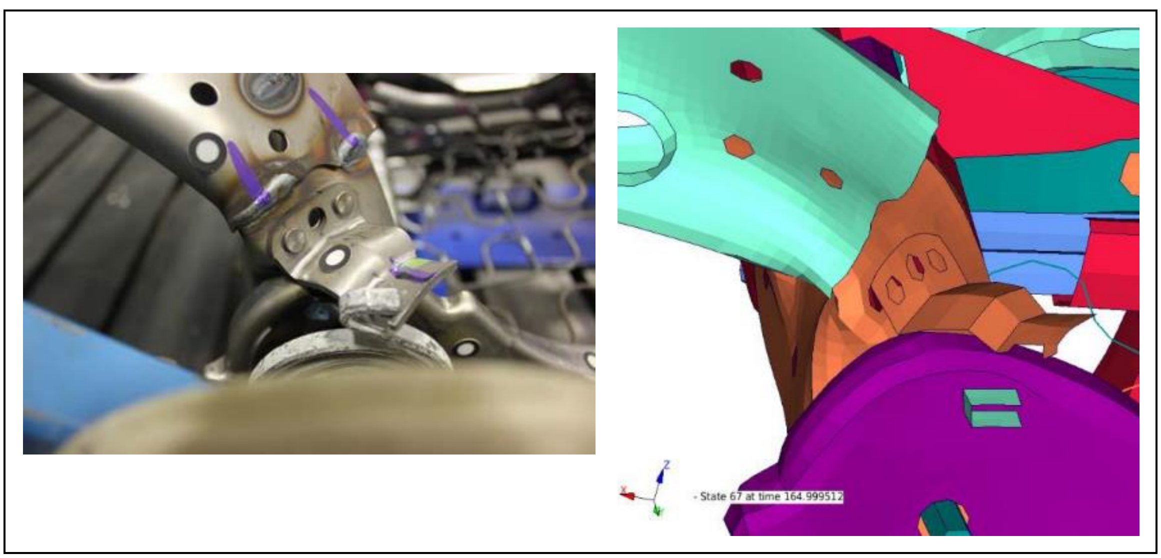

Figure 14: Similar Deformation of LHS Seat Frame Test Versus FEA –Manual Seat

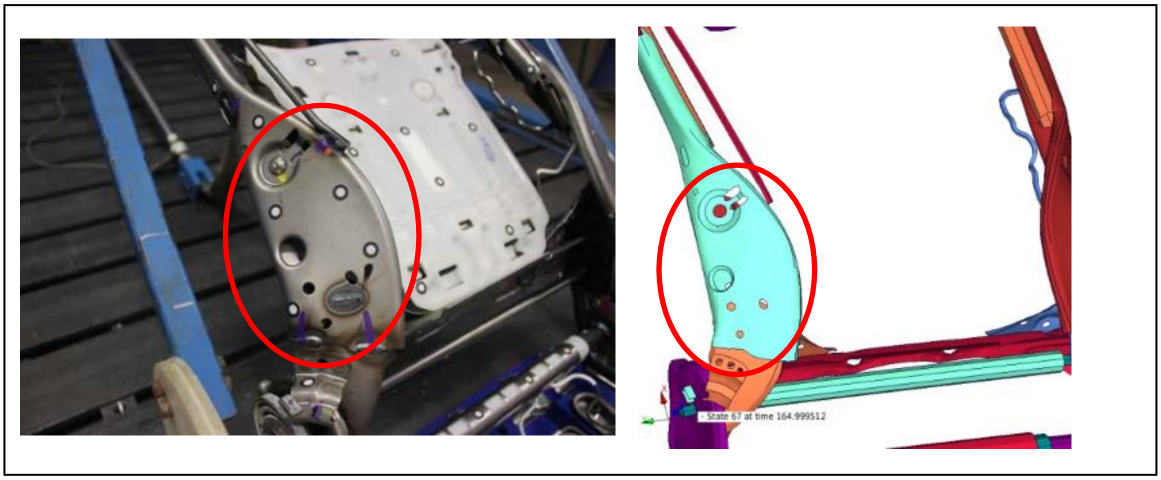

Figure 15: Similar Deformation of RHS Seat Frame Test Versus FEA – Manual Seat

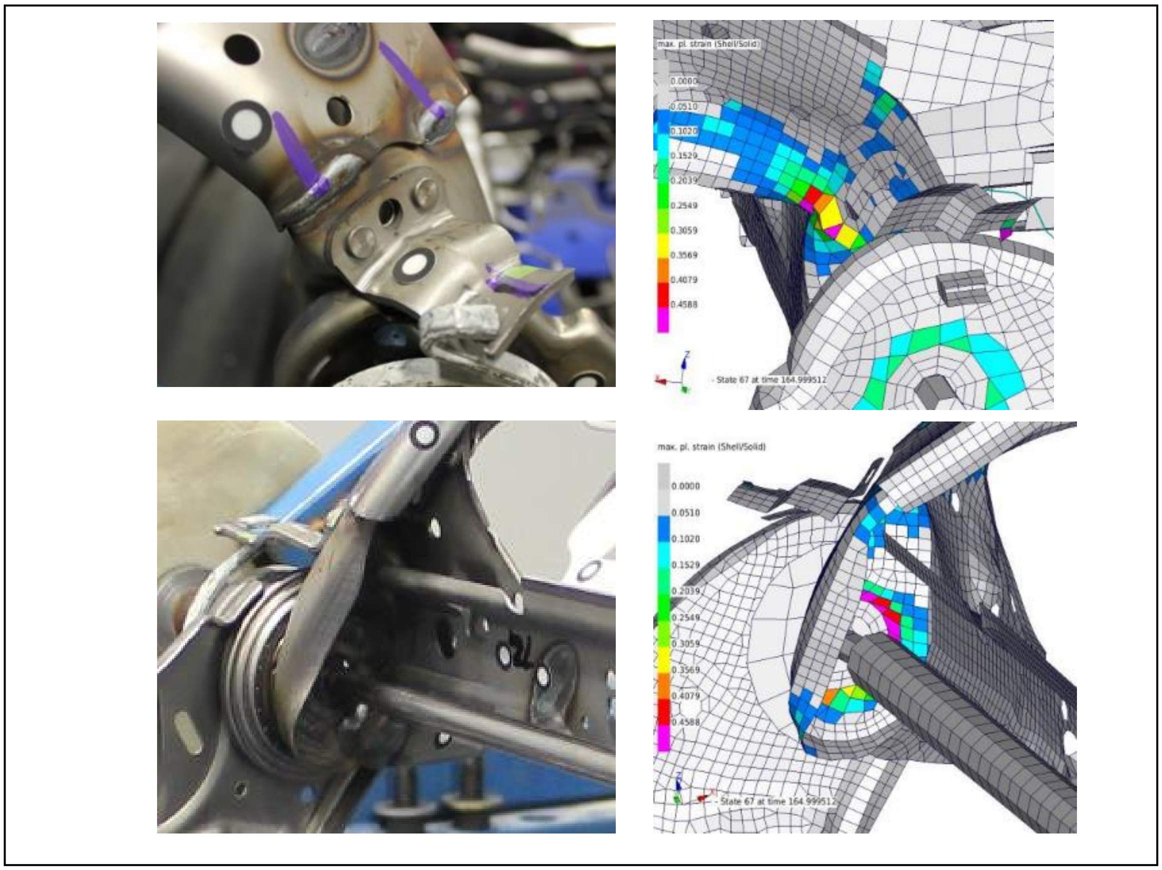

Figure 16: Manual Seat Deformation at Failure Area Similar to Test

The gussets folded inward and failed symmetrically in both Test and FEA. In addition to the frame deformation, the seat back strength was compared in terms of stiffness or force versus displacement plots. The displacement of the seat back along the loading direction, which is the representation of the piston displacement in the physical test, was measured and plotted against the applied load profile. The comparison of FD curves of FE simulation and physical test is shown in Figure 17.

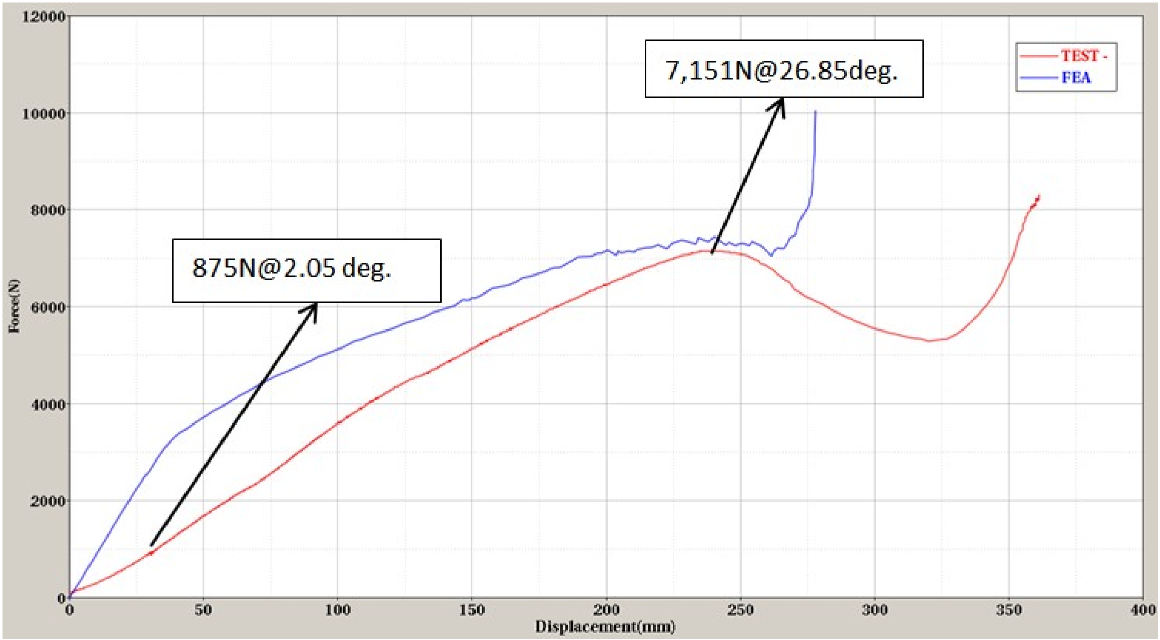

Figure 17: Force Versus Displacement Curves – Manual Seat

A commercially available curve comparison tool called CORA was used to compare the CAE and test FD curves. The FD curve shows a correlation rating of about 78 percent, which is a generally acceptable rating for such curves as good correlation.

From the above comparisons of frame deformation and stiffness (FD curve), it can be concluded that the manual seat correlated well with the physical test. Thus, the manual FE seat was modeled with acceptable detail and accuracy.

3.2.5 Power Seat – Seat Back Pull Test Correlation

Similarly, the power seat FE model was also set up to full down, full rear position by adjusting the seat position mechanism. The same method was followed from the manual seat modeling to set up and run power seat pull test simulation. The load application and boundary conditions setup are similar to the manual seat as shown in Figure 11, but the loading curve is slightly different. The loading curve used for power seat is shown in Figure 18.

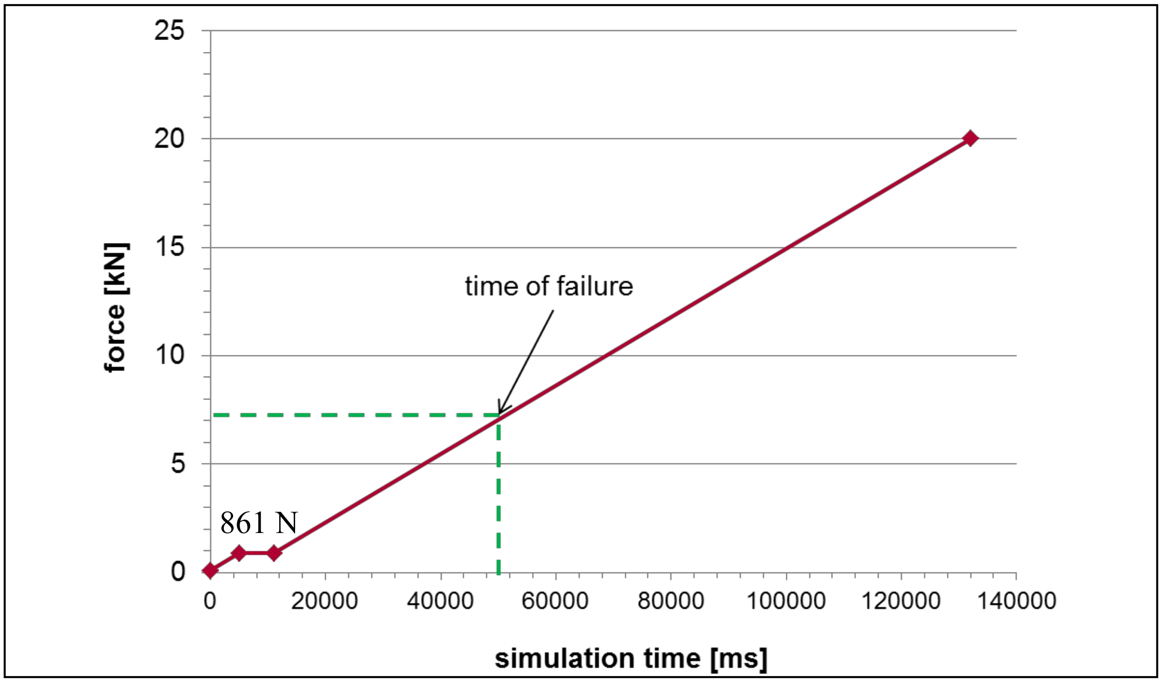

Figure 18: Loading Curve – Power Seat

FE simulation results of the power seat back pull test were compared with the physical test. Figure 19 shows the comparison of the deformed shape of the seat. Figures 20, 21 and 22 show the deformation of the collapsed seat frames at the failed area. The gussets folded non- symmetrically due to the motor that is located on the right side gusset, The LHS frame collapsed first at 37.1 degrees and RHS collapsed later at 20 degrees respectively.

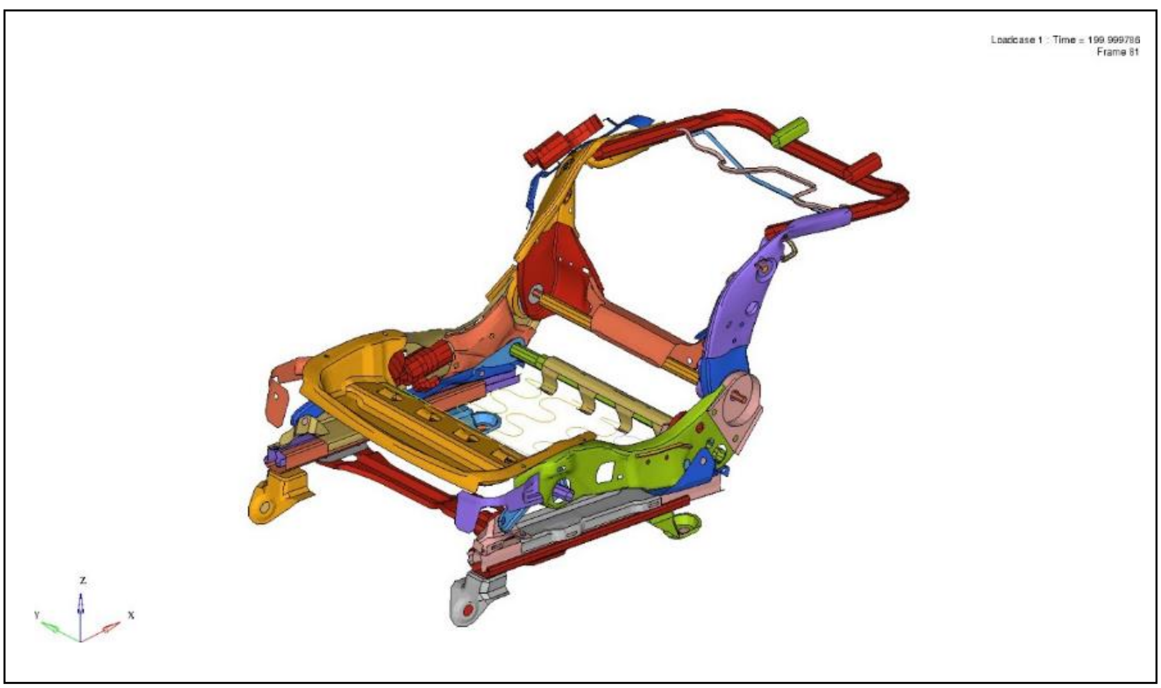

Figure 19: Global Deformation the Seat Frame – Power Seat

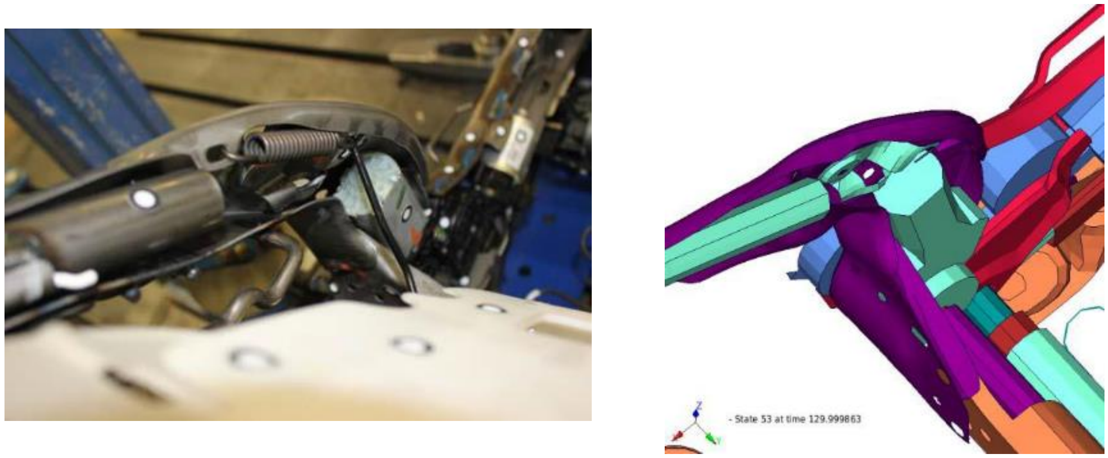

Figure 20: Similar Deformation of LHS Seat Frame Test Versus FEA – Power Seat

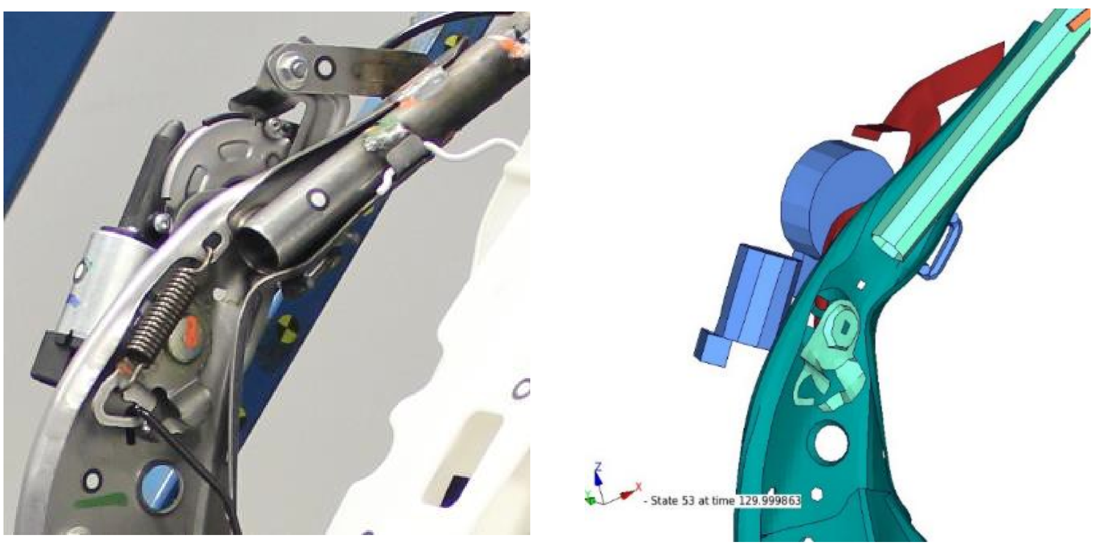

Figure 21: Similar Deformation of RHS Seat Frame Test Versus FEA – Power Seat

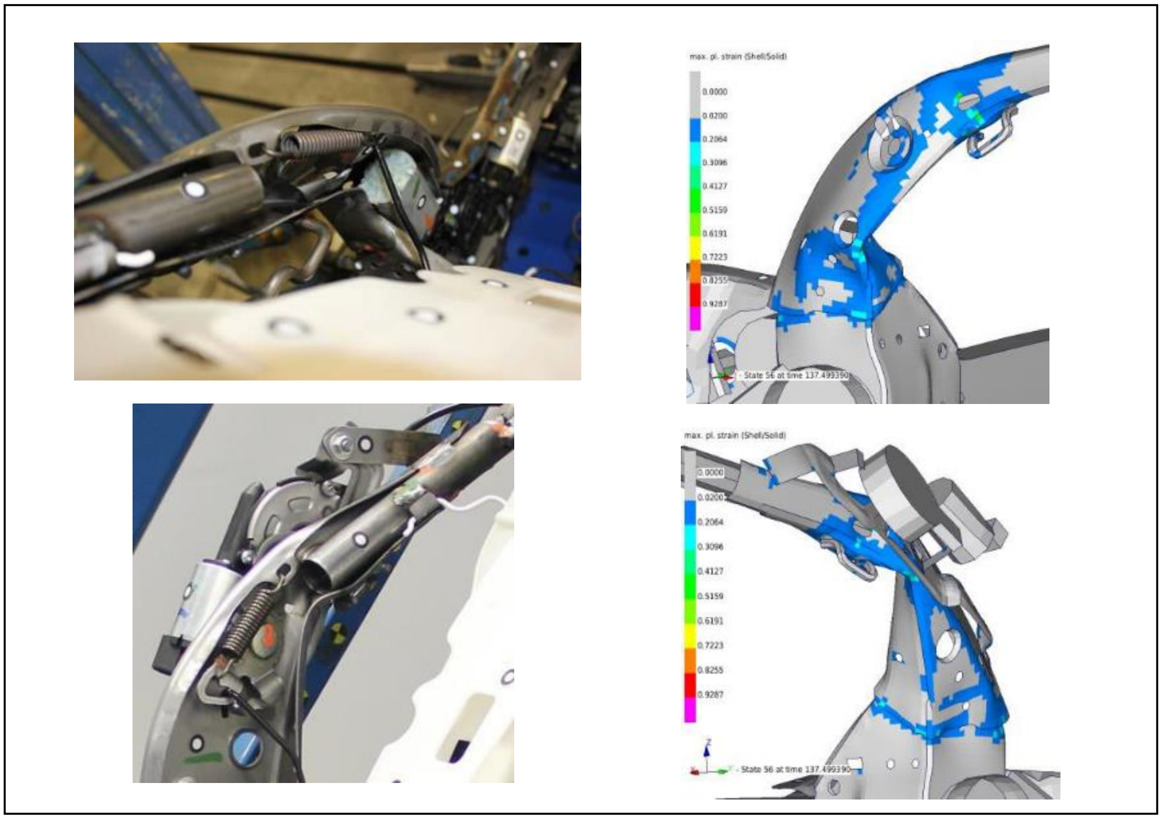

Figure 22: Power Seat Deformation at Failure Area Similar to Test

In addition to the frame deformation, the seat back strength was compared in terms of stiffness or force versus displacement plots. The displacement of the seat back along the loading direction, which is the representation of the piston displacement in the physical test, was measured and plotted against the applied load profile. The comparison of FD curves of FE simulation and physical test is shown in Figure 23.

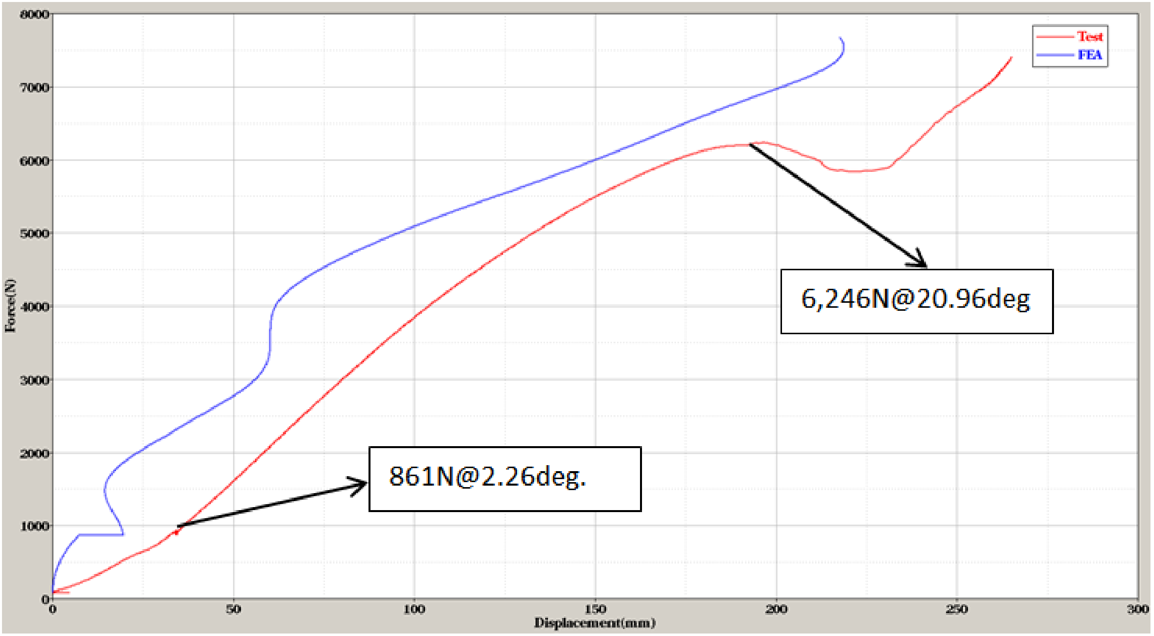

Figure 23: Force Versus Displacement Curves – Power Seat

The commercially available curve comparison tool called CORA was used to compare the CAE and test FD curves. The FD curve shows a correlation rating of about 76 percent that is a generally acceptable rating for such curves as good correlation.

From the above comparisons of frame deformation and stiffness (FD curve), it can be concluded that the power seat also correlated well with the physical test. Thus the power FE seat was modeled with acceptable detail and accuracy.

4 FMVSS 301 High Speed Rear Impact Sled Test

The objective of this project is to study the front seat back strength in rear crash events. While the low-speed rear impact study is limited to the whiplash and neck injury measures of the occupant, this study is aimed at rear seat passenger protection in high-speed impact such as FMVSS 301 rear impact scenario. The FMVSS 301 rear impact subjects the vehicle to rear impact by a moving deformable barrier (MDB) at 55 mph with 70 percent offset. This test generates an acceleration pulse of the vehicle. In order to study the front seat back strength requirements with occupant seated on it, it was decided to conduct the FMVSS 301 test with a physical sled and Bio-RID II dummy positioned on the front seat using the vehicle acceleration pulse.

EDAG sub-contracted the testing company MGA to conduct the rear impact sled test for the manual and power seat. The necessary vehicle pulse was computed by running the FMVSS 301 rear impact simulation using MY2014 Honda Accord structural model (Ref. Section 3.1). The rear impact vehicle pulse is shown in Figure 24.

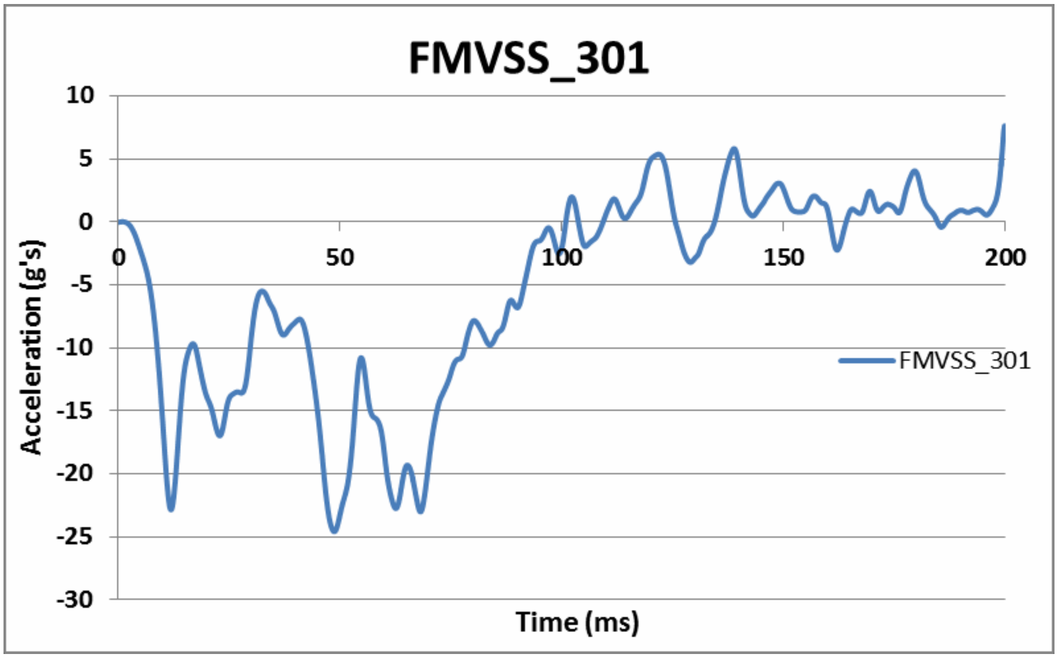

Figure 24: FMVSS 301 Rear Impact Vehicle Pulse (CAE Simulation)

The Bio-RID II rear impact dummy was used in the sled test. The Bio-RID II dummy was supplied by NHTSA. The rear impact dummy was calibrated with 22 necessary channels. Considering the Bio-RID II dummy's loading capacity limited to a rear impact speed of 17 mph, the vehicle pulse was tuned to approximately 20 G. The vehicle pulse was a generic vehicle pulse calculated based on the FMVSS 301 rear impact pulse obtained from the CAE simulation (shown in Figure 24). The generic vehicle pulse used in the sled test is shown in Figure 25.

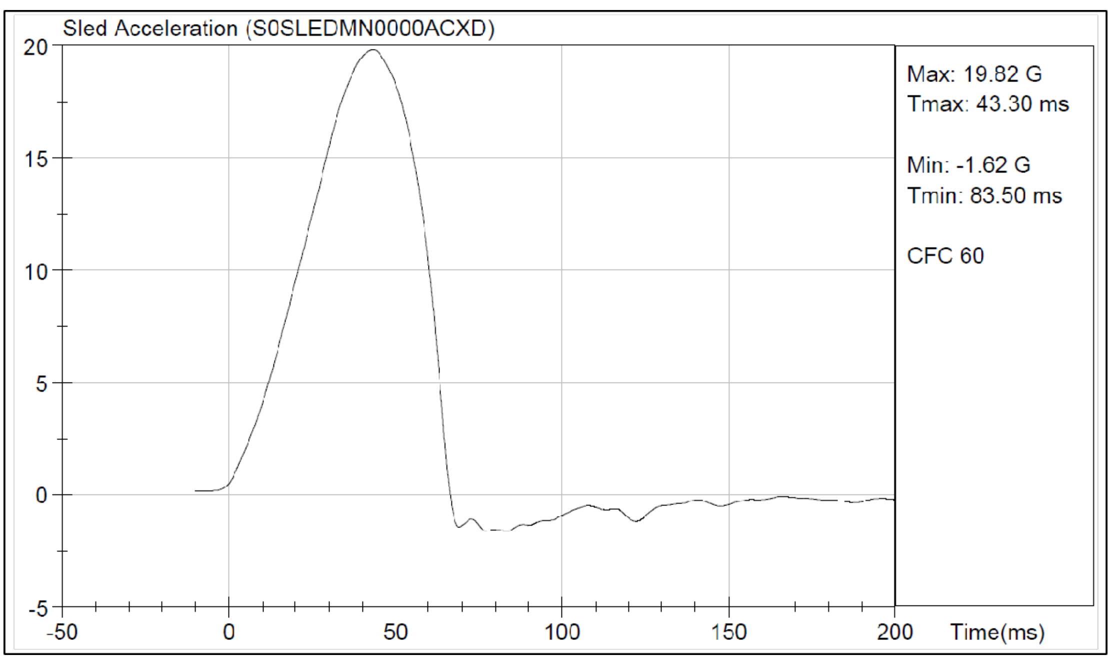

Figure 25: FMVSS 301 Sled Pulse (Generic, 20G Pulse)

The dummy position data such as H-Point location and torso angle were computed based on MY2014 Honda Accord Vehicle structure and seat models. The FMVSS 301 rear impact Sled test setups for fully trimmed manual and power seat are shown in Figure 26.

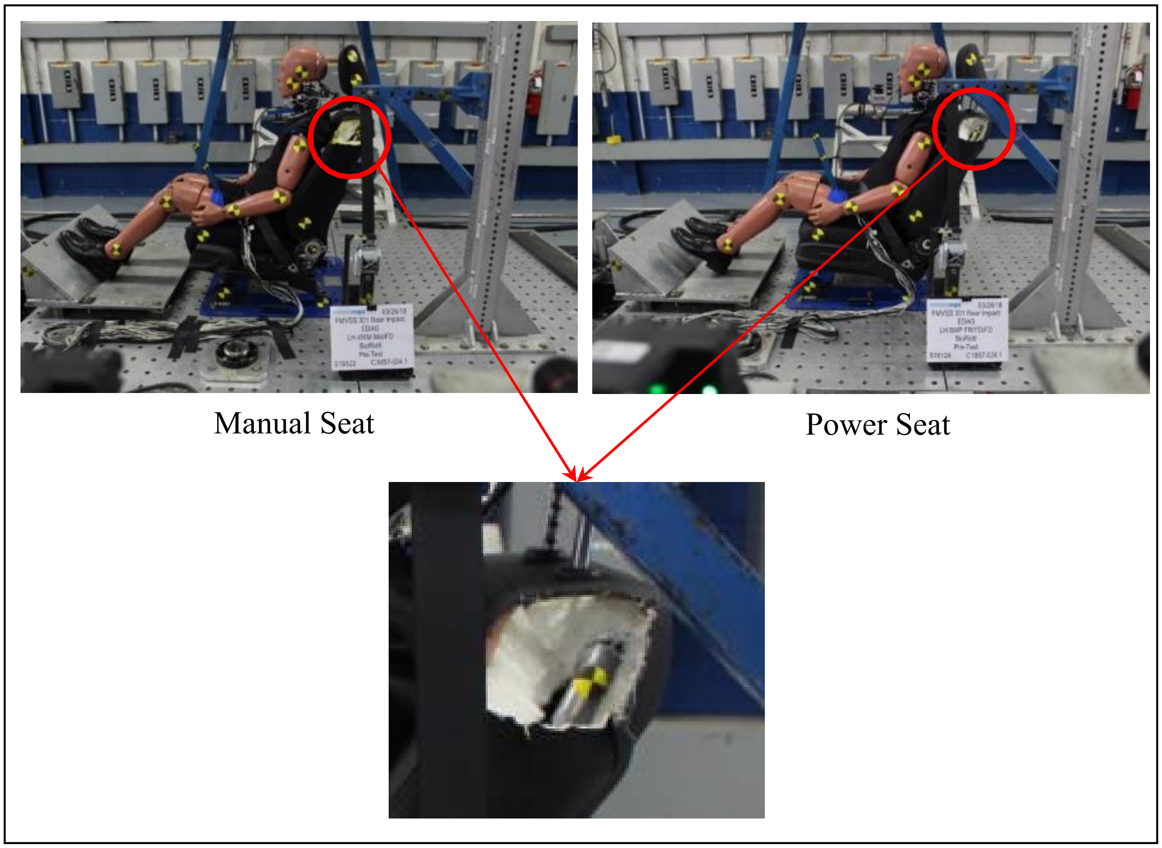

Figure 26: FMVSS 301 Sled Test Setup

The manual seat was tested in mid track and full down seat position. The power seat was tested in full rear track and full down seat position. The reason for conducting the sled tests for two different seat positions is to understand the seat back strength requirements for nominal and extreme conditions of occupant seating. Occupant characteristics including head acceleration, neck injury parameters and seat back measurements were recorded appropriately. Considering the scope of this project to study the seat back strength, a target point location was marked on the top of the seat back frame to track the seatback angle (shown in Figure 26). Measured from the initial position, the manual seat recorded a dynamic seat back deflection of 38.4° and post-test static permanent deflection of 9.4°. The power seat recorded a dynamic seat back rotation of 38.5° and post-test static permanent deflection of 9°. The following Figure 27 and 28 show the pre and post-test photographs of the FMVSS 301 Sled Test of manual and power seats respectively. In the dynamic seat back test there is no significant deformation is observed on both power and manual seat similar to the quasi-static pull test.

Pre Test Post Test

Figure 27: FMVSS301 Sled Test – Manual Seat

Pre Test Post Test

Figure 28: FMVSS301 Sled Test – Power Seat

The dynamic seat deflections (in degrees) of manual seat and power seat are shown in Figures 27 and 28, respectively.

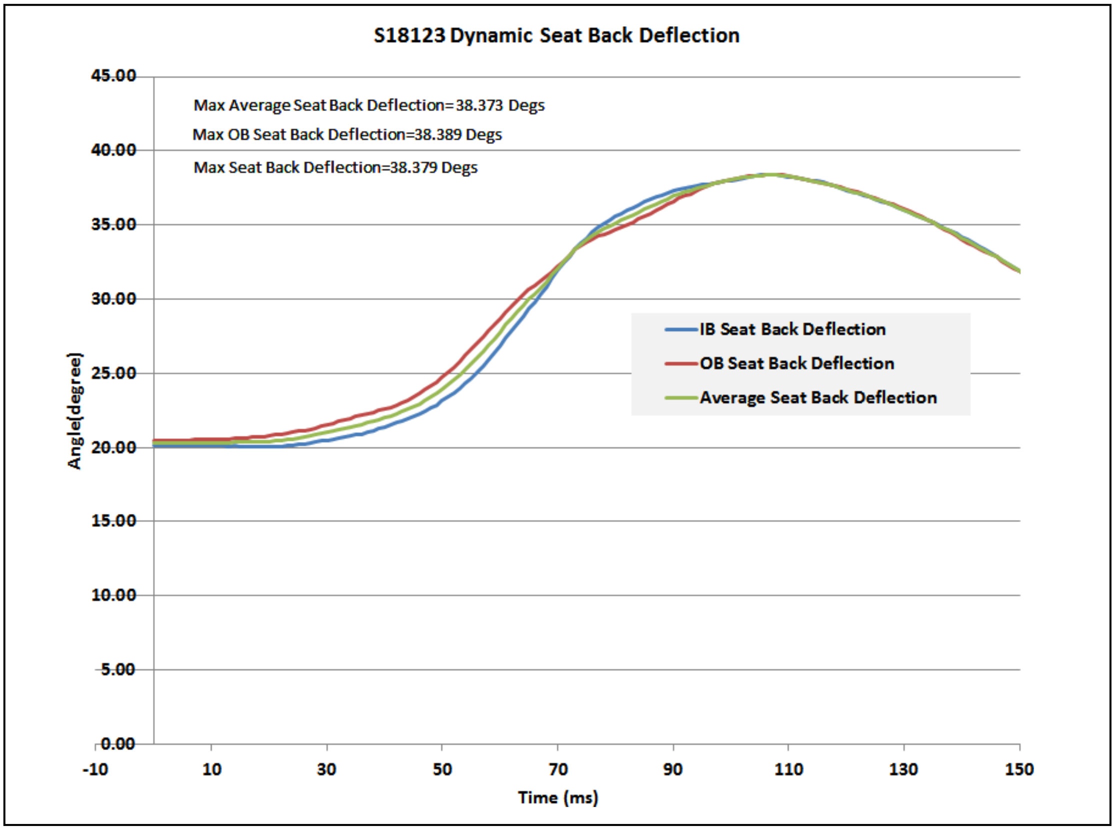

Figure 29: Seat Back Dynamic Deflection - Manual Seat

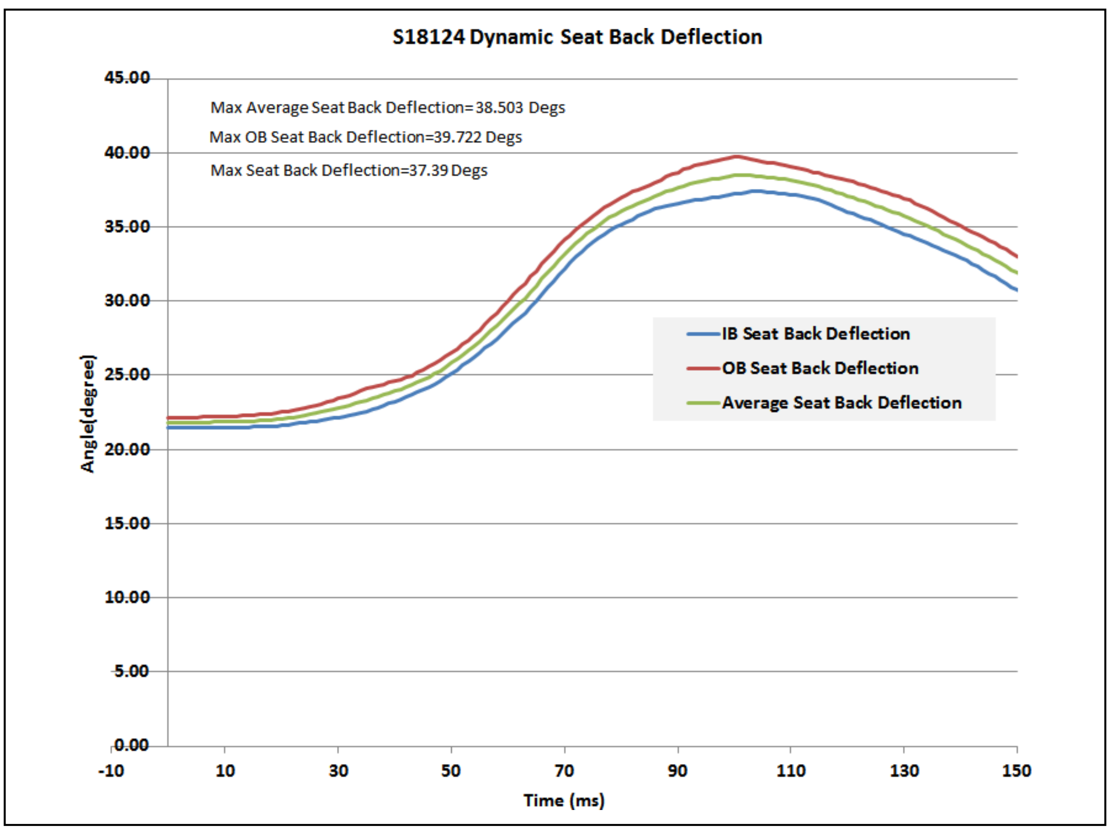

Figure 30: Seat Back Dynamic Deflection - Power Seat

Detailed sled test reports of manual and power seat testing are provided in **Appendix A.3a and A.3b** where occupant head acceleration and neck injury measures are given accordingly. The occupant characteristics from the sled tests have been referred accordingly in the FEA model development, as described in the following sections.

5 FMVSS 301 Model Development

After developing and validating the FE seat models by correlating to the physical test, the FE seat models were used in the FMVSS 301 FE modeling.

5.1 FMVSS 301 FEM Development

The FMVSS 301 rear impact simulation included the Bio-RID II dummy FE model positioned on the fully trimmed front seats. For this purpose, MY2014 Honda Accord FE structural model was used as a rigid sled. The study focused on the driver side of the vehicle. Therefore, only the driver side half (left hand side) of the FE model was converted to a rigid sled model.

The above validated seat models were integrated by including the standard seat bottom and seat back cushion (or foam) modeling for realistic dummy to seat interaction. The seat structure, seat position mechanism, and cushions are shown in Figure 31.

Figure 31: Seat FEM –Mechanism and Cushions (Ex. Manual Seat)

The seat cushions were modeled as solid elements and were assigned foam material properties. Another important requirement to have more realistic occupant kinematics is to have the seat cushions pre-deformed due to weight of the dummy to match the lower torso profile impression on the seat bottom cushion and upper torso impression over the seat back cushion. The model was gravity settled prior to simulation. The seat cushions were deformed to the Bio-RID II dummy shapes by using LS-DYNA pre-simulations. Figure 32 shows the pre-deformed seat cushions attached to the seat structure.

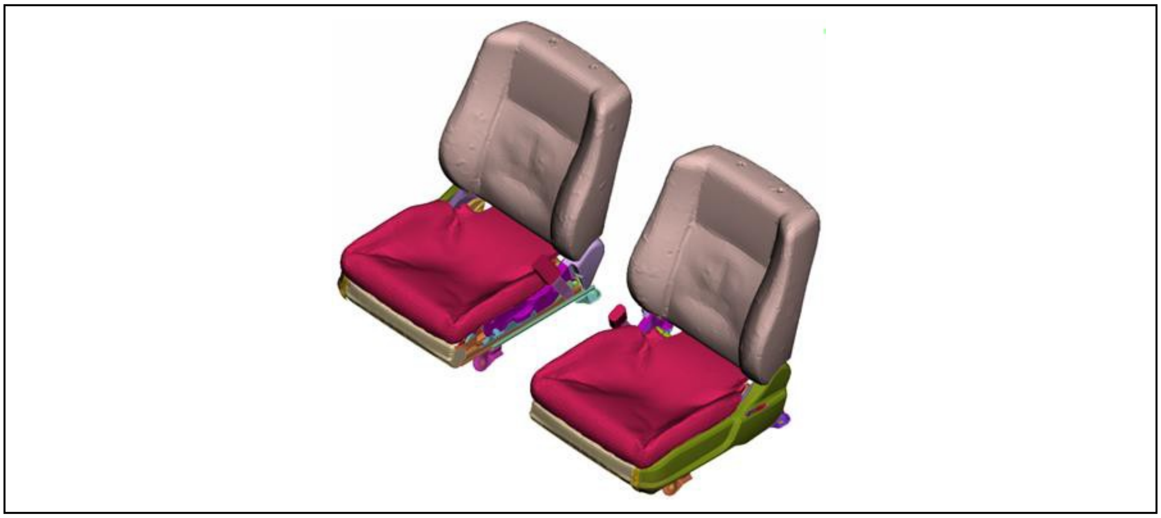

Figure 32: Manual and Power Seat Models With Pre-deformed Cushions

5.2 FMVSS 301 Sled Test CAE, Test Comparison

Two different FE models were developed using the manual and power seat FE models. All the FE parts of the sled model were assigned with rigid materials and attached globally to one freely moving master rigid part.

5.2.1 Manual Seat – Sled Test Comparison

The manual seat was integrated with seat position and seat back angle as per the test. Bio-RID II occupant dummy was positioned as per the required H-Point and seat back angle. Shoulder belt and lap belt were modeled and wrapped over the Bio-RID II dummy. Gravity was applied to Bio-RID II dummy. The sled pulse (shown in Figure 25) was applied to the master rigid part.

LS-DYNA simulation was run for 200 milliseconds and the characteristics of Bio-RID II dummy and seat structure were computed. In particular, the seat back rotation, occupant head acceleration and neck forces were obtained, plotted, and compared to that of physical test. The kinematics of the seat back rotation and occupant position are shown in Figure 33 for several frames of the simulation and test.

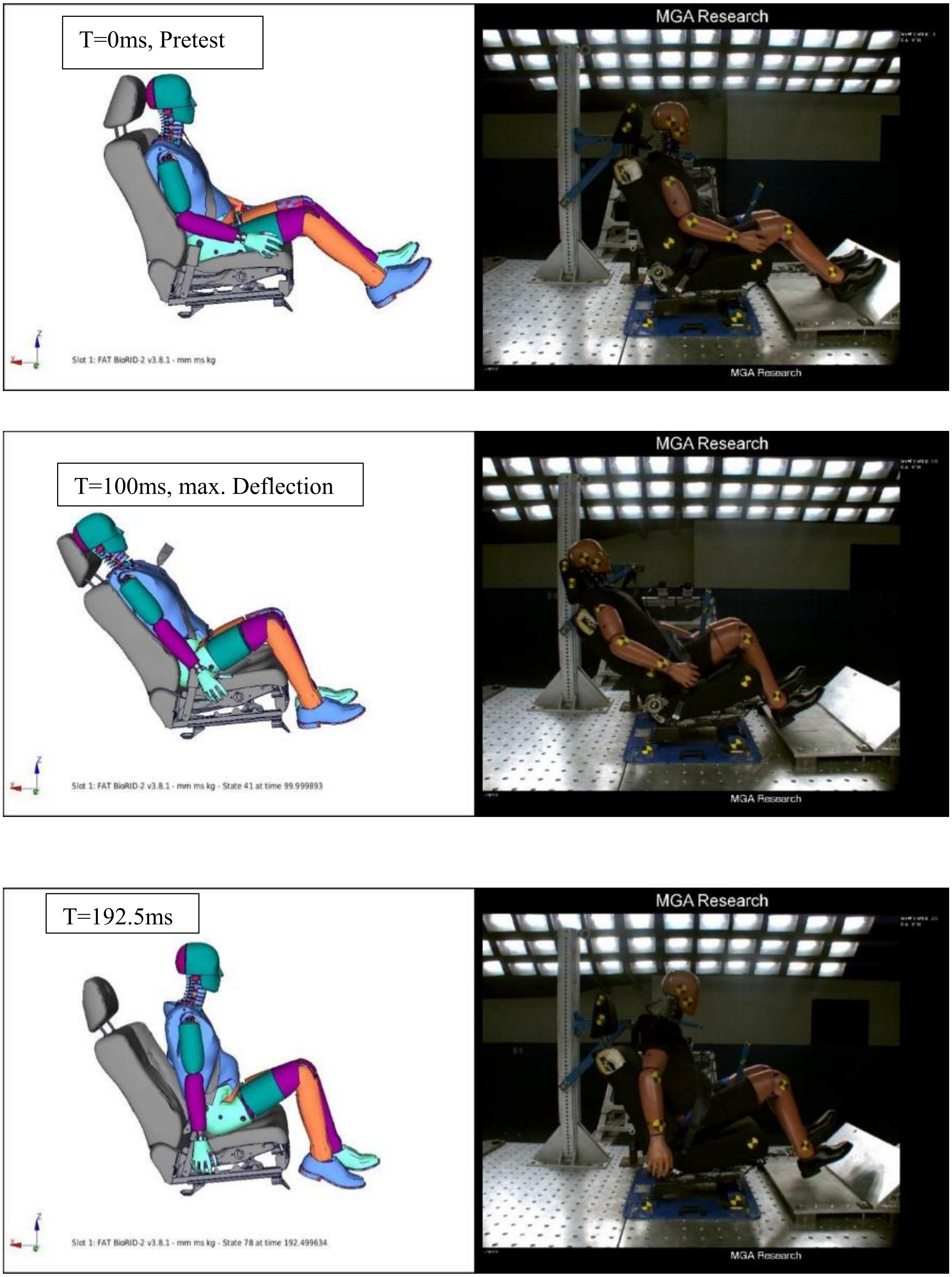

Figure 33: FMVSS301 Sled Test FEA and Test – Manual Seat

The manual seat FE simulation and sled test results comparison including seat back dynamic deflection, occupant head acceleration plot, Head Injury Criteria (HIC) value and neck forces for Neck Injury Criteria (NIJ) are given in Figures 34, 35 and 36.

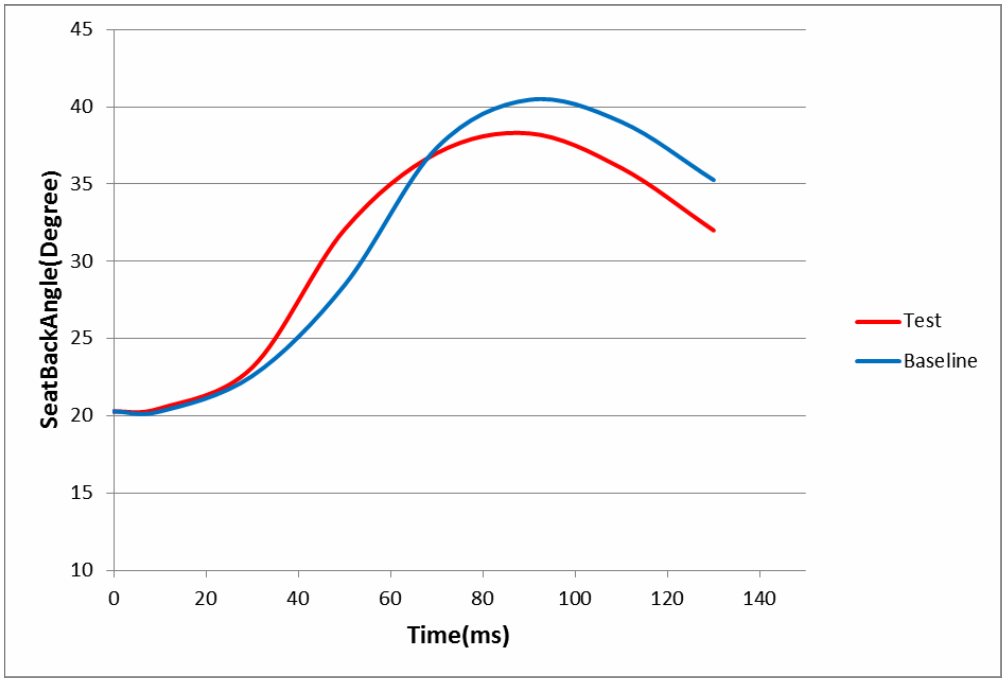

Figure 34: Seat Back Rotation – Manual Seat

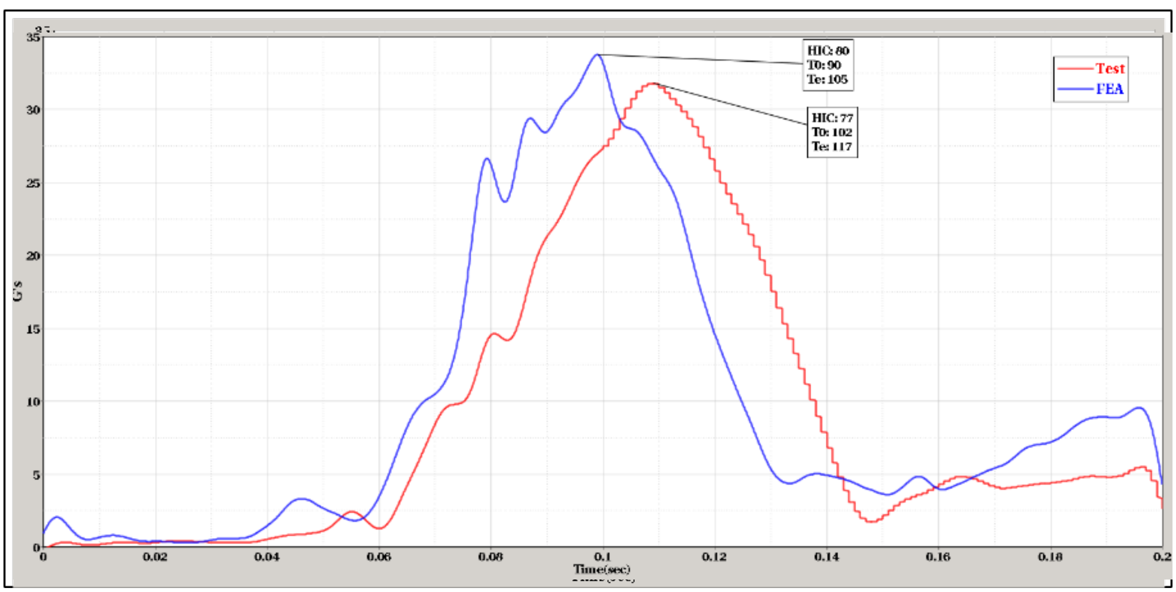

Figure 35: Head Acceleration – Manual Seat

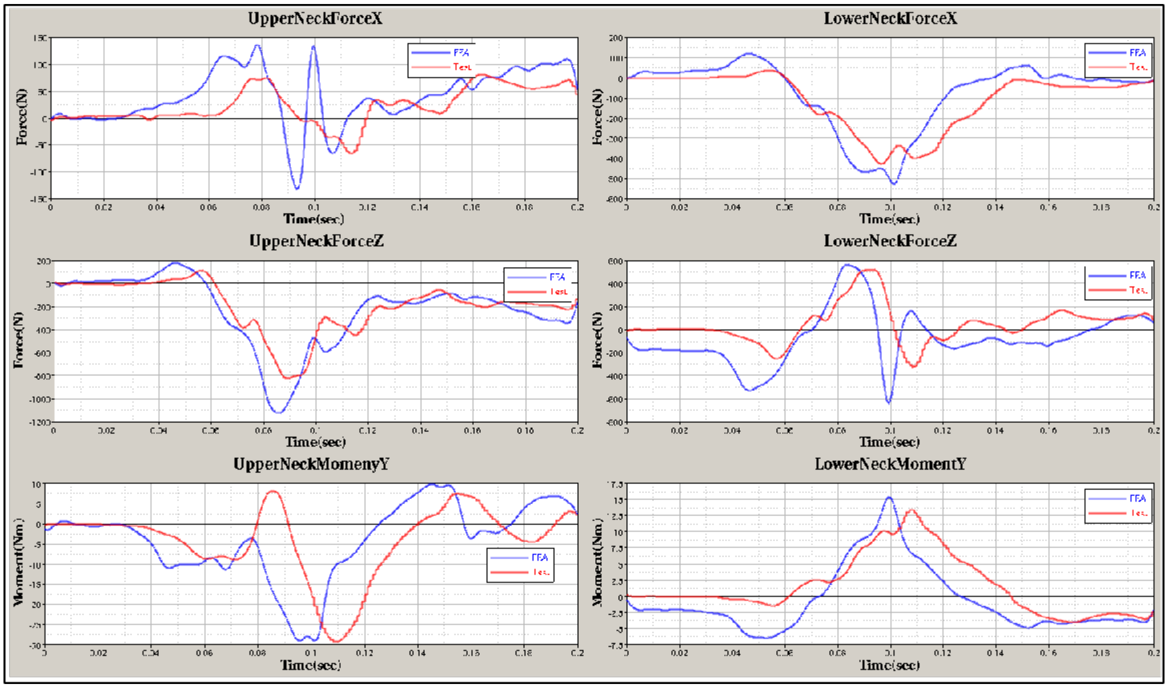

Figure 36: Neck Forces – Manual Seat

In Figure 34, significant offset between test and simulations are observed, the reason being, the test had idle time for the first 10sec that the test curve was offset to match with FEA, and FEA did not represent this test idle time during simulation. Even though the main objective of comparison of FE simulation in this case was for validating the FE model for seat back strength, it was always a general practice to obtain a reasonable seat and occupant kinematics similar to that of the physical test. The FE animation and physical test video showed similar kinematics. The comparisons of HIC, NIJ are listed in Table 4.

No.	Injury measures	FEA	Test
1	HIC 15	80	77
2	NIJ	0.18	0.28

Table 4: FMVSS 301 Sled Test FE Simulations and Test Comparison – Manual Seat

5.2.2 Power Seat – Sled Test Comparison

Similarly, the power seat was integrated with seat position and seat back angle as per the test. The same method was followed from the manual seat sled test modeling to set up and run power seat sled test simulation. The kinematics of the seat back rotation and occupant position of power seat are shown in Figure 37 for several frames of the simulation and test.

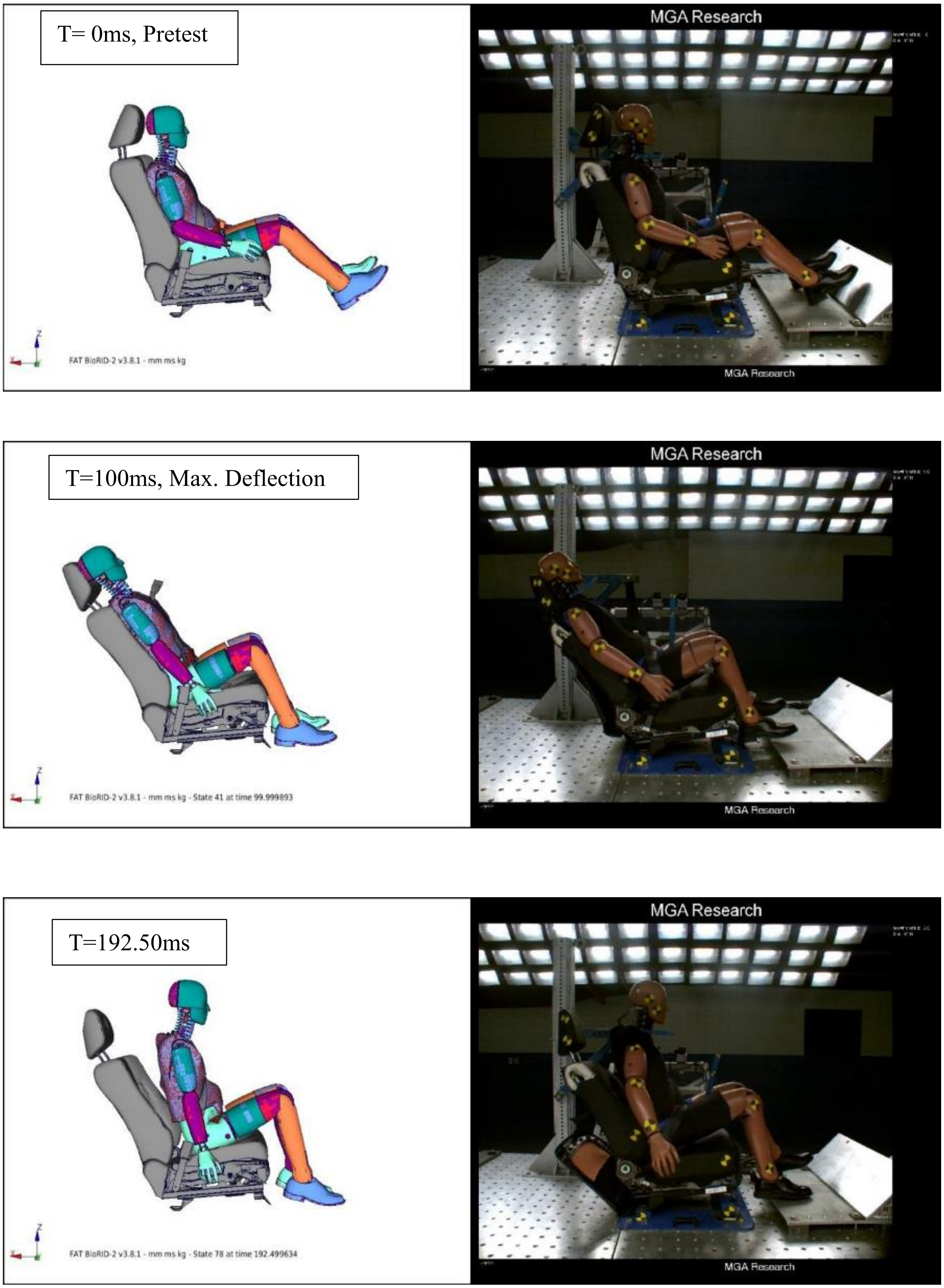

Figure 37: FMVSS301 Sled Test FEA and Test – Power Seat

The power seat FE simulation and sled test results comparison including seat back dynamic deflection, occupant head acceleration plot, HIC value and neck forces for Neck Injury are given in Figures 38, 39 and 40.

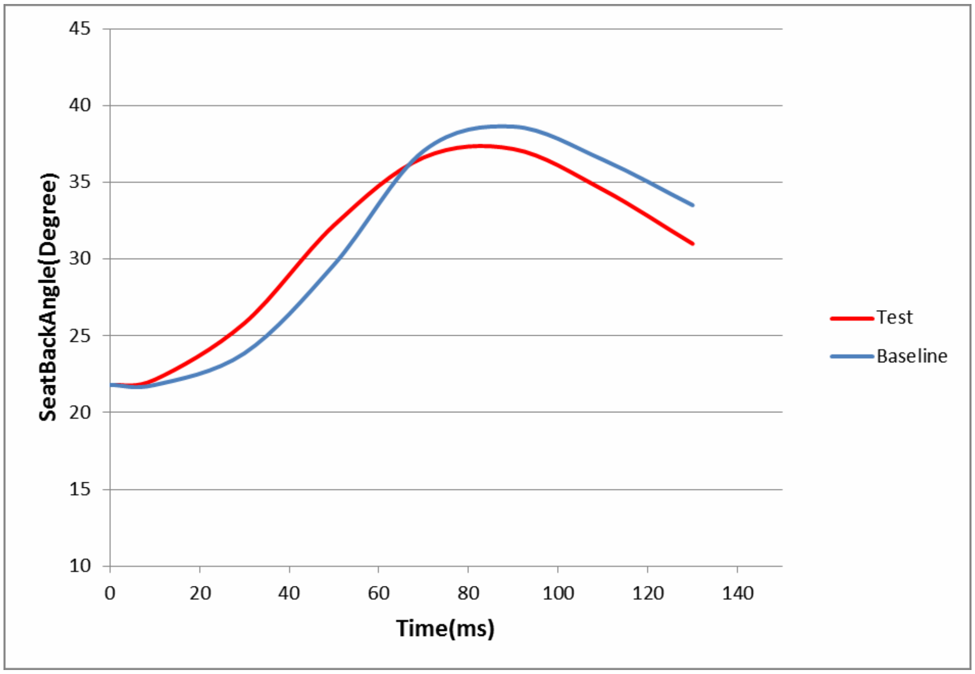

Figure 38: Seat Back Rotation – Power Seat

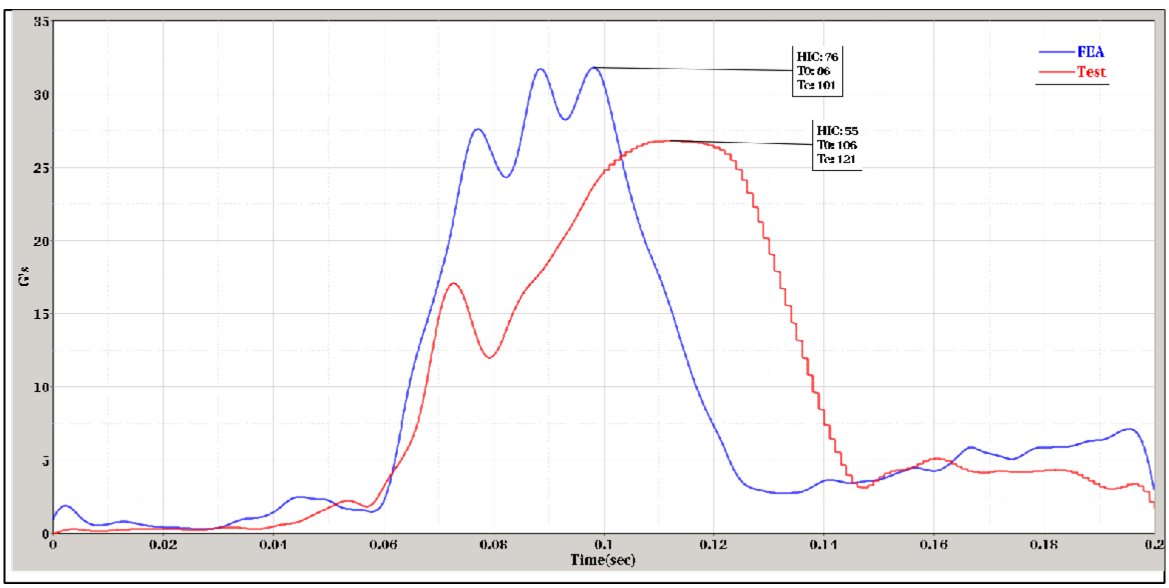

Figure 39: Head Acceleration – Power Seat

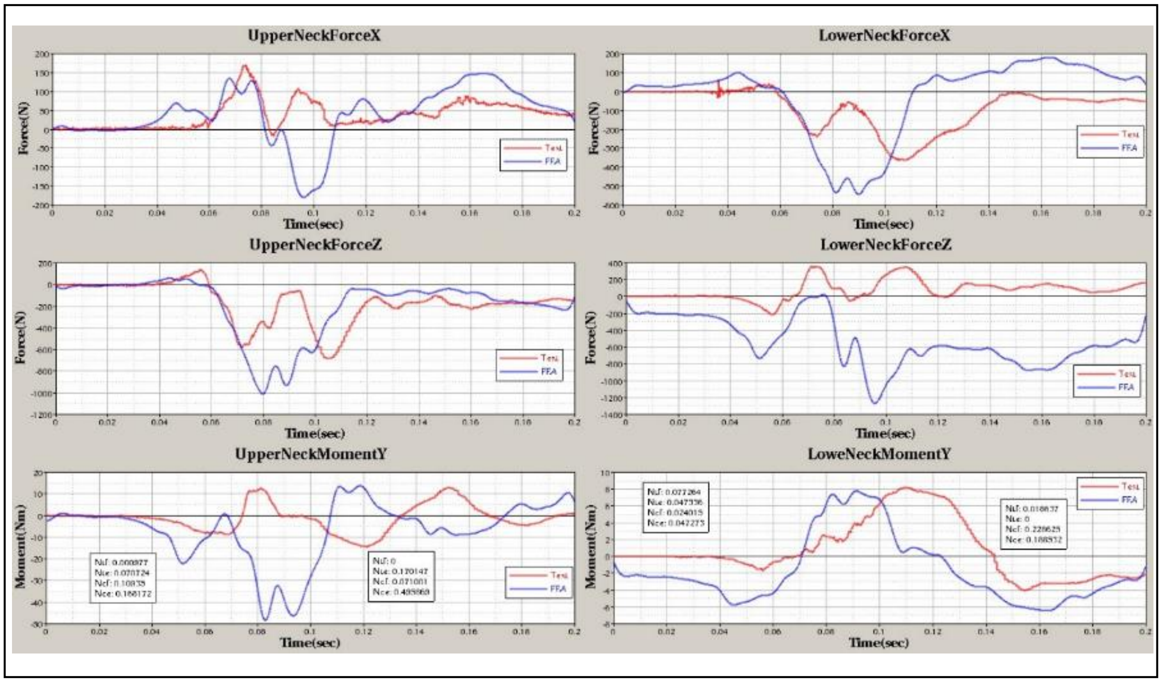

Figure 40: Neck Forces – Power Seat

It should be noted FEA and test curves offset in Figure 38 is due to a 10secs test idle time. The neck forces and moments shown in Figure 40 were not used directly for seat back strength study. From the project scope point of view, the main purpose of comparison of FE simulation in this case was for validating the seat FE model for seat back strength. It was decided to obtain a reasonable global seat kinematics only similar to that of the physical test. The FE animation and physical test video showed similar kinematics. Therefore, with this level of comparison, the results were deemed sufficient for this project. The comparison of HIC and NIJ are listed in the Table 5 for additional references for comparison purpose during seat back countermeasures.

No.	Injury measures	FEA	Test
1	HIC 15	55	76
2	NIJ	0.42	0.08

Table 5: FMVSS 301 Sled Test FE Simulations and Test Comparison – Power Seat

6 Seat Back Strength Requirements Study

6.1 FMVSS 301 Simulations With Rear Seat Passenger

Once the front seat models were developed and integrated with acceptable accuracy in terms of structural integrity and strength (comparing to seat back pull test), seat and occupant kinematics, dynamic characteristics (comparing FMVSS301 high-speed rear impact sled test), the next step was to study the seat back strength requirements to avoid rear seat passenger injuries. This study was intended to observe the seat back movement that could potentially cause injuries to rear seat passenger in the rear crash events. As discussed with notable rear crash cases (Section 2.1), the rapid rear seat movement due to impact forces and occupant reaction on the seat back could cause severe injuries to the rear seat occupants such as children or adults due to interaction with the front seat or front seat occupant.

Therefore, the necessary seat back strength has to be investigated with the rear seat occupant seated at the impact side of the vehicle, in this case the driver side. The detailed FE front seat models, driver side FE model of the Honda Accord MY 2014 full vehicle and Bio-RID II FE model were used to simulate the rear crash scenario. In this study 2 FEA models (for manual seat and power seat) with rear seat passenger were developed and investigated for the seat back strength.

6.1.1 Manual Seat – FMVSS 301 Simulation With Rear Seat Passenger

The FEA model used for sled test simulation in Section 5.2.1 was set up with a rear seat occupant dummy for FMVSS 301 rear crash. In this case Bio-RID II FE dummy model itself was used as rear seat passenger and positioned on the rear seat behind the driver side seat (manual seat) under investigation. The necessary rear seat head restraint was modeled and integrated in the full vehicle representation of FE model. Figure 41 shows the FMVSS 301 FE model with rear seat occupant dummy.

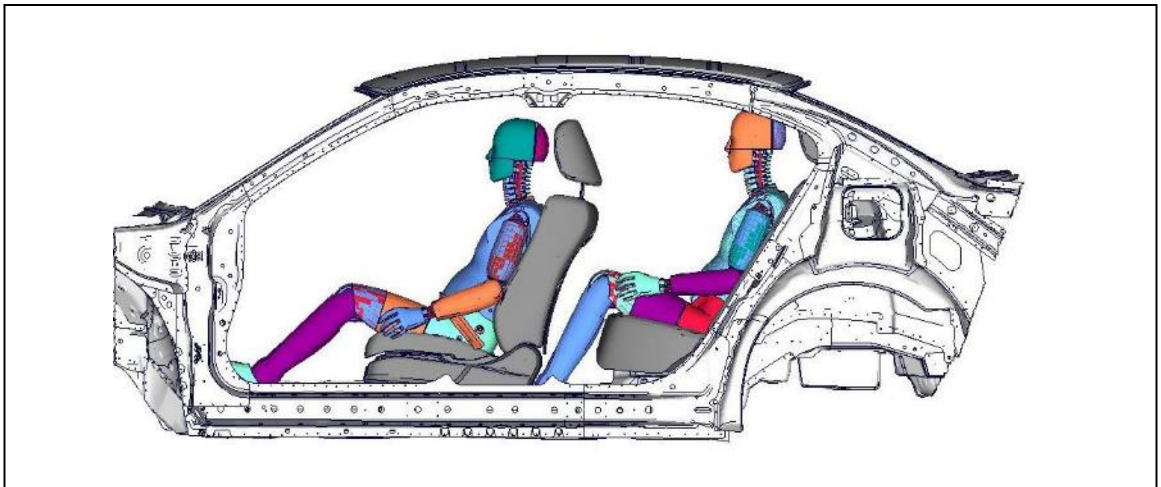

Figure 41: FMVSS 301 FE Model With Rear Seat Occupant Dummy – Manual Seat

LS-DYNA simulation was run for 200 milliseconds. The front seat back rotation and the rear seat occupant interaction with the front seat were observed. The front seat back movements are illustrated in Figure 42.

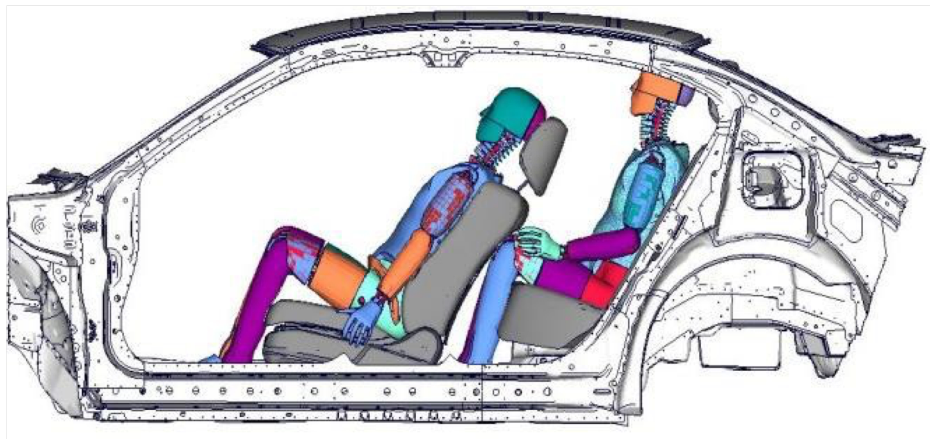

Front seat in contact with rear occupant knee

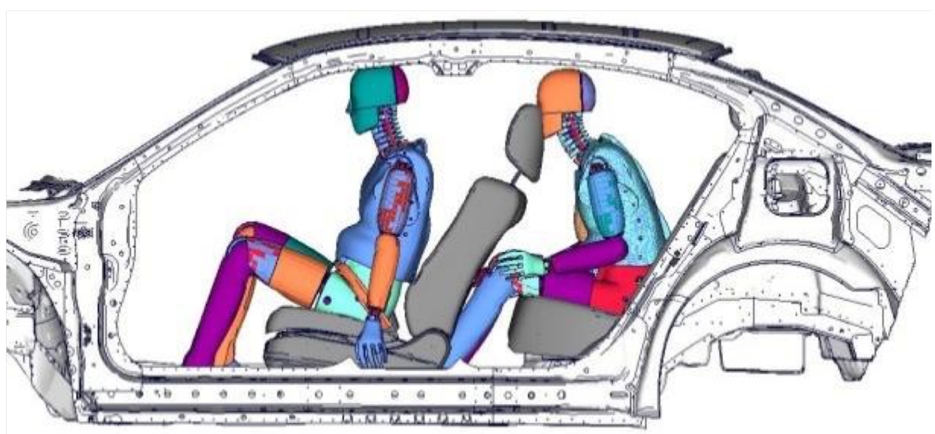

Front seat in at maximum impact with rear occupant

Figure 42: Front Seat Back and Rear Seat Occupant Interaction – Manual Seat

6.1.2 Power Seat – FMVSS 301 Simulation With Rear Seat Passenger

Similarly, the FEA model used for sled test simulation in Section 5.2.2 was set up with rear seat occupant dummy for FMVSS 301 rear crash. The Bio-RID II FE dummy model was used as rear seat passenger in unbelted condition as shown in Figure 43. LS-DYNA simulation was run for 200 milliseconds. The front seat back rotation and the rear seat occupant interaction with the front seat were observed for power seat. The front seat back movements of the power seat are illustrated in Figure 44.

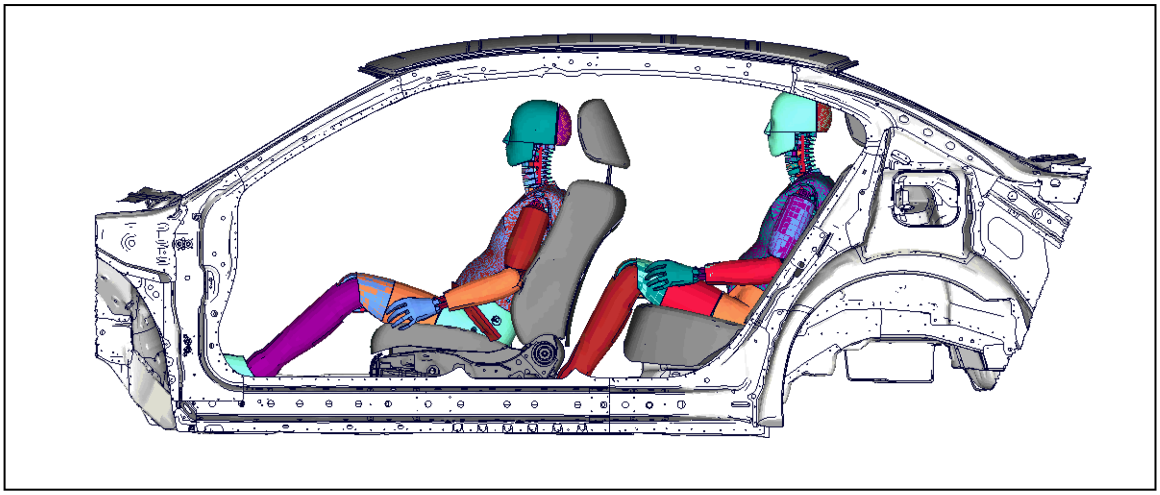

Figure 43: FMVSS 301 FE Model With Rear Seat Occupant Dummy – Power Seat

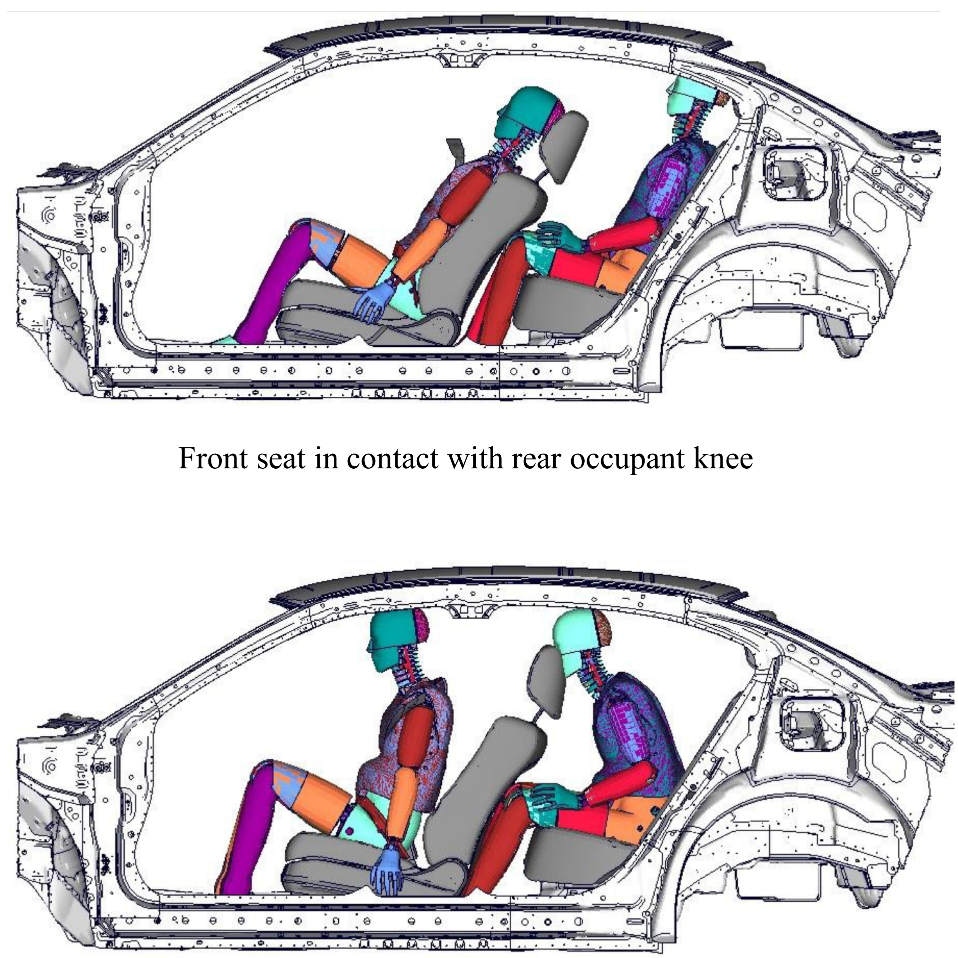

Front seat in contact with rear occupant knee

Front seat in at maximum impact with rear occupant

Figure 44: Front Seat Back and Rear Seat Occupant Interaction – Power Seat

7 Seat Back Strength Improvements

7.1 Countermeasures and Design Changes

FMVSS 301 FEA simulations of driver seat with rear seat passenger clearly showed the front seat back impact on the unbelted rear seat passenger seat behind the driver seat. The HIC value of the rear seat passenger was observed to be less than 500 when the head impacts on the front seat head rest. The front seat interaction on the rear seat occupant knee showed significant contact and femur force that was above 3.5 kN. These observations are good evidences that the baseline seat would need to be modified to avoid seat back to knee contact and head restraint to head contact. EDAG performed the countermeasures actions on the seat back and seat bottom frames to achieve reduced rear seat occupant HIC value and femur force in terms of the following performance targets shown in Table 6.

No.	Criteria	Target	Baseline	Improvements for
1	Seat back angle	< 35 deg	38 deg	No knee contact
2	Seat frame to knee clearance	> 10 mm	3.76 mm	No knee contact
3	Femur force	< 1.5 kN	3.5 kN	Reduced knee impact

Table 6: Seat back strength improvement targets

Several countermeasure ideas were attempted on both manual and power seats. The countermeasures that showed significant improvements are listed in **Appendix A.4**. The countermeasures were implemented on manual and power seat and FEA simulations were run to investigate the improvements. Observing the static deformation of 9.4 mm of the seat back in the FMVSS 301 test, the modification of strengthening the seat back frame by thickness (gauge) and material (grade) update, head rest forward tilt did not show any improvements of seat back angle. Further deeper investigation of kinematics of the seat back movement from FEA simulations with rear seat passenger, it was observed that, the seat bottom upward movement by the 4-way or 6-way seat mechanism influenced the seat back frame rotation more than the deformation of the seat frame alone. Therefore 2G (gauge and grade) optimization was undertaken on the seat bottom frame and bracket members. This approach showed good improvements in reducing the seat back angle. The seat bottom frame and mechanism support parts were optimized and FEA simulations were compared with the baseline seats. The gauge and grade changes of the seat bottom frame are shown in Figure 45.

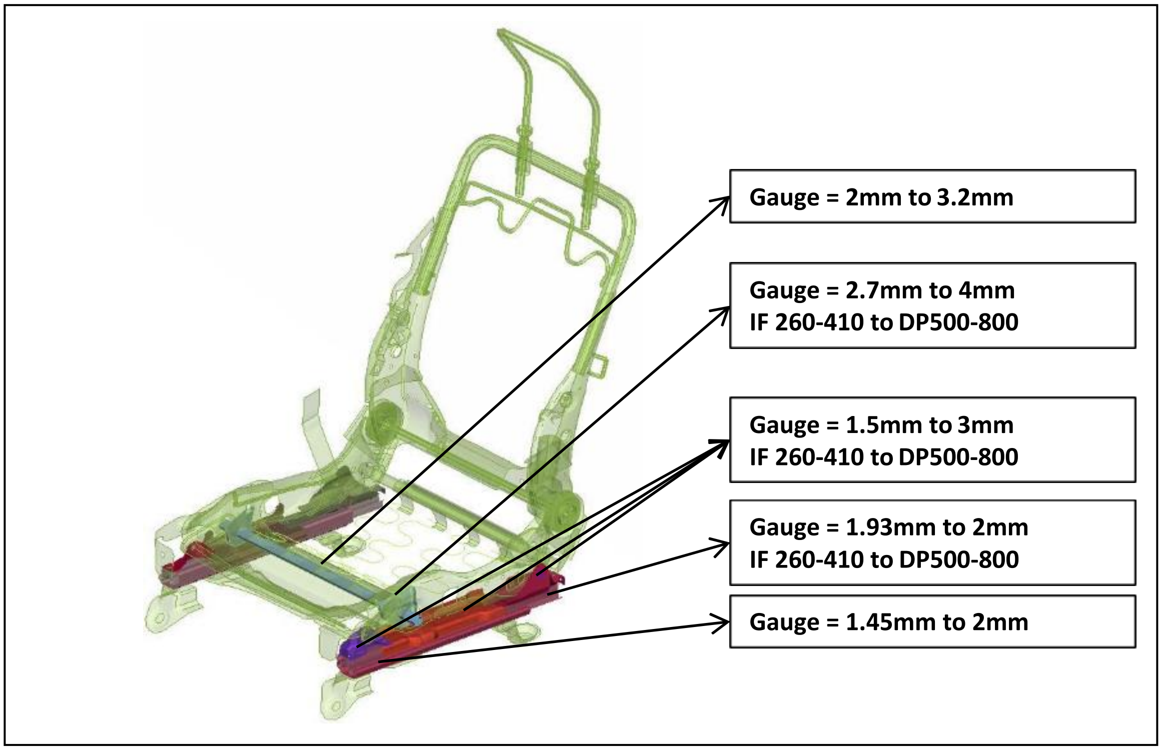

Figure 45: Seat Bottom Countermeasure (Manual and Power Seats)

It should be noted that, since the countermeasures were on the seat bottom frame parts, it is common for both manual and power seats. This means, the same changes of the parts on the manual seat were implemented on the respective parts of the power seat also.

7.2 Updated Manual Seat – FMVSS 301 Simulations With Rear Seat Passenger

The 2G optimized seat model was integrated in to the FMVSS301 FEA model and simulations was carried out. Seat back rotation of simulation was compared to the baseline and post-test seat back rotation curves as shown in Figure 46. Comparison of seat back kinematics and rear seat occupant characteristics between the countermeasures implemented seat model and baseline model is provided in Figures 47 – 49.

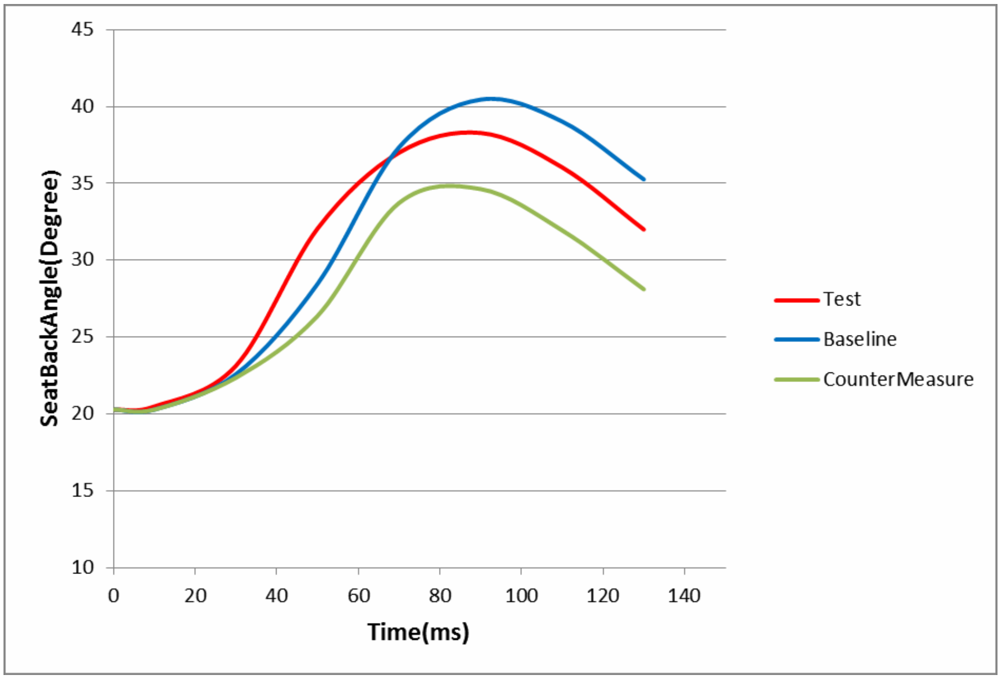

Figure 46: Seat Back Rotation Comparison (Manual Seat)

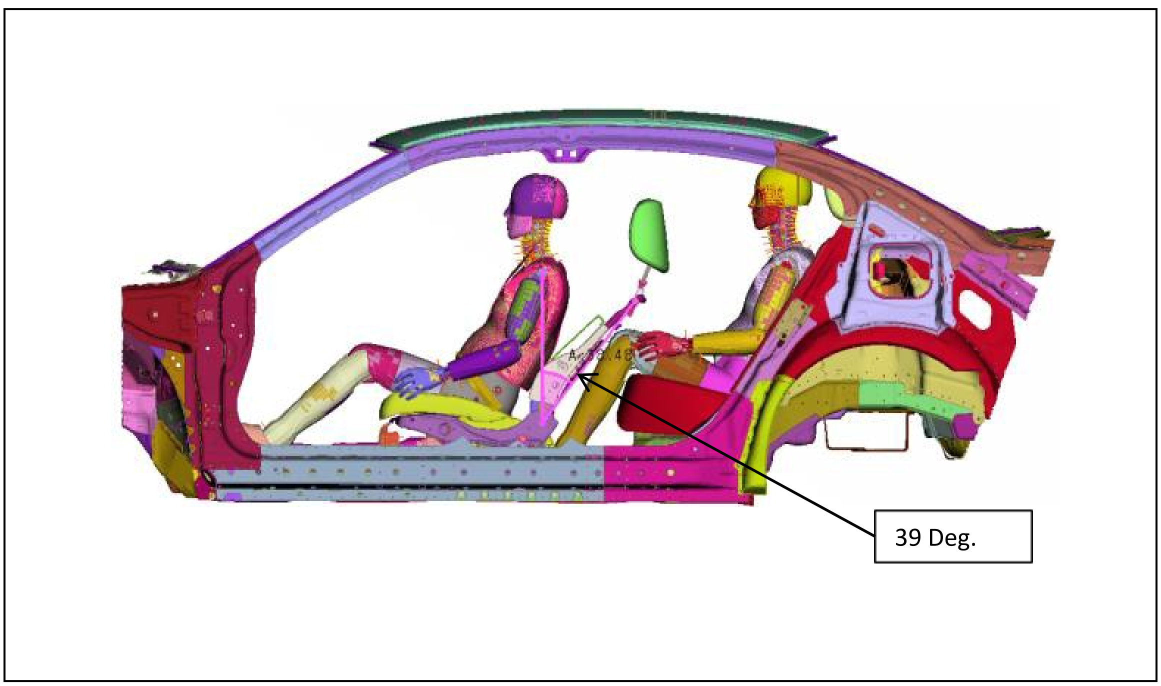

Figure 47: Seat Back Angle (Baseline – Manual Seat)

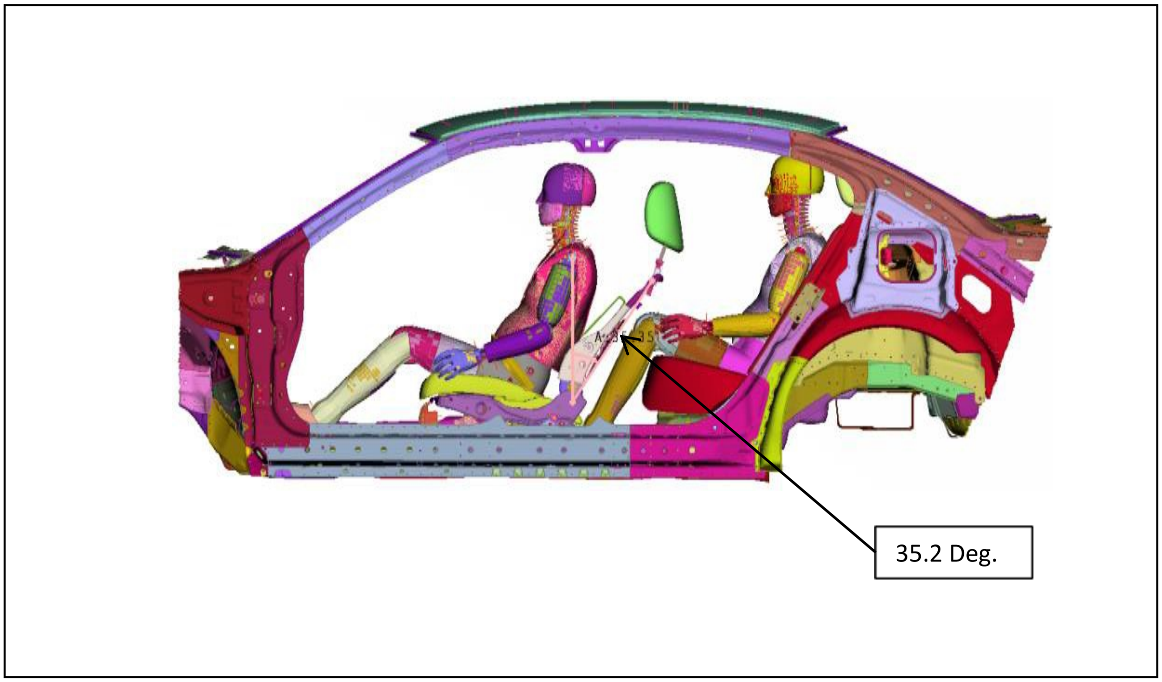

Figure 48: Seat Back Angle (Countermeasure – Manual Seat)

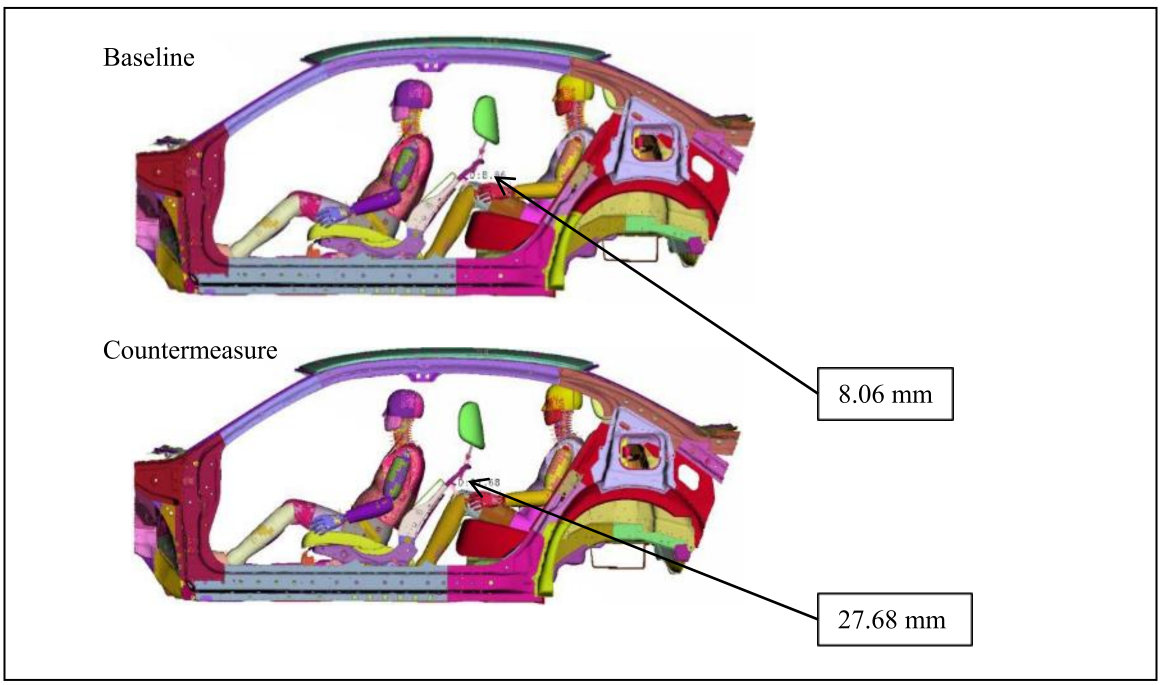

Figure 49: Seat Back to Knee Clearance (Baseline and Countermeasure – Manual Seat)

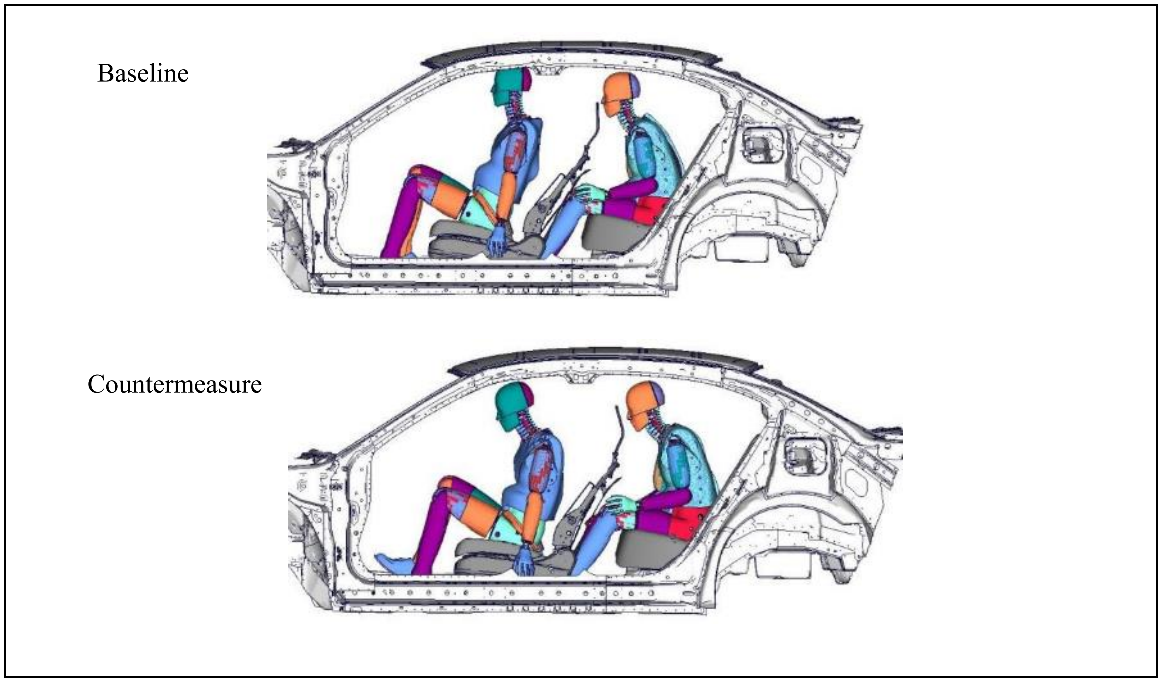

Figure 50: Head Rest Clearance (Baseline and Countermeasure – Manual Seat)

The knee impact force and HIC value of the rear seat occupant also reduced due to the effectiveness of the countermeasure. Figures 50 and 51 show the rear seat occupant knee force and head acceleration compared to the baseline model.

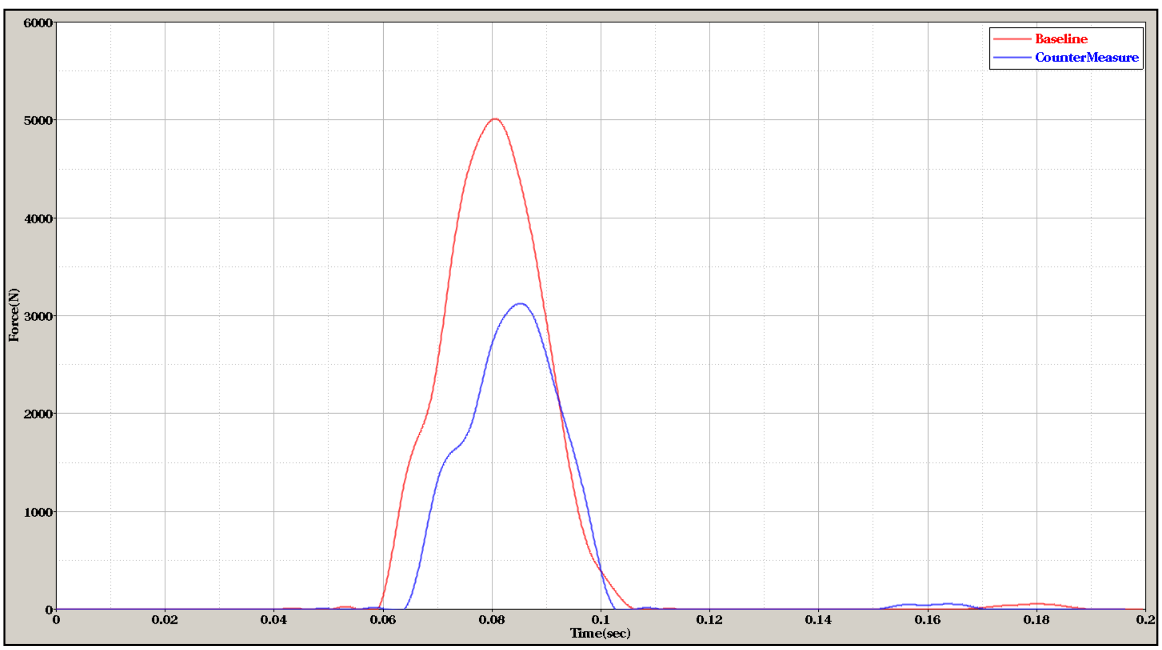

Figure 51: Knee Impact Force Baseline and Countermeasure (Manual Seat)

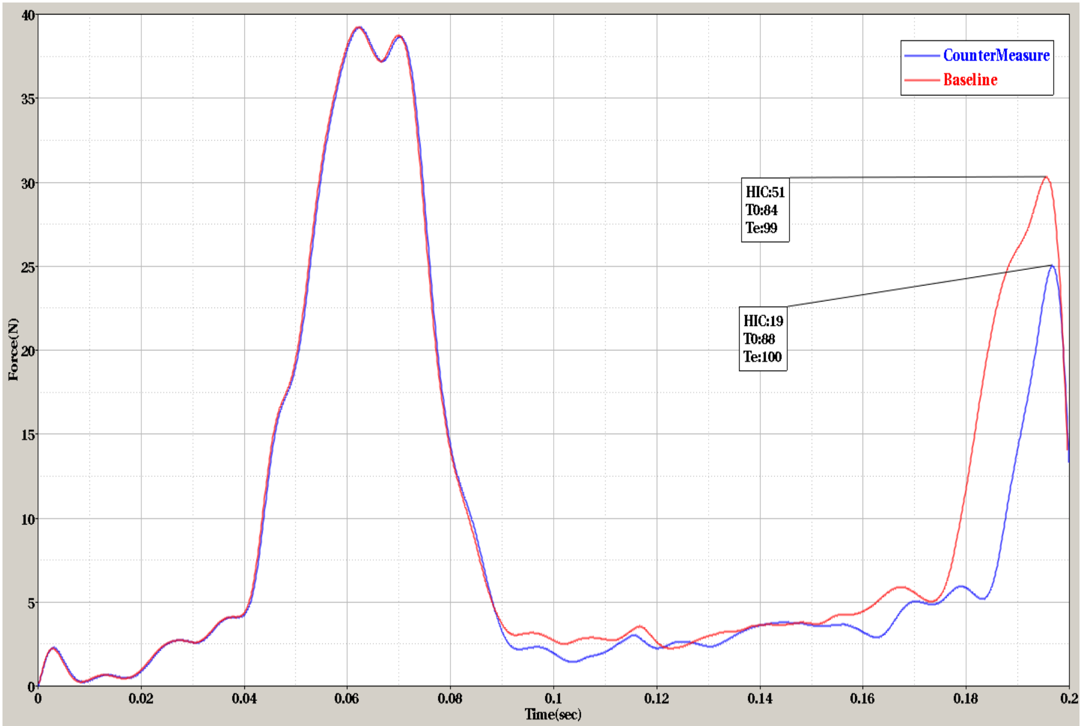

Figure 52: Head Acceleration Baseline and Countermeasure (Manual Seat)

Table 7 shows the countermeasure improvements to the target performance measures.

No.	Criteria	Target	Baseline	Countermeasure
1	Seat back angle	< 35 deg	39 deg	35.2 deg
2	Seat frame to knee clearance	> 10 mm	8.06 mm	27.68 mm
3	Femur force	< 1.5 kN	5 kN	3.1 kN

Table 7: Countermeasure Improvement Measures (Manual Seat)

7.3 Updated Power Seat – FMVSS 301 Simulations With Rear Seat Passenger

Using the similar countermeasures of the manual seat, the power seat bottom members were updated without affecting the seat mechanism. Seat back rotation from simulation was compared to the baseline, and post-test seat back rotation curves as shown in Figure 53. Comparison of seat back kinematics and rear seat occupant characteristics between the countermeasures implemented seat model and baseline model is provided in Figures 54 to 56.

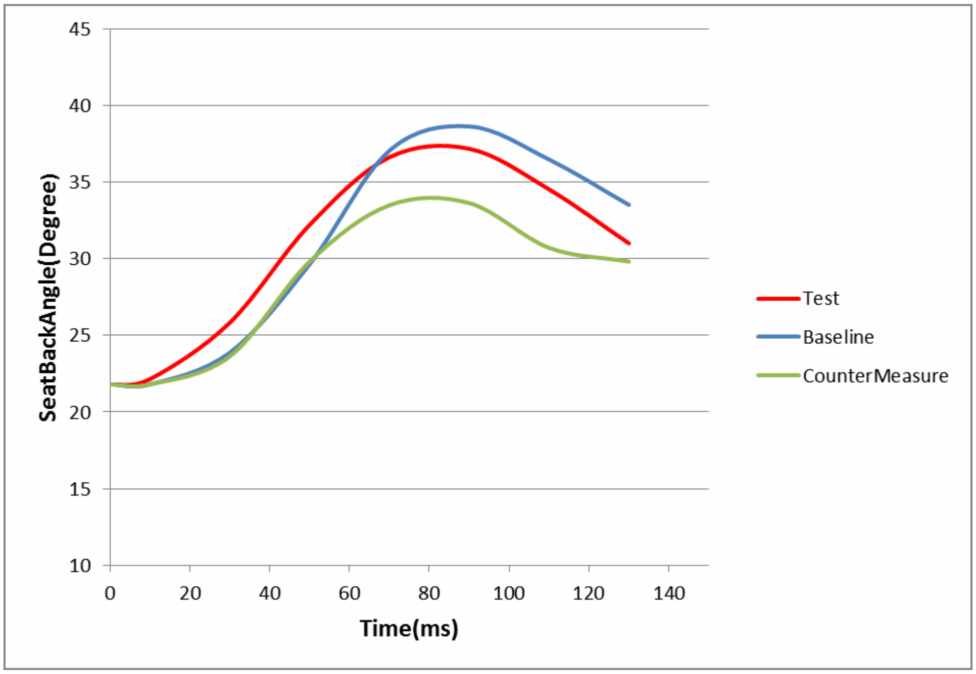

Figure 53: Seat Back Rotation Comparison (Power Seat)

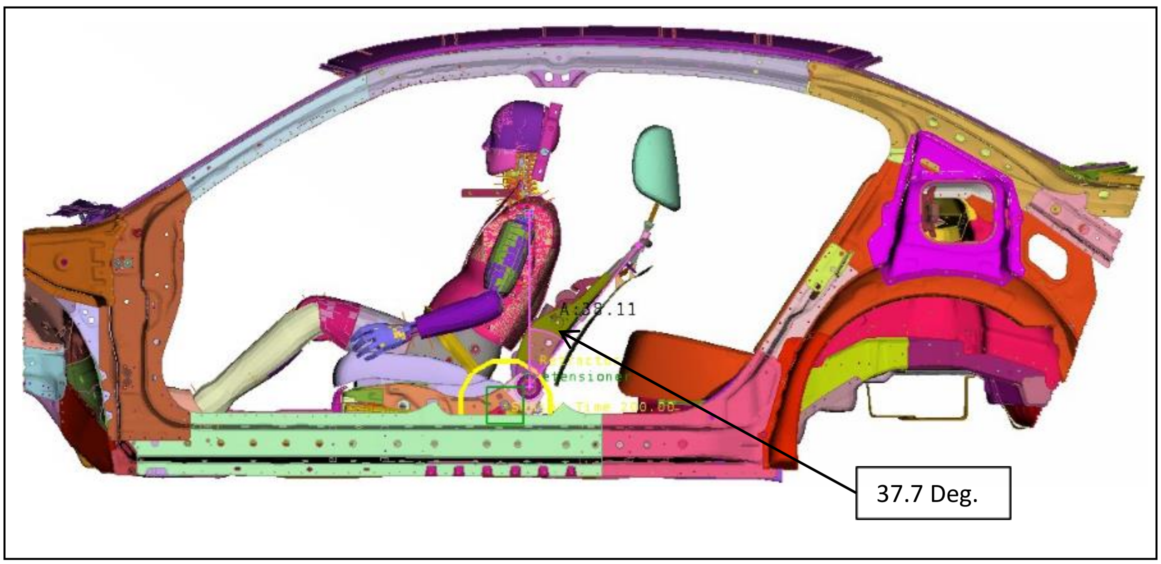

Figure 54: Seat Back Angle (Baseline – Power Seat)

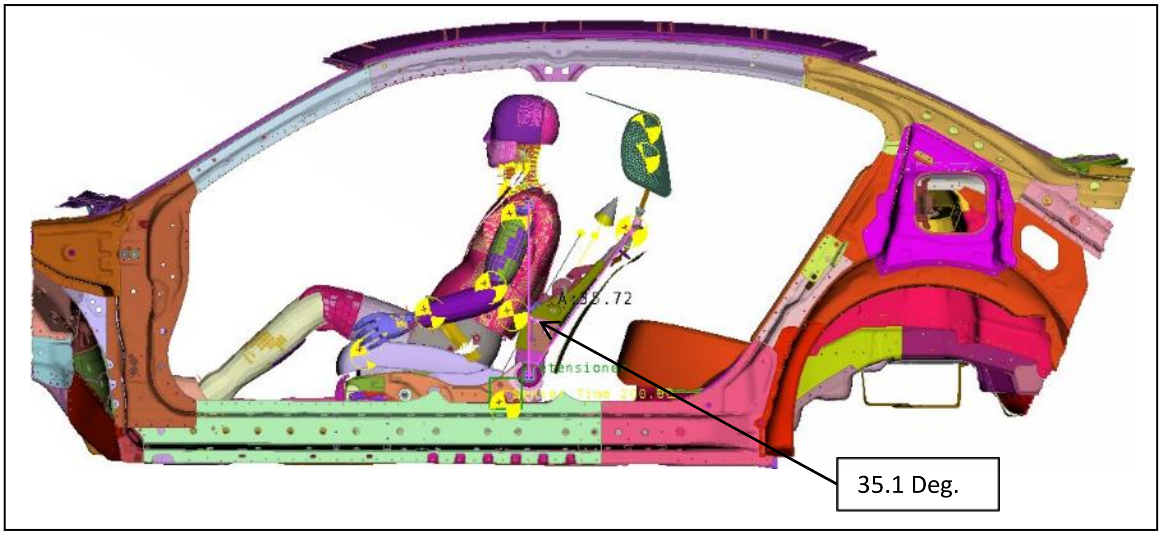

Figure 55: Seat Back Angle (Countermeasure – Power Seat)

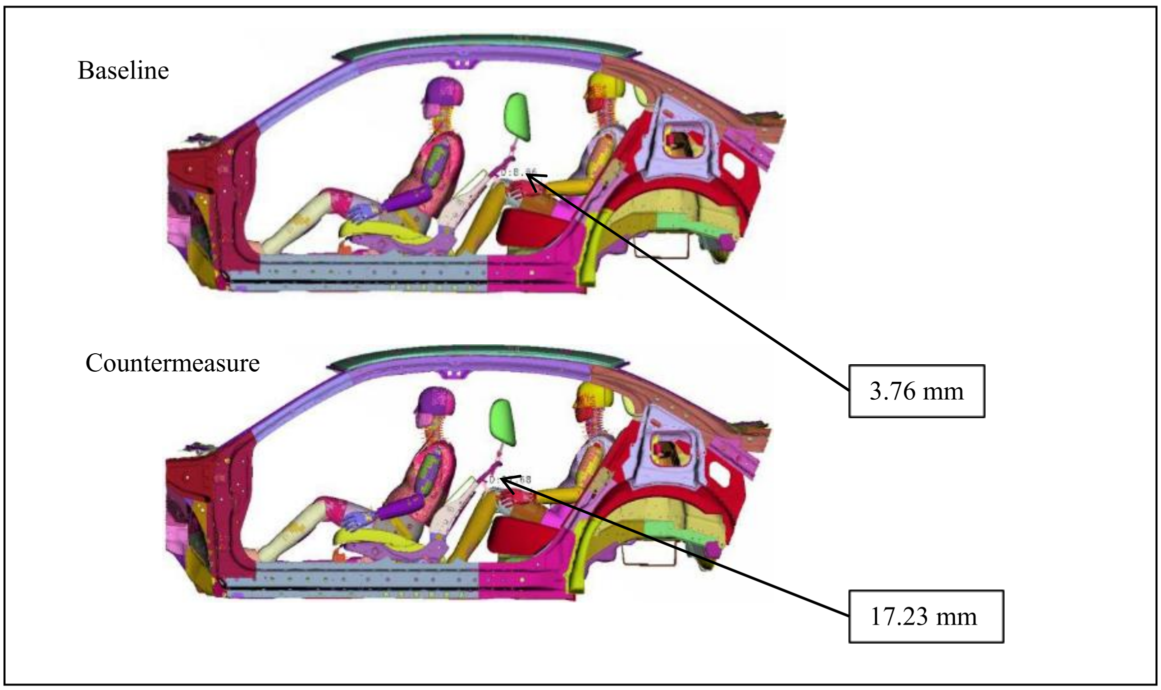

Figure 56: Seat Back to Knee Clearance (Baseline and Countermeasure – Power Seat)

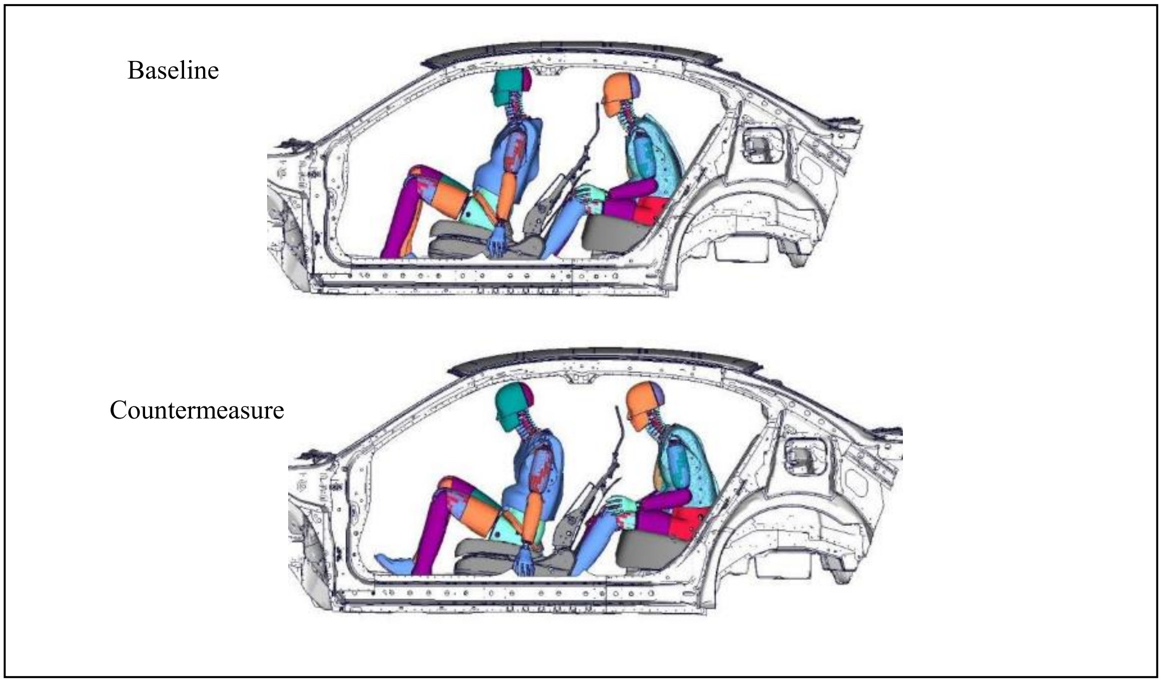

Figure 57: Head Rest Clearance (Baseline and Countermeasure – Power Seat)

The knee impact force and HIC value of the rear seat occupant also reduced due to the effectiveness of the countermeasure. Figures 57 and 58 show the rear seat occupant knee force and head acceleration compared to the baseline model.

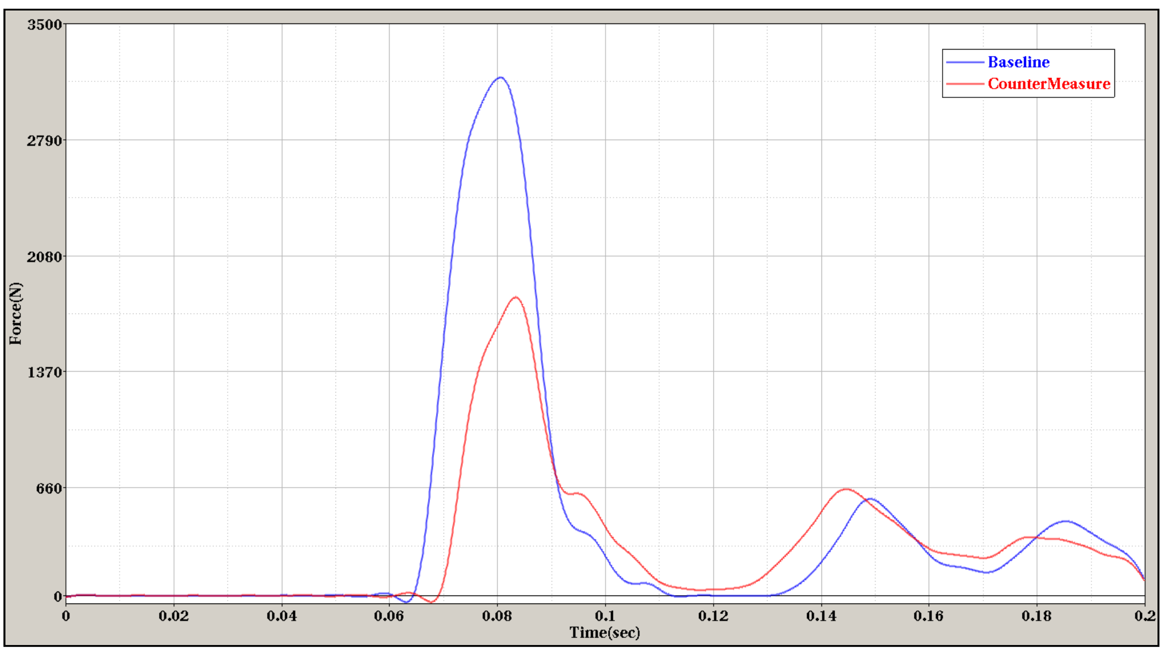

Figure 58: Knee Impact Force Baseline and Countermeasure (Power Seat)

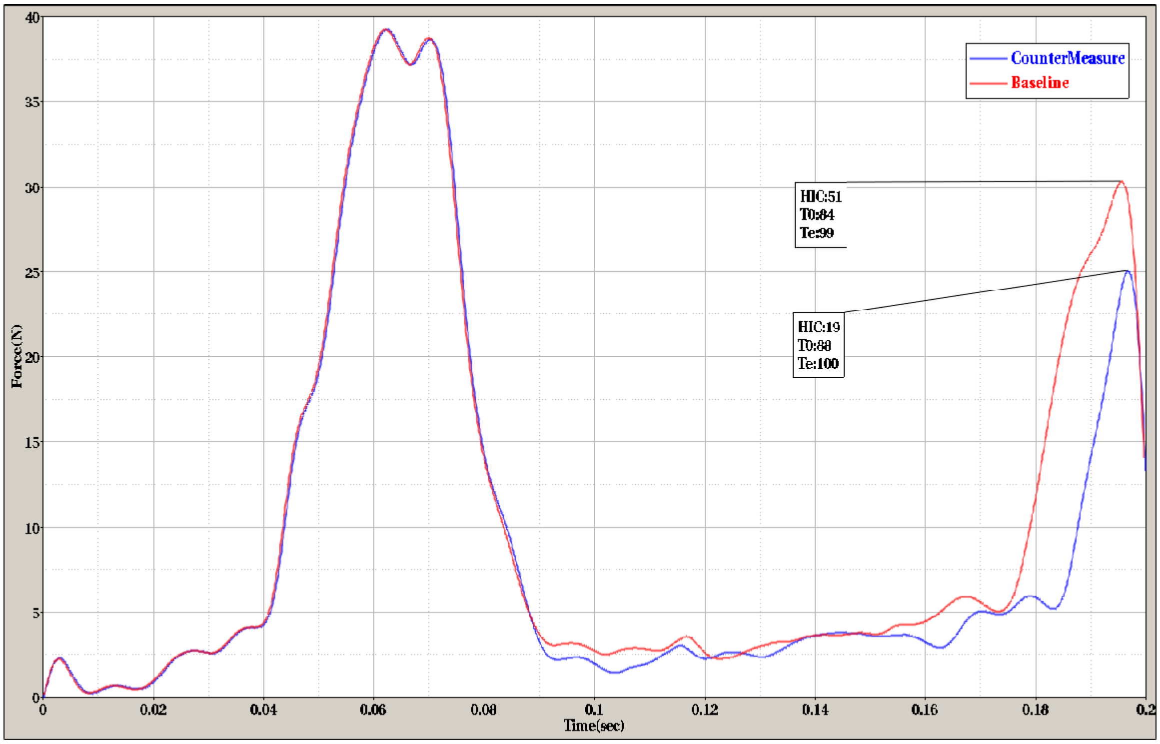

Figure 59: Head Acceleration Baseline and Countermeasure (Power Seat)

Table 8 shows the countermeasure improvements to the target performance measures.

No.	Criteria	Target	Baseline	Countermeasure
1	Seat back angle	< 35 deg	38 deg	35 deg
2	Seat frame to knee clearance	> 10 mm	3.76 mm	17.23 mm
3	Femur force	< 1.5 kN	3.5 kN	1kN

Table 8: Countermeasure Improvement Measures (Power Seat)

7.4 Countermeasure Validation for Low-Speed Rear Impact

Once the seat models were updated to achieve the target requirements of reduced dynamic motions of the seat back, it was intended to verify the countermeasures would not affect the regulatory requirements such as low-speed rear impact cases. For this purpose existing IIHS vehicle seat head restraint dynamic test results of Honda Accord MY2013 were compared. The test vehicle was a Honda Accord MY2013 had manual seats. Therefore, FEA model for the IIHS vehicle seat head restraint dynamic test setup was developed by using the manual seat FEA model. A baseline model was developed to validate the FEA model was comparable to the test results. The baseline model setup for IIHS vehicle seat head restraint dynamic test for manual seat is shown in Figure 60.

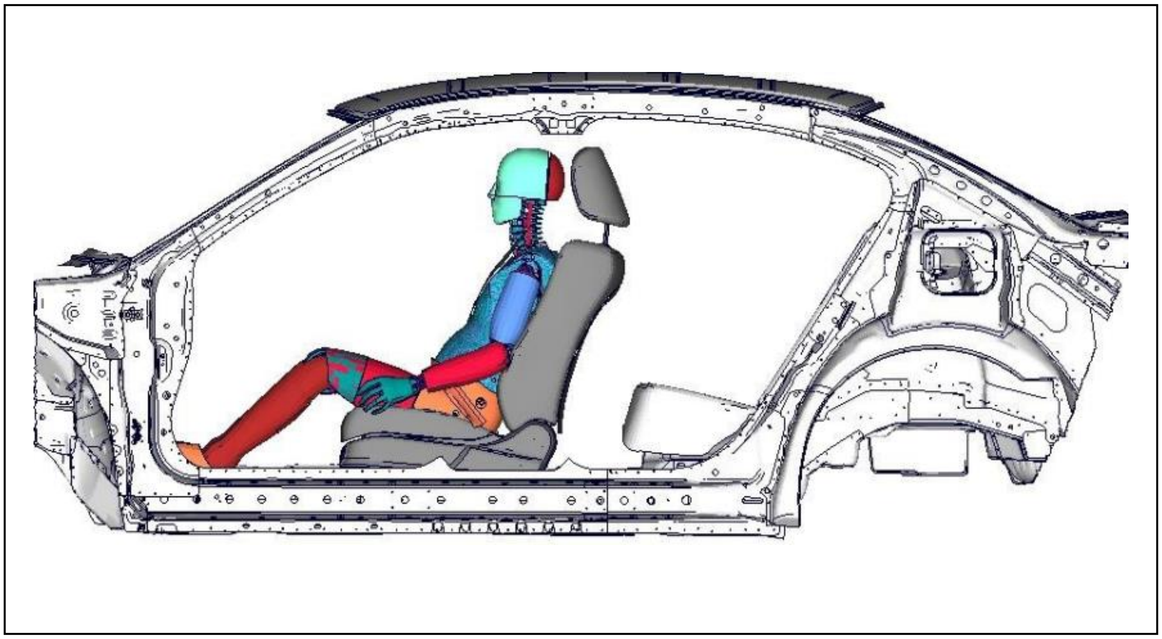

Figure 60: IIHS Vehicle Seat Head Restraint Test – Baseline (Manual Seat)

The FEA simulation of baseline model was carried out for 200 milliseconds duration by using LS-DYNA. The baseline model results were compared to the test results to verify the baseline model was in good correlation. FEA simulation results of the baseline model and the comparison to the test results is provided in Figure 61.

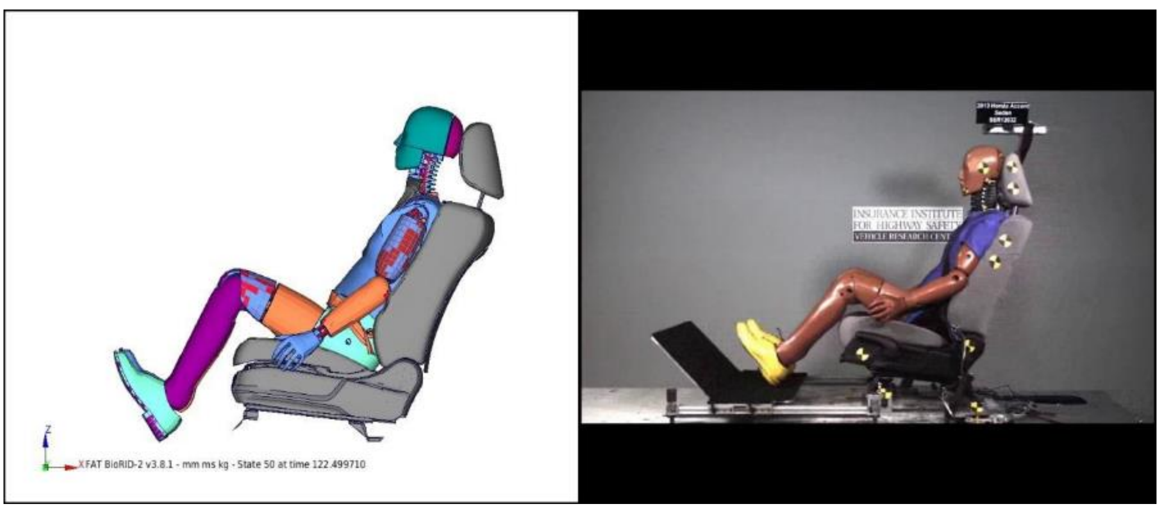

Figure 61: IIHS Vehicle Seat Head Restraint Test – Baseline Versus Test (Manual Seat)

The neck injury criteria for baseline and test were also compared as shown in the IIHS neck injury rating graph Figure 62.

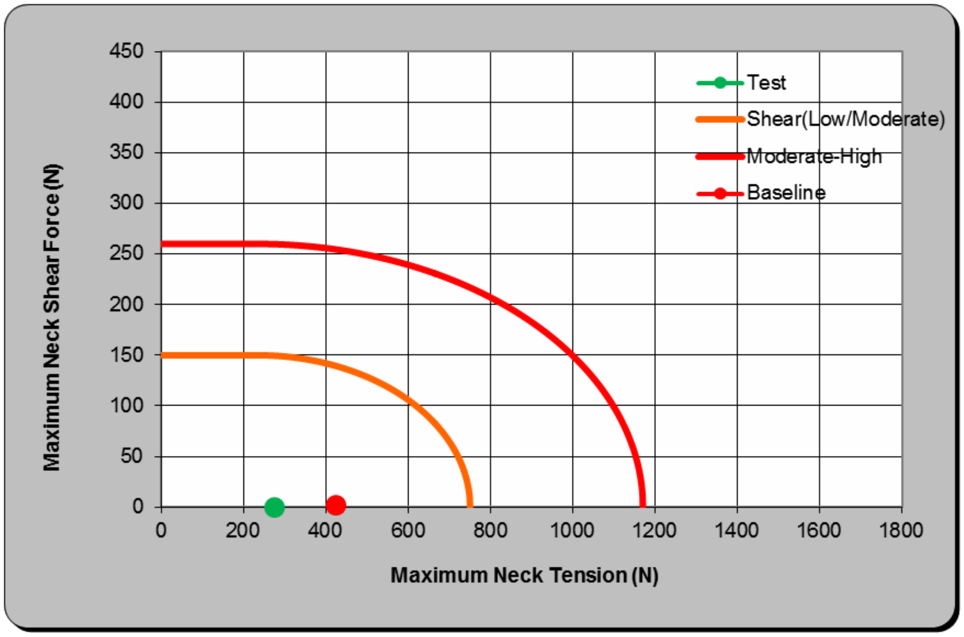

Figure 62: IIHS Vehicle Seat Head Restraint Test – Neck Injury Rating, Baseline Versus Test

From the above results comparison, it can be seen that both test and baseline FEA model ratings are within the "Good" corridor of IIHS rating chart. Therefore, the FEA model is deemed reasonable to use for countermeasure verification. The scope of the project included the power seat, so another baseline model for IIHS vehicle seat head restraint dynamic test also was developed by replacing the manual seat by the power seat. The FEA model setup for baseline IIHS load case with power seat is shown in Figure 63.

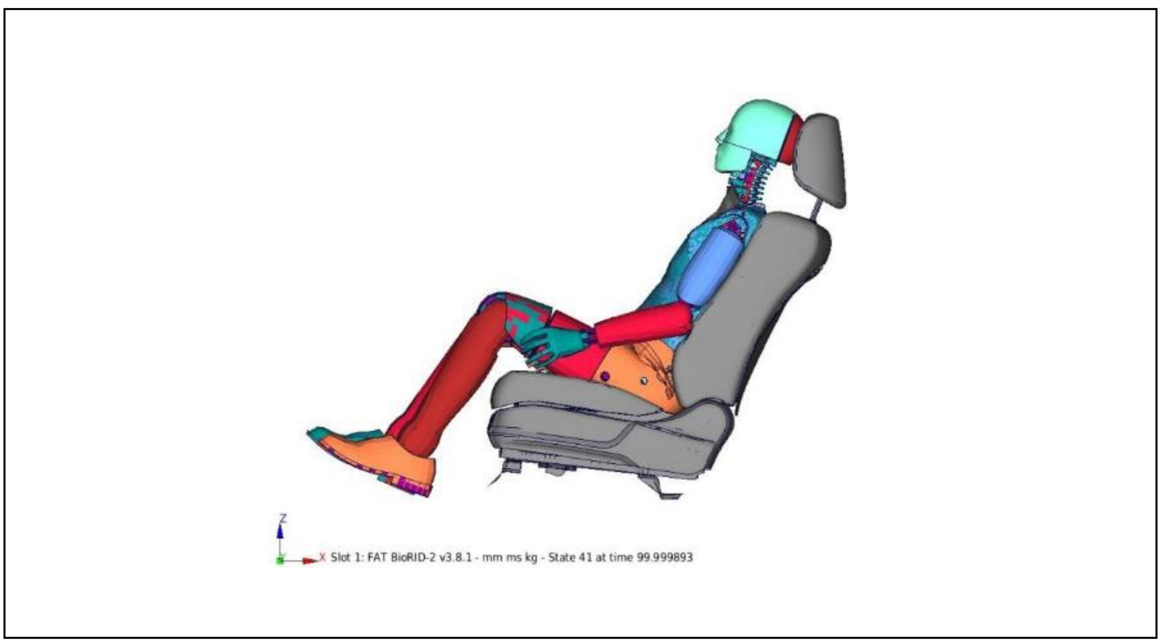

Figure 63: IIHS Vehicle Seat Head Restraint Test – Baseline (Power Seat)

Similarly, FEA simulation of baseline model for power seat was carried out for 200 milliseconds duration using LS-DYNA. The neck injury criteria for the power seat baseline are shown in the IIHS neck injury rating graph Figure 64. The rating was recorded above the Moderate-Higher corridor. It should be noted that, there was no test result available for power seat case. Correlating the FEA model to a better rating of within the Moderate-High corridor is out of the scope, the FEA model was intended for comparison purpose only for validating the countermeasures.

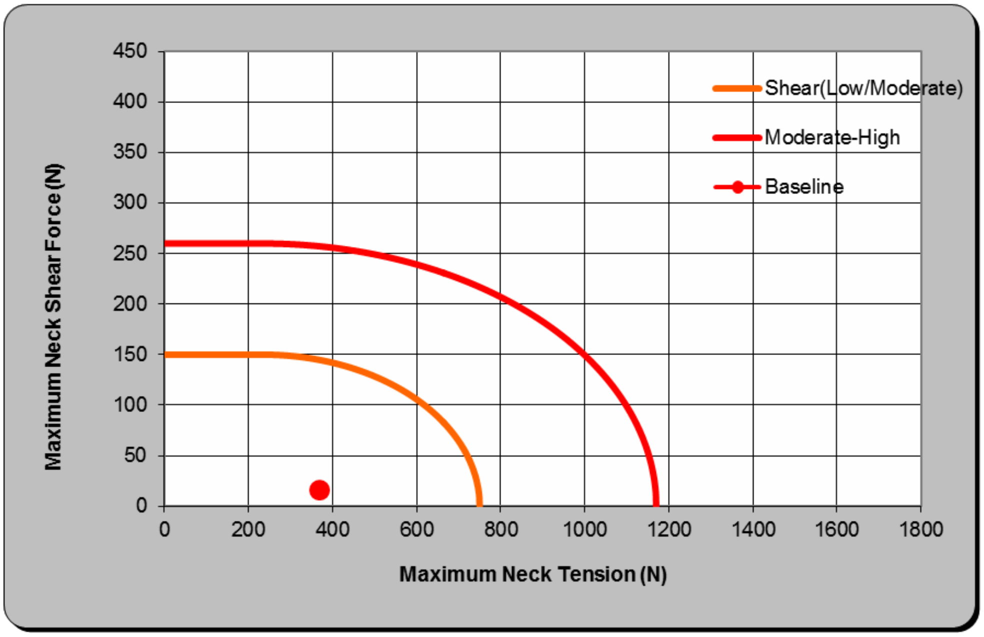

Figure 64: IIHS Vehicle Seat Head Restraint Test – Neck Injury Rating, Baseline (Power Seat)

These two baseline models and results were used for validating the countermeasures using the countermeasure seats respectively. The baseline seat FE modules in the IIHS test baseline models were replaced with corresponding countermeasure seat FE modules. The test conditions and load case setup were maintained as same as the IIHS test baseline models. Once the simulations of the countermeasure models were run, the results were compared to the baseline results, which is the neck injury rating chart. The neck injury rating chart for the countermeasure seats are shown in Figures 64 and 65.

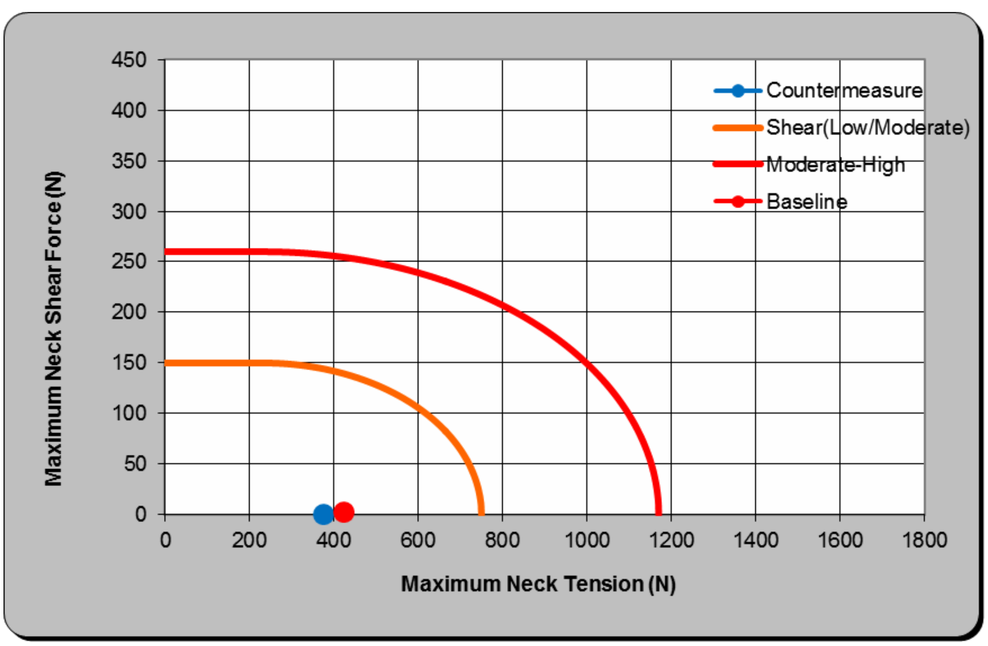

Figure 65: IIHS Neck Injury Rating Chart – Countermeasure Versus Baseline (Manual Seat)

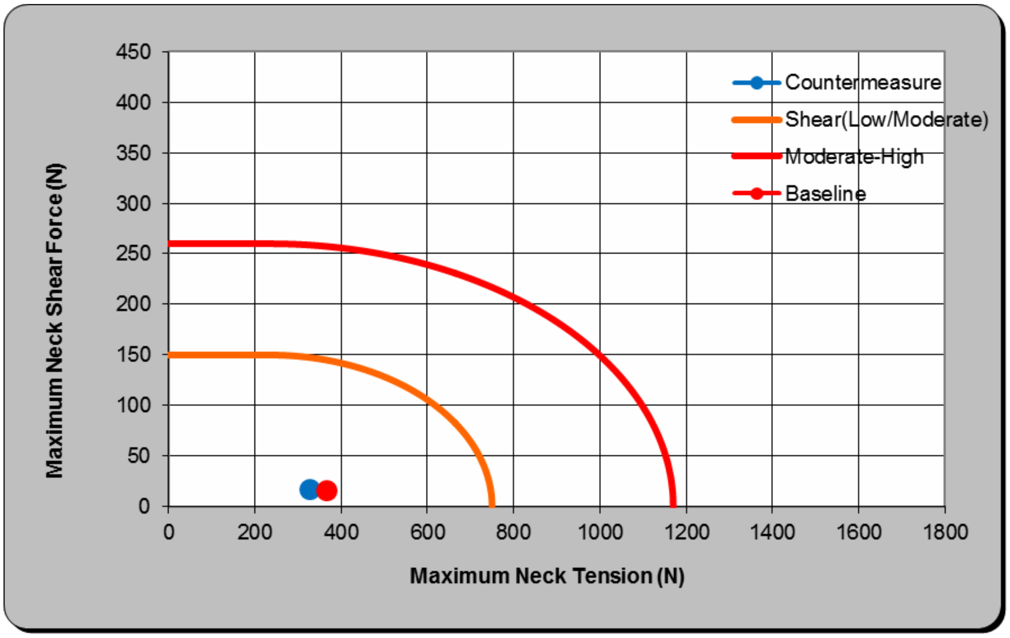

Figure 66: IIHS Neck Injury Rating Chart – Countermeasure Versus Baseline (Power Seat)

Thus, it is noted that, from the above investigation using IIHS vehicle seat head restraint test in low-speed rear impact scenario, the countermeasures on the front seats did not affect the IIHS rating with much deviation from baseline or test. Therefore, the proposed countermeasures of the front seats to reduce the dynamic seat back rotation should be acceptable in both high-speed and low-speed rear crash events.

7.5 Cost Estimation

The seat back strength investigation of this project also studied the cost impact of going from baseline seat to improved seat to reduce the dynamic seat back rotation. The proposed countermeasures are within the gauge and grade changes, with no design changes of the part. The countermeasure ideas discussed in this study provides directional inputs about seat strength improvements to be able to protect the rear seat occupant by reducing the injury levels. When it is necessary to implement the countermeasures by the seat manufacturers, the cost impact of the changes also needs to be considered in the product development. EDAG performed the cost estimate for the baseline and countermeasure seats using standard MIT cost model process sheets. Cost difference was estimated for the countermeasure parts obtained from 2G optimization (seat bottom frame and mechanism components). The cost estimation was performed for manual seat and power seat separately due to a small difference found in one of the countermeasure parts geometry of the power seat.

7.5.1 Cost Estimate – Manual Seat

The weight of the baseline manual seat was calculated from baseline FEA seat model as 18.81 kg and the weight of the countermeasure seat was calculated from countermeasure FEA seat model as 20.94 kg. The cost estimation was performed only for the parts changed by the countermeasure with the manufacturing and assembling processes are assumed to be remaining same as existing seat. The parts affected weighed originally 3.87 kg and the countermeasure added 2.13 kg due to gauge and grade changes. The countermeasure parts weighed 6 kg. Using standard material price and grade premium for the upgraded materials and using EDAG cost model worksheet, the baseline parts cost was estimated to be $2.24 and the countermeasure parts cost was found to be $4.17, and the delta cost was estimated as $1.94 for the manual seat.

The seat countermeasures, weight and cost differences due to the countermeasure are shown in Figure 67 for the manual seat.

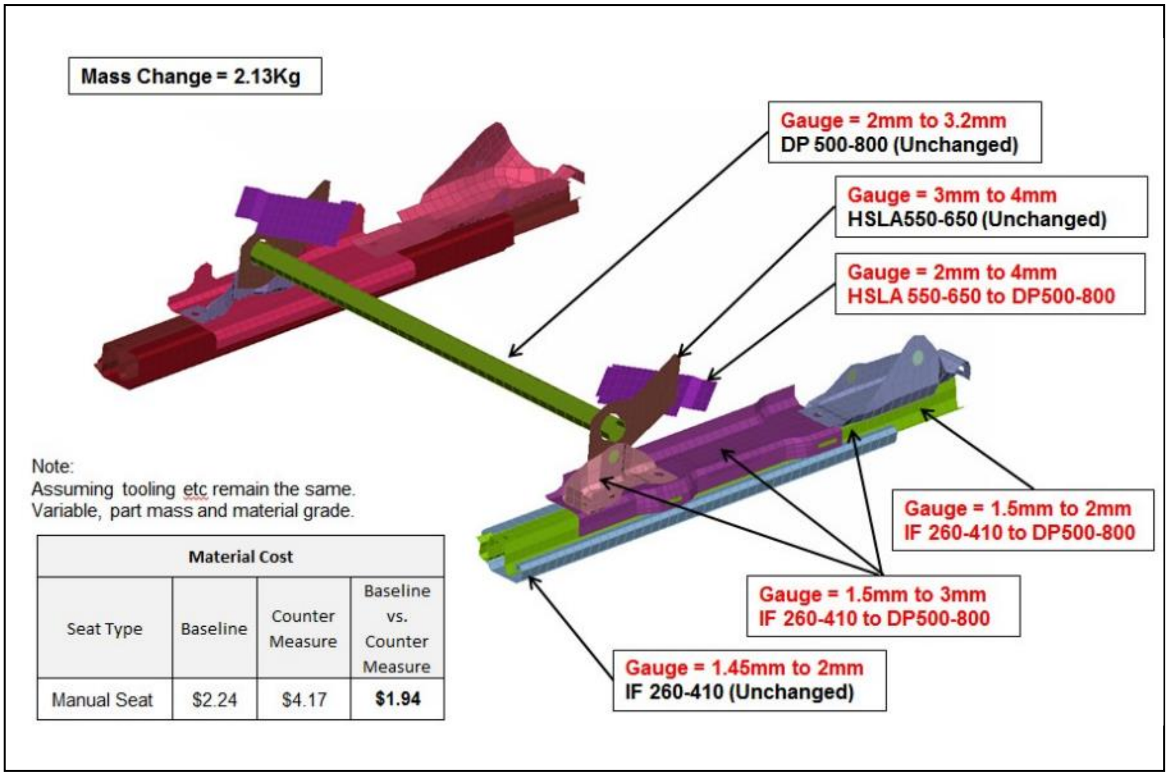

Seat Type	Baseline	Counter Measure	Baseline vs. Counter Measure
Manual Seat	$2.24	$4.17	**$1.94**

Figure 67: Countermeasure Parts and Cost Estimate (Manual Seat)

7.5.2 Cost Estimate – Power Seat

Similarly, the weight of the baseline power seat was calculated from baseline FEA seat model as 23.41 kg and the weight of the countermeasure seat was calculated from countermeasure FEA seat model as 25.10 kg. The cost estimation was performed only for the parts changed by the countermeasure with the manufacturing and assembling processes are assumed to be remaining same as existing seat. The parts affected weighed originally 3.87 kg and the countermeasure added 1.69 kg due to gauge and grade changes. The countermeasure parts weighed 6 kg. Using standard material price and grade premium for the upgraded materials and using EDAG cost model worksheet, the baseline parts cost was estimated to be $9.69 and the countermeasure parts cost was found to be $14.01, and the delta cost was estimated as $4.62 for the power seat.

The seat countermeasures, weight, and cost differences due to the countermeasure are shown in Figure 68 for the power seat.

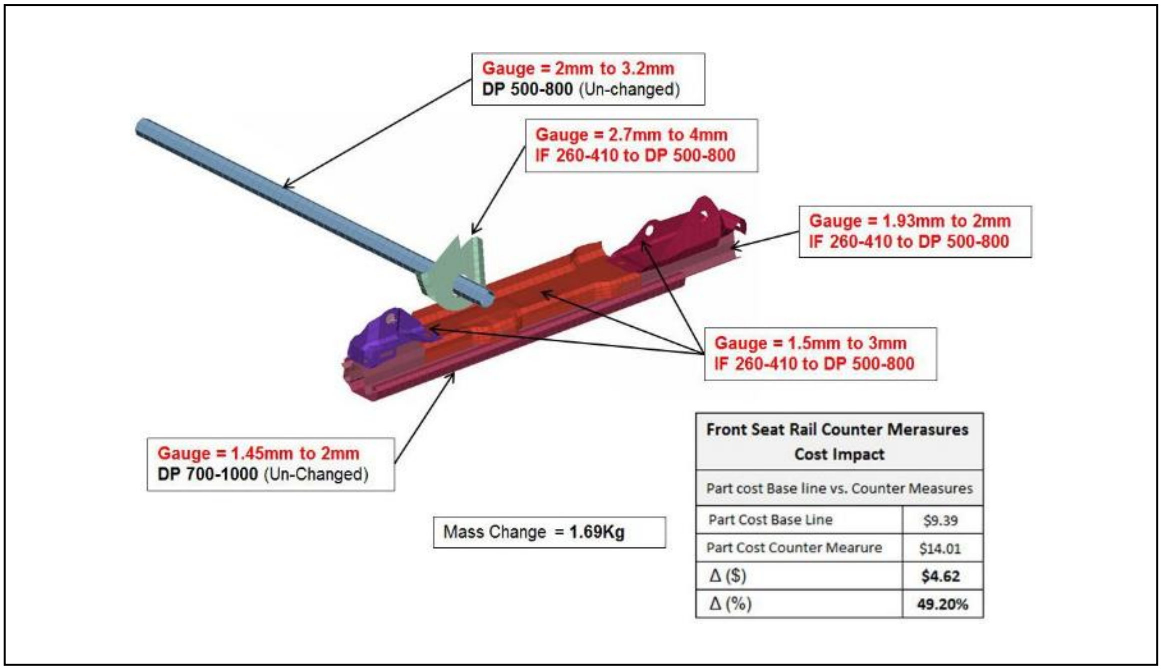

Figure 68: Countermeasure Parts and Cost Estimate (Power Seat)

An overview of the cost impact for the countermeasures is shown in Table 9.

No.	Description	Manual Seat	Power Seat
1	Baseline seat weight (kg)	18.81	23.41
2	Countermeasure seat weight (kg)	20.94	25.10
3	Baseline weight of parts affected (kg)	3.87	4.13
4	Countermeasure weight of parts affected (kg)	6.00	5.82
5	**Δ weight (kg) / seat**	**2.13**	**1.69**
6	Baseline cost of parts affected	$2.24	$ 9.39
7	Countermeasure cost of parts affected	$4.17	$ 14.01
8	**Δ cost / seat**	**$1.94**	**$ 4.62**
9	Cost / kg increase	$0.91	$ 2.73

Table 9: Cost Impact of Countermeasure Seats

8 Conclusion and Recommendations

The primary objective of the project to identify the required seat tests and validate the front seat back strength was met. One quasi-static seat back pull test based on FMVSS 207 with extended loading until seat collapse was proposed. And, the other test to include the high-speed rear impact scenario was also proposed. The seat back strength improvement investigation and study for the front seat driver seat was carried out by using CAE techniques in a systematic approach. Starting with identifying the front seats of a good performing vehicle, the study was conducted by following the steps listed below.

1. Identified a vehicle that is currently in the market
2. Procured the necessary front seats (manual seat and power seat)
3. Developed the FEA model of the seats
4. Conducted quasi-static seat pull test and validated the FEA seat models by comparing the FEA simulations and tests
5. Integrated the FEA seat models into the full vehicle FEA model

6. Developed FMVSS 301 high-speed rear impact FEA model by including Bio-RID II dummy model on the front seat.
7. Conducted FMVSS 301 high-speed rear impact Sled test using Bio-RID II dummy and validate the FEA models.
8. Developed FMVSS 301 high-speed rear impact FEA model by including front and rear seat occupant models
9. Investigated the dynamic seat back motion of the front seat against the rear seat occupant.
10. Having found significant injuries on the rear seat occupant, seat back strength was improved by necessary countermeasures on the seat bottom frame parts to reduce the injury level.
11. Verified the improved seats did not affect the low-speed rear impact performance using IIHS vehicle head restraint dynamic test simulations.
12. Estimated the cost impact of seat modifications.

Summary of the study and recommended actions are provided in the following sections.

8.1 Summary of Project Results

In this project Honda Accord MY2014 was chosen for CAE based study. The reason being for this selection, EDAG had developed fully functional and validated FEA model of Honda Accord MY2014 for the previous projects. The FEA model could be used without a need for developing full vehicle model. The front seats of Honda Accord MY2014, readily available in the market were procured for the purpose of developing much more detailed seat models. Both manually operated and power operated front seats were purchased. Upon review of the seats, it was found that there were significant geometry changes. So, the FEA seat model already available in the full vehicle model was updated to reflect the changes. The Manual seat and Power seat were modeled separately with necessary details including the recliner mechanism. Two physical tests, FMVSS207 based quasi static seat back strength test and dynamic rear impact test were identified for model validation and seat back improvement study purposes respectively. The FEA seat models were validated by correlating the quasi-static seat back pull strength simulations to the physical test. Third party testing organization MGA was sub-contracted to conduct the quasi- static seat back pull tests for both manual and power seats. The seat model simulations results in terms of seat back rotation kinematics, static deflection were correlated to an acceptable 78 percent conformation and the seat models were considered to be good FEA models.

As per the scope, it was needed to study the occupant interaction with seats in the rear impact scenarios. The seat back strength and dynamic motion of the front seat in terms of front and rear seat occupant injury during rear impact was preliminary measurements to investigate the need for seat back improvement. Therefore, two rear impact scenarios modeling of occupant simulation were considered in the study. First, the front seat occupant interaction on the driver seat in the rear impact event was critical to observe the dynamic motion of the seat back towards the rear seat. Second, the rear seat occupant injuries due to the interaction of the front seat back.

FEA models for these two scenarios were developed. In order to validate the modeling of the front seat occupant interaction on the driver seat, the high-speed rear impact sled test was conducted for manual and power sets. Generic vehicle pulse based on FMVSS301 high-speed rear impact pulse (20 G) was used for the sled speed. Bio-RID II 50th percentile male occupant dummy was calibrated and supplied by NHTSA. The results from the sled tests were used to compare the simulation results. Even though higher degree of correlation was not the scope of the project, good comparison was achieved and the occupant FEA models were considered good for the study. Two parts of the results, seat kinematics and occupant injuries were included for comparison. Seat back motion of manual and power seats with occupant dummies closely matched to that of the sled test respectively. The HIC values of occupant dummy of tests and simulations were compared to be less than 2 percent difference. The NIJ values were also comparable with a difference of 5 percent. Considering the objective of the project to determine the need for seat back strength improvement by reducing the dynamic motion of the seat back towards the rear set occupant, a directional outcome was intended rather than focusing on achieving higher degree of occupant model development. However, good correlated seat models were included in the study to reason the outcome to be valid.

The next part of the project involved the study of seat back strength requirement by including the rear seat occupant behind the driver seat. Both manual and power seats were studied separately by developing two separate rear impact occupant models. The occupant dummy chosen for the rear seat was the same Bio-RID II, 50th percentile male dummy in unbelted condition. The worst-case scenario of front seat, full down and full rear position was set up as initial condition. The rear impact pulse of 20 G was applied as the sled speed. The front seat kinematics, front seat occupant injury and rear seat occupant injury were observed from the simulations. It was clearly seen that the rear seat rotated about 40° and hit the rear seat occupant knee. The rear seat occupant head hit the front seat back at an acceleration of 30G and HIC value of 51. The knee impact force was observed to be 3.5 kN. The seat back rotation observed from this study was considered high potential to cause injuries to the rear seat occupants of all types such as children and adults. It was evident to reduce the seat back dynamic motion by improving the seat strength.

Countermeasure actions were undertaken by FEA simulation iterations to reduce the seat back movement by setting necessary performance targets for optimization in terms of seat back rotation and occupant characteristics such as HIC, NIJ, and knee force. Seat parts modifications were made based on gauge and grade (2G) optimization of the highly deformed/displaced parts of seat back and seat bottom. It was noted that, modification of the seat back parts or recliner mechanism showed no improvement. Most of the seat back dynamic rotation was caused by weakness of the seat bottom frame parts and seat mechanism. EDAG countermeasure actions took place on the seat bottom frame parts only and any modification of the seat mechanism was assumed to increase the cost to seat manufacturers. While performing the countermeasures, attention was paid not to add weight more than 10 percent and not to involve any expensive design change. Out of several countermeasures, gauge increase to 3.0 mm from 1.8 mm and grade change to high strength steel on the seat bottom frames yielded the performance meeting the targets. This added 1.69 kg per seat and $2.73 cost increase per kg weight increase.

In the final stage of project, it was necessary to make sure that the countermeasures did not increase the seat rigidity that will affect the low-speed rear impact regulatory requirements.

For this purpose, the modified seats performances were verified by FEA simulations of one IIHS low-speed rear impact case for vehicle head restraint dynamic test. Additionally, the results of the manual seat simulation were compared with the available test results from IIHS. Thus it was verified that the obtained countermeasures from this study did not affect any of the low-speed rear impact regulatory requirements.

8.2 Recommendations

It can be noted that the entire study was limited to one type of occupant that was 50th percentile male. Both front seat strength observation in rear impact scenario and front seat back rotation to rear seat occupant involved only Bio-RID II 50th percentile male dummy. The observation of front seat back dynamic rotation causing potential injuries to rear seat occupant and the implemented countermeasures are from the occupant injuries of 50th percentile male. However, the severity of the injury can vary depending on different occupant (children, adult, etc.) and different riding condition such as belted, unbelted, add-on restraint systems for babies and young children such as child seat etc.

From this investigation and CAE based studies discussed in this report, with the evidence of front seats under certain configuration (seat position) causing injuries to the rear seat occupant (unbelted 50th percentile male), it is duly recommended that seat back dynamic rotation should be reduced to less than 35°. Currently it is estimated that for FMVSS 301 without rear passenger the seat back rotation could reach up to 40° and cause head injuries and knee injuries to the 50th percentile male occupant. Apart from using 50th percentile male occupant in the rear seat, the directional outcome of this study, the seat back rotation range of 38.5° is useful to illustrate potentials of serious injuries to different occupant and different seating conditions. Figures 69 to 71 show different rear seat occupants with more than 38.5°. It should be noted that, a minimum seat back rotation (less than 38.5°) could cause injury to 95th percentile male occupant.

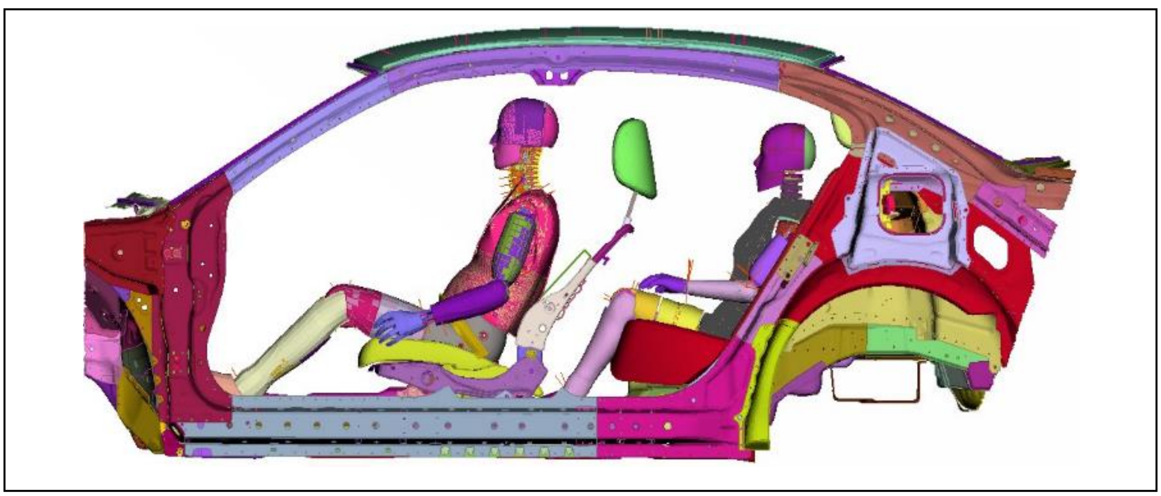

Figure 69: Illustration of Front Seat Interaction on 5th Percentile Rear Seat Occupant

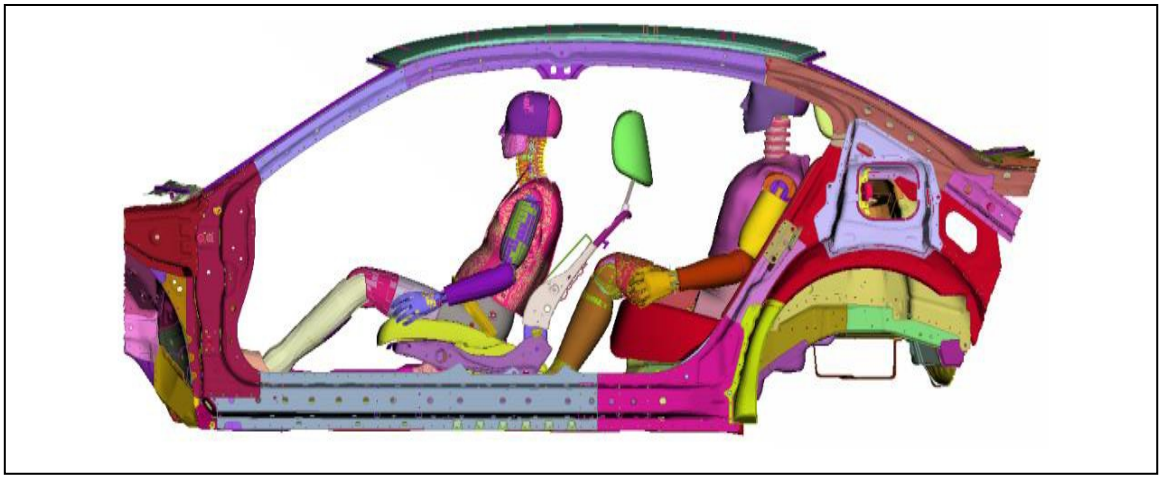

Figure 70: Illustration of Front Seat Interaction on 90th Percentile Rear Seat Occupant

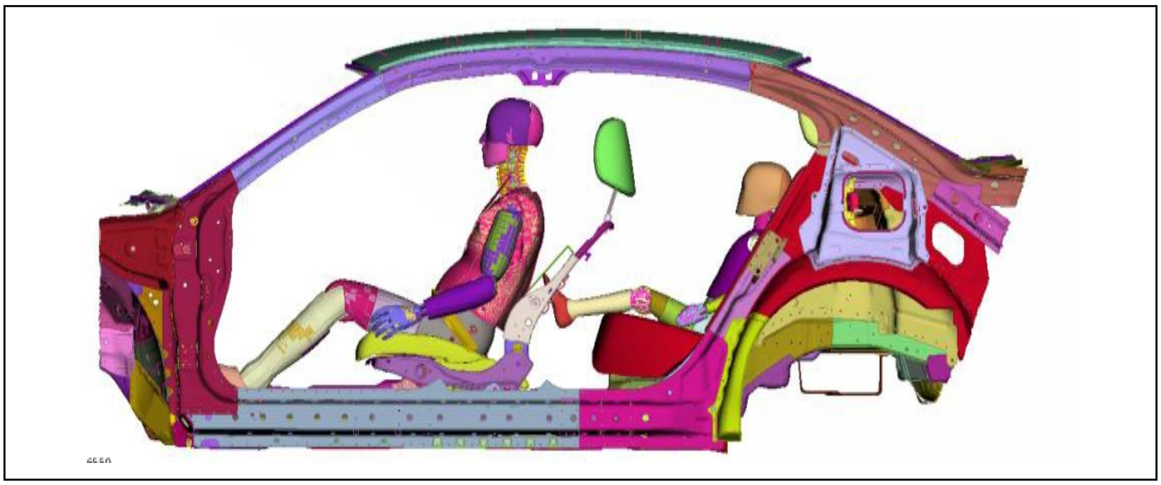

Figure 71: Illustration of Front Seat Interaction on Child Rear Seat Occupant

From the seat back dynamic rotation stand point, the countermeasures discussed here are for the Honda Accord MY2014 vehicle. The countermeasure on the seat back was not effective, but update of the parts on the seat bottom was effective. The advantage is observed, being only modifications on the seat bottom is that seat back kinematics and dynamic deformation characteristics in a high-speed frontal crash should be less affected. Further, the countermeasure requirements could vary for different vehicle and different seat structures. By observing the rear seat and occupant kinematics against the front seat back motions, the countermeasure actions can be studied for case by case for each rear seat occupant type. The future work can be extended to (1) verify the seat back characteristics in the high-speed frontal impact events, (2) optimize the countermeasures by including occupant types and extensive design changes of the seat back and head rest.

Appendix A. Seat Back Pull Test Report

mga research corporation

EDAG, INC.
2014 HONDA ACCORD 1ST ROW DRIVER SEATS REARWARD MOMENT TEST SERIES (PO #1160013891)

TEST REPORT

MGA REPORT NO.:	C17Q7-082.1
TEST(S) PERFORMED ON:	January 9, 2018
TEST REFERENCE NUMBER(S):	M18000-M18001
PROCEDURE NUMBER:	MGATP_207_UB Date of last revision: 7/14/2016
TEST LABORATORY:	MGA Research Corporation 446 Executive Drive Troy, Michigan 48083
SUBMITTED TO:	Velayudham Ganesan EDAG, Inc. 1875 Research Drive, Suite 200 Troy, MI 48083
REPORT DATE:	January 11, 2018
MGA PERSONNEL:	John Puckett Project Leader <u>Test Personnel:</u> Dirrell Echols Mark Pytell

* The results presented in this report relate only to the specified test items.
** This report shall not be reproduced except in full, without the written approval of the laboratory.

446 executive drive • troy, mi 48083
248 / 577-5001 • fax 248 / 577-5025
www.mgaresearch.com

ACCREDITED TESTING
CERT #0850-01

Test Specification

The provided sample was tested to the customer's requirements with similar loads stated in FMVSS 207 Rearward Moment (49 CFR 571.207 S4.2d, dated 10/1/2016).

Equipment

The following instrumentation was used to perform this test. All equipment and data has been calibrated by a source traceable to the National Institute of Standards and Technology (NIST). Calibration certificates can be furnished upon request.

Sensor ID Number	Data Type	Calibration Date	Calibration Due Date
M-Frame	DAS	9/27/2017	9/27/2018
237	Load Cell	10/16/2017	10/16/2018
A1600456A	Displacement	7/19/2017	7/19/2018
I2208857A	Displacement	7/19/2017	7/19/2018
TPM004-74	Tape Measure	7/17/2017	7/17/2018
MGA00730	Inclinometer	7/31/2017	7/31/2018
MI0094	Temp/Humidity Gauge	8/30/2017	8/30/2018

Procedure/Method

The fixturing of the sample consisted of attaching the sample to the fixture and then bolting the fixture to a T-slot plate. The H-point dimensions were provided by the customer. Linear transducers were placed at the LH and RH recliner. The load was applied at the uppermost member of the seatback at -9°. Representatives from EDAG were present to verify setup and witness the tests.

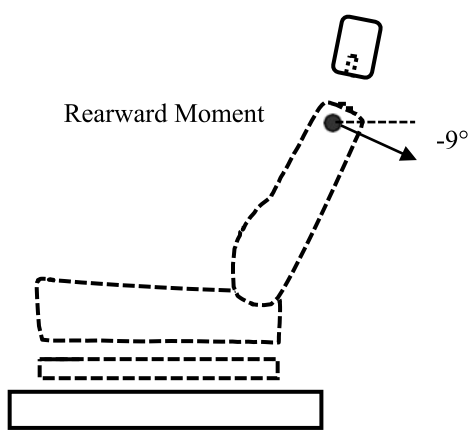

Figure 1 Schematic of Rearward Moment Test Setup
(Rigid Fixture)

Test Results

Photographs as well as all data processing and graphs can be found in Appendix B. All data is traceable to the National Institute of Standards and Technology (NIST).

Test No.	Sample Desc.	Max. Load (N)	Max. Moment (Nm)	Max. Cyl. Disp't. (mm)	Max. Angle (deg)		Post-Test Comments
					LH	RH	
M18000	1st Row 6 Way Manual Driver Seat	7,152	3,047	239.0	50.1	53.5	• Met the customer requirements. • The seatback collapsed/bent.
M18001	1st Row 8 Way Power Driver Seat	6,246	2,704	196.5	37.1	20.0	• Met the customer requirements. • The seatback collapsed/bent.

Additional test documentation can be found in the following appendices.

Appendix A
Customer Test Requests and Related Documents

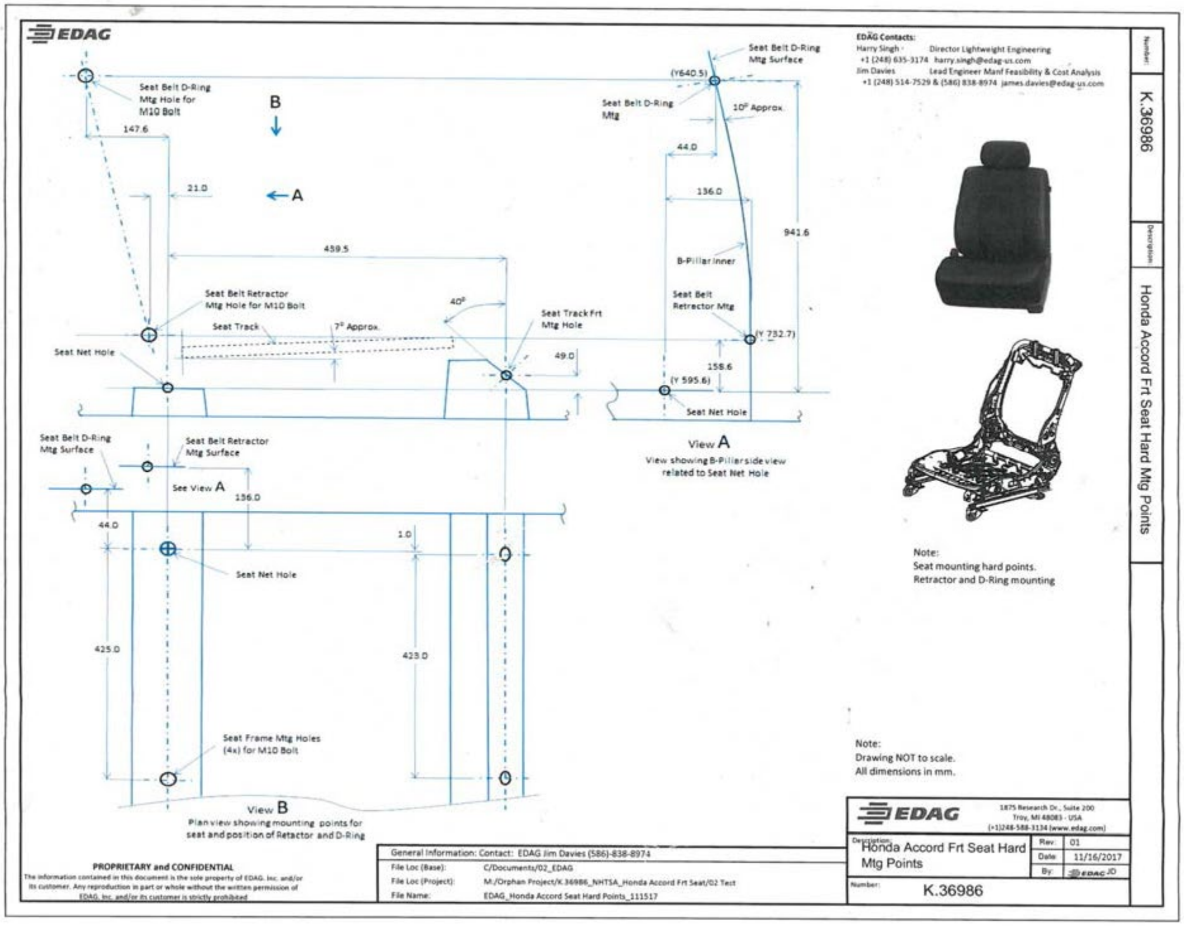

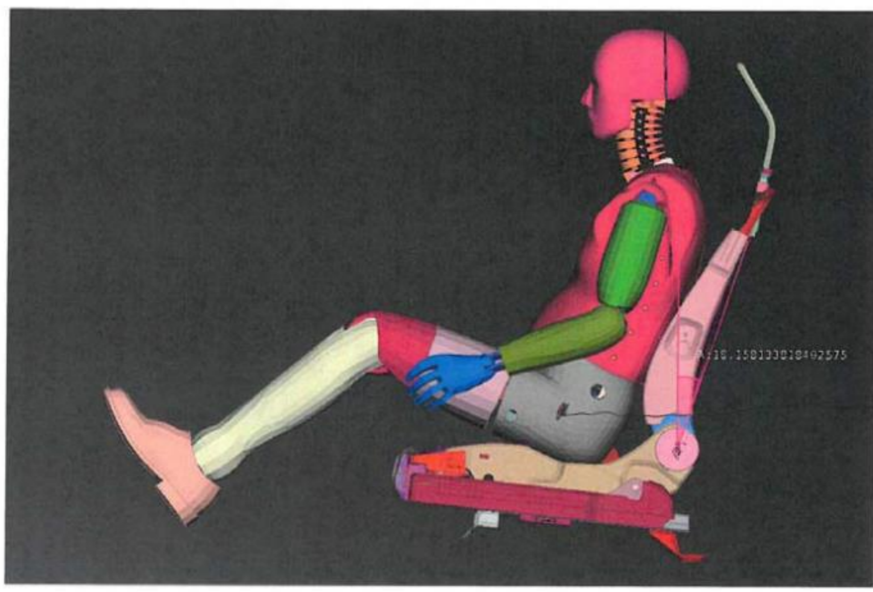

426

19124

Appendix B
Test Data and Photographs

Test M18000 Data

Seat Type: 1st Row 6 Way Manual Driver Seat	
Seat Function	**Test Position**
Track Position	Full Rearward
Vertical Position	Full Down
Seat Back Angle (Ref: See drawing)	18°
H-point (Ref: Rear lower cross tube)	159 mm Above
Moment Arm (Ref: H-Point)	426 mm Above
Load Angle	-9°
Temperature	72°F
Humidity	22%

Load Profile	
Time (second)	**Load (N)**
0	88
5	875
11	875
132	20,000

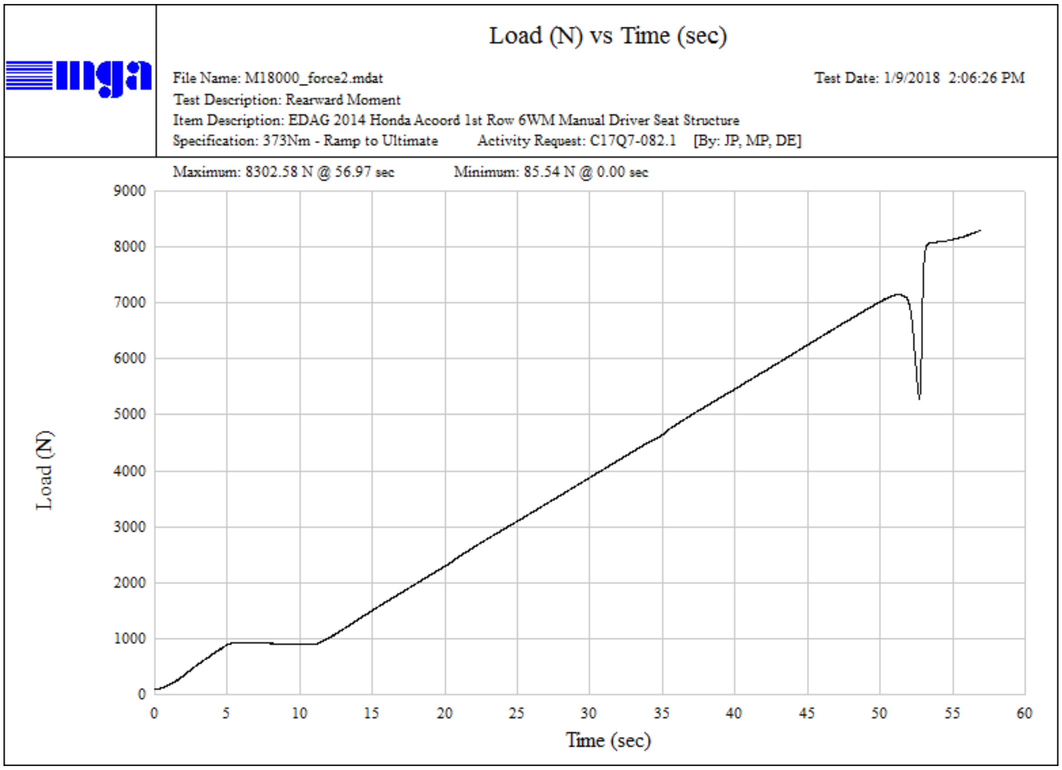
Load (N) vs Time (sec)
File Name: M18000_force2.mdat
Test Date: 1/9/2018 2:06:26 PM
Test Description: Rearward Moment
Item Description: EDAG 2014 Honda Accord 1st Row 6WM Manual Driver Seat Structure
Specification: 373Nm - Ramp to Ultimate
Activity Request: C17Q7-082.1 [By: JP, MP, DE]
Maximum: 8302.58 N @ 56.97 sec
Minimum: 85.54 N @ 0.00 sec
Load (N)
Time (sec)

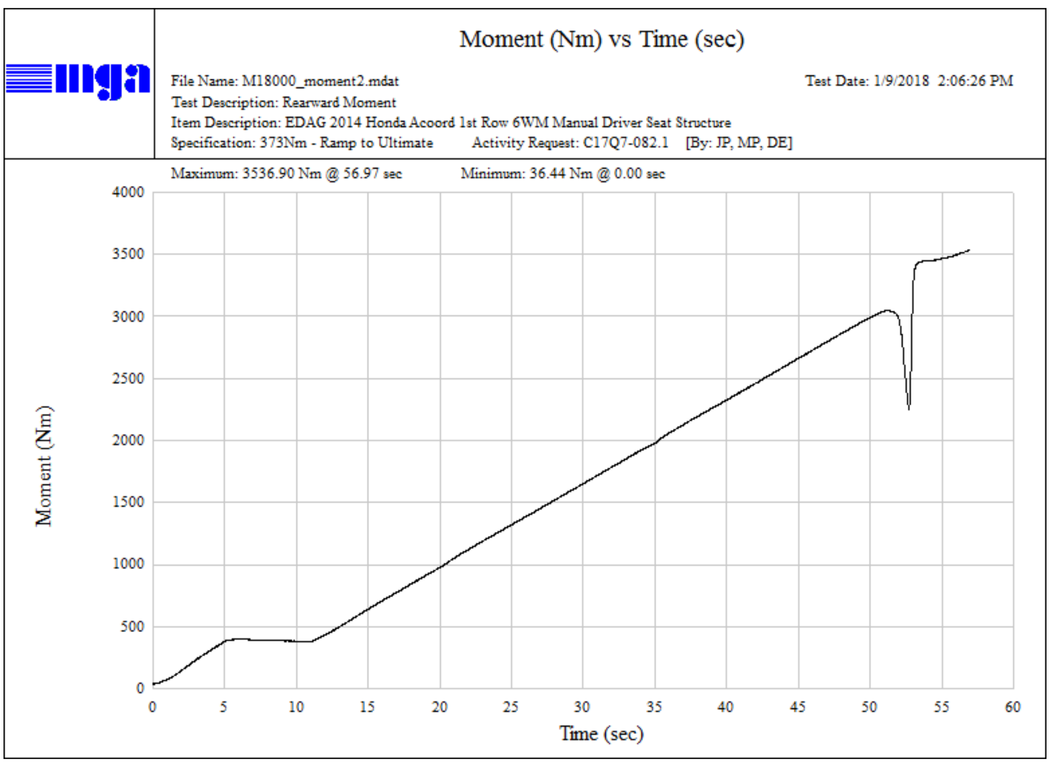
Moment (Nm) vs Time (sec)
File Name: M18000_moment2.mdat
Test Date: 1/9/2018 2:06:26 PM
Test Description: Rearward Moment
Item Description: EDAG 2014 Honda Accord 1st Row 6WM Manual Driver Seat Structure
Specification: 373Nm - Ramp to Ultimate
Activity Request: C17Q7-082.1 [By: JP, MP, DE]
Maximum: 3536.90 Nm @ 56.97 sec
Minimum: 36.44 Nm @ 0.00 sec
Moment (Nm)
Time (sec)

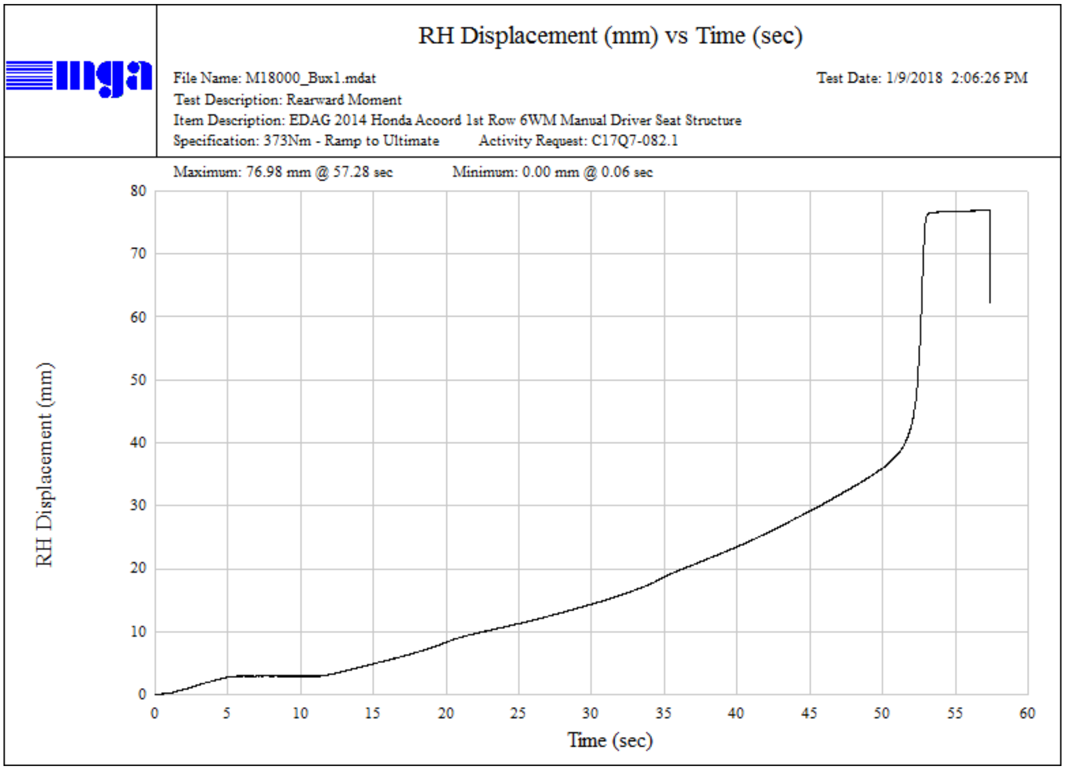
RH Displacement (mm) vs Time (sec)
File Name: M18000_Bux1.mdat
Test Date: 1/9/2018 2:06:26 PM
Test Description: Rearward Moment
Item Description: EDAG 2014 Honda Accord 1st Row 6WM Manual Driver Seat Structure
Specification: 373Nm - Ramp to Ultimate
Activity Request: C17Q7-082.1
Maximum: 76.98 mm @ 57.28 sec
Minimum: 0.00 mm @ 0.06 sec
RH Displacement (mm)
Time (sec)

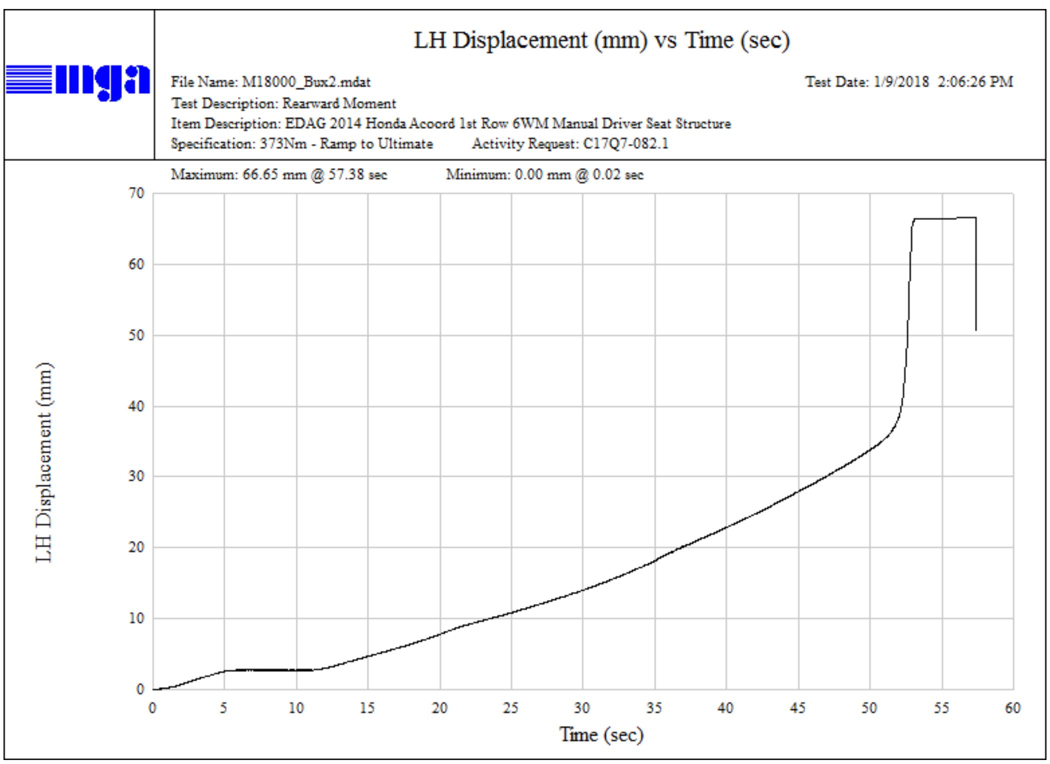
LH Displacement (mm) vs Time (sec)
File Name: M18000_Bux2.mdat
Test Date: 1/9/2018 2:06:26 PM
Test Description: Rearward Moment
Item Description: EDAG 2014 Honda Accord 1st Row 6WM Manual Driver Seat Structure
Specification: 373Nm - Ramp to Ultimate
Activity Request: C17Q7-082.1
Maximum: 66.65 mm @ 57.38 sec
Minimum: 0.00 mm @ 0.02 sec
LH Displacement (mm)
Time (sec)

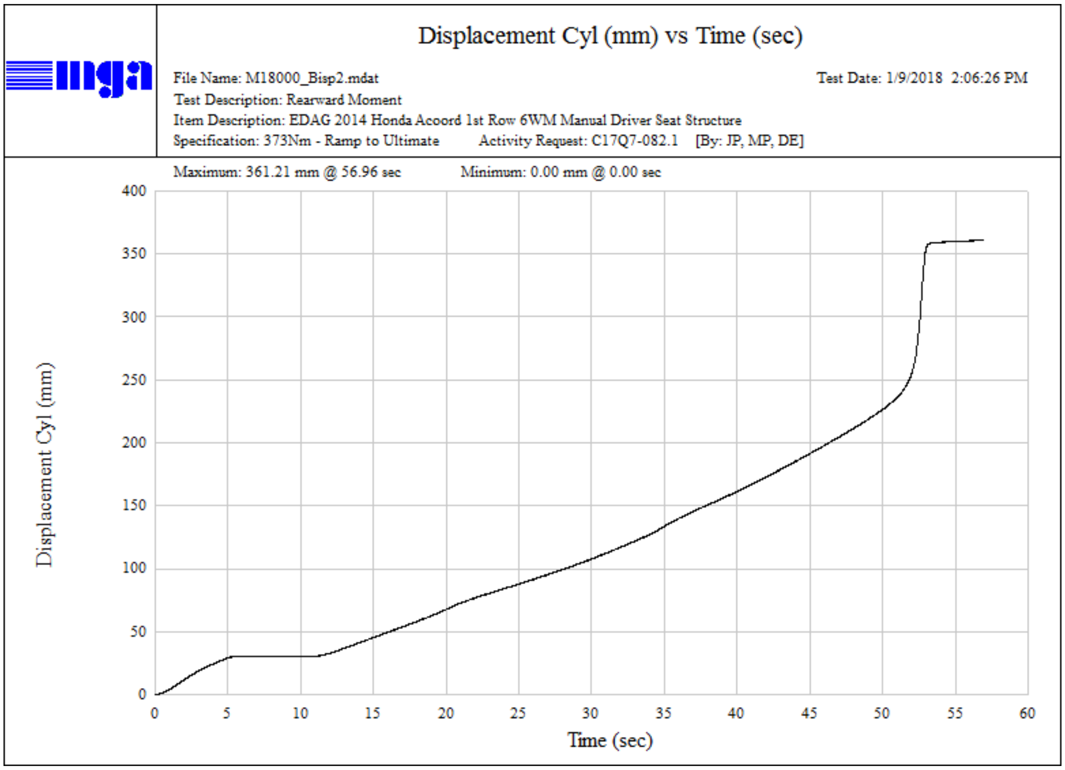
Displacement Cyl (mm) vs Time (sec)
mga
File Name: M18000_Bisp2.mdat
Test Date: 1/9/2018 2:06:26 PM
Test Description: Rearward Moment
Item Description: EDAG 2014 Honda Accord 1st Row 6WM Manual Driver Seat Structure
Specification: 373Nm - Ramp to Ultimate
Activity Request: C17Q7-082.1 [By: JP, MP, DE]
Maximum: 361.21 mm @ 56.96 sec
Minimum: 0.00 mm @ 0.00 sec
Displacement Cyl (mm)
Time (sec)

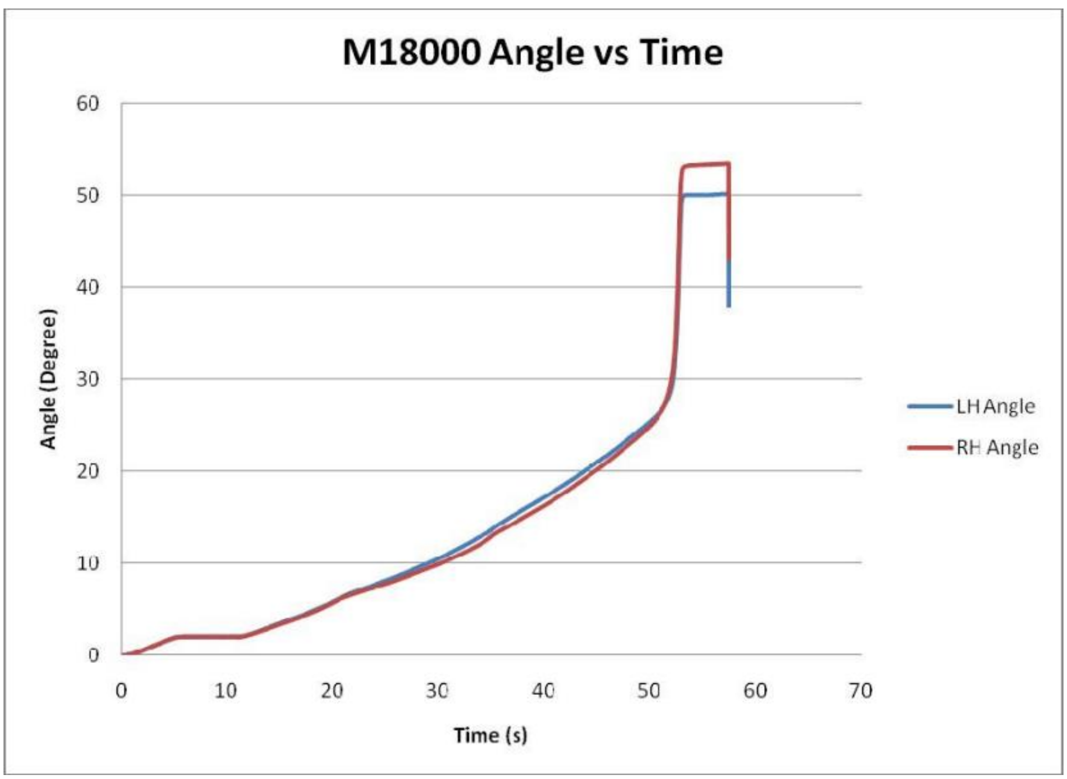
M18000 Angle vs Time
Angle (Degree)
Time (s)
LH Angle
RH Angle

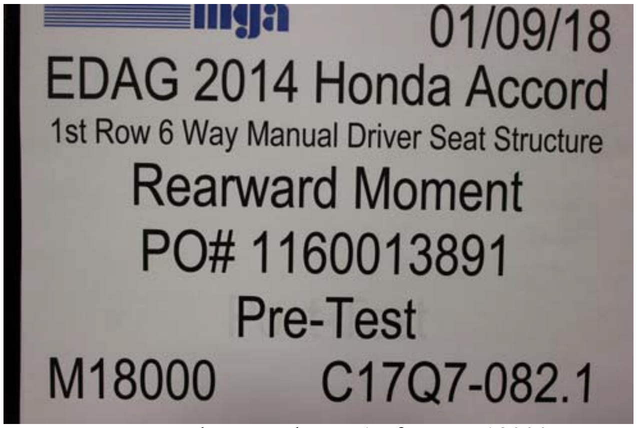

Pre-Test Photograph No. 1 of Test M18000

Pre-Test Photograph No. 2 of Test M18000

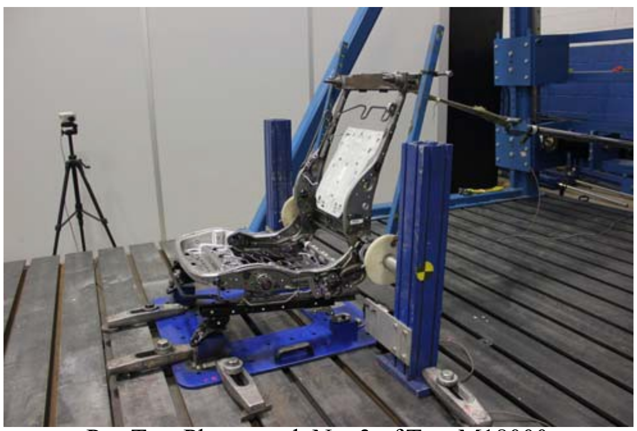

Pre-Test Photograph No. 3 of Test M18000

Pre-Test Photograph No. 4 of Test M18000

Pre-Test Photograph No. 5 of Test M18000

Pre-Test Photograph No. 6 of Test M18000


Pre-Test Photograph No. 7 of Test M18000

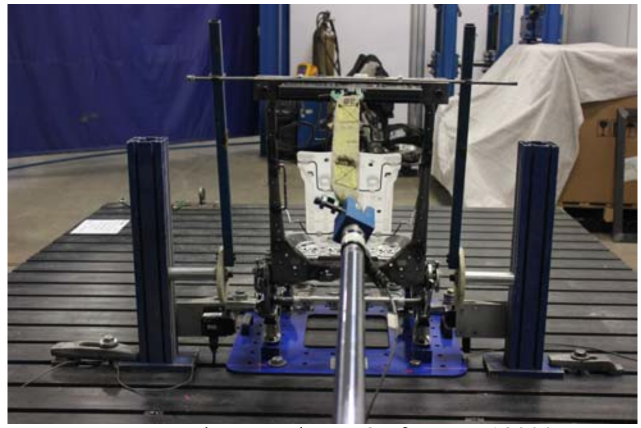
Pre-Test Photograph No. 8 of Test M18000


Pre-Test Photograph No. 9 of Test M18000


Pre-Test Photograph No. 10 of Test M18000

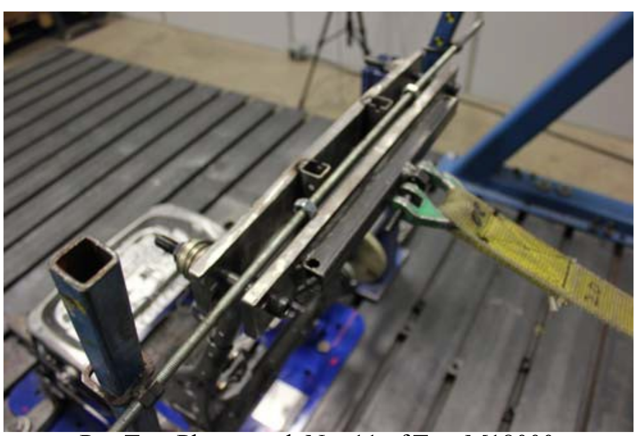
Pre-Test Photograph No. 11 of Test M18000

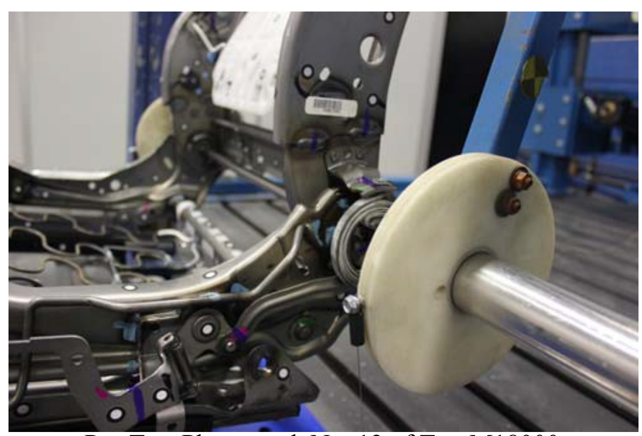
Pre-Test Photograph No. 12 of Test M18000

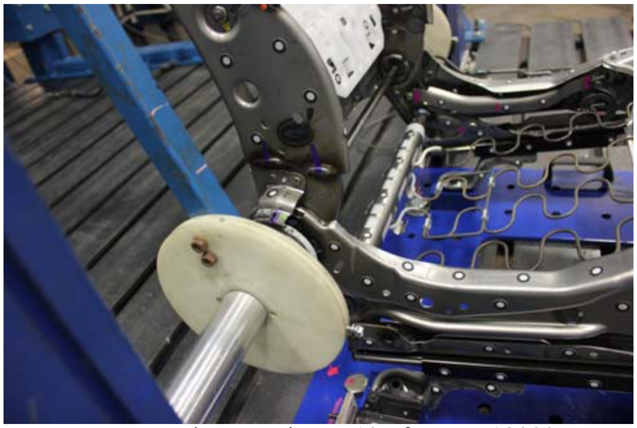
Pre-Test Photograph No. 13 of Test M18000


Pre-Test Photograph No. 14 of Test M18000

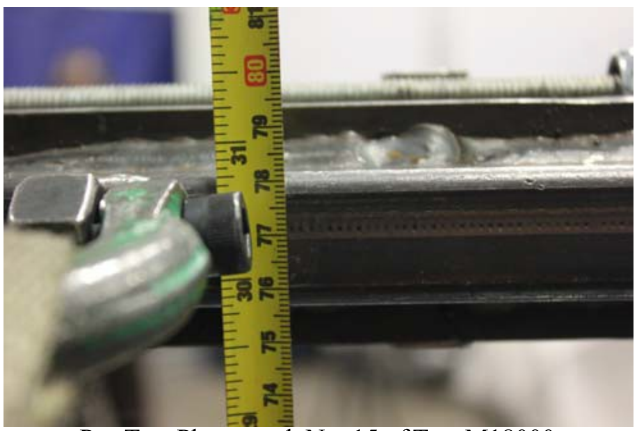
Pre-Test Photograph No. 15 of Test M18000


Pre-Test Photograph No. 16 of Test M18000

Post-Test Photograph No. 1 of Test M18000


Post-Test Photograph No. 2 of Test M18000

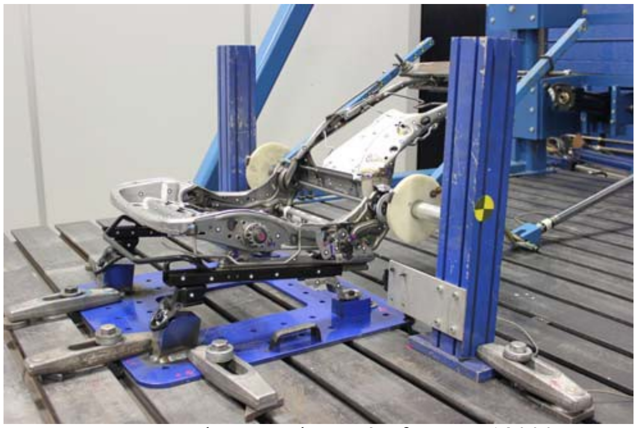
Post-Test Photograph No. 3 of Test M18000

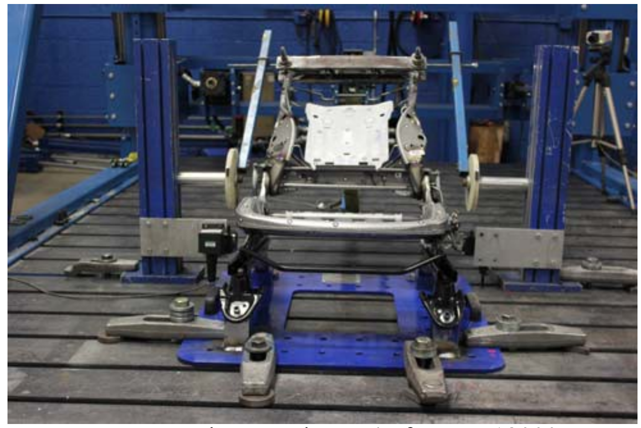
Post-Test Photograph No. 4 of Test M18000


Post-Test Photograph No. 5 of Test M18000


Post-Test Photograph No. 6 of Test M18000


Post-Test Photograph No. 7 of Test M18000


Post-Test Photograph No. 8 of Test M18000


Post-Test Photograph No. 9 of Test M18000


Post-Test Photograph No. 10 of Test M18000

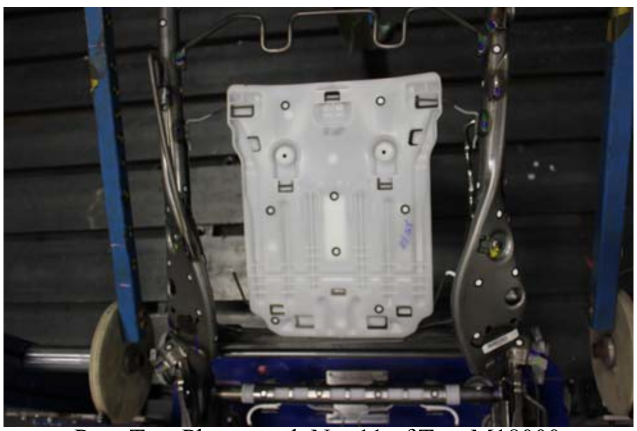
Post-Test Photograph No. 11 of Test M18000

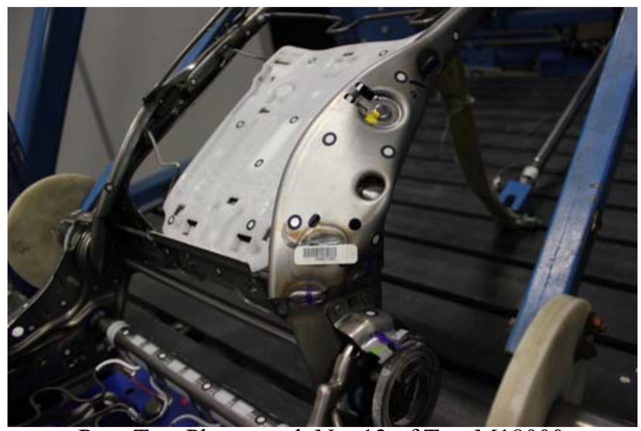
Post-Test Photograph No. 12 of Test M18000


Post-Test Photograph No. 13 of Test M18000

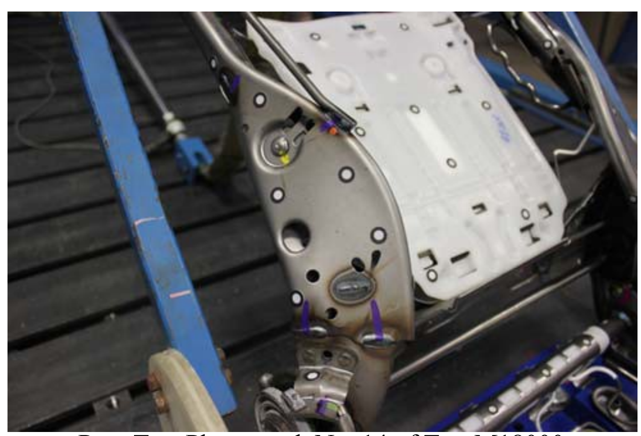
Post-Test Photograph No. 14 of Test M18000

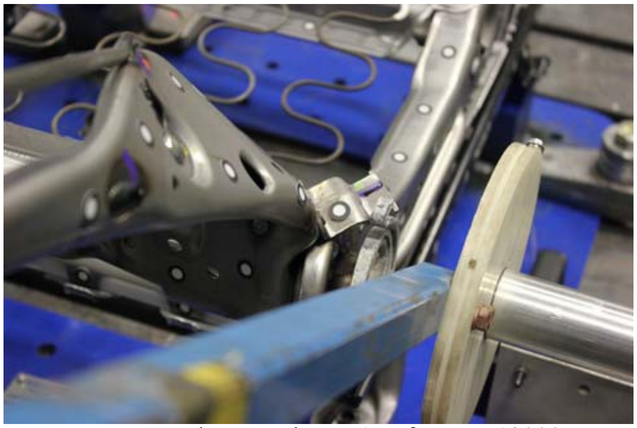
Post-Test Photograph No. 15 of Test M18000

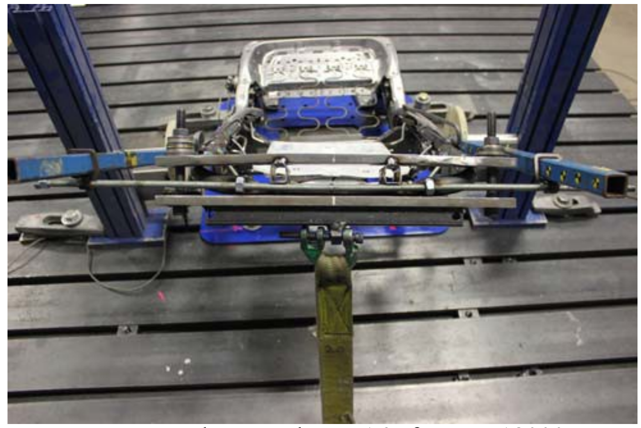
Post-Test Photograph No. 16 of Test M18000

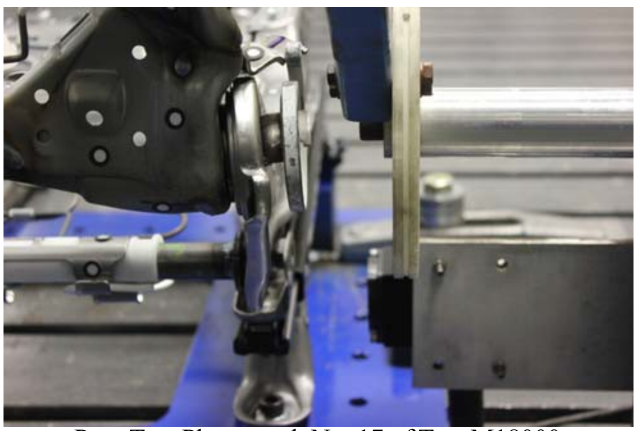
Post-Test Photograph No. 17 of Test M18000

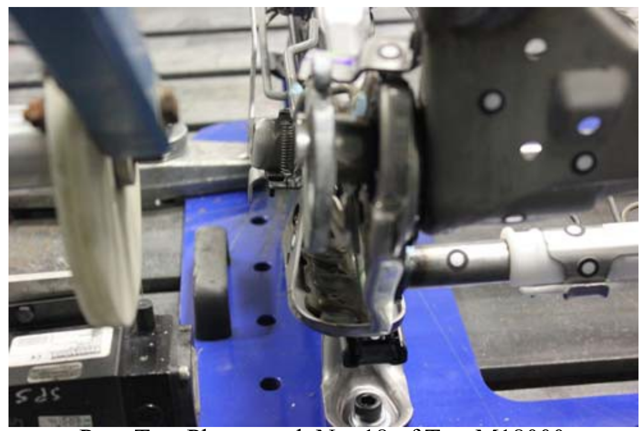
Post-Test Photograph No. 18 of Test M18000

Test M18001 Data

Seat Type: 1st Row 8 Way Power Driver Seat	
Seat Function	**Test Position**
Track Position	Full Rearward
Vertical Position	Full Down
Seat Back Angle (Ref: See drawing)	18°
H-point (Ref: Rear lower cross tube)	159 mm Above
Moment Arm (Ref: H-Point)	433 mm Above
Load Angle	-9°
Temperature	73°F
Humidity	22%

Load Profile	
Time (second)	**Load (N)**
0	86
5	861
11	861
132	20,000

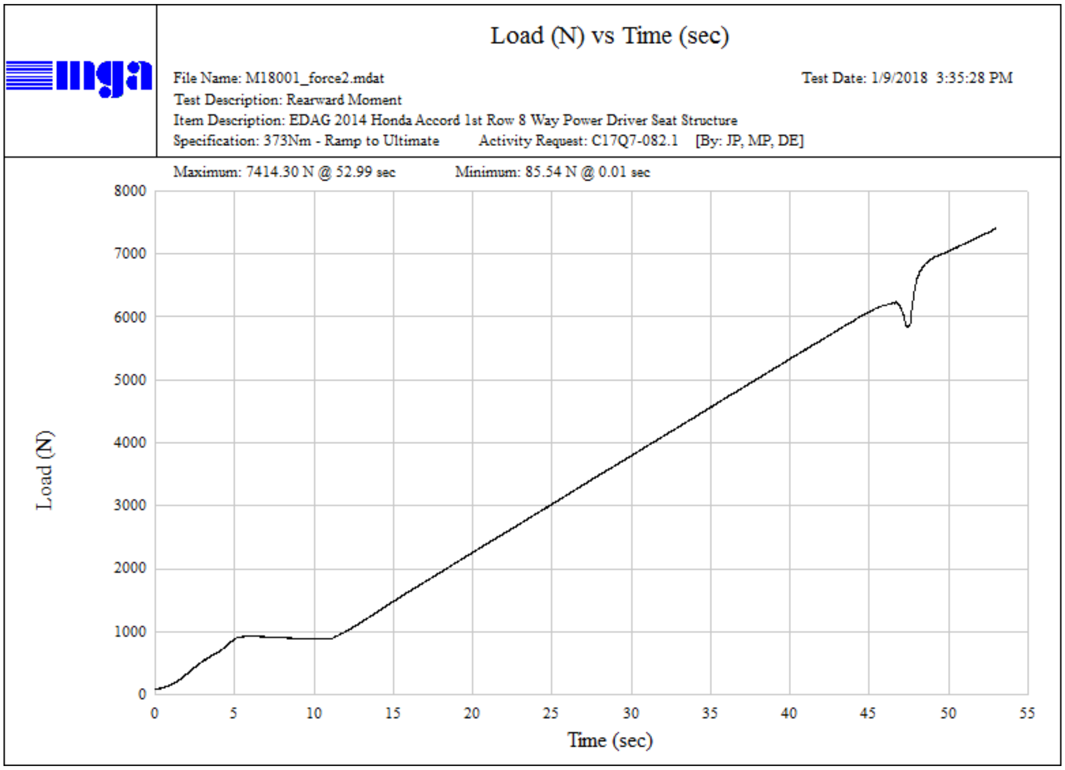
Load (N) vs Time (sec)
File Name: M18001_force2.mdat
Test Date: 1/9/2018 3:35:28 PM
Test Description: Rearward Moment
Item Description: EDAG 2014 Honda Accord 1st Row 8 Way Power Driver Seat Structure
Specification: 373Nm - Ramp to Ultimate
Activity Request: C17Q7-082.1 [By: JP, MP, DE]
Maximum: 7414.30 N @ 52.99 sec
Minimum: 85.54 N @ 0.01 sec
Load (N)
Time (sec)

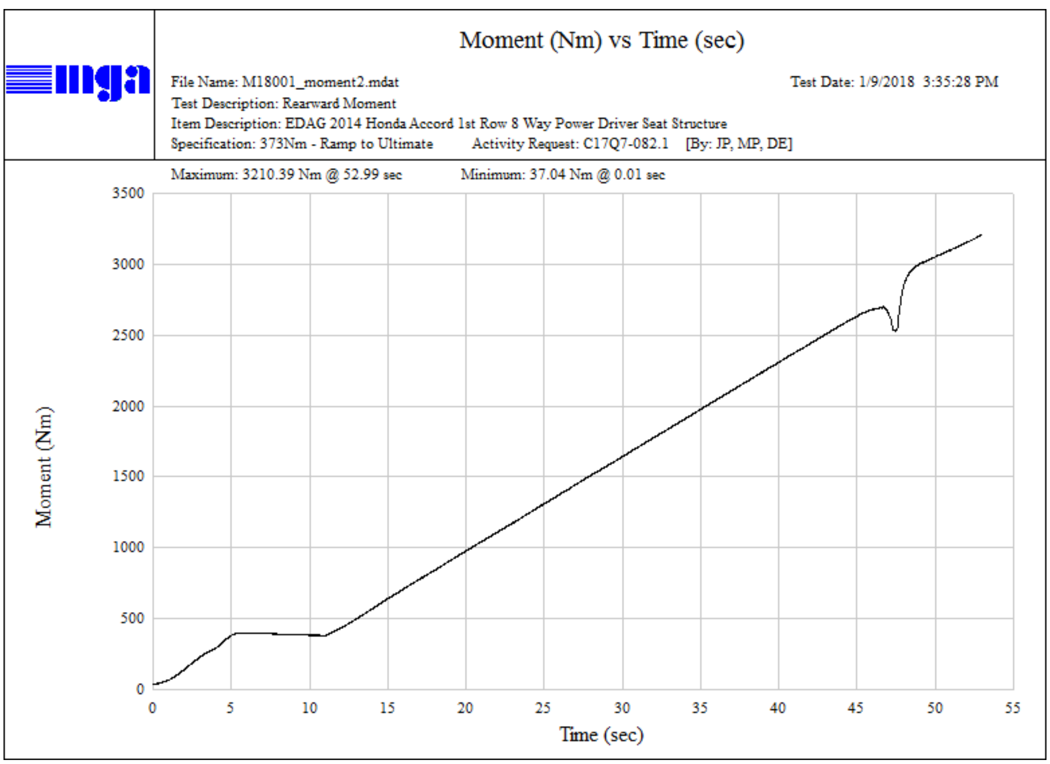
Moment (Nm) vs Time (sec)
File Name: M18001_moment2.mdat
Test Date: 1/9/2018 3:35:28 PM
Test Description: Rearward Moment
Item Description: EDAG 2014 Honda Accord 1st Row 8 Way Power Driver Seat Structure
Specification: 373Nm - Ramp to Ultimate
Activity Request: C17Q7-082.1 [By: JP, MP, DE]
Maximum: 3210.39 Nm @ 52.99 sec
Minimum: 37.04 Nm @ 0.01 sec
Moment (Nm)
Time (sec)

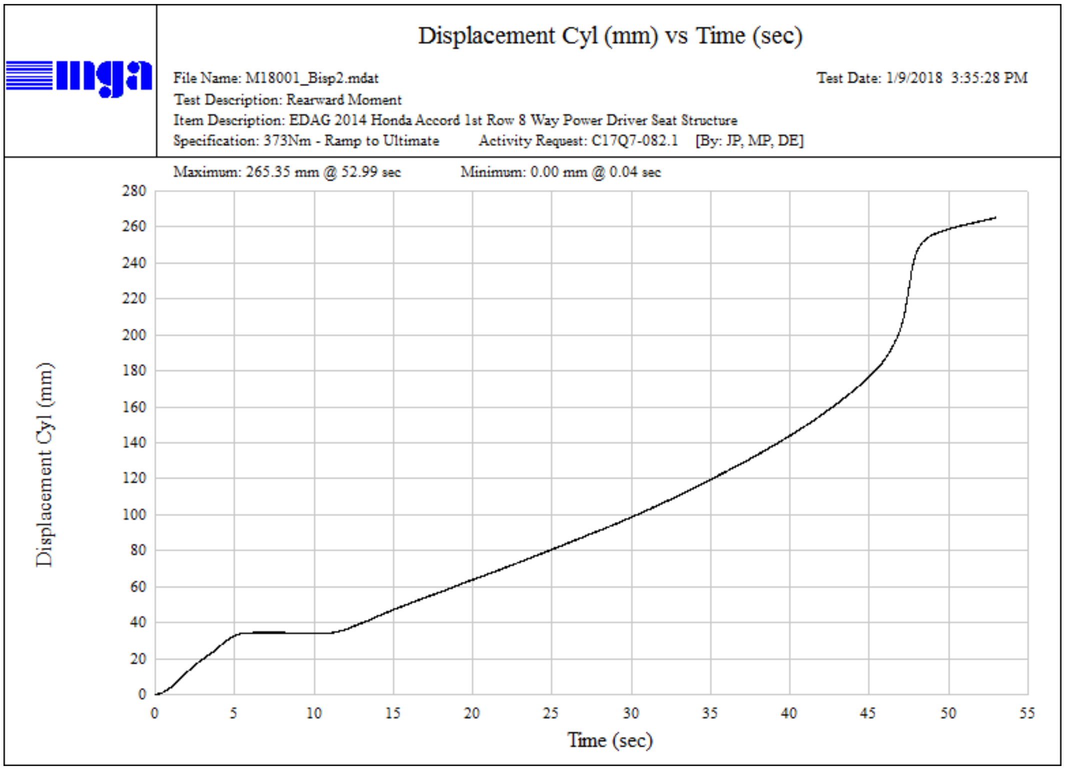
Displacement Cyl (mm) vs Time (sec)
File Name: M18001_Bisp2.mdat
Test Date: 1/9/2018 3:35:28 PM
Test Description: Rearward Moment
Item Description: EDAG 2014 Honda Accord 1st Row 8 Way Power Driver Seat Structure
Specification: 373Nm - Ramp to Ultimate
Activity Request: C17Q7-082.1 [By: JP, MP, DE]
Maximum: 265.35 mm @ 52.99 sec
Minimum: 0.00 mm @ 0.04 sec
Displacement Cyl (mm)
Time (sec)

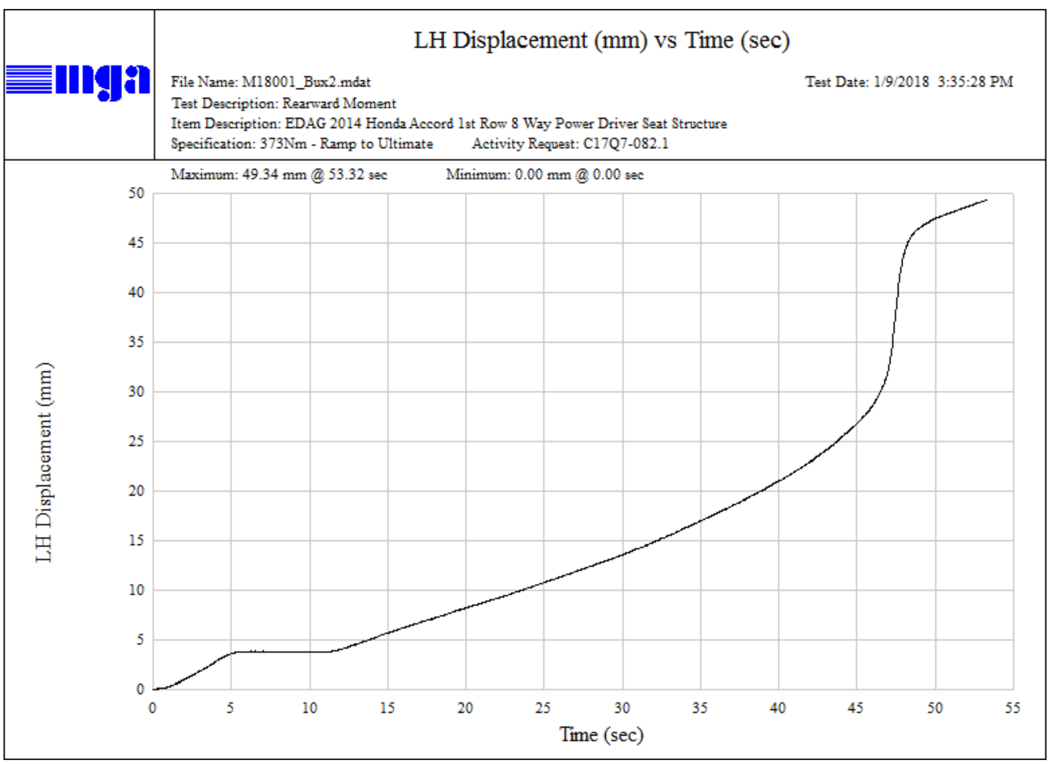
LH Displacement (mm) vs Time (sec)
File Name: M18001_Bux2.mdat
Test Date: 1/9/2018 3:35:28 PM
Test Description: Rearward Moment
Item Description: EDAG 2014 Honda Accord 1st Row 8 Way Power Driver Seat Structure
Specification: 373Nm - Ramp to Ultimate
Activity Request: C17Q7-082.1
Maximum: 49.34 mm @ 53.32 sec
Minimum: 0.00 mm @ 0.00 sec
LH Displacement (mm)
Time (sec)

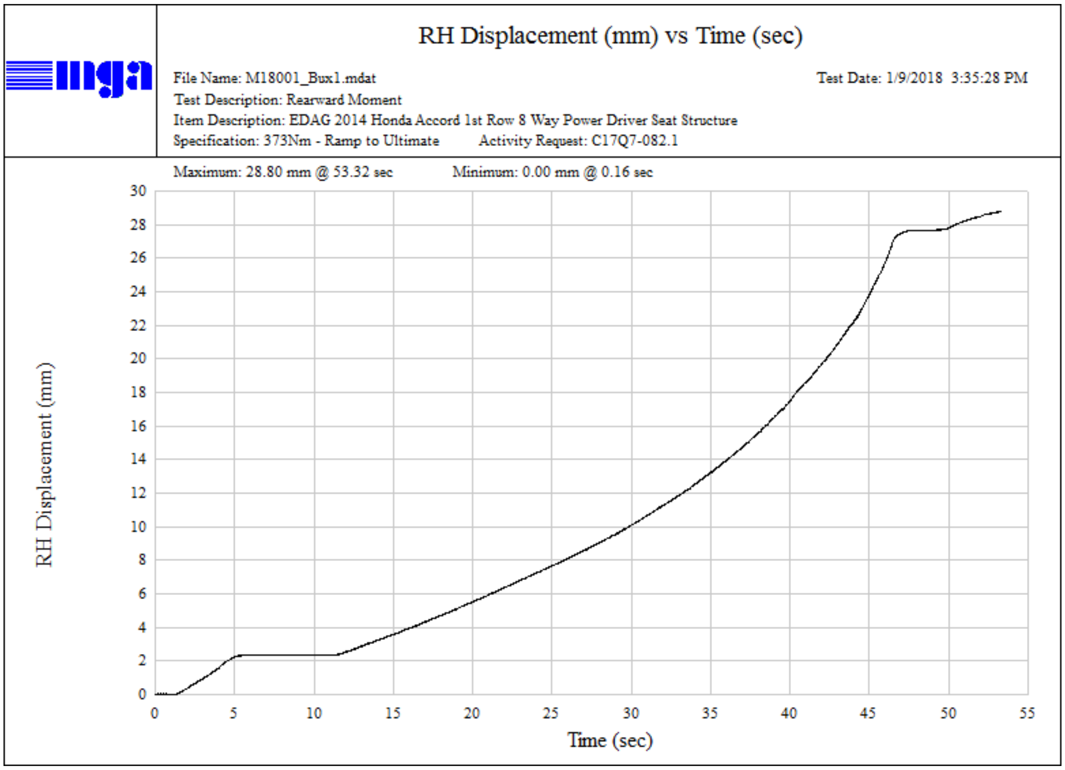
RH Displacement (mm) vs Time (sec)
File Name: M18001_Bux1.mdat
Test Date: 1/9/2018 3:35:28 PM
Test Description: Rearward Moment
Item Description: EDAG 2014 Honda Accord 1st Row 8 Way Power Driver Seat Structure
Specification: 373Nm - Ramp to Ultimate
Activity Request: C17Q7-082.1
Maximum: 28.80 mm @ 53.32 sec
Minimum: 0.00 mm @ 0.16 sec
RH Displacement (mm)
Time (sec)
0
2
4
6
8
10
12
14
16
18
20
22
24
26
28
30
5
15
25
35
40
45
50
55

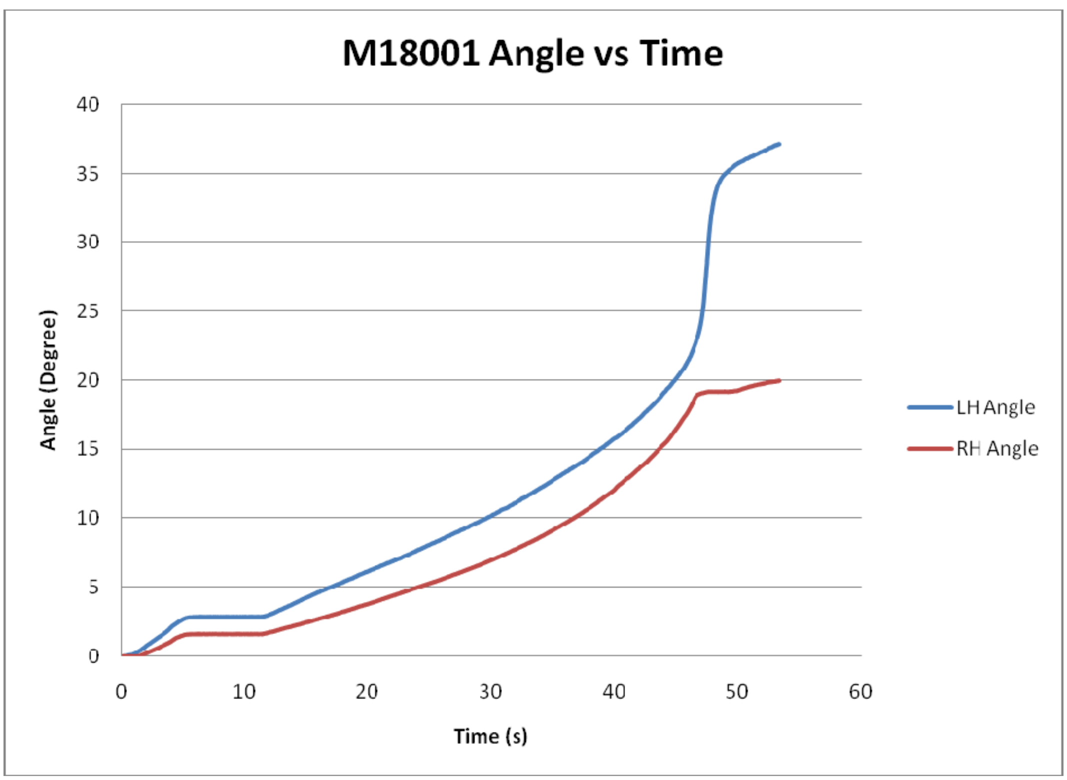
M18001 Angle vs Time
Angle (Degree)
Time (s)
LH Angle
RH Angle
0
5
10
15
20
25
30
35
40
50
60

Pre-Test Photograph No. 1 of Test M18001

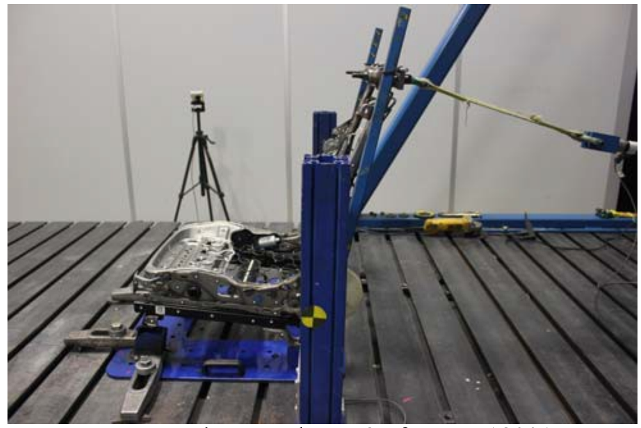
Pre-Test Photograph No. 2 of Test M18001


Pre-Test Photograph No. 3 of Test M18001

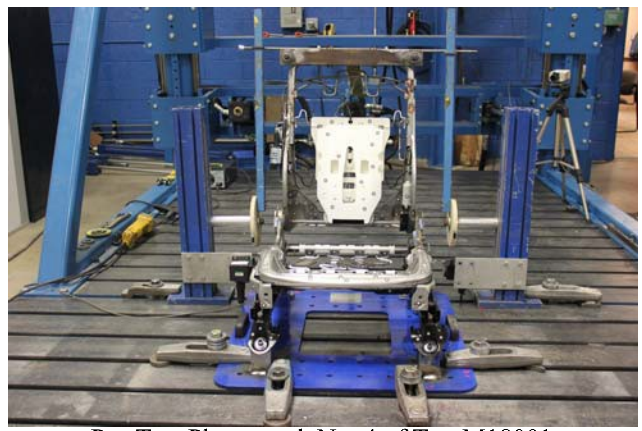
Pre-Test Photograph No. 4 of Test M18001


Pre-Test Photograph No. 5 of Test M18001


Pre-Test Photograph No. 6 of Test M18001


Pre-Test Photograph No. 7 of Test M18001

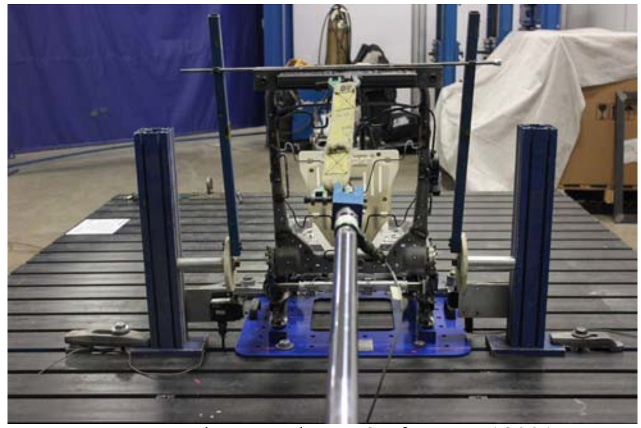
Pre-Test Photograph No. 8 of Test M18001


Pre-Test Photograph No. 9 of Test M18001


Pre-Test Photograph No. 10 of Test M18001

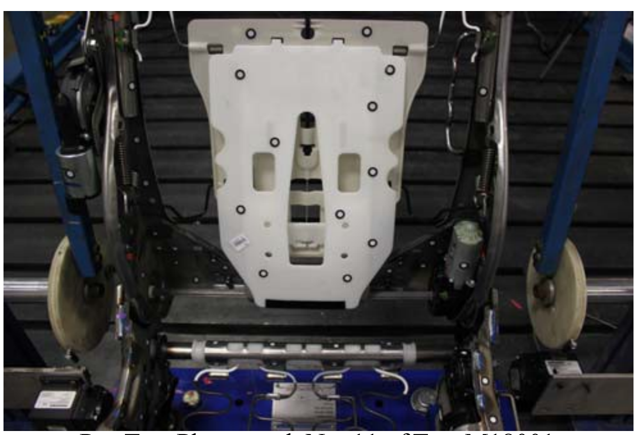
Pre-Test Photograph No. 11 of Test M18001

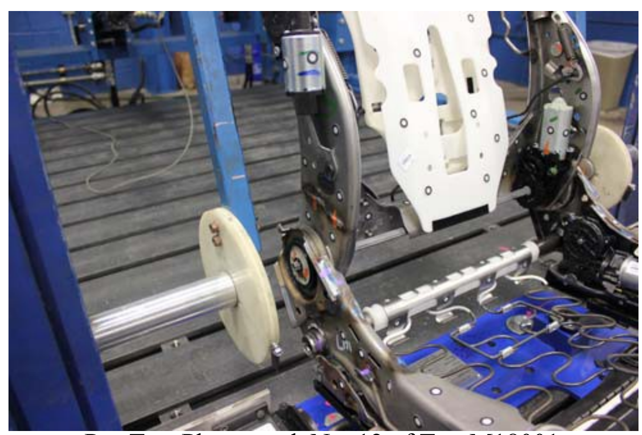
Pre-Test Photograph No. 12 of Test M18001

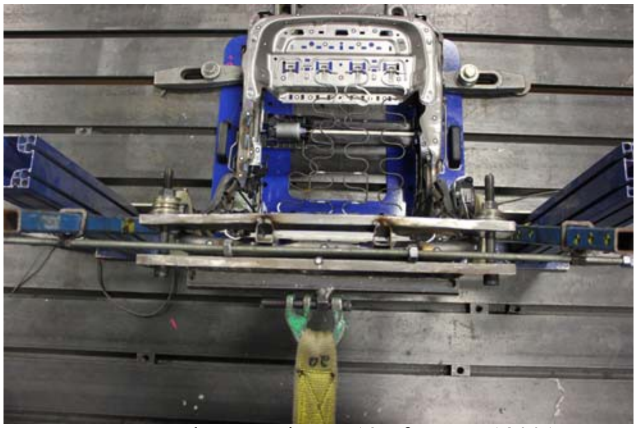
Pre-Test Photograph No. 13 of Test M18001

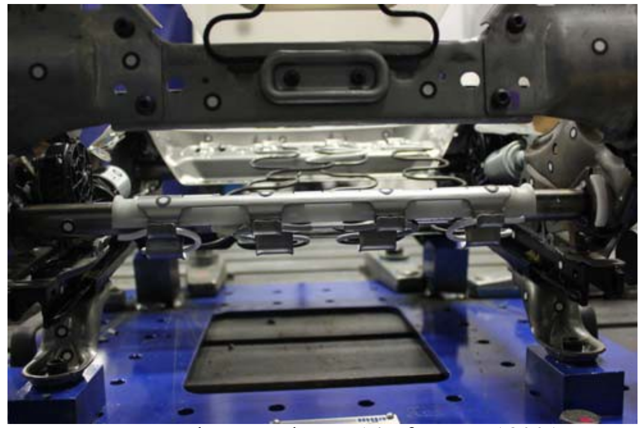
Pre-Test Photograph No. 14 of Test M18001


Pre-Test Photograph No. 15 of Test M18001

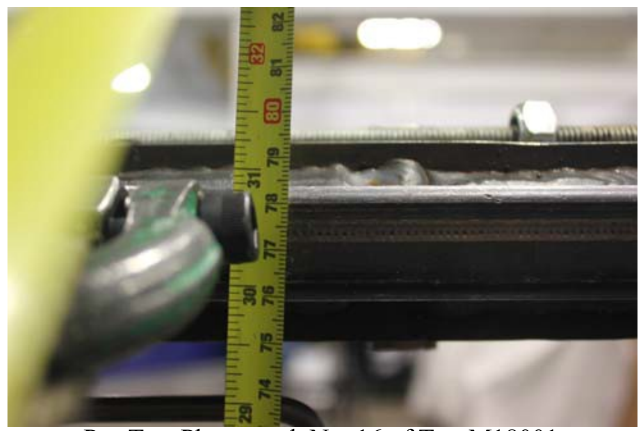
Pre-Test Photograph No. 16 of Test M18001

Pre-Test Photograph No. 17 of Test M18001

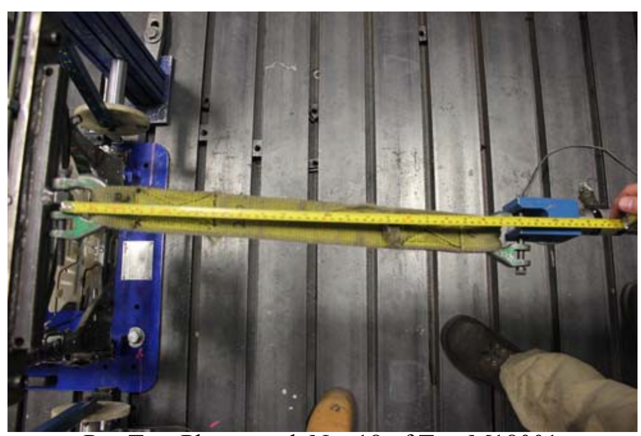
Pre-Test Photograph No. 18 of Test M18001

Pre-Test Photograph No. 19 of Test M18001

Post-Test Photograph No. 1 of Test M18001

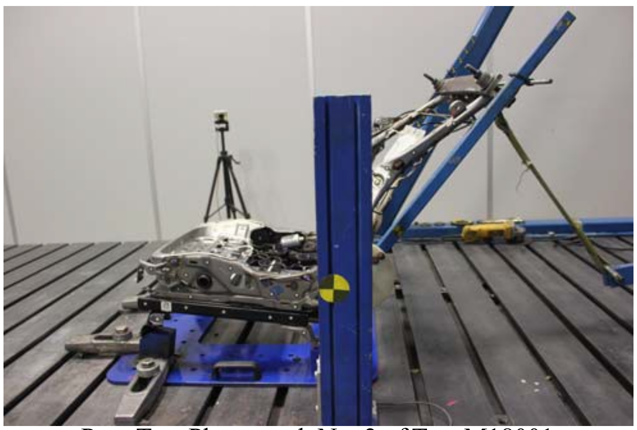

Post-Test Photograph No. 2 of Test M18001

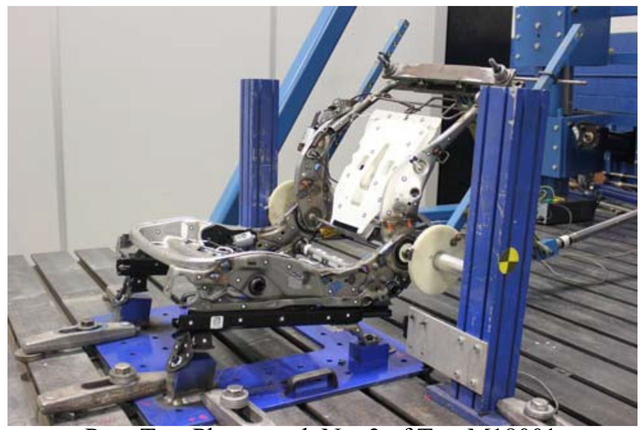

Post-Test Photograph No. 3 of Test M18001

Post-Test Photograph No. 4 of Test M18001

Post-Test Photograph No. 5 of Test M18001

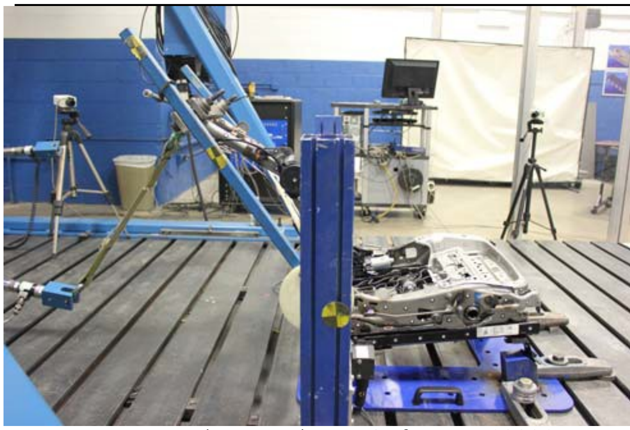
Post-Test Photograph No. 6 of Test M18001

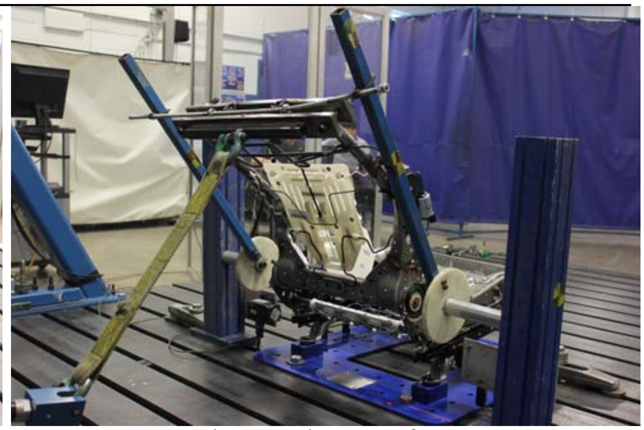
Post-Test Photograph No. 7 of Test M18001

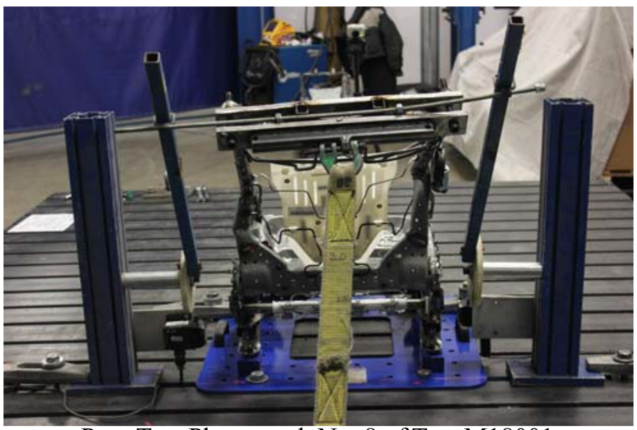
Post-Test Photograph No. 8 of Test M18001


Post-Test Photograph No. 9 of Test M18001

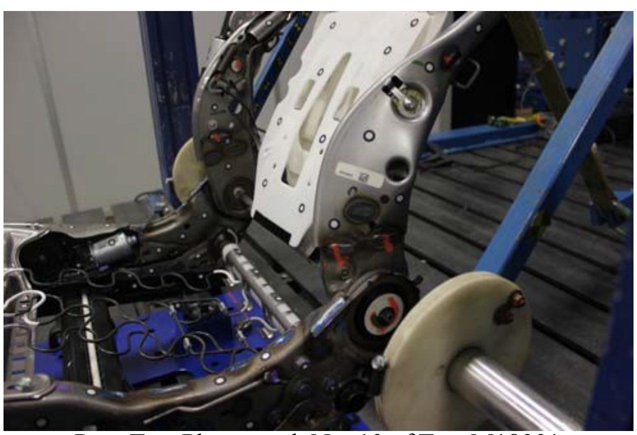
Post-Test Photograph No. 10 of Test M18001

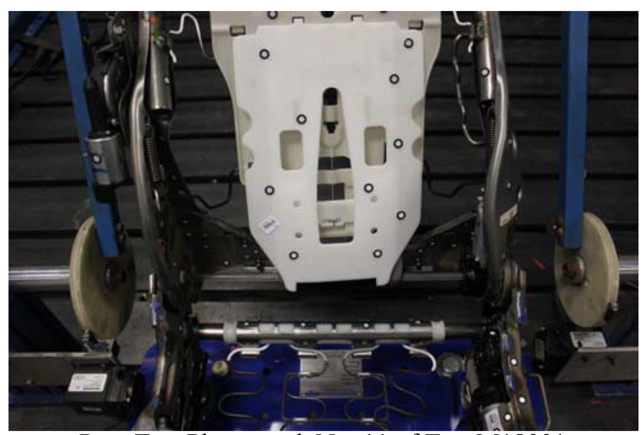
Post-Test Photograph No. 11 of Test M18001

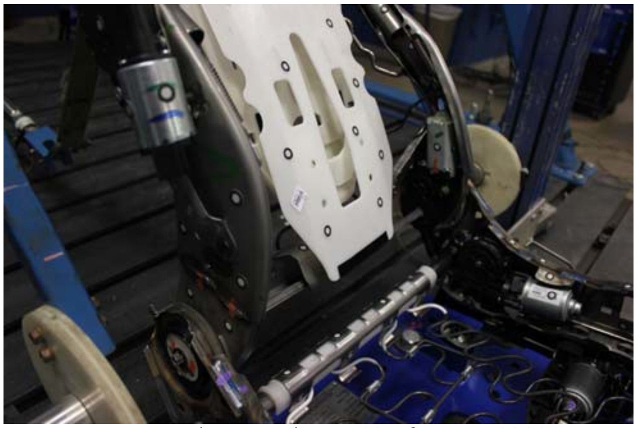
Post-Test Photograph No. 12 of Test M18001

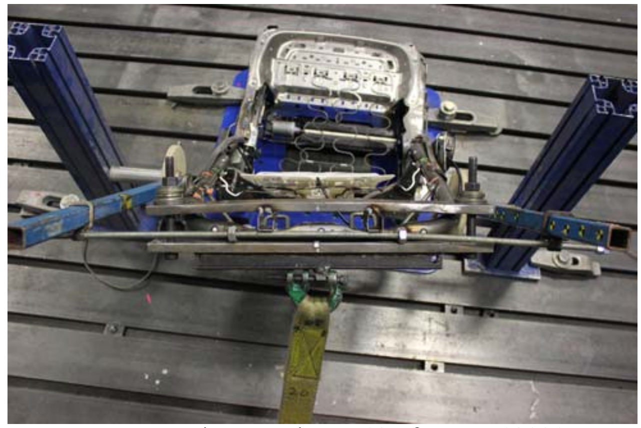
Post-Test Photograph No. 13 of Test M18001

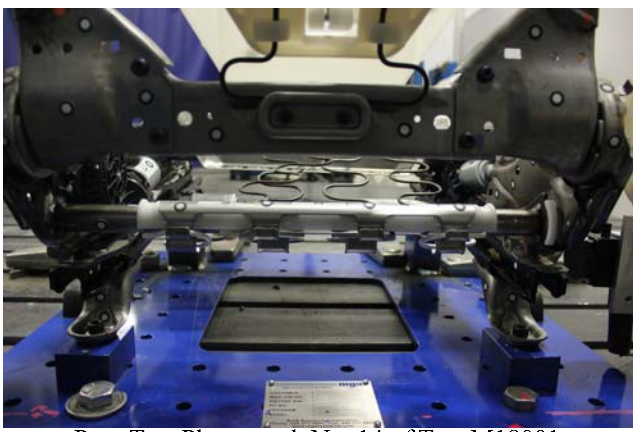
Post-Test Photograph No. 14 of Test M18001


Post-Test Photograph No. 15 of Test M18001

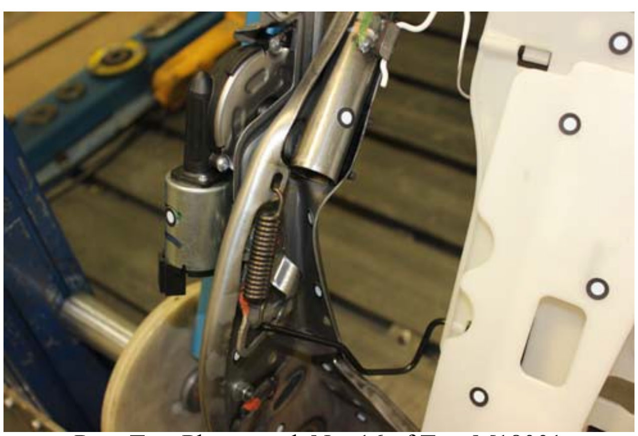
Post-Test Photograph No. 16 of Test M18001

Appendix B. Seat Model Differences

Seat Model Differences Between MY2012 and MY2014 Honda Accord and FEA Model

Updates

Seat model update, **manual seat**

Main differences

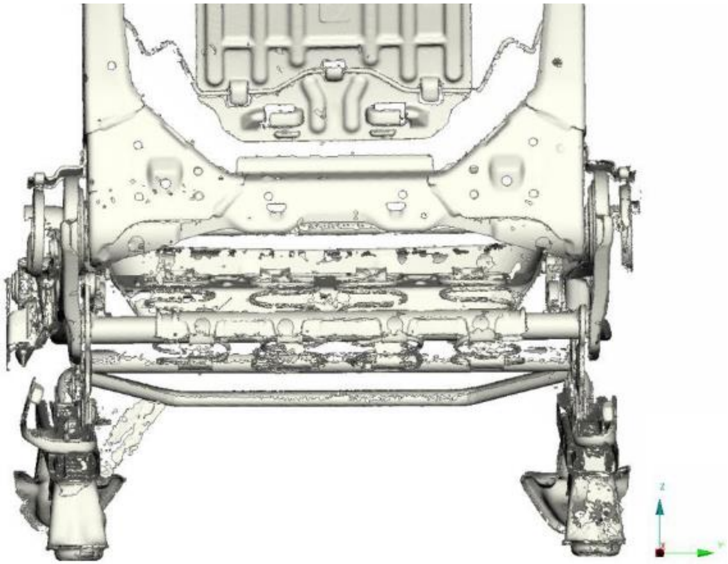

Rear view, scanned model

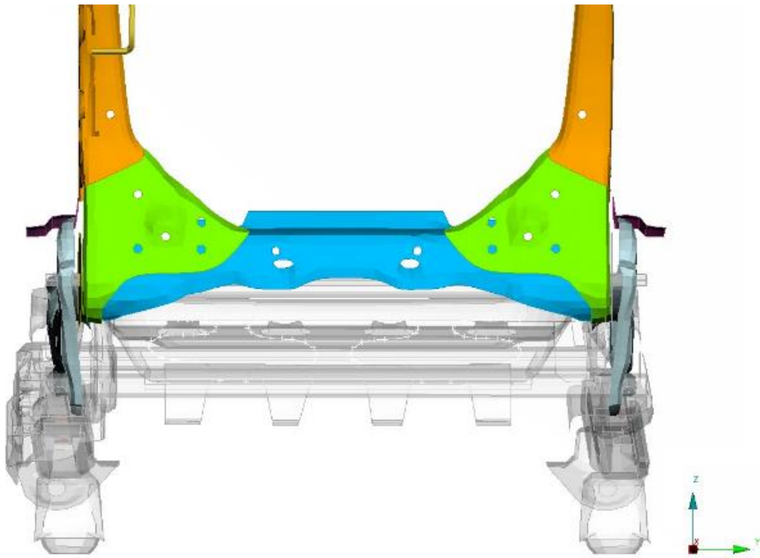

Rear view, simulation model

Seat model update, **manual seat**

Main differences

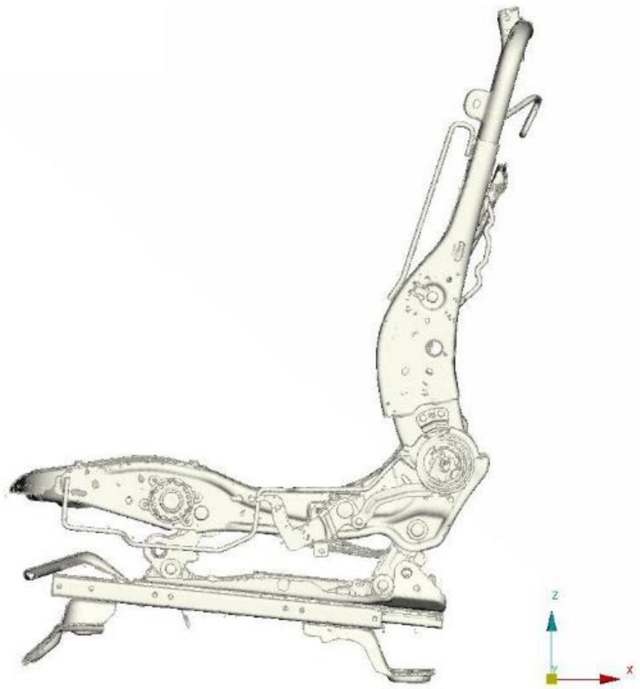

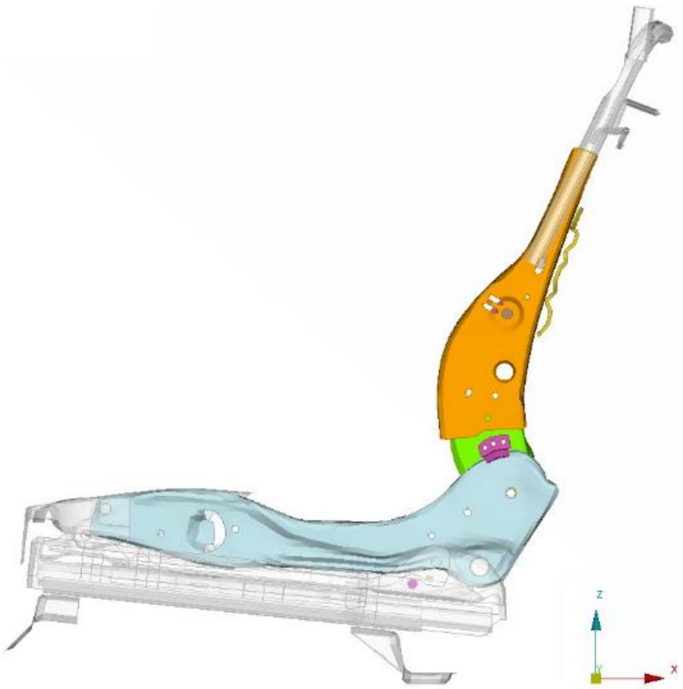

Seat model update, **power seat**

Updated parts

Original scan data

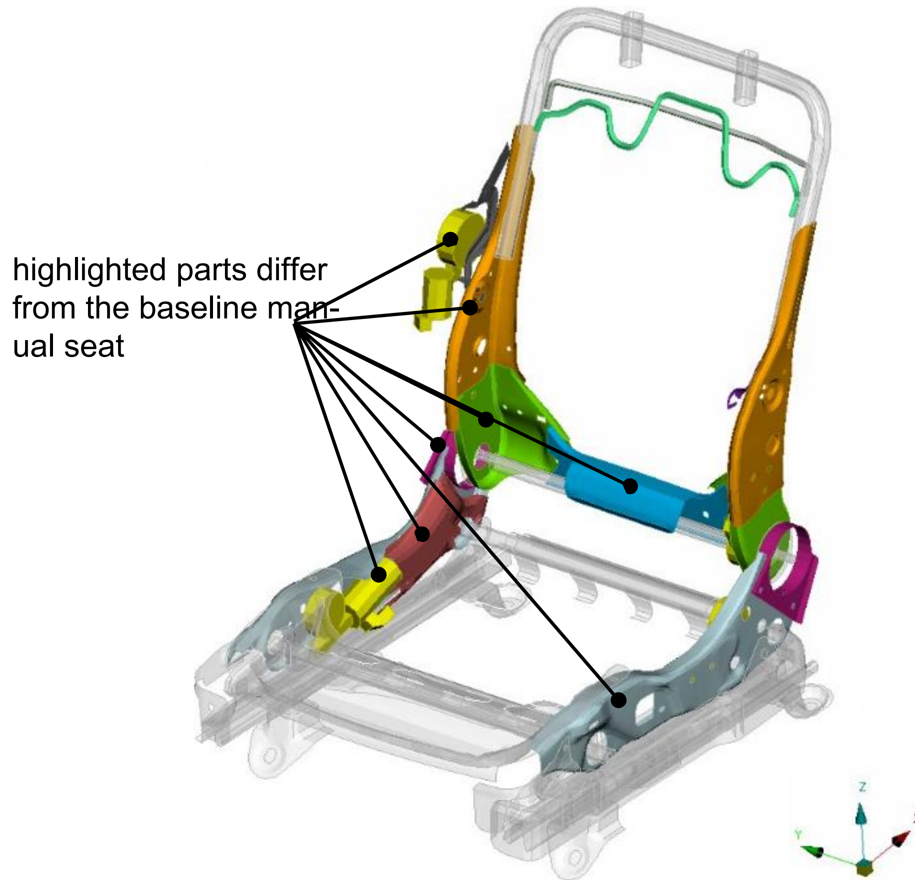

Updated simulation model

Seat model update, **power seat**

<u>Updated parts</u>

Original scan data

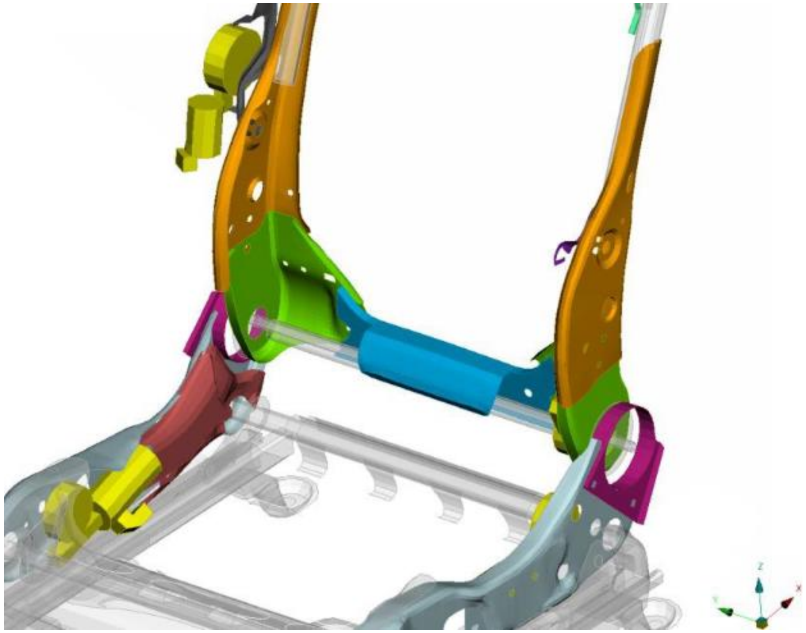

Simulation model

Seat model update, **power seat**

Updated parts

Original scan data

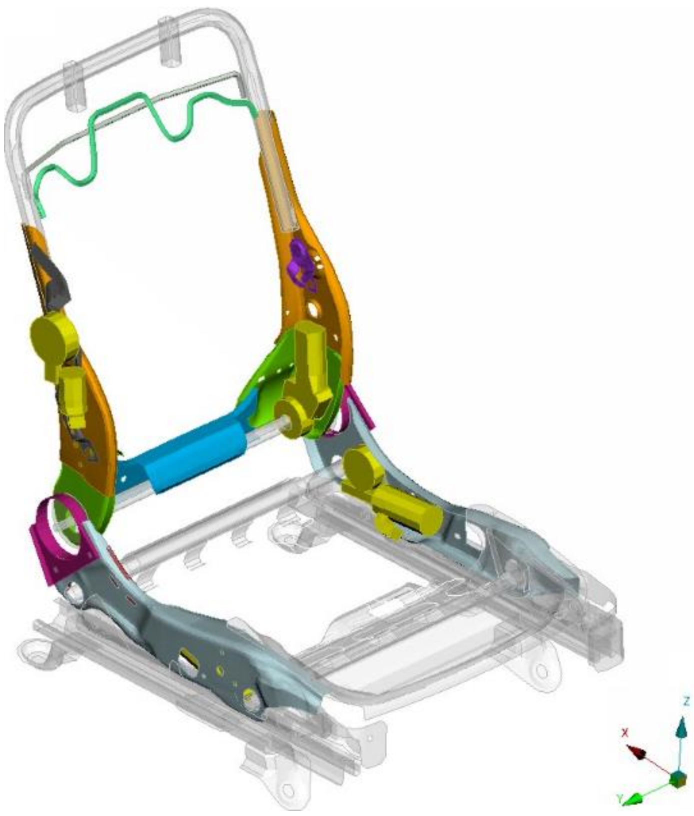

Simulation model

Seat model update, **power seat**

Main differences

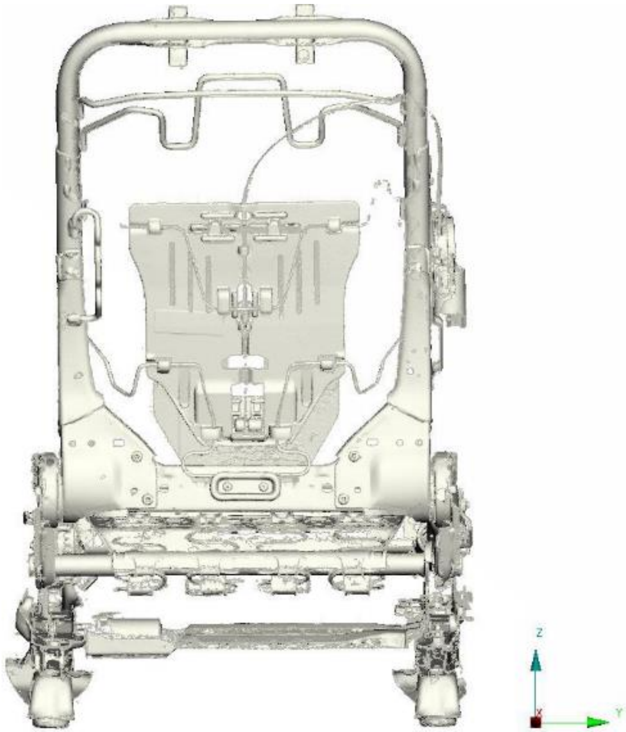

Rear view, scanned model

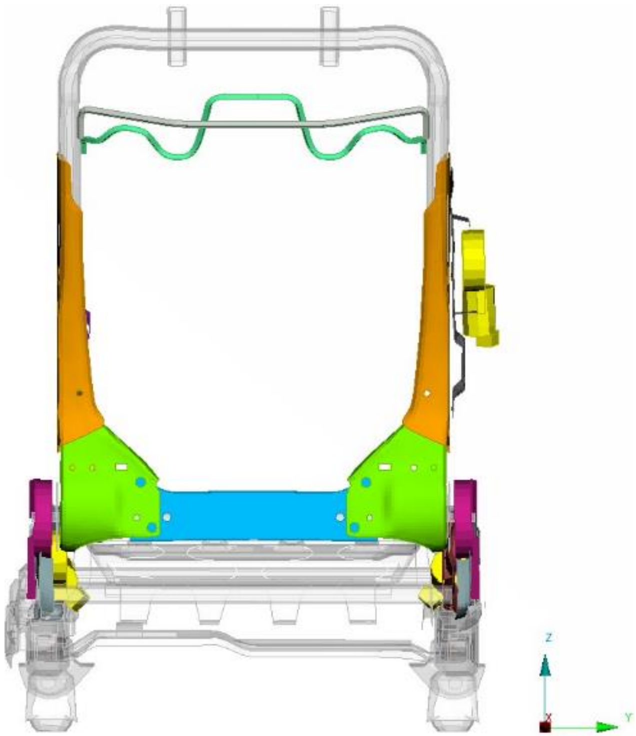

Rear view, simulation model

Seat model update, **power seat**

Main differences

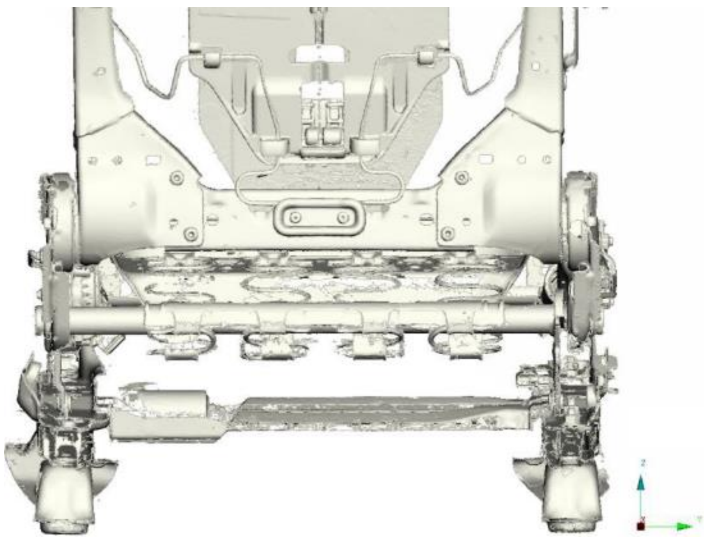

Rear view, scanned model

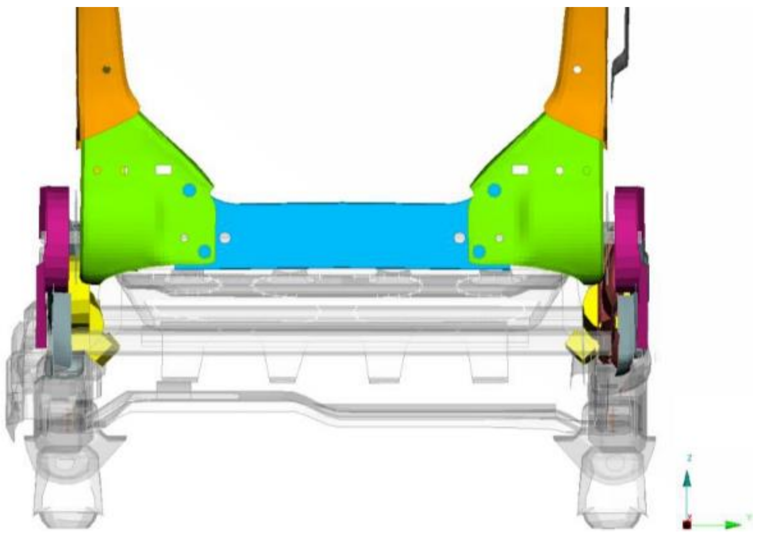

Rear view, simulation model

Seat model update, **power seat**

Main differences

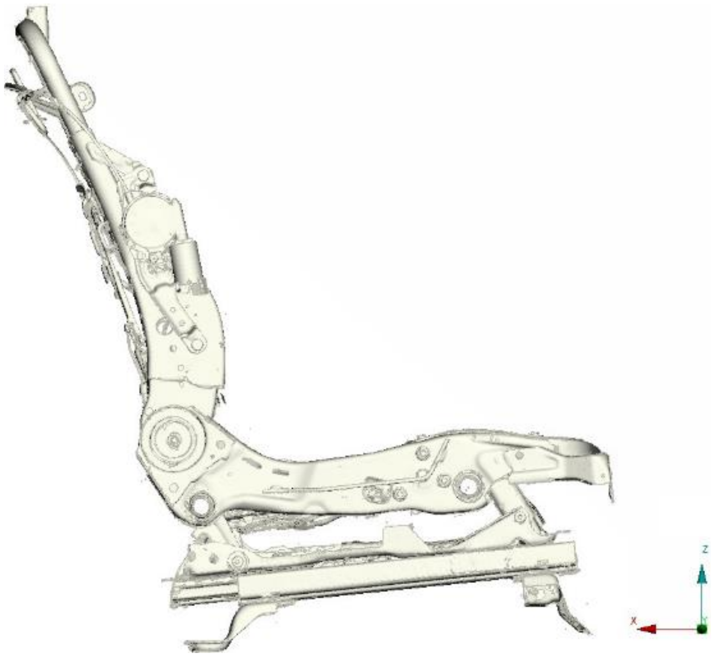

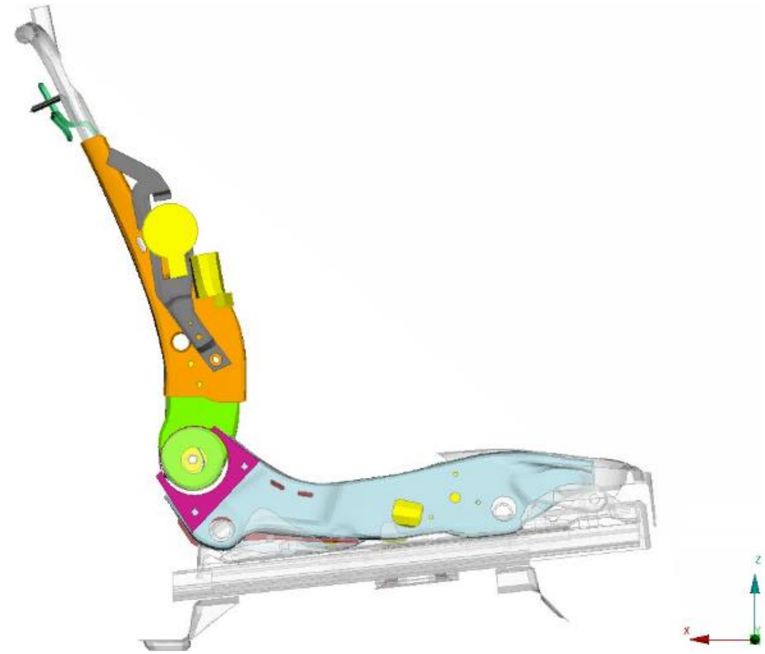

<u>Main differences</u>

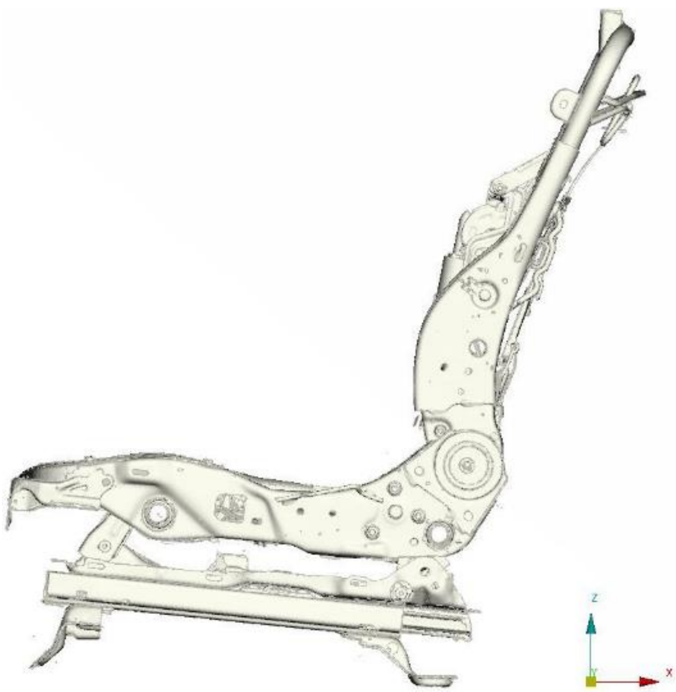

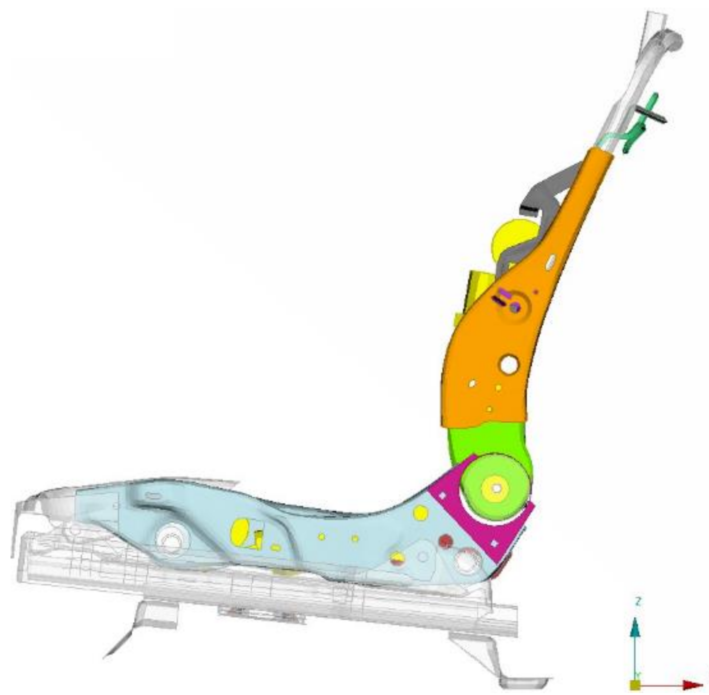

Appendix C. FMVSS 301 Sled Test Report (Power Seat)

FMVSS 301 Sled Test Report (Power Seat)

Summary of the Test

Setup Information

Customer: EDAG
Job No.: C18S7-024.1
Sample ID: Sample 1
ATD: BioRID-II
Direction: Rearward
Seat Position: Mid/FD

Time: 12:15:02
Temperature: 22.9 °C
Humidity: 53 %RH

Test Results

	Accelerometer 1 (S0SLED010000ACXD)			
Peak Acceleration	19.82	G	43.30	ms
Peak Velocity Change	27.34	km/h	65.90	ms
HIC 15 (Time Duration = 15.000 ms)	76.94		102.400 to 117.400	ms
NIC Normalized Neck Injury Criterion	564.36		179.95	ms
One Meter Trap Verification	1010.314	mm	1.03	%
Video Strobe Time Shift from Raw Data			-4.20	ms

Post-Test Comments: See Result Table
Test Series Performed By: Scott McCarter, Carl Prange

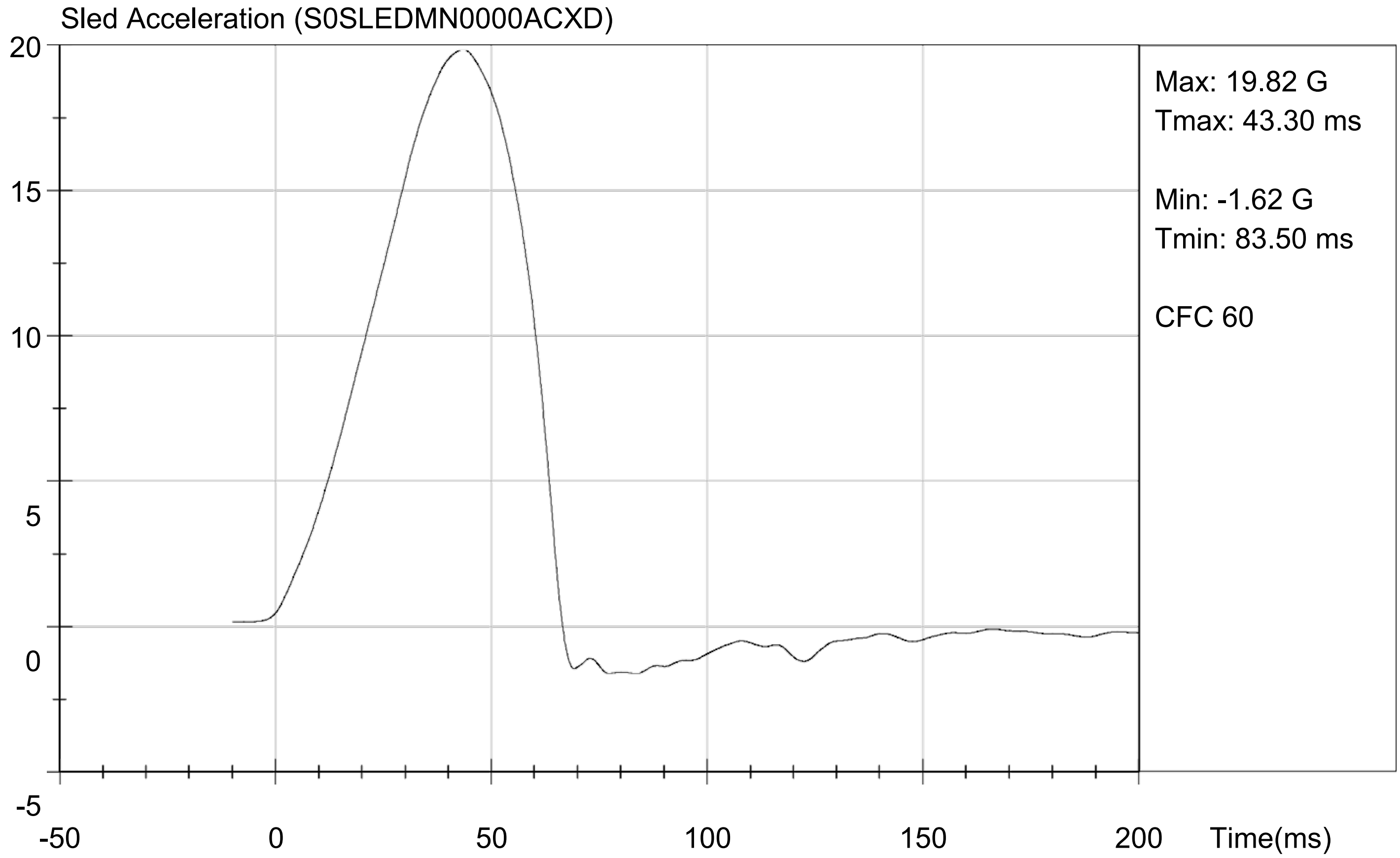
Sled Acceleration (S0SLEDMN0000ACXD)
20
15
10
5
0
-5
-50
0
50
100
150
200
Time(ms)
Max: 19.82 G
Tmax: 43.30 ms
Min: -1.62 G
Tmin: 83.50 ms
CFC 60

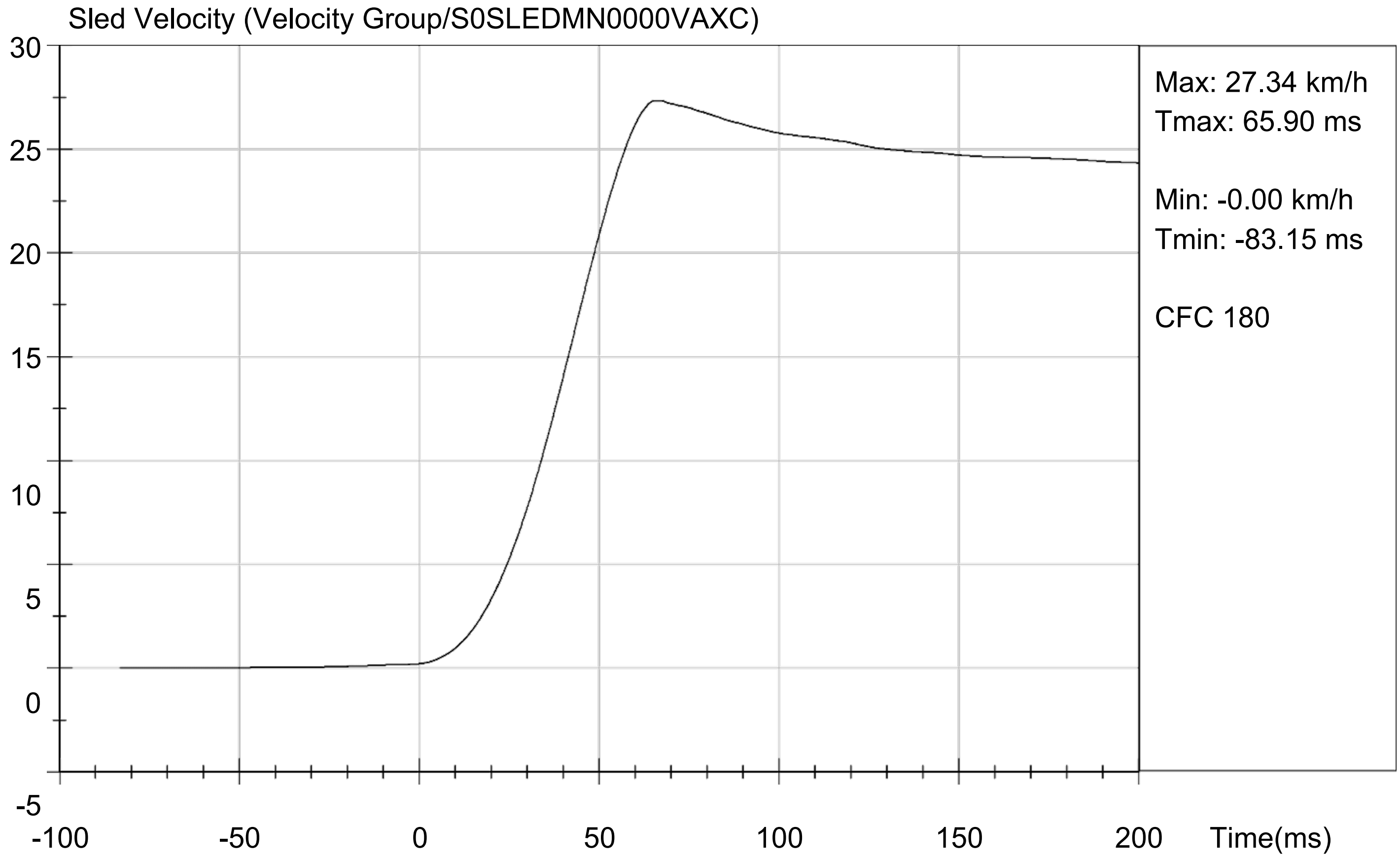
Sled Velocity (Velocity Group/S0SLEDMN0000VAXC)
30
25
20
15
10
5
0
-5
-100
-50
0
50
100
150
200
Time(ms)
Max: 27.34 km/h
Tmax: 65.90 ms
Min: -0.00 km/h
Tmin: -83.15 ms
CFC 180

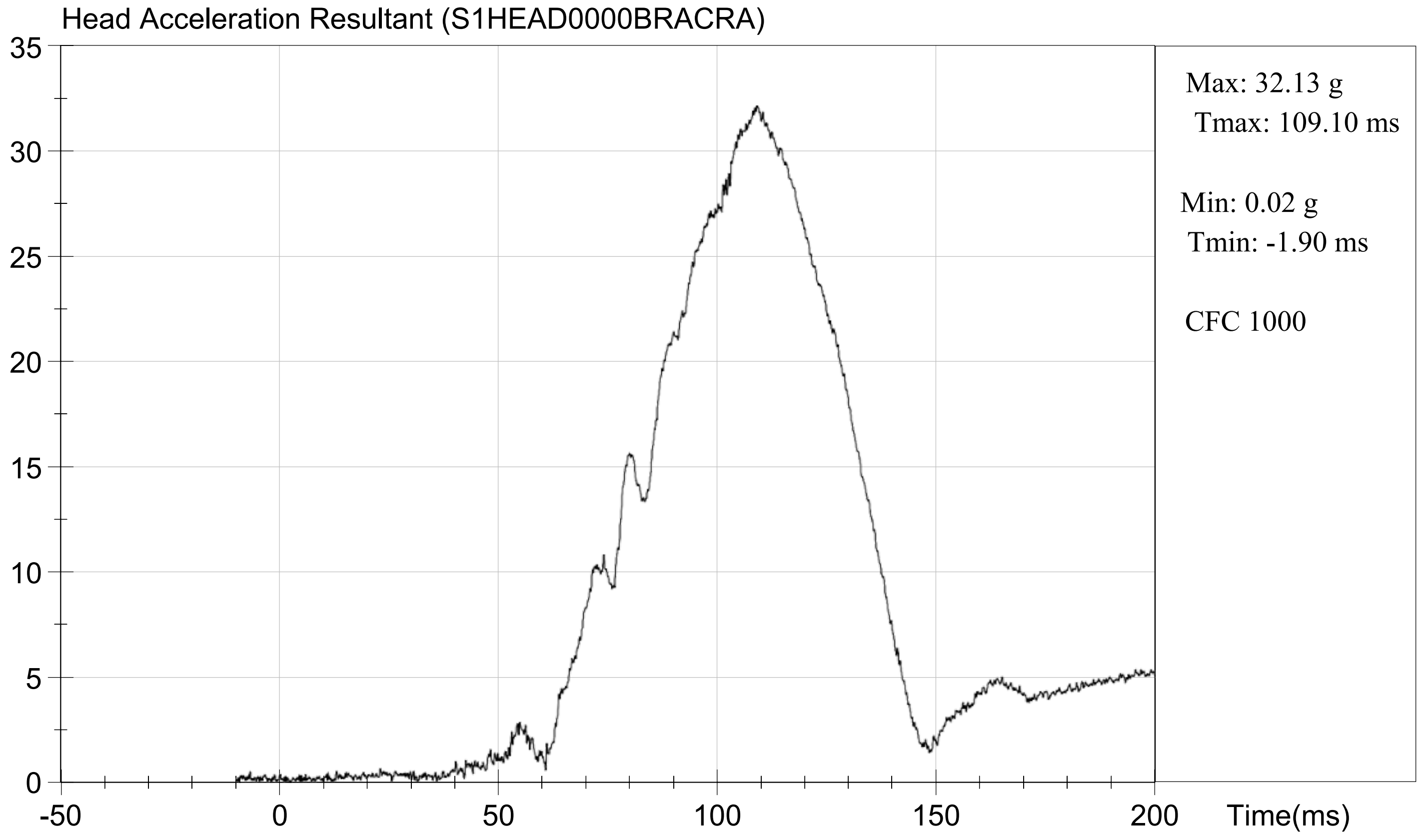
Head Acceleration Resultant (S1HEAD0000BRACRA)
35
30
25
20
15
10
5
0
-50
0
50
100
150
200
Time(ms)
Max: 32.13 g
Tmax: 109.10 ms
Min: 0.02 g
Tmin: -1.90 ms
CFC 1000

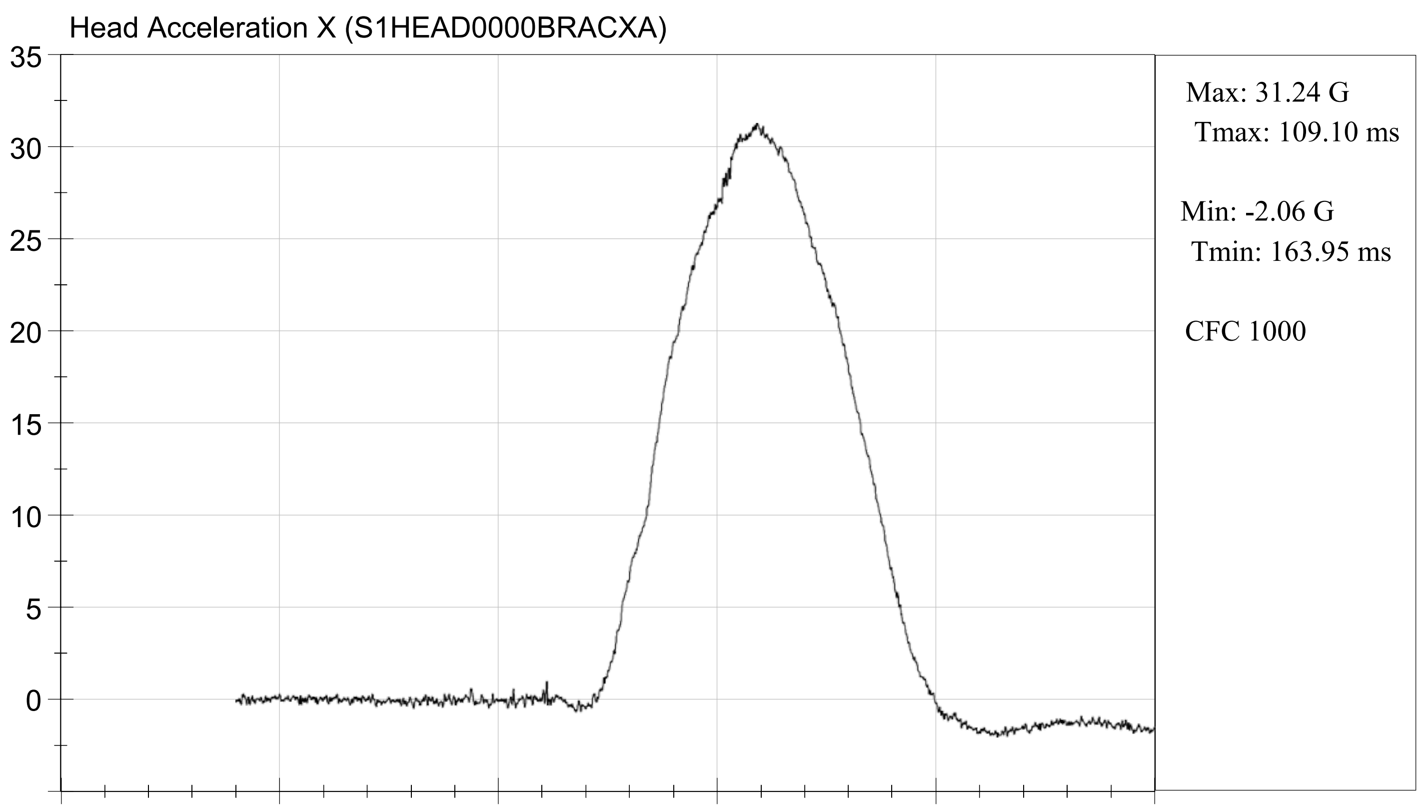
Head Acceleration X (S1HEAD0000BRACXA)
35
30
25
20
15
10
5
0
Max: 31.24 G
Tmax: 109.10 ms
Min: -2.06 G
Tmin: 163.95 ms
CFC 1000

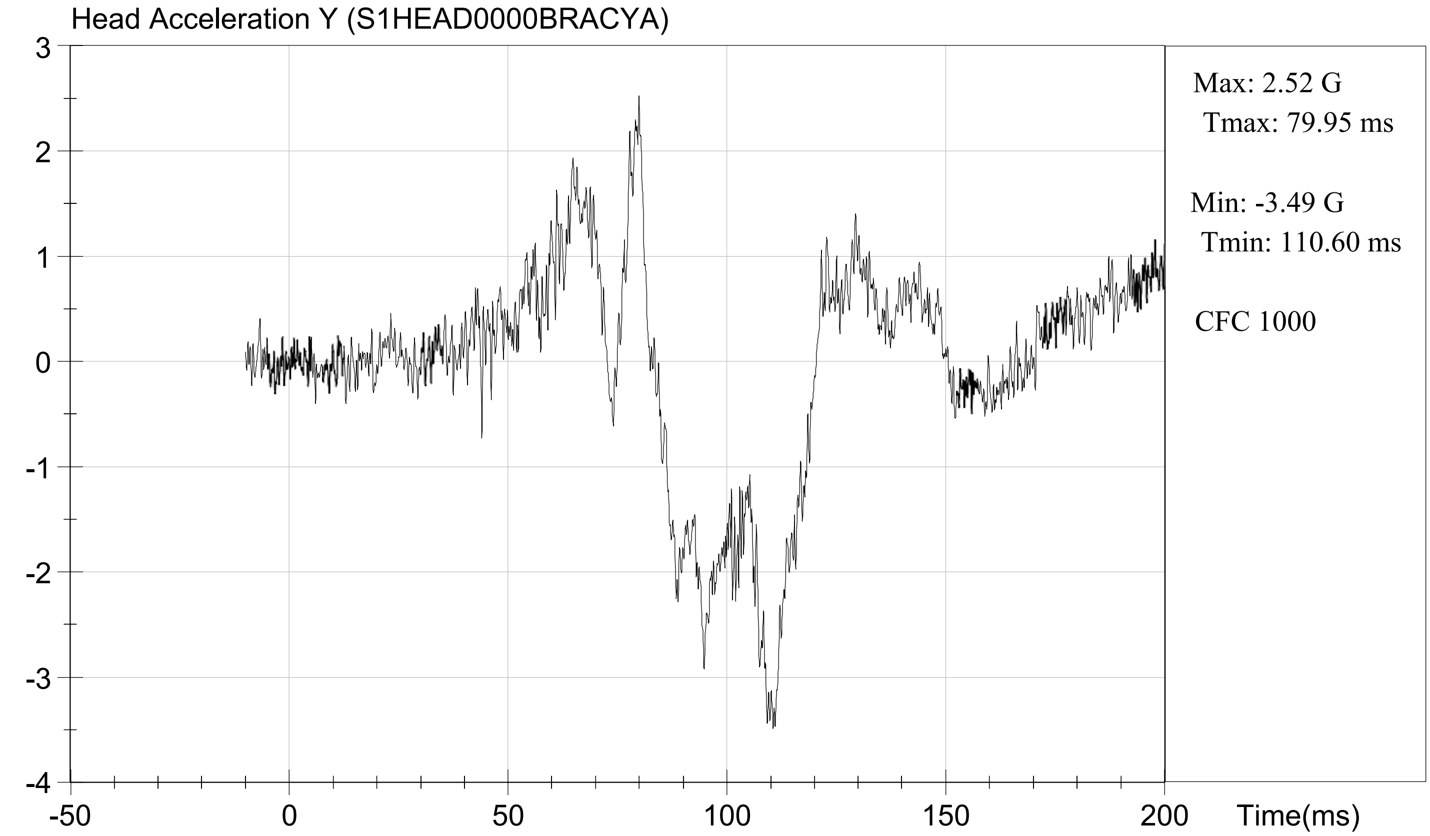
Head Acceleration Y (S1HEAD0000BRACYA)
3
2
1
0
-1
-2
-3
-4
-50
0
50
100
150
200
Time(ms)
Max: 2.52 G
Tmax: 79.95 ms
Min: -3.49 G
Tmin: 110.60 ms
CFC 1000

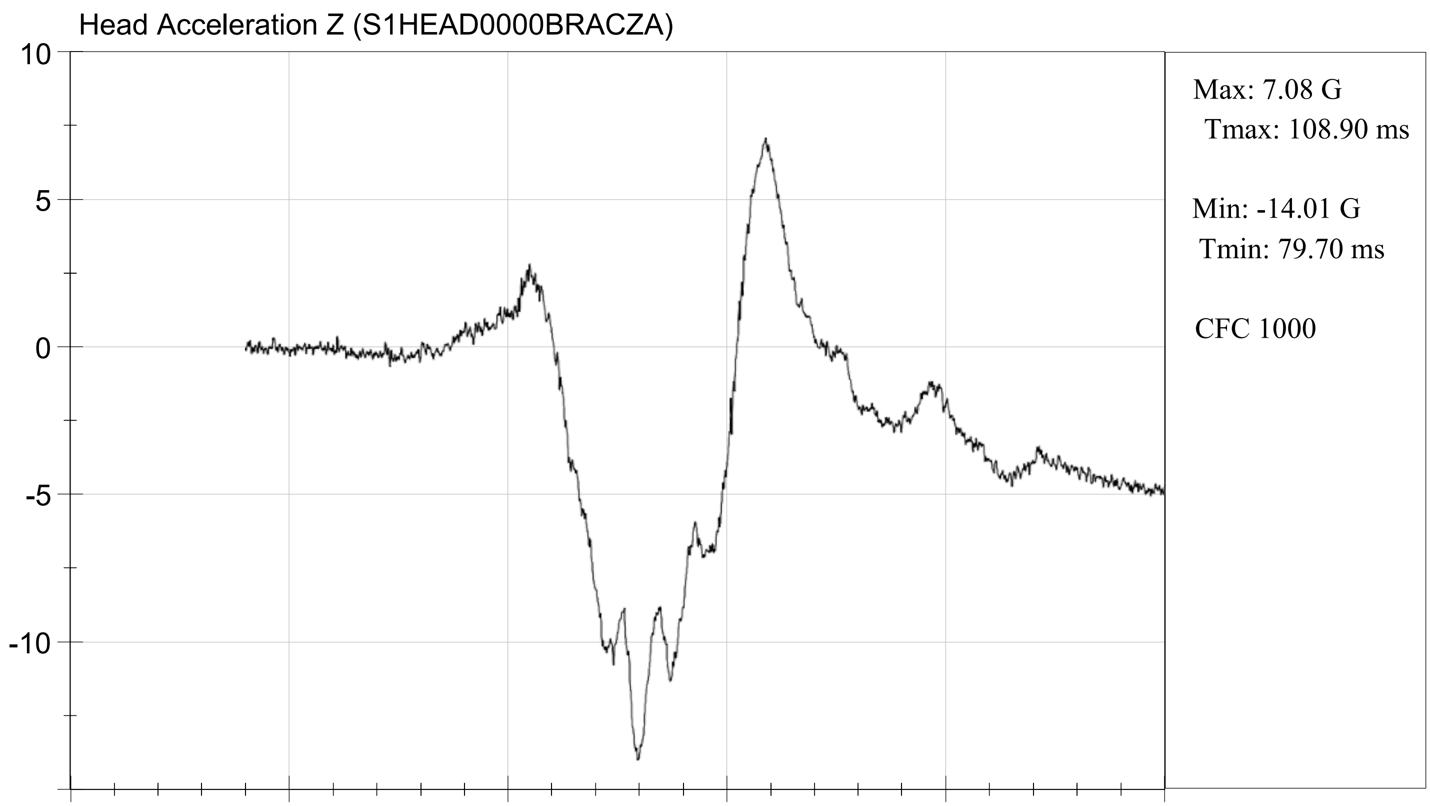
Head Acceleration Z (S1HEAD0000BRACZA)
10
5
0
-5
-10
Max: 7.08 G
Tmax: 108.90 ms
Min: -14.01 G
Tmin: 79.70 ms
CFC 1000

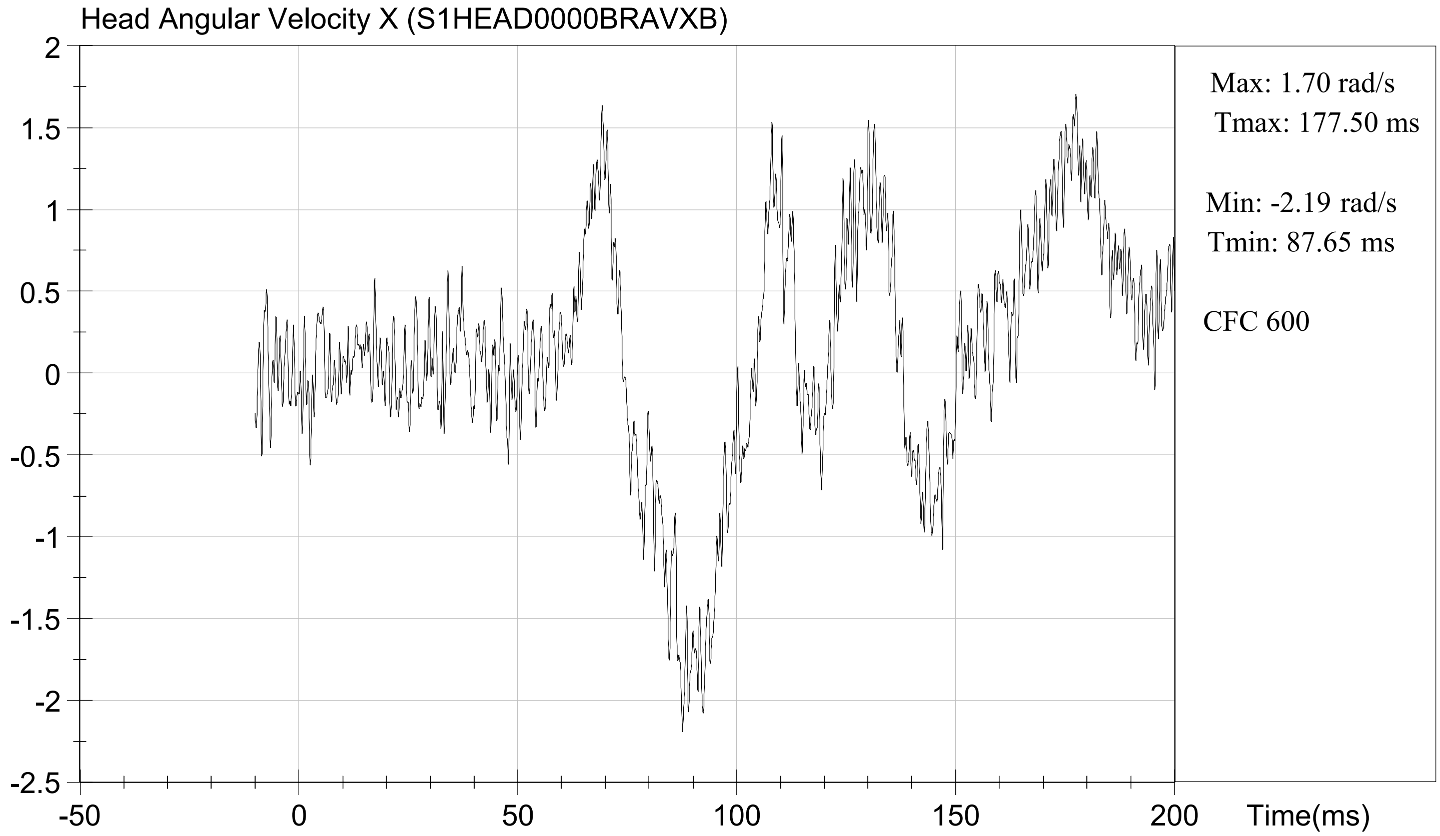
Head Angular Velocity X (S1HEAD0000BRAVXB)
2
1.5
1
0.5
0
-0.5
-1
-1.5
-2
-2.5
-50
0
50
100
150
200
Time(ms)
Max: 1.70 rad/s
Tmax: 177.50 ms
Min: -2.19 rad/s
Tmin: 87.65 ms
CFC 600

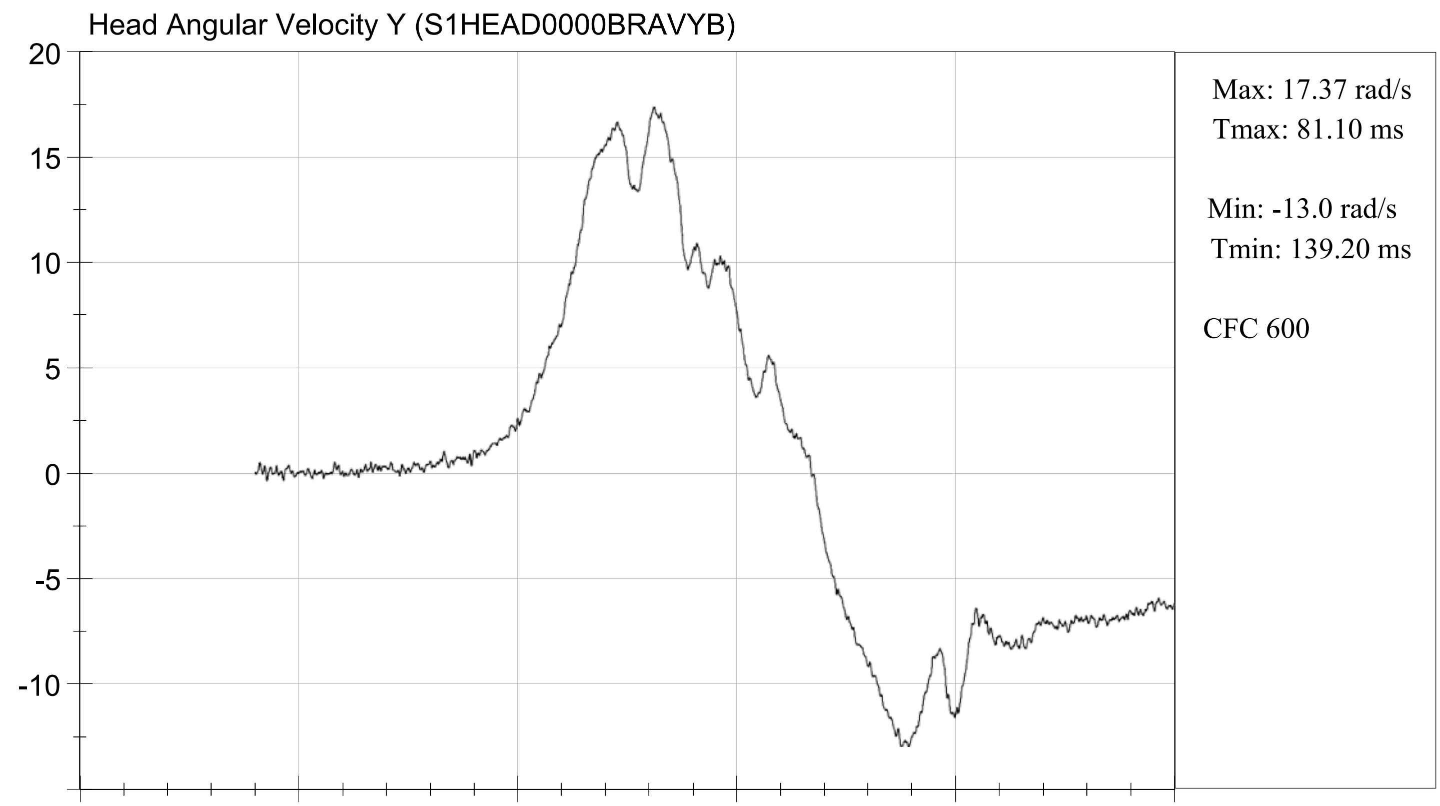
Head Angular Velocity Y (S1HEAD0000BRAVYB)
20
15
10
5
0
-5
-10
Max: 17.37 rad/s
Tmax: 81.10 ms
Min: -13.0 rad/s
Tmin: 139.20 ms
CFC 600

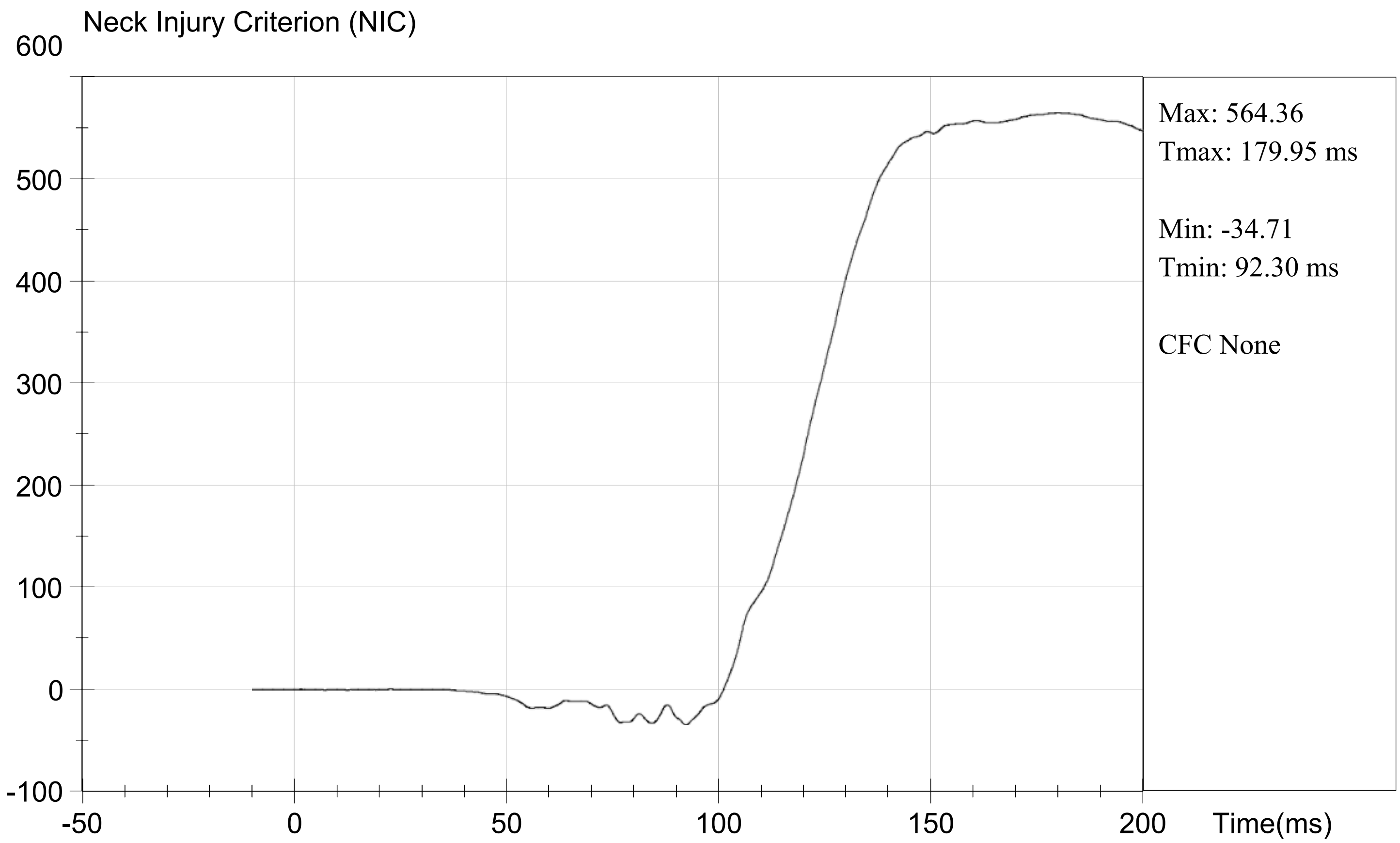
Neck Injury Criterion (NIC)
600
500
400
300
200
100
0
-100
-50
0
50
100
150
200
Time(ms)
Max: 564.36
Tmax: 179.95 ms
Min: -34.71
Tmin: 92.30 ms
CFC None

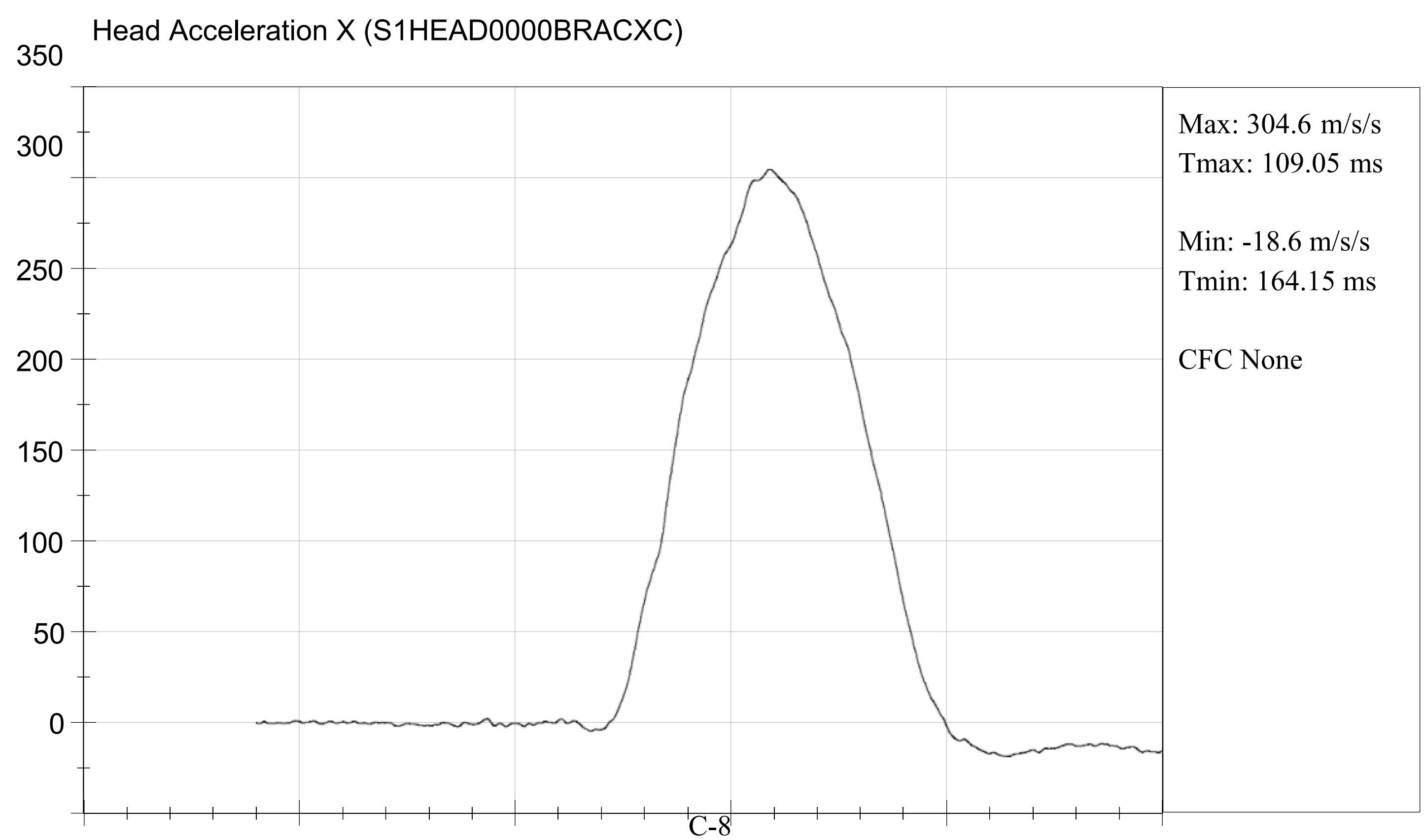
Head Acceleration X (S1HEAD0000BRACXC)
350
300
250
200
150
100
50
0
Max: 304.6 m/s/s
Tmax: 109.05 ms
Min: -18.6 m/s/s
Tmin: 164.15 ms
CFC None

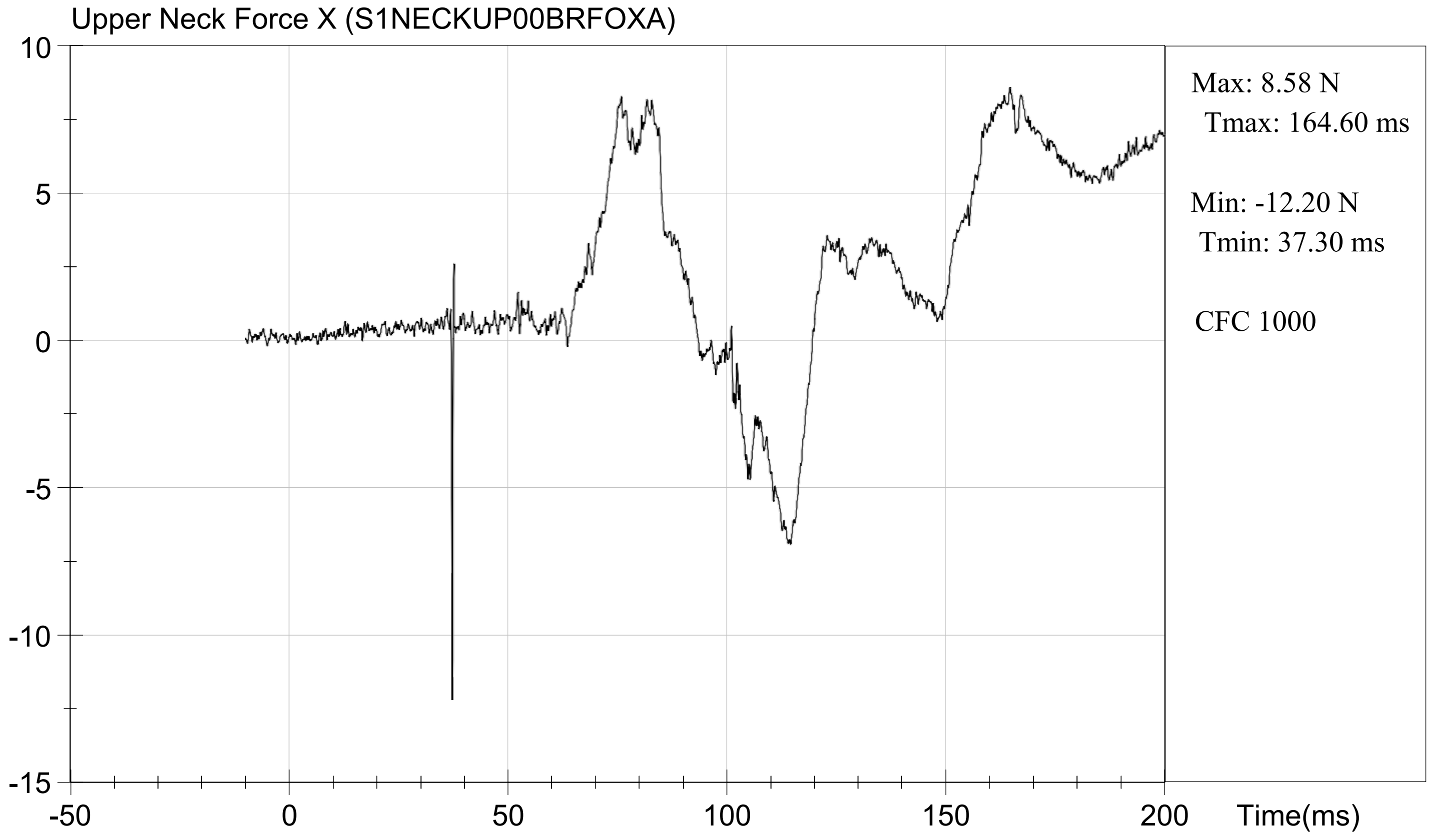
Upper Neck Force X (S1NECKUP00BRFOXA)
10
5
0
-5
-10
-15
-50
0
50
100
150
200
Time(ms)
Max: 8.58 N
Tmax: 164.60 ms
Min: -12.20 N
Tmin: 37.30 ms
CFC 1000

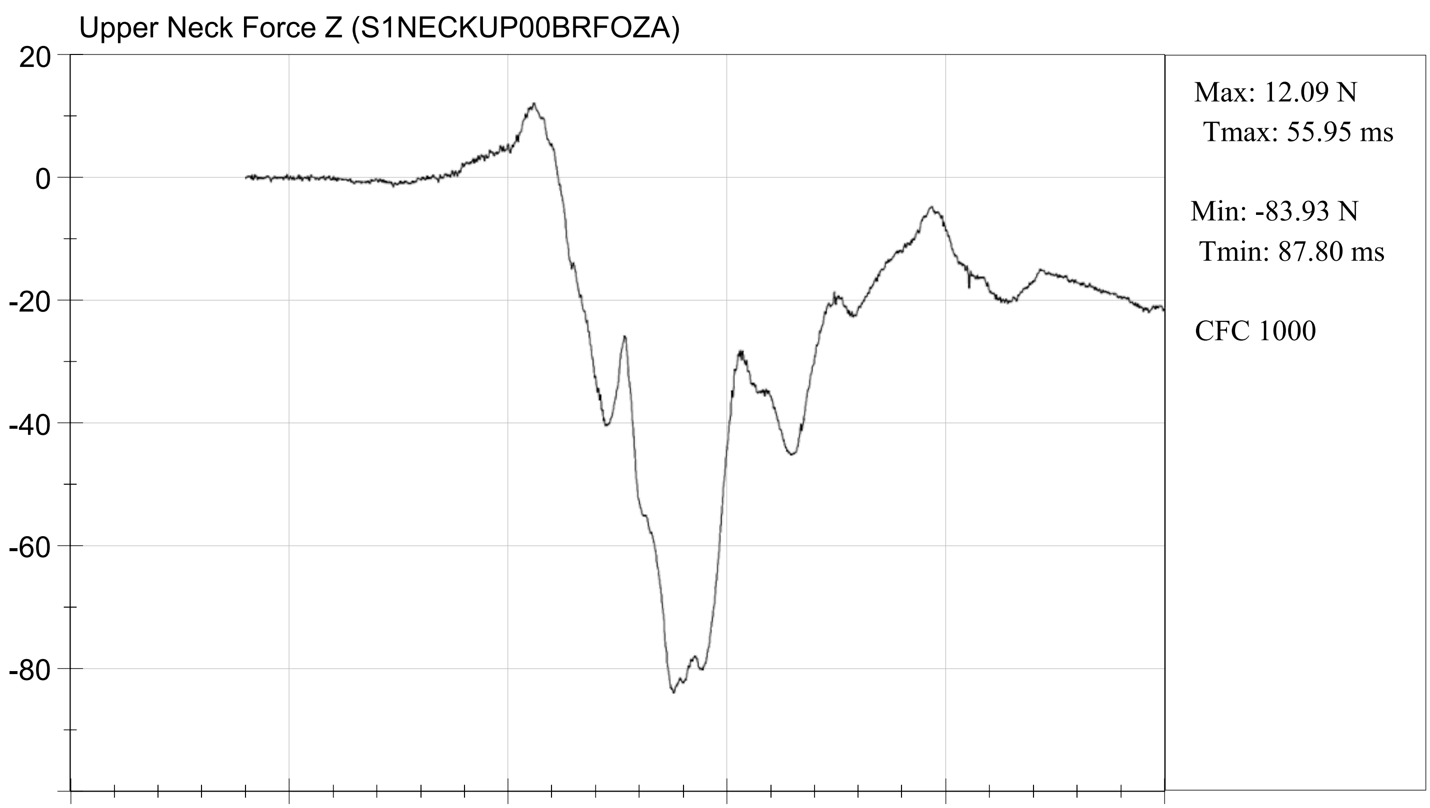
Upper Neck Force Z (S1NECKUP00BRFOZA)
20
0
-20
-40
-60
-80
Max: 12.09 N
Tmax: 55.95 ms
Min: -83.93 N
Tmin: 87.80 ms
CFC 1000

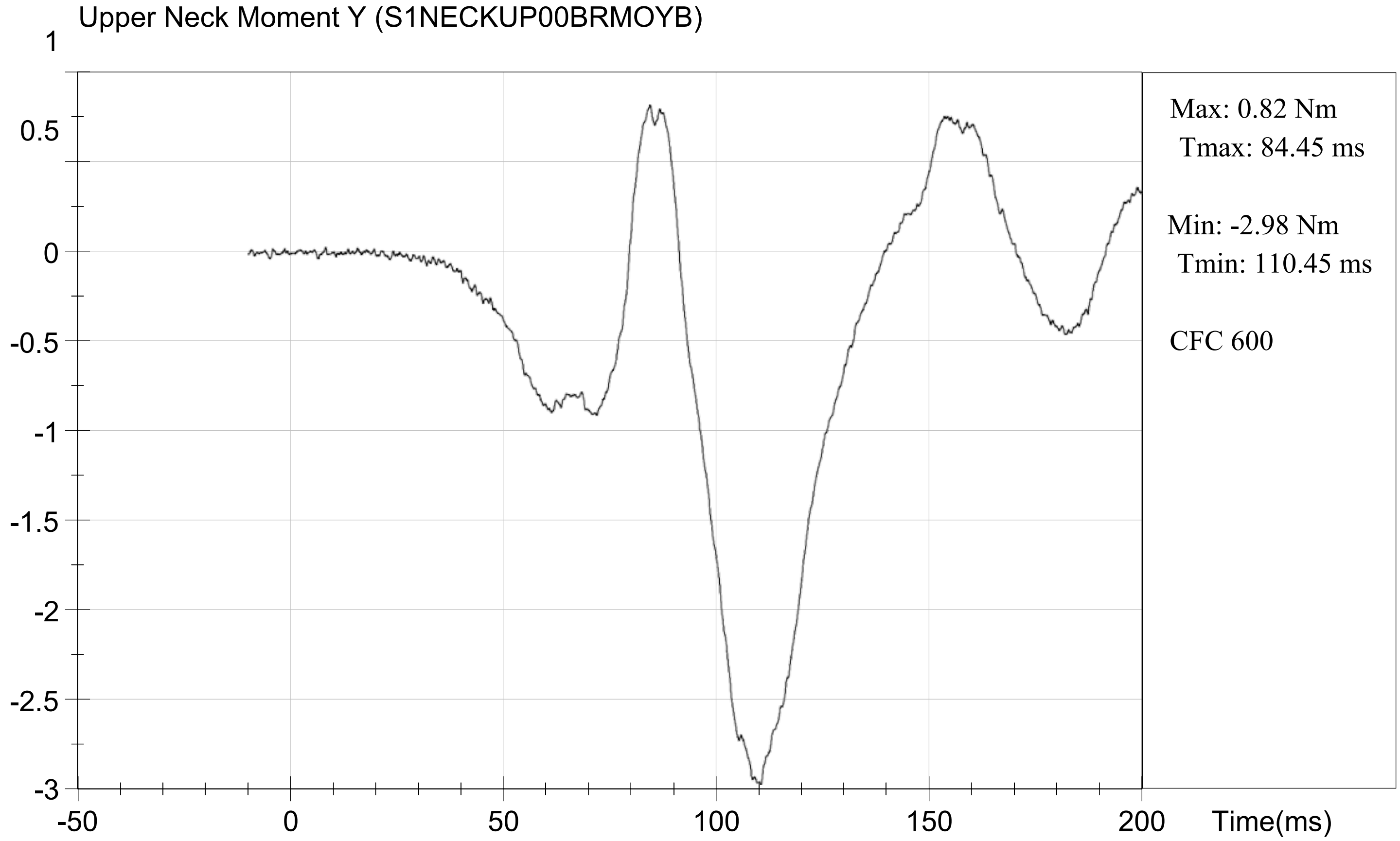
Upper Neck Moment Y (S1NECKUP00BRMOYB)
1
0.5
0
-0.5
-1
-1.5
-2
-2.5
-3
-50
0
50
100
150
200
Time(ms)
Max: 0.82 Nm
Tmax: 84.45 ms
Min: -2.98 Nm
Tmin: 110.45 ms
CFC 600

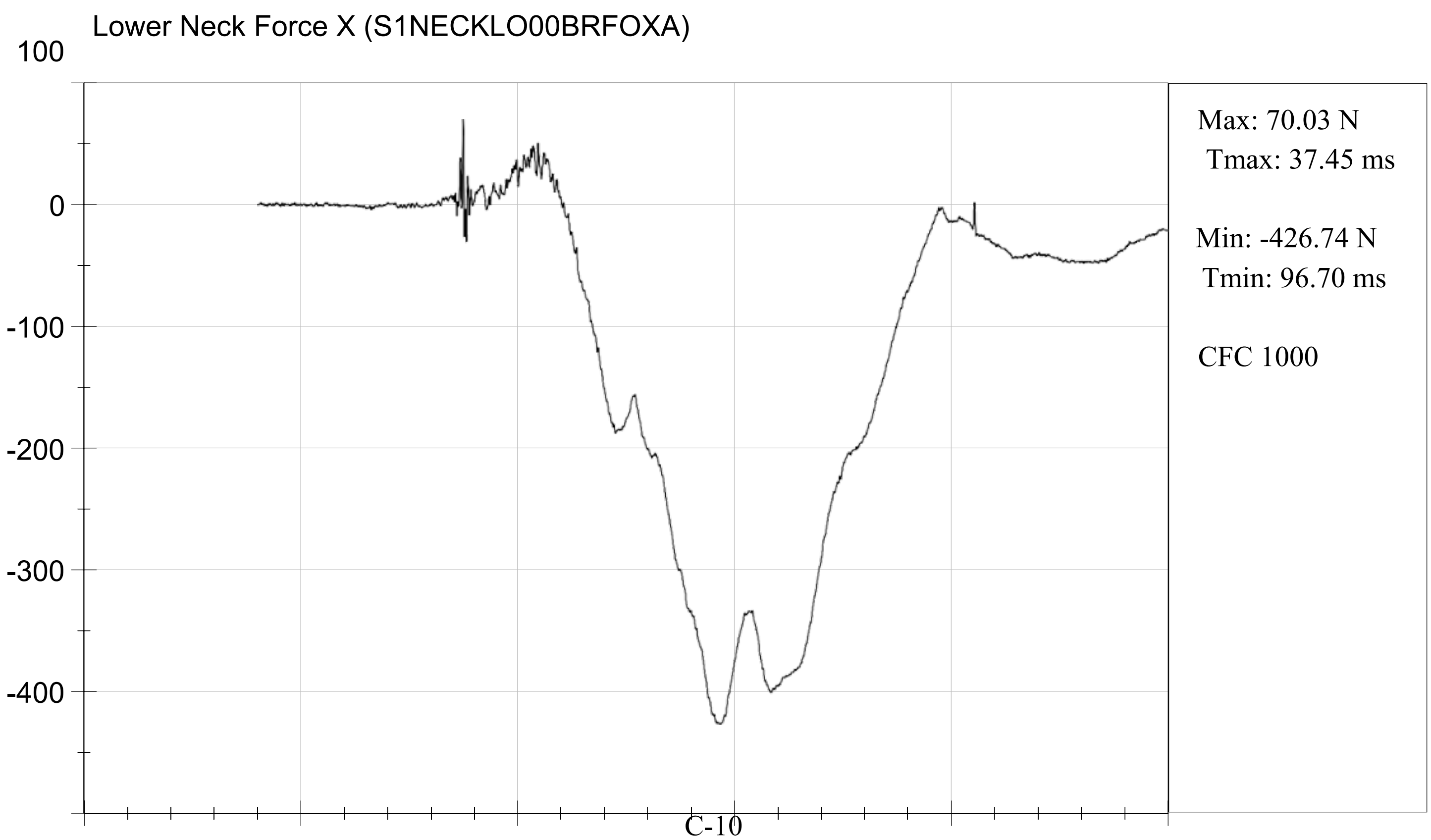
Lower Neck Force X (S1NECKLO00BRFOXA)
100
0
-100
-200
-300
-400
Max: 70.03 N
Tmax: 37.45 ms
Min: -426.74 N
Tmin: 96.70 ms
CFC 1000

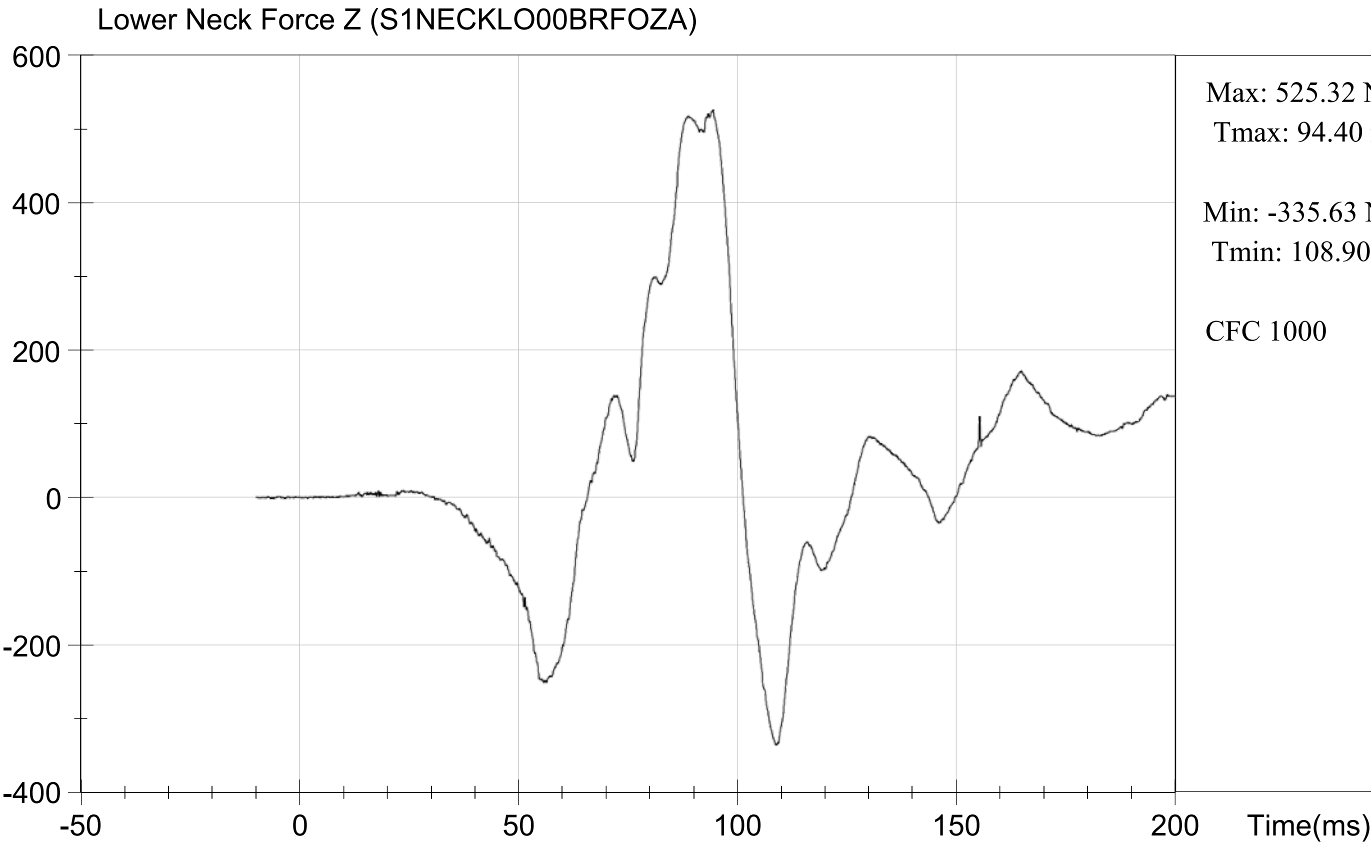
Lower Neck Force Z (S1NECKLO00BRFOZA)
600
400
200
0
-200
-400
-50
0
50
100
150
200
Time(ms)
Max: 525.32 N
Tmax: 94.40 ms
Min: -335.63 N
Tmin: 108.90 ms
CFC 1000

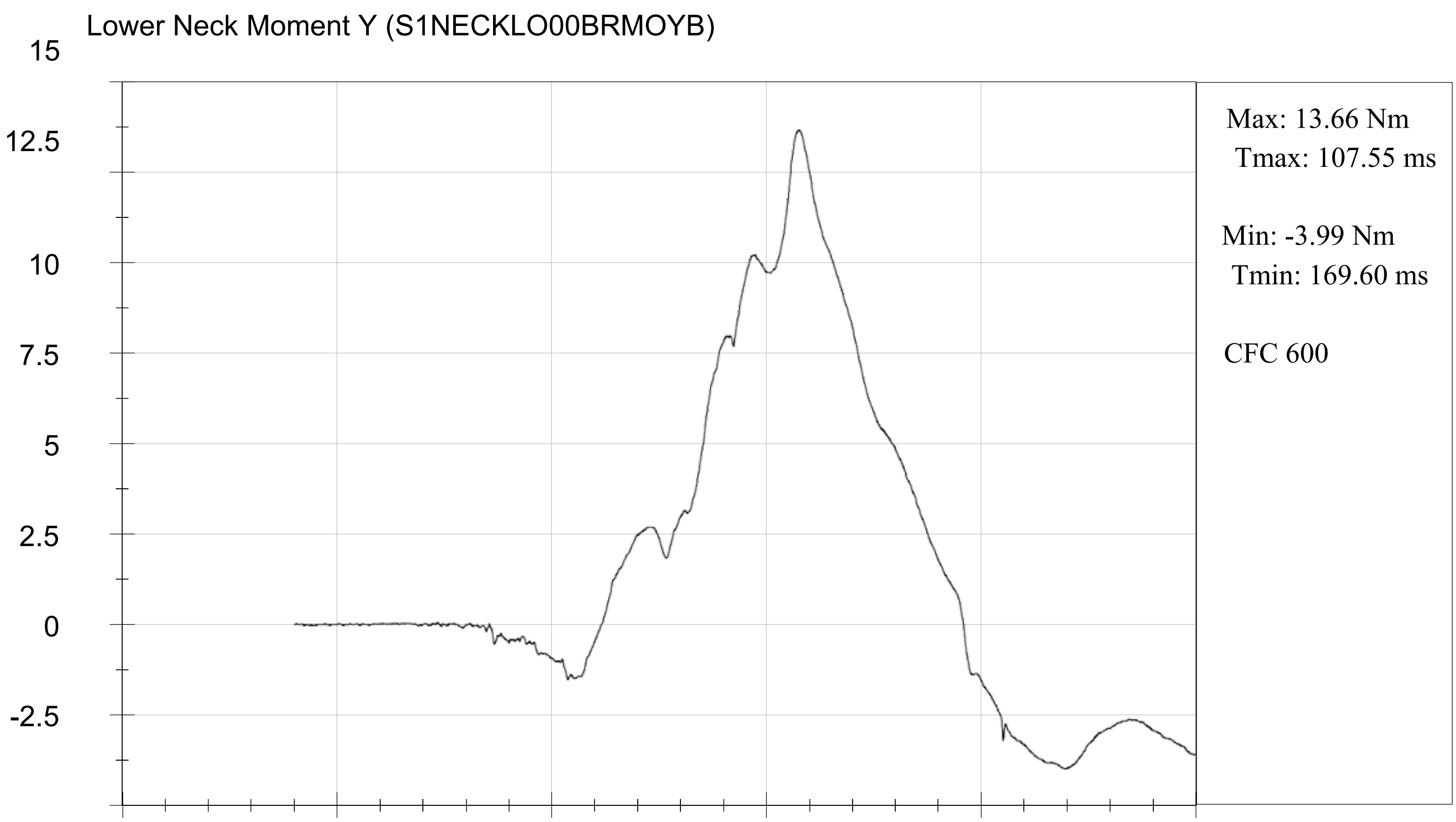
Lower Neck Moment Y (S1NECKLO00BRMOYB)
15
12.5
10
7.5
5
2.5
0
-2.5
Max: 13.66 Nm
Tmax: 107.55 ms
Min: -3.99 Nm
Tmin: 169.60 ms
CFC 600

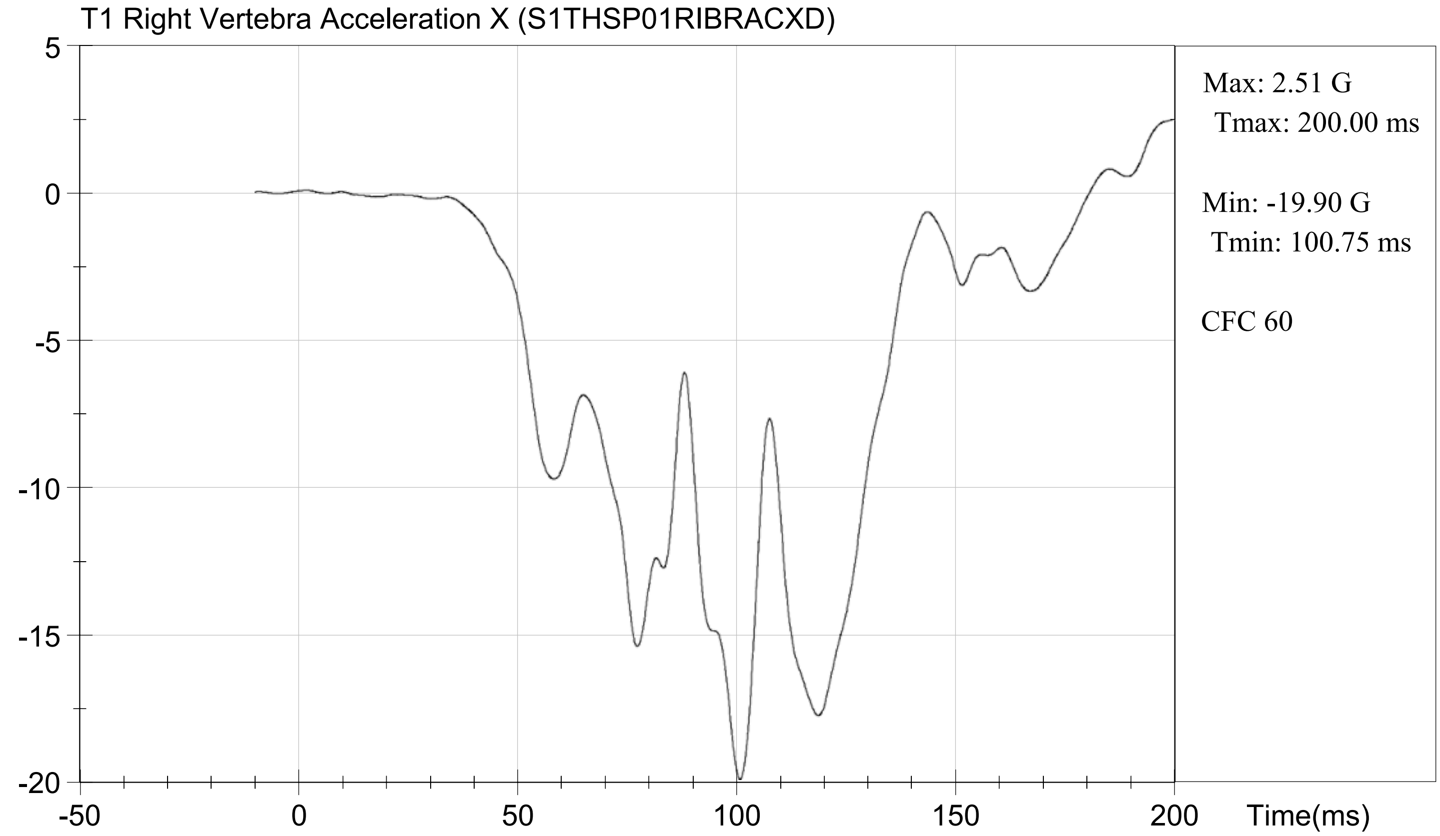
T1 Right Vertebra Acceleration X (S1THSP01RIBRACXD)
Max: 2.51 G
Tmax: 200.00 ms
Min: -19.90 G
Tmin: 100.75 ms
CFC 60
5
0
-5
-10
-15
-20
-50
0
50
100
150
200
Time(ms)

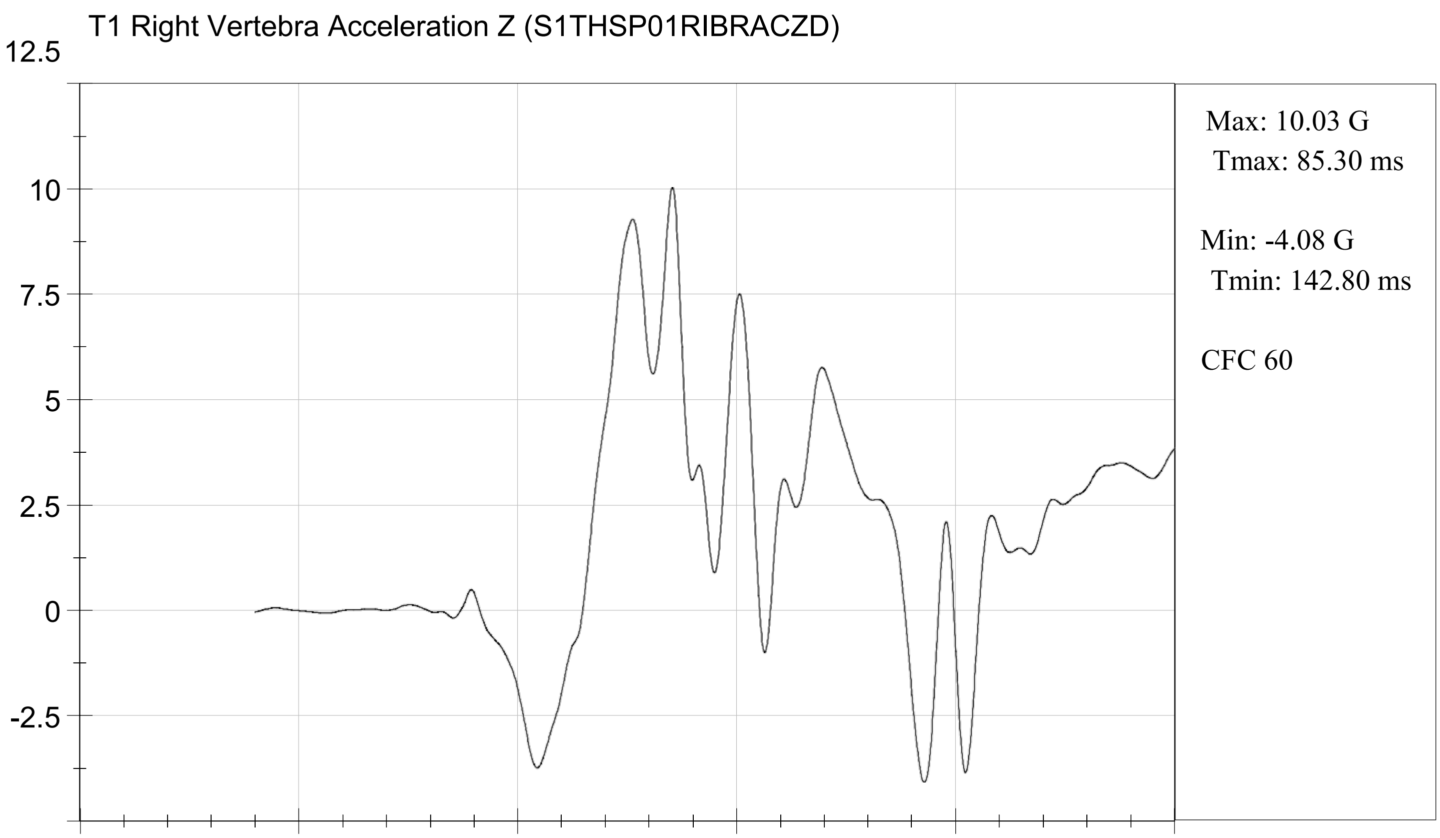
T1 Right Vertebra Acceleration Z (S1THSP01RIBRACZD)
Max: 10.03 G
Tmax: 85.30 ms
Min: -4.08 G
Tmin: 142.80 ms
CFC 60
12.5
10
7.5
5
2.5
0
-2.5

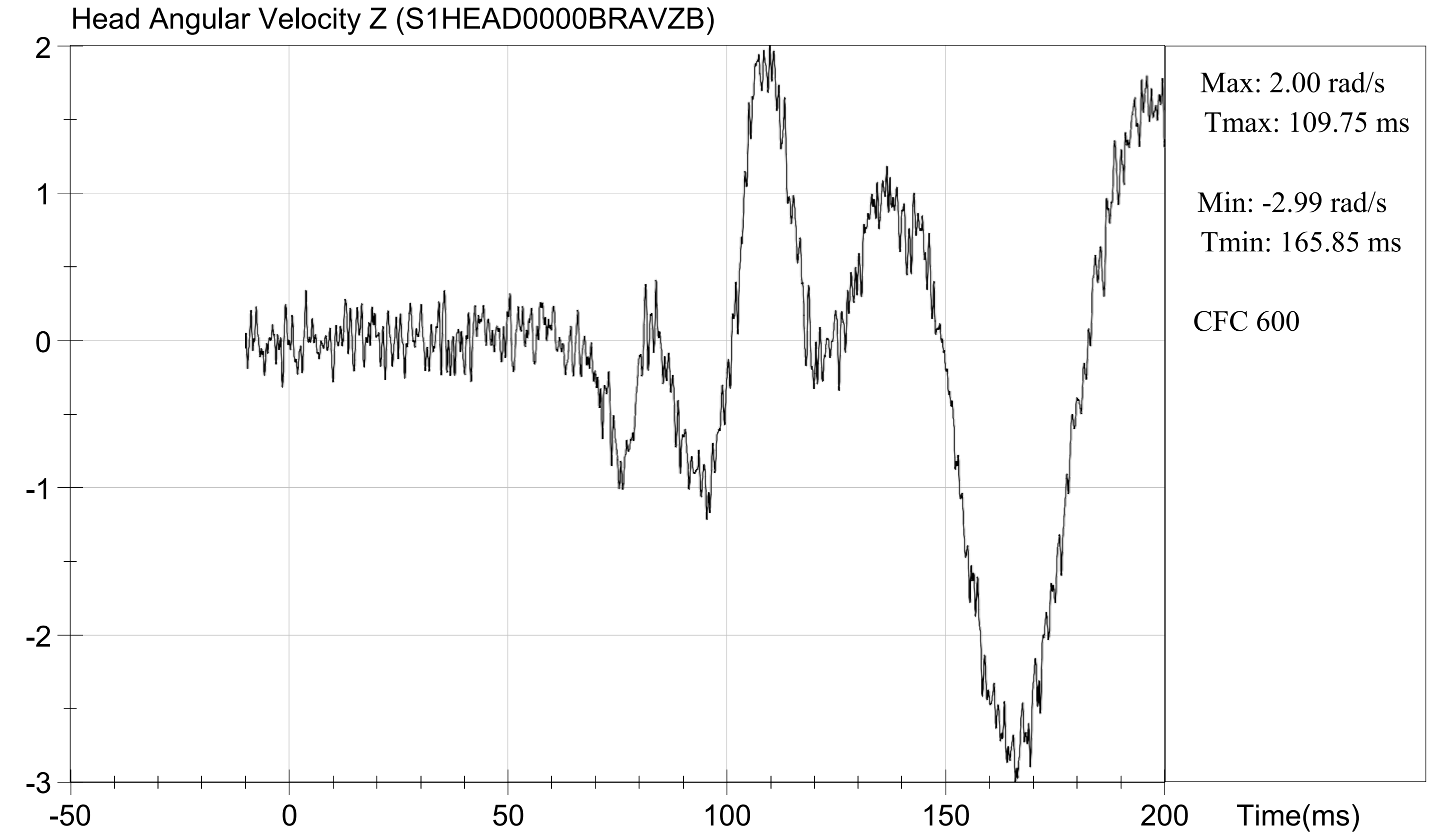
Head Angular Velocity Z (S1HEAD0000BRAVZB)
2
1
0
-1
-2
-3
-50
0
50
100
150
200
Time(ms)
Max: 2.00 rad/s
Tmax: 109.75 ms
Min: -2.99 rad/s
Tmin: 165.85 ms
CFC 600

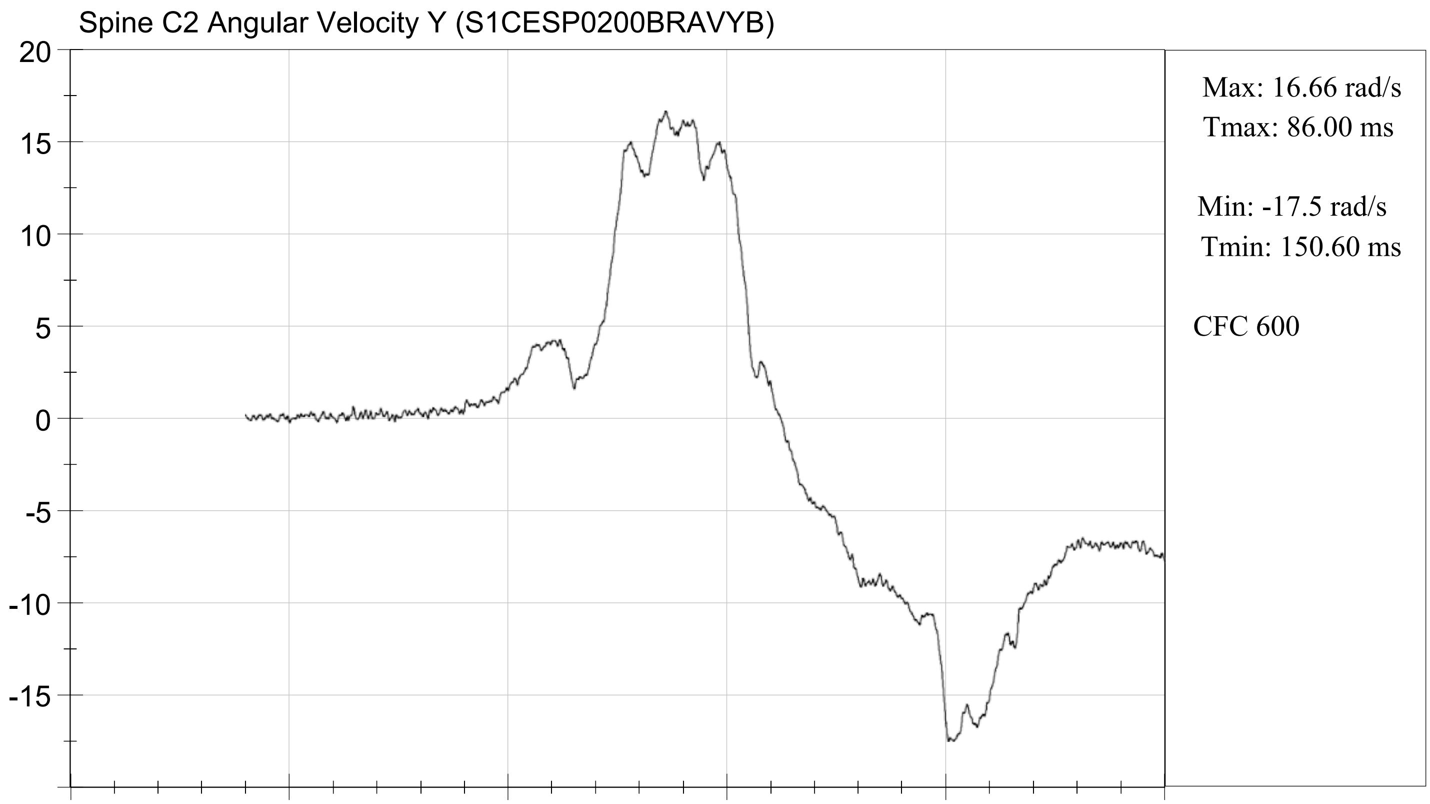
Spine C2 Angular Velocity Y (S1CESP0200BRAVYB)
20
15
10
5
0
-5
-10
-15
Max: 16.66 rad/s
Tmax: 86.00 ms
Min: -17.5 rad/s
Tmin: 150.60 ms
CFC 600

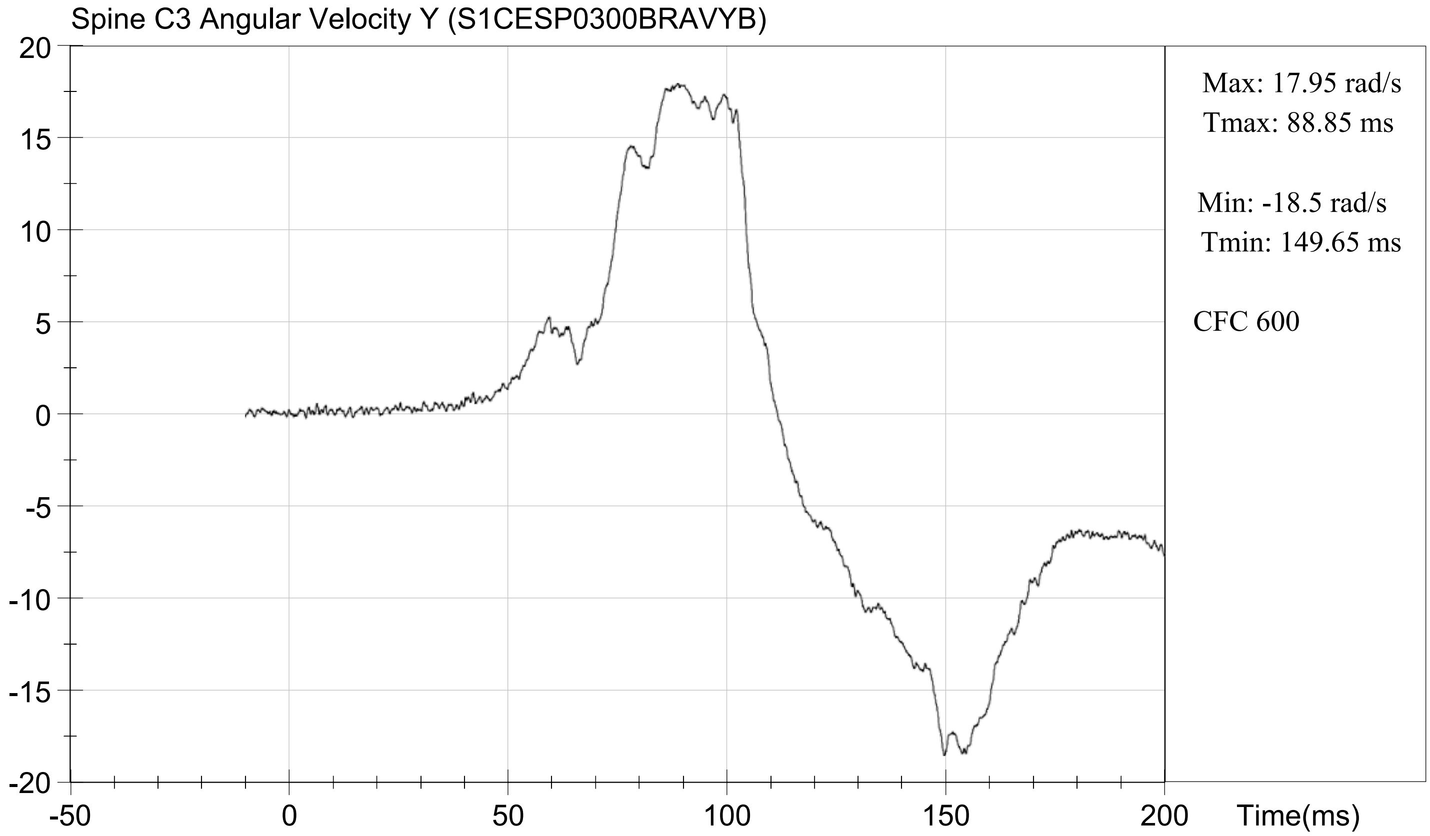
Spine C3 Angular Velocity Y (S1CESP0300BRAVYB)
20
15
10
5
0
-5
-10
-15
-20
-50
0
50
100
150
200
Time(ms)
Max: 17.95 rad/s
Tmax: 88.85 ms
Min: -18.5 rad/s
Tmin: 149.65 ms
CFC 600

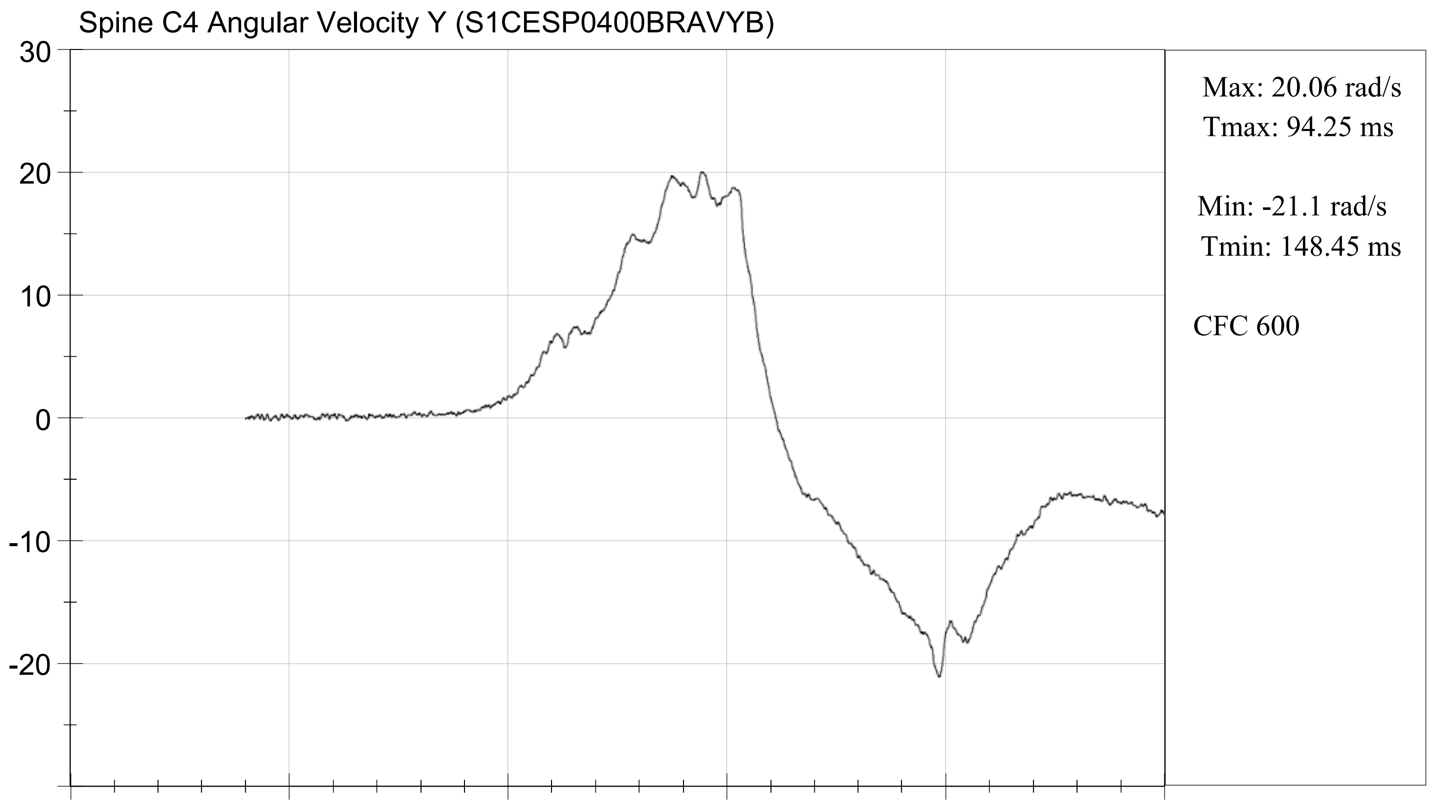
Spine C4 Angular Velocity Y (S1CESP0400BRAVYB)
30
20
10
0
-10
-20
Max: 20.06 rad/s
Tmax: 94.25 ms
Min: -21.1 rad/s
Tmin: 148.45 ms
CFC 600

Spine C5 Angular Velocity Y (S1CESP0500BRAVYB)

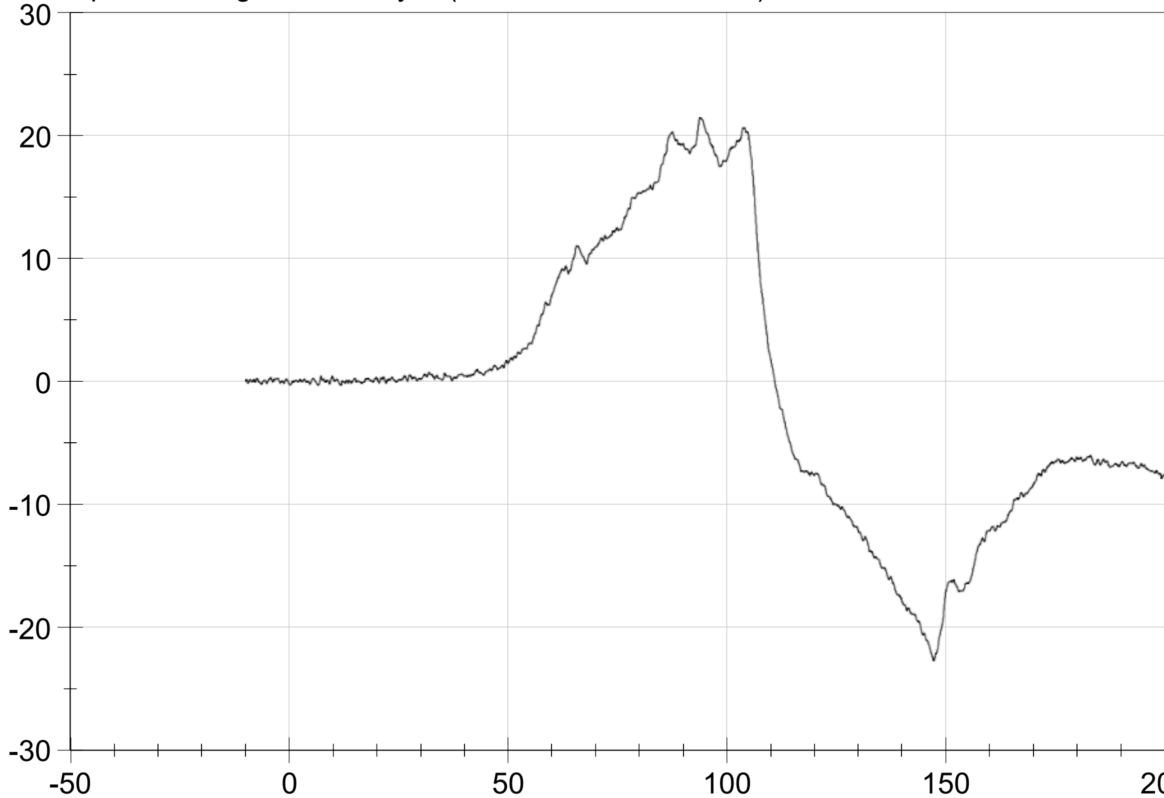

Max: 21.51 rad/s
Tmax: 93.85 ms

Min: -22.7 rad/s
Tmin: 147.15 ms

CFC 600

Spine C6 Angular Velocity Y (S1CESP0600BRAVYB)

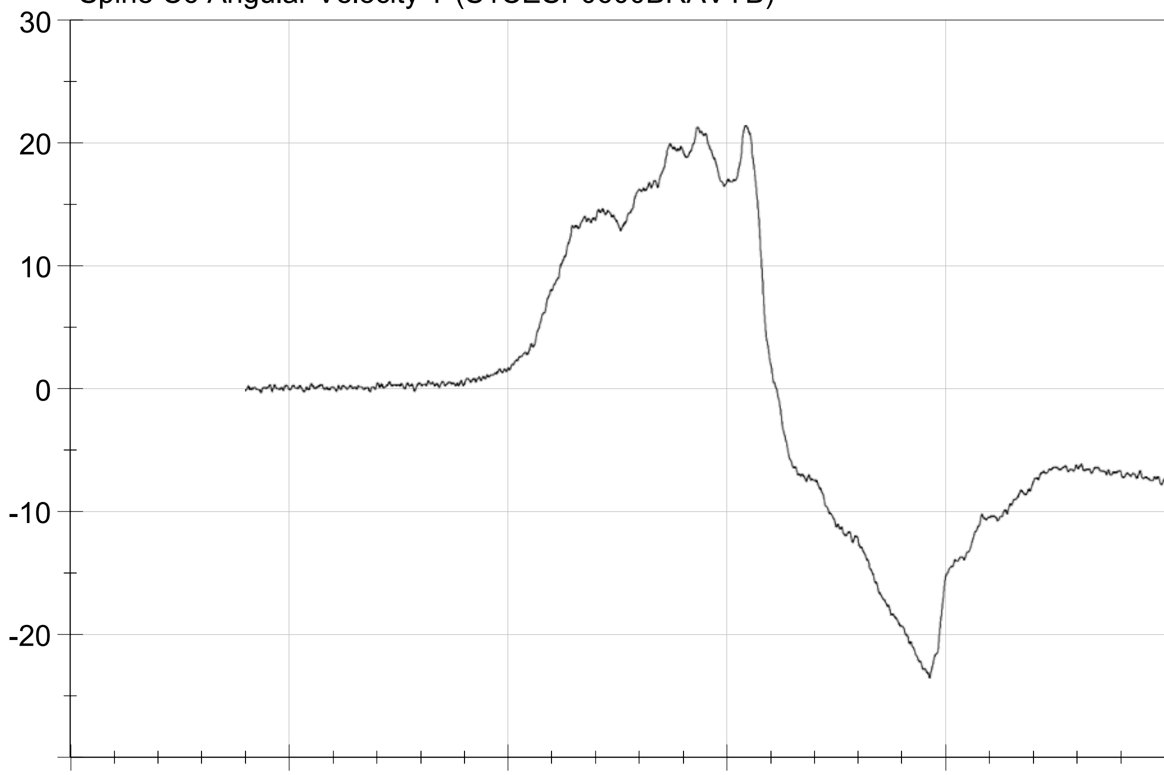

Max: 21.42 rad/s
Tmax: 104.30 ms

Min: -23.5 rad/s
Tmin: 146.25 ms

CFC 600

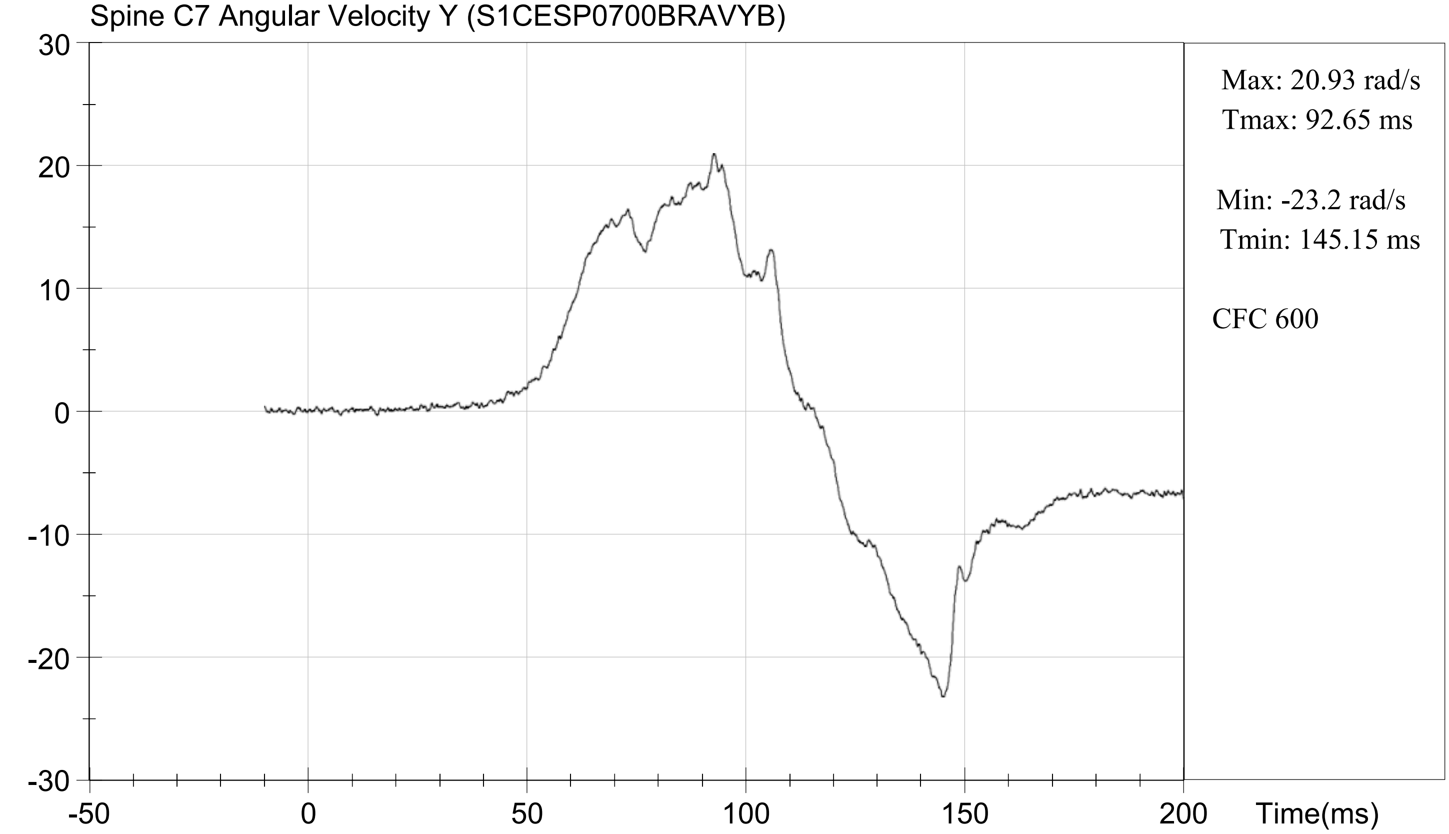
Spine C7 Angular Velocity Y (S1CESP0700BRAVYB)
30
20
10
0
-10
-20
-30
-50
0
50
100
150
200
Time(ms)
Max: 20.93 rad/s
Tmax: 92.65 ms
Min: -23.2 rad/s
Tmin: 145.15 ms
CFC 600

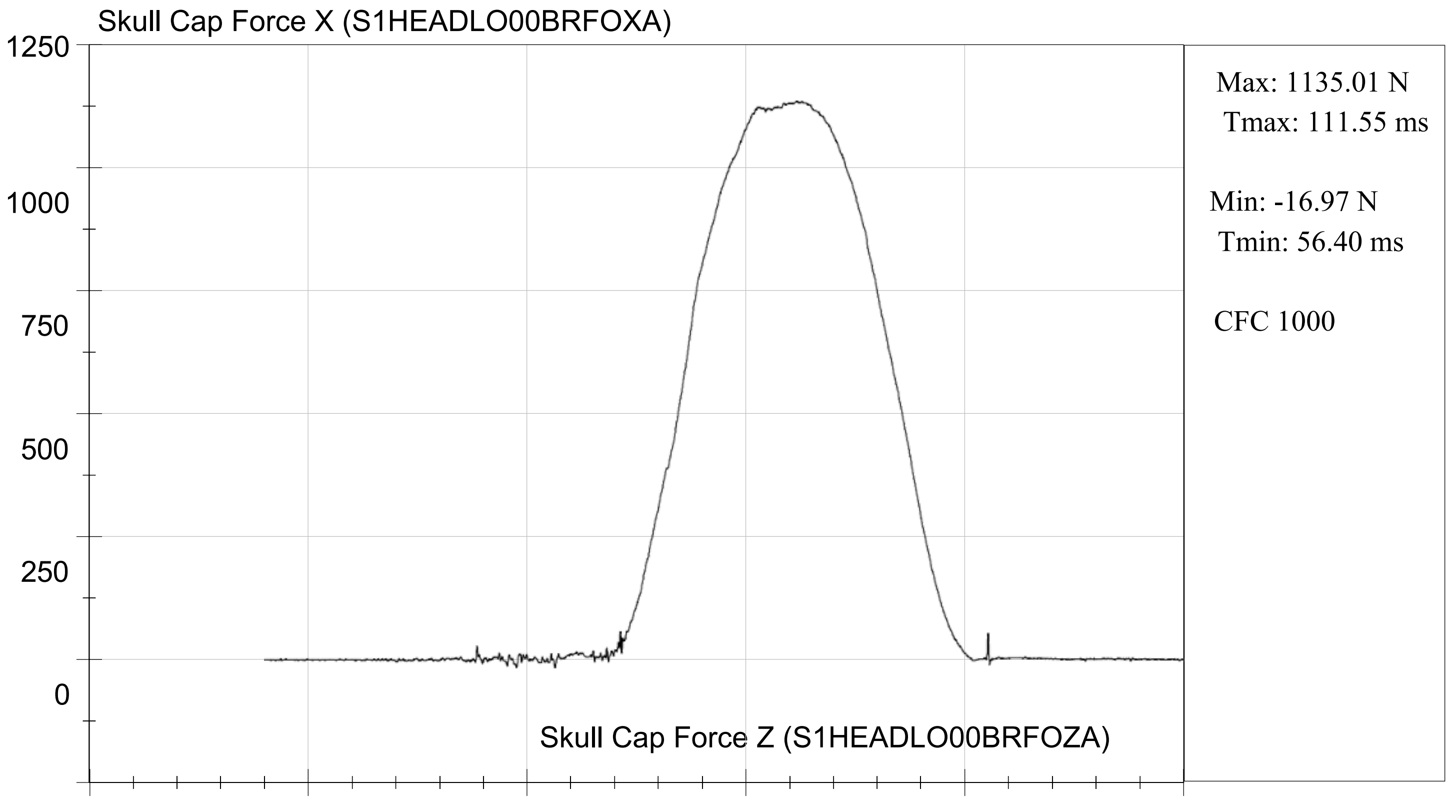
Skull Cap Force X (S1HEADLO00BRFOXA)
1250
1000
750
500
250
0
Max: 1135.01 N
Tmax: 111.55 ms
Min: -16.97 N
Tmin: 56.40 ms
CFC 1000
Skull Cap Force Z (S1HEADLO00BRFOZA)

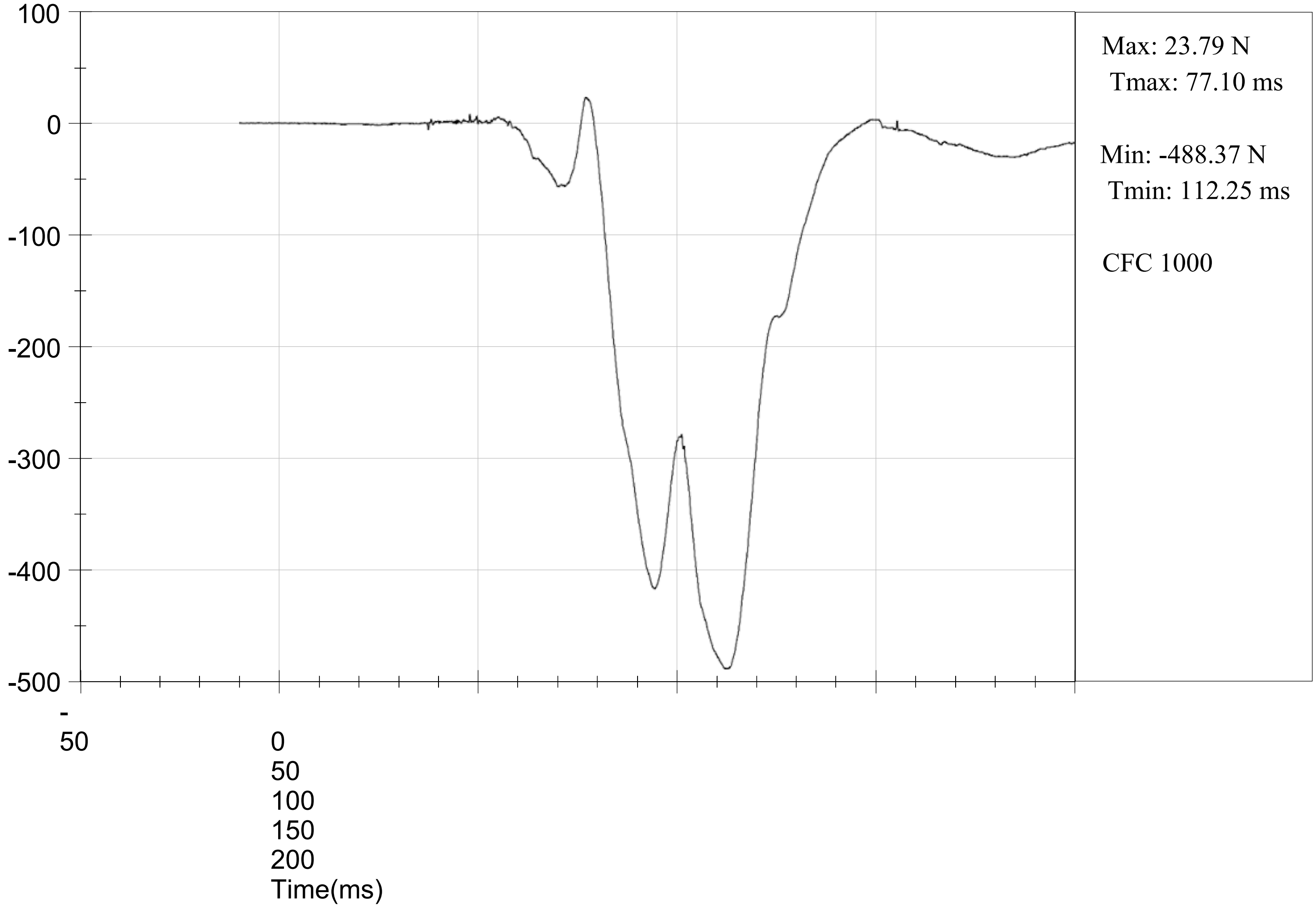
100
0
-100
-200
-300
-400
-500
-
50
0
50
100
150
200
Time(ms)
Max: 23.79 N
Tmax: 77.10 ms
Min: -488.37 N
Tmin: 112.25 ms
CFC 1000

Appendix D. FMVSS 301 Sled Test Report (Manual Seat)

Summary of the Test

Setup Information

Customer: EDAG
Job No.: C18S7-024.1
Sample ID: Sample 2
ATD: BioRID-II
Direction: Rearward
Seat Position: FR/FD/FD

Time: 15:00:30
Temperature: 22.9 °C
Humidity: 53 %RH

Test Results

Accelerometer 1 (S0SLED010000ACXD)

Peak Acceleration	19.86	G	42.65	ms
Peak Velocity Change	27.30	km/h	65.25	ms
HIC 15 (Time Duration = 15.000 ms)	55.06		105.900 to 120.900	ms
NIC Normalized Neck Injury Criterion	552.98		184.65	ms
One Meter Trap Verification	1010.638	mm	1.06	%
Video Strobe Time Shift from Raw Data			-4.20	ms

Post-Test Comments: See Result Table
Test Series Performed By: Scott McCarter, Carl Prange

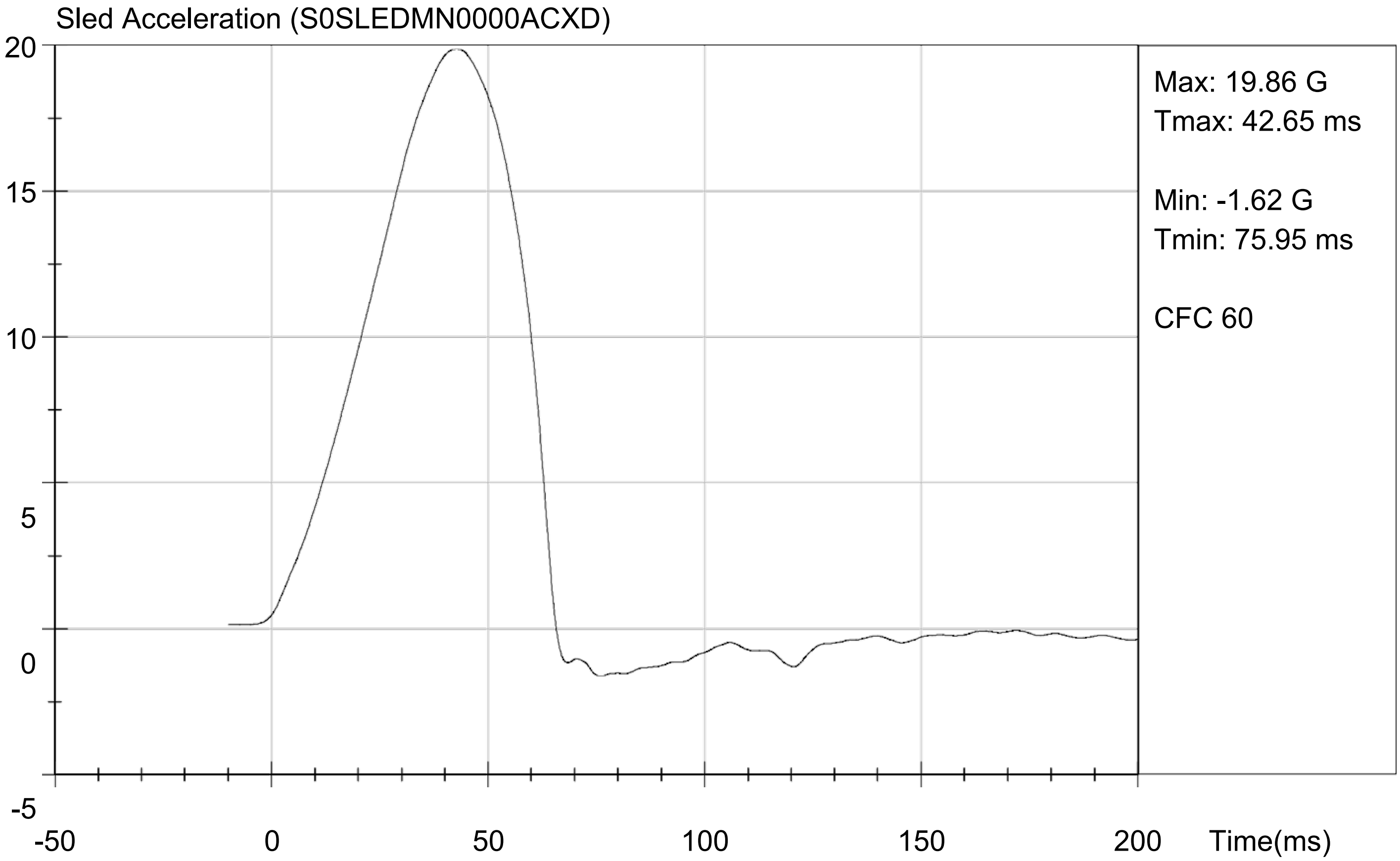

Sled Acceleration (S0SLEDMN0000ACXD)
20
15
10
5
0
-5
-50
0
50
100
150
200
Time(ms)
Max: 19.86 G
Tmax: 42.65 ms
Min: -1.62 G
Tmin: 75.95 ms
CFC 60

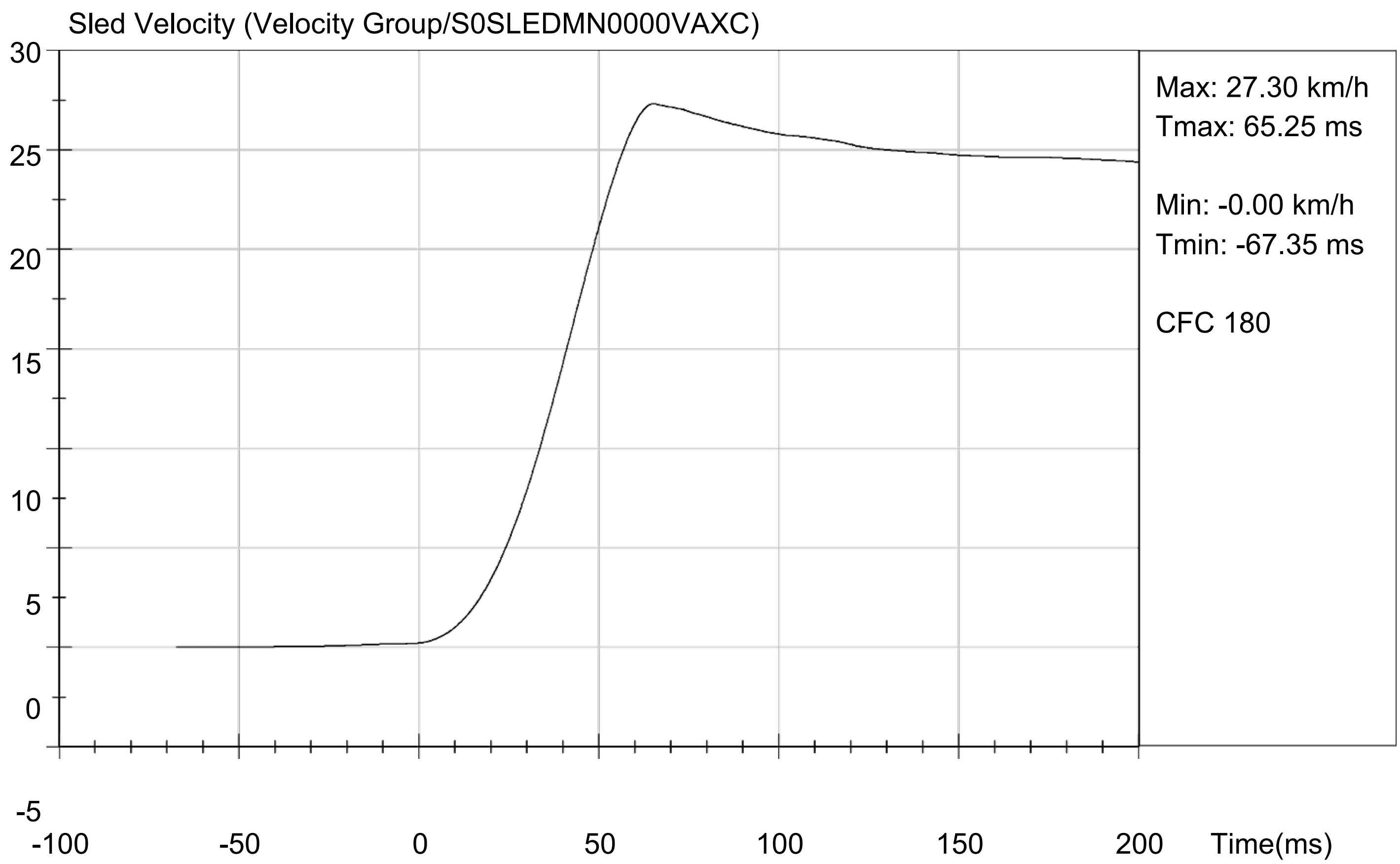

Sled Velocity (Velocity Group/S0SLEDMN0000VAXC)
30
25
20
15
10
5
0
-5
-100
-50
0
50
100
150
200
Time(ms)
Max: 27.30 km/h
Tmax: 65.25 ms
Min: -0.00 km/h
Tmin: -67.35 ms
CFC 180

Head Acceleration Resultant (S1HEAD0000BRACRA)

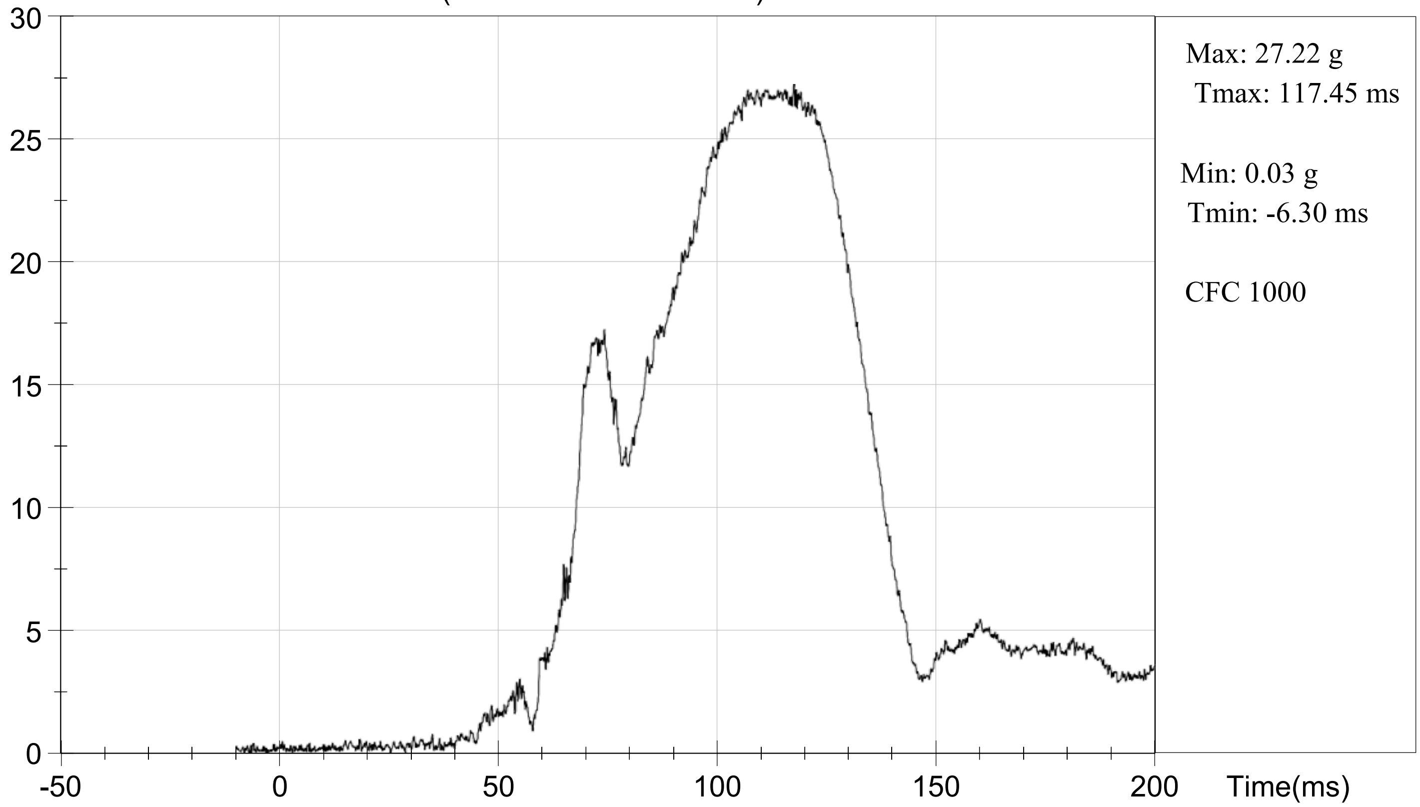

Head Acceleration X (S1HEAD0000BRACXA)

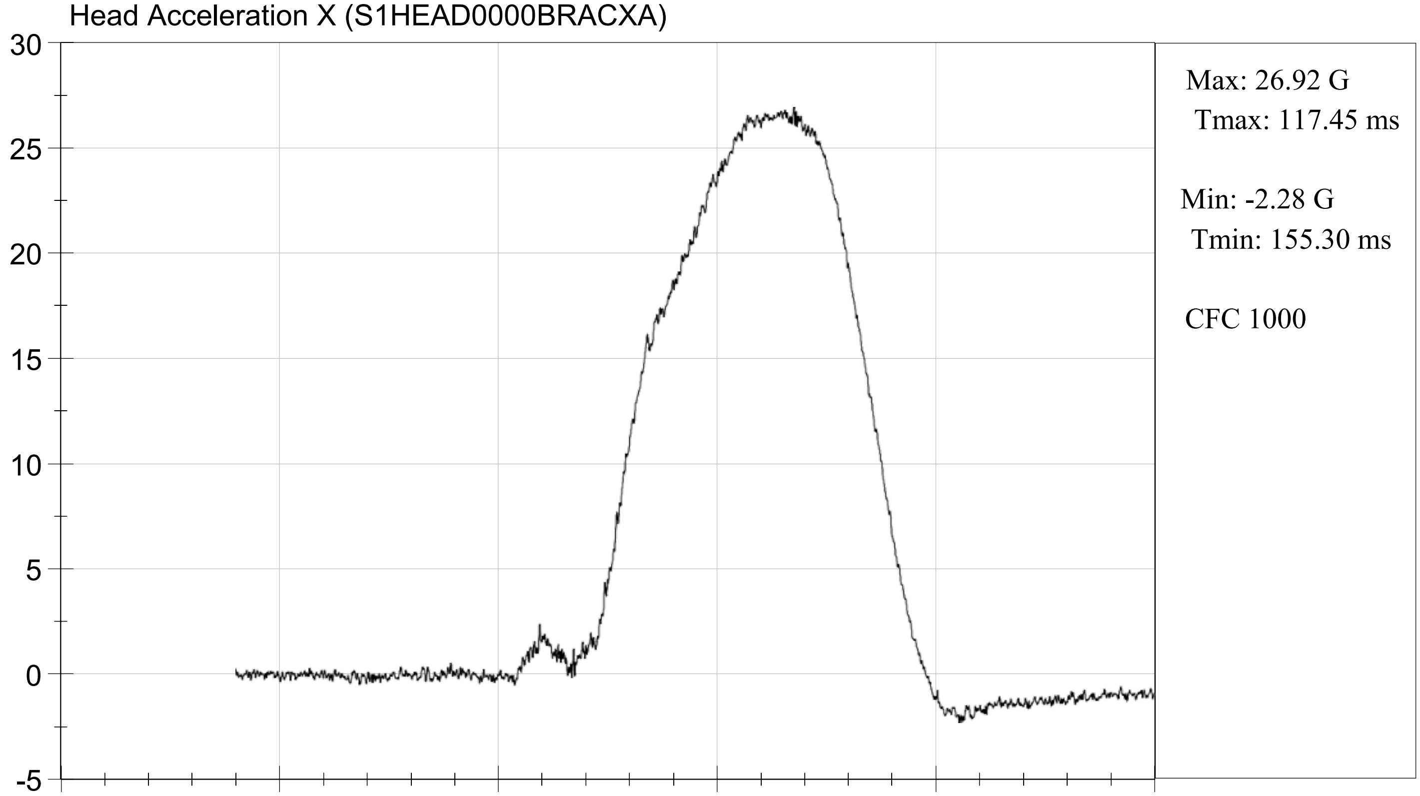

Head Acceleration Y (S1HEAD0000BRACYA)

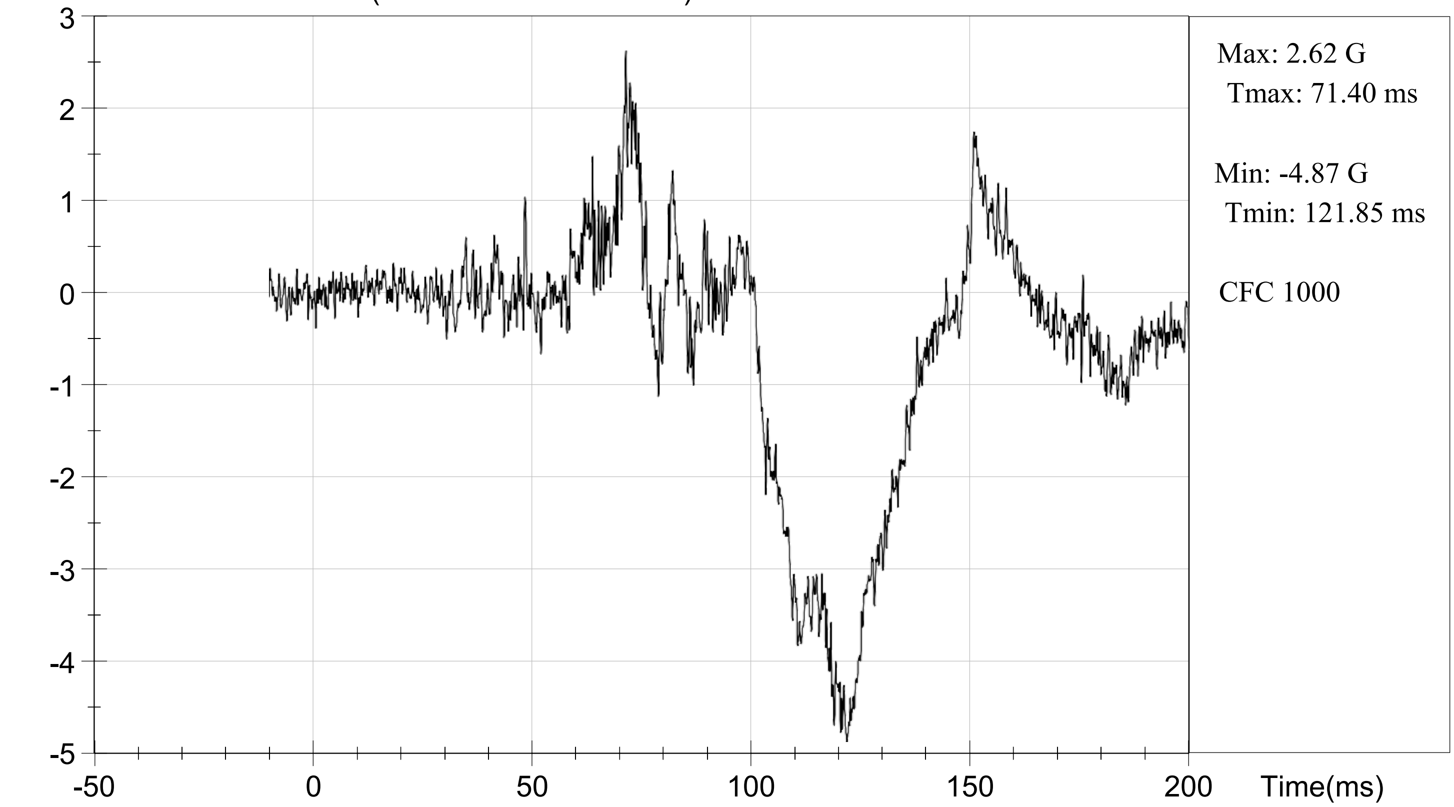

Head Acceleration Z (S1HEAD0000BRACZA)

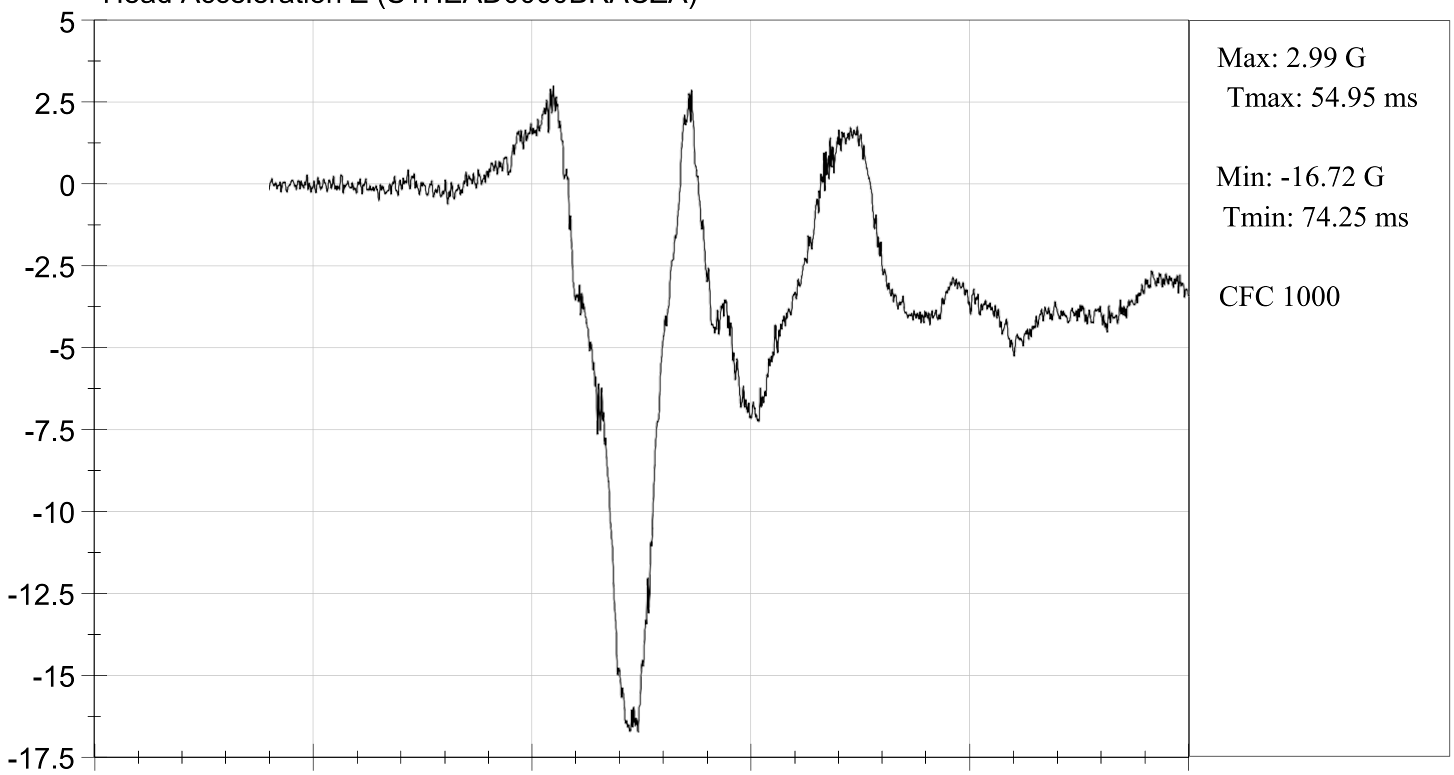

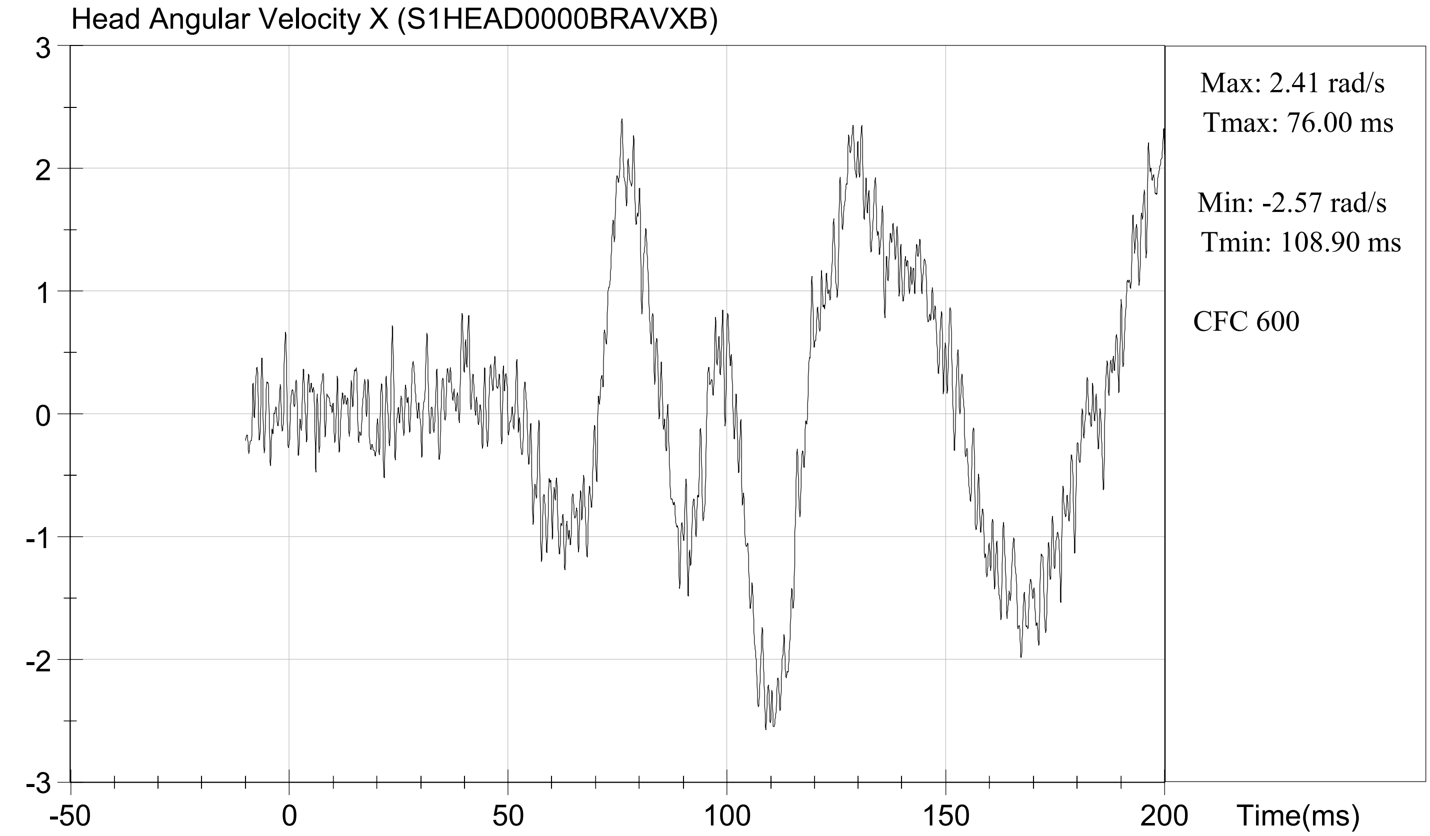
Head Angular Velocity X (S1HEAD0000BRAVXB)
Max: 2.41 rad/s
Tmax: 76.00 ms
Min: -2.57 rad/s
Tmin: 108.90 ms
CFC 600
Time(ms)
3
2
1
0
-1
-2
-3
-50
0
50
100
150
200

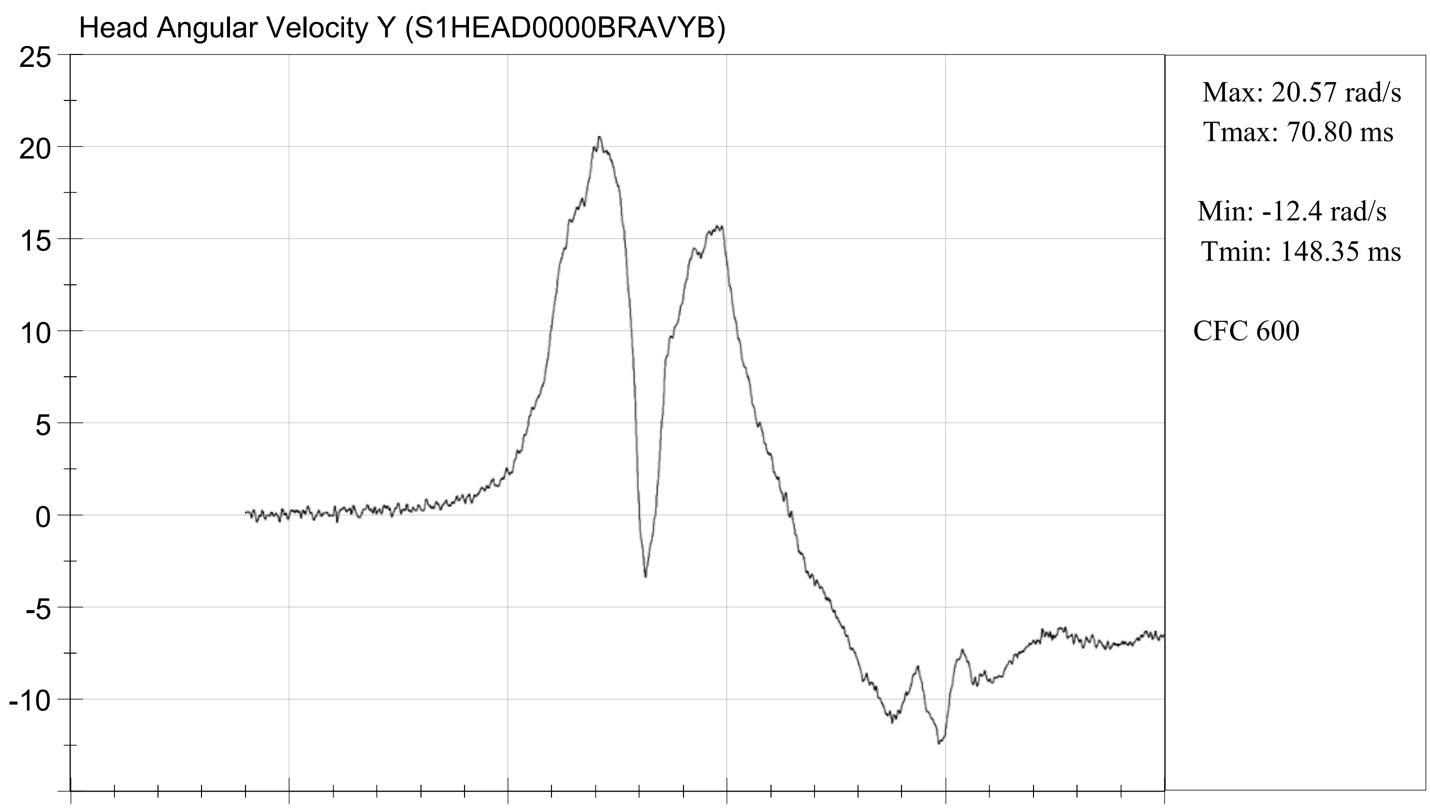
Head Angular Velocity Y (S1HEAD0000BRAVYB)
Max: 20.57 rad/s
Tmax: 70.80 ms
Min: -12.4 rad/s
Tmin: 148.35 ms
CFC 600
25
20
15
10
5
0
-5
-10

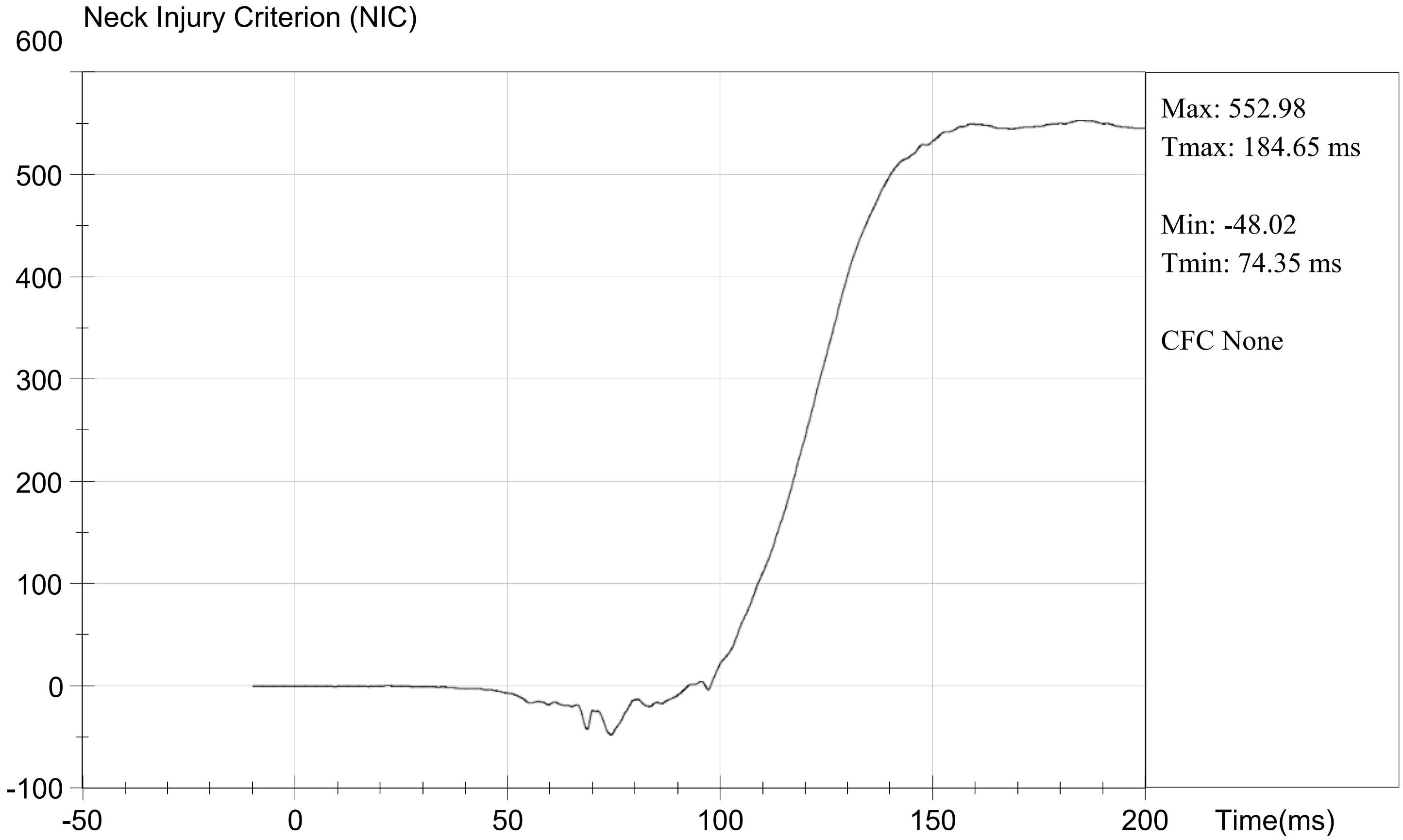
Neck Injury Criterion (NIC)
600
500
400
300
200
100
0
-100
-50
0
50
100
150
200
Time(ms)
Max: 552.98
Tmax: 184.65 ms
Min: -48.02
Tmin: 74.35 ms
CFC None

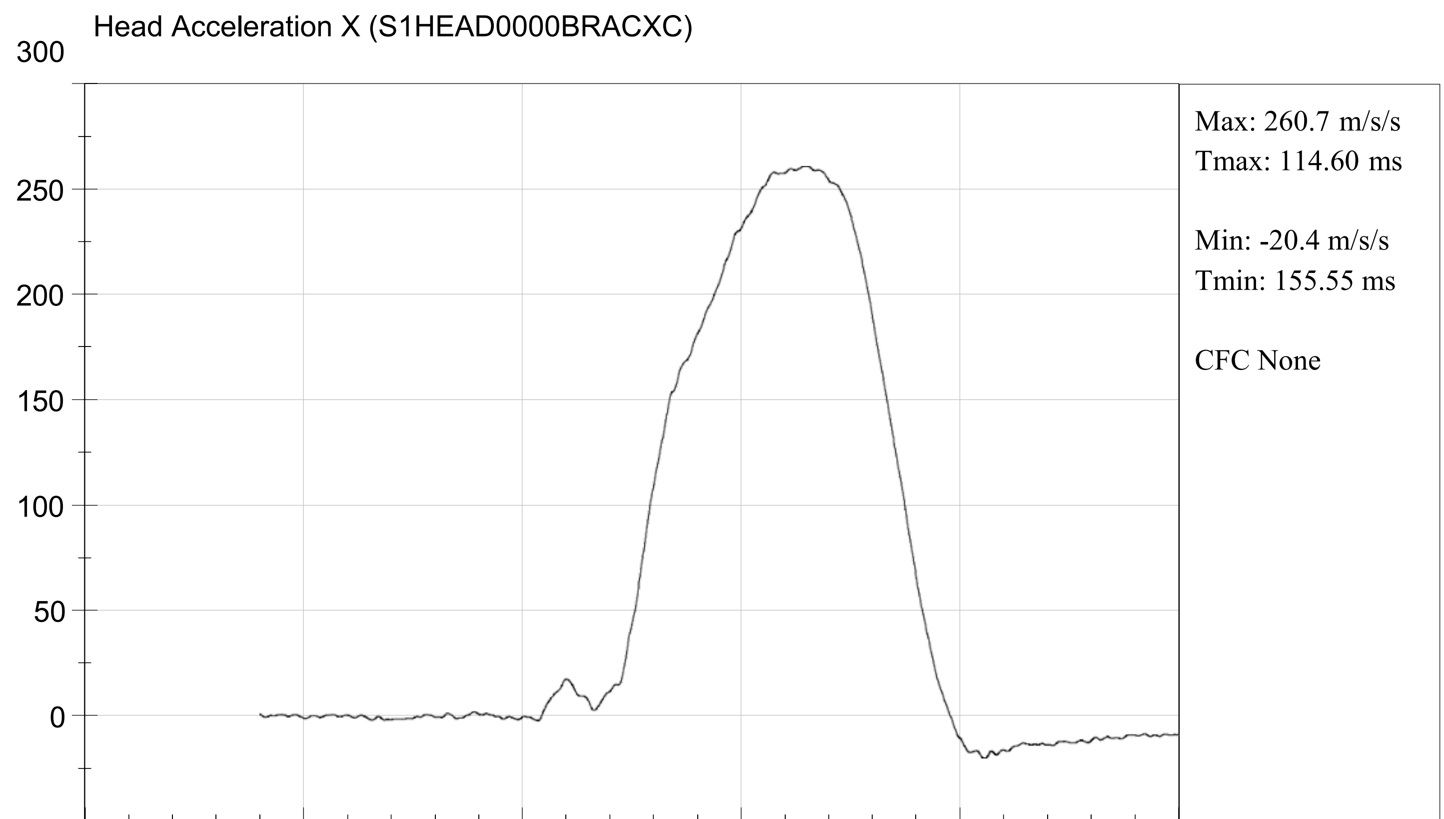
Head Acceleration X (S1HEAD0000BRACXC)
300
250
200
150
100
50
0
Max: 260.7 m/s/s
Tmax: 114.60 ms
Min: -20.4 m/s/s
Tmin: 155.55 ms
CFC None

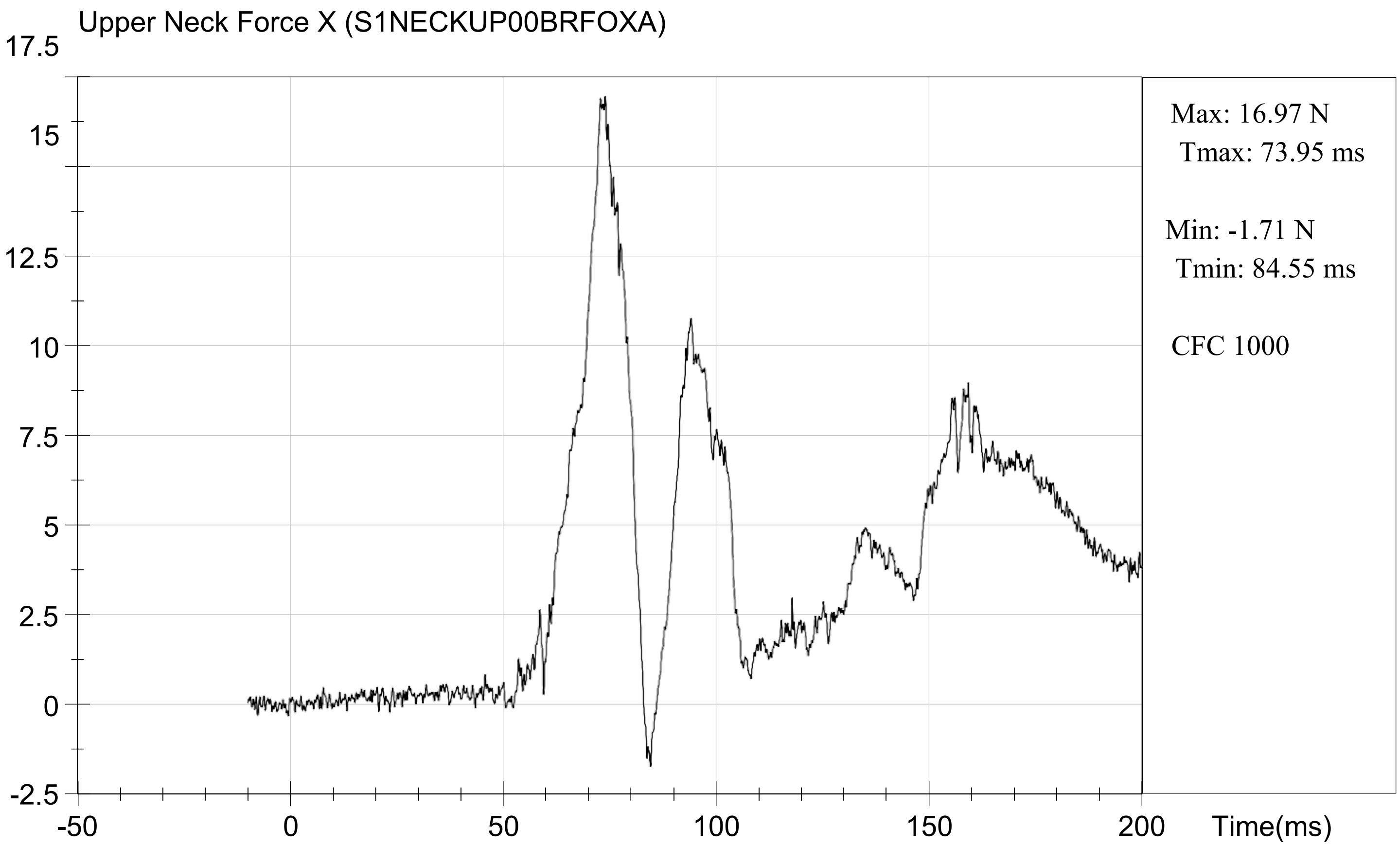
Upper Neck Force X (S1NECKUP00BRFOXA)
17.5
15
12.5
10
7.5
5
2.5
0
-2.5
-50
0
50
100
150
200
Time(ms)
Max: 16.97 N
Tmax: 73.95 ms
Min: -1.71 N
Tmin: 84.55 ms
CFC 1000

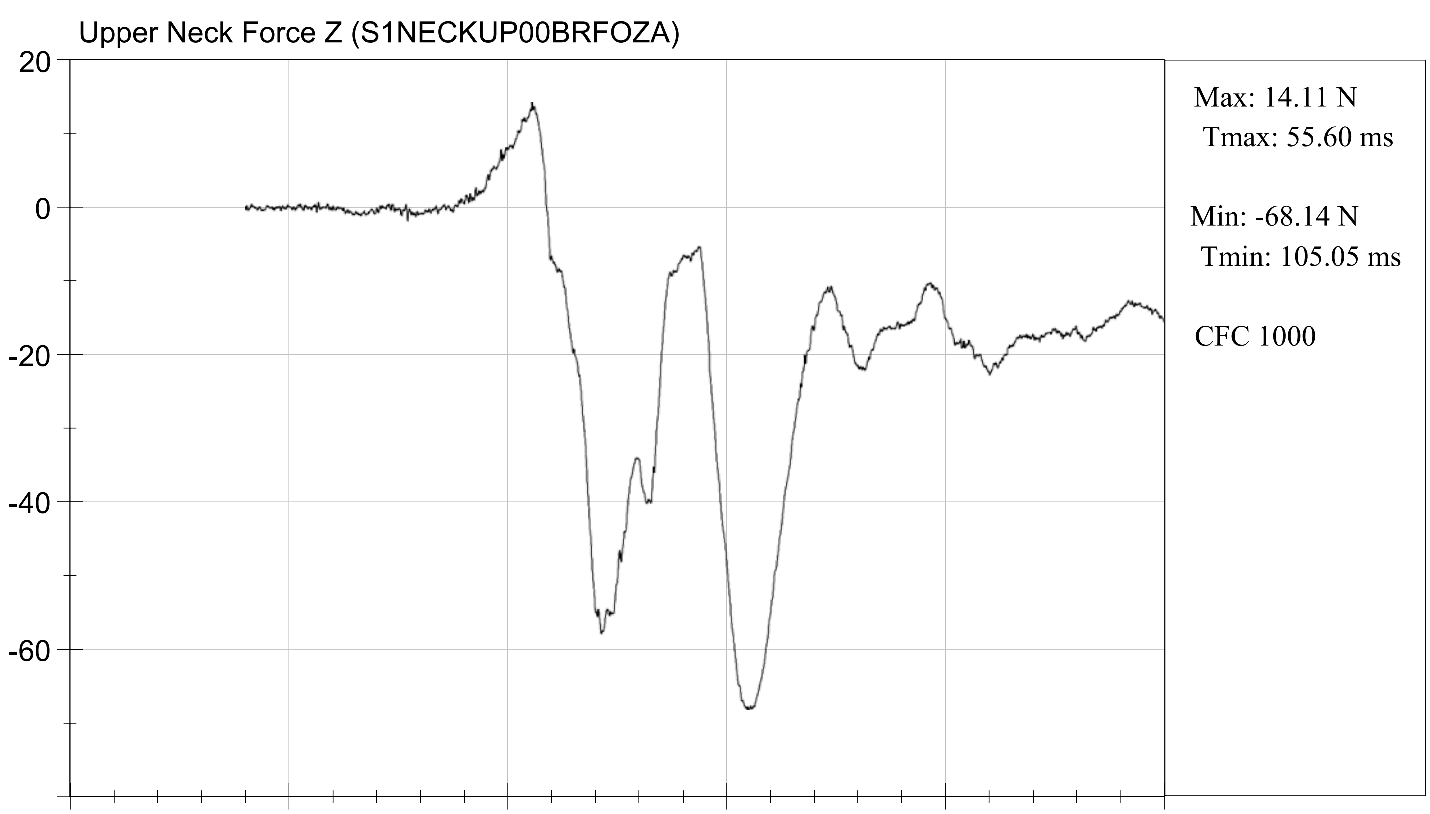
Upper Neck Force Z (S1NECKUP00BRFOZA)
20
0
-20
-40
-60
Max: 14.11 N
Tmax: 55.60 ms
Min: -68.14 N
Tmin: 105.05 ms
CFC 1000

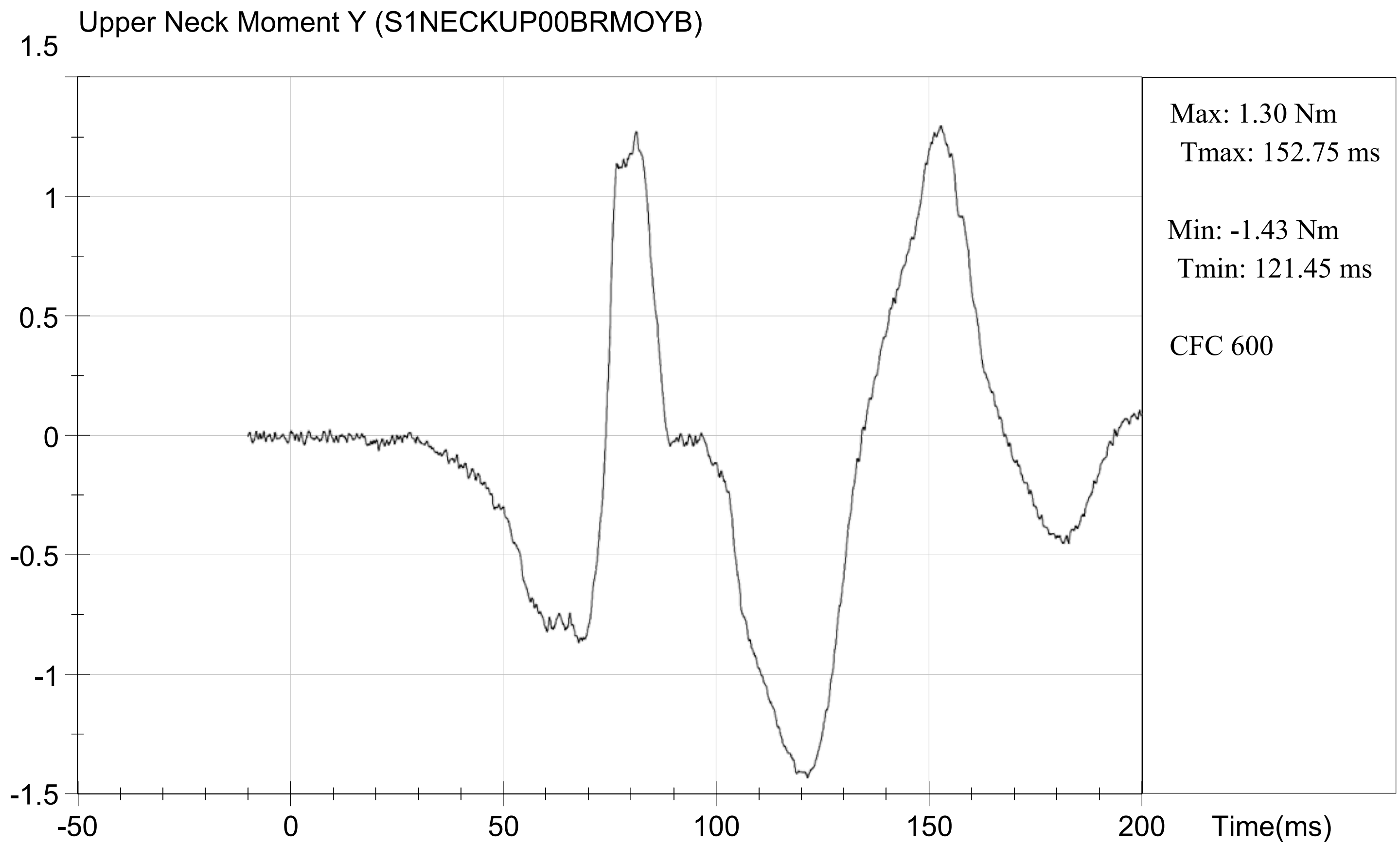
Upper Neck Moment Y (S1NECKUP00BRMOYB)
1.5
1
0.5
0
-0.5
-1
-1.5
-50
0
50
100
150
200
Time(ms)
Max: 1.30 Nm
Tmax: 152.75 ms
Min: -1.43 Nm
Tmin: 121.45 ms
CFC 600

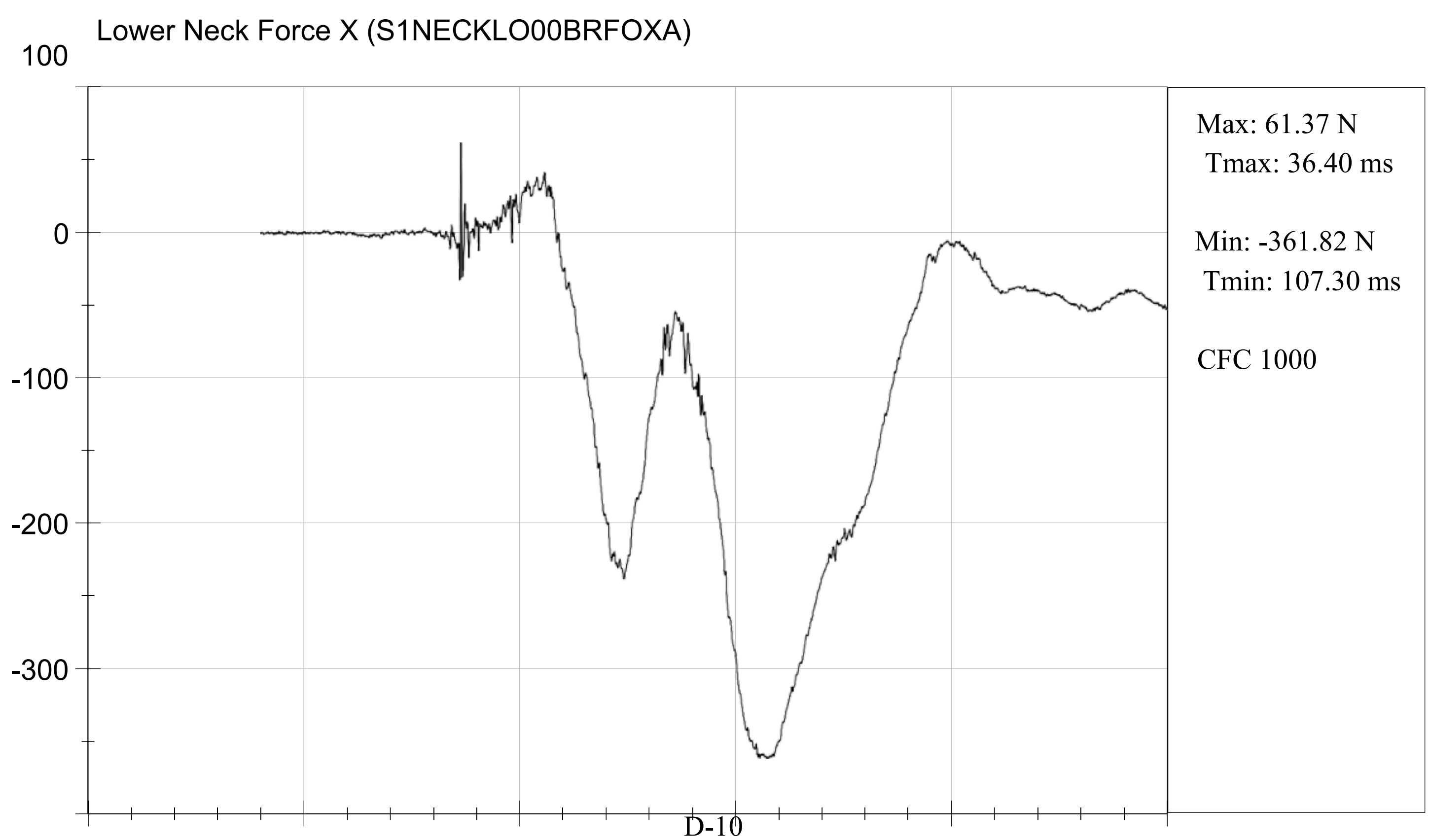
Lower Neck Force X (S1NECKLO00BRFOXA)
100
0
-100
-200
-300
Max: 61.37 N
Tmax: 36.40 ms
Min: -361.82 N
Tmin: 107.30 ms
CFC 1000

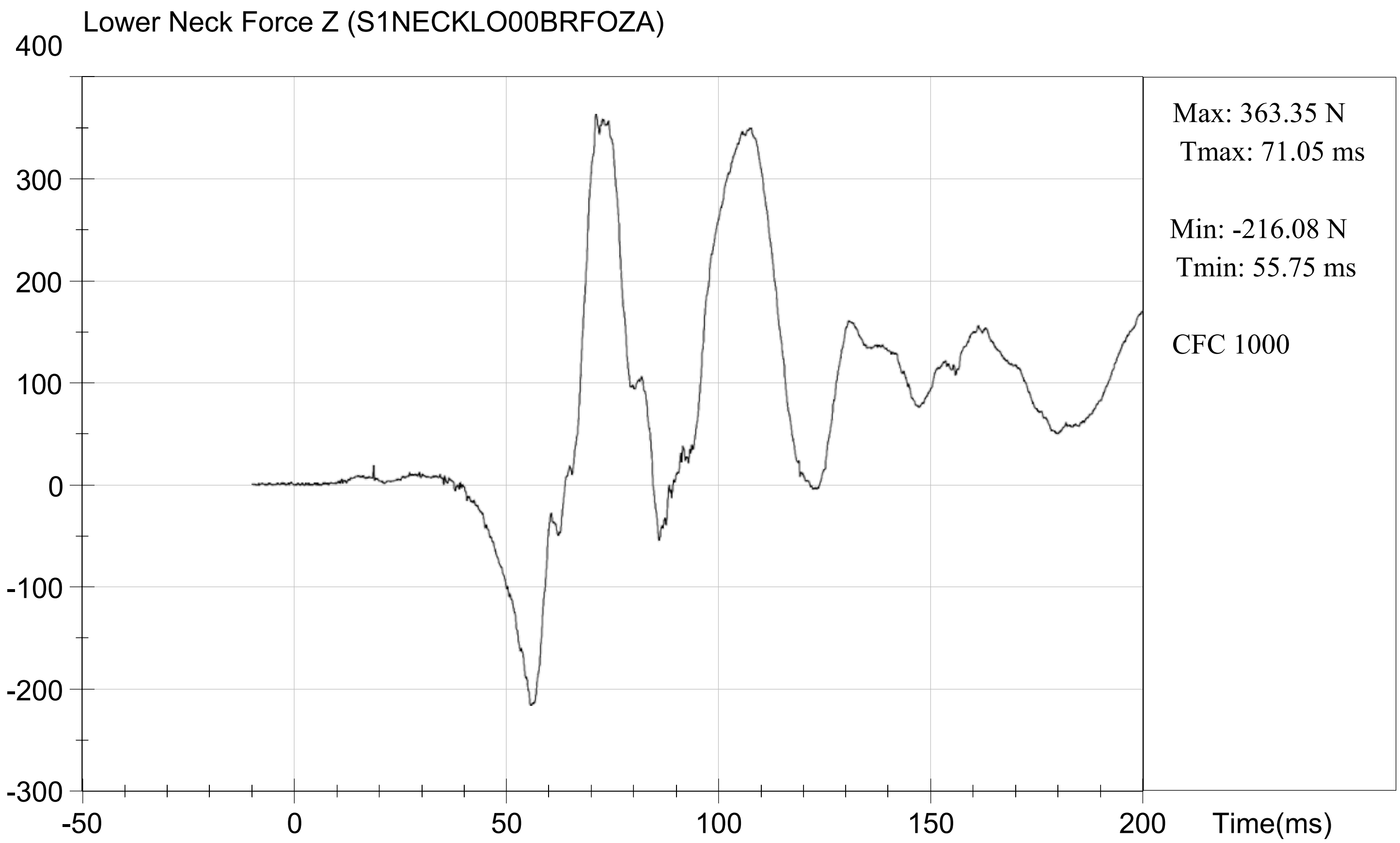
Lower Neck Force Z (S1NECKLO00BRFOZA)
400
300
200
100
0
-100
-200
-300
-50
0
50
100
150
200
Time(ms)
Max: 363.35 N
Tmax: 71.05 ms
Min: -216.08 N
Tmin: 55.75 ms
CFC 1000

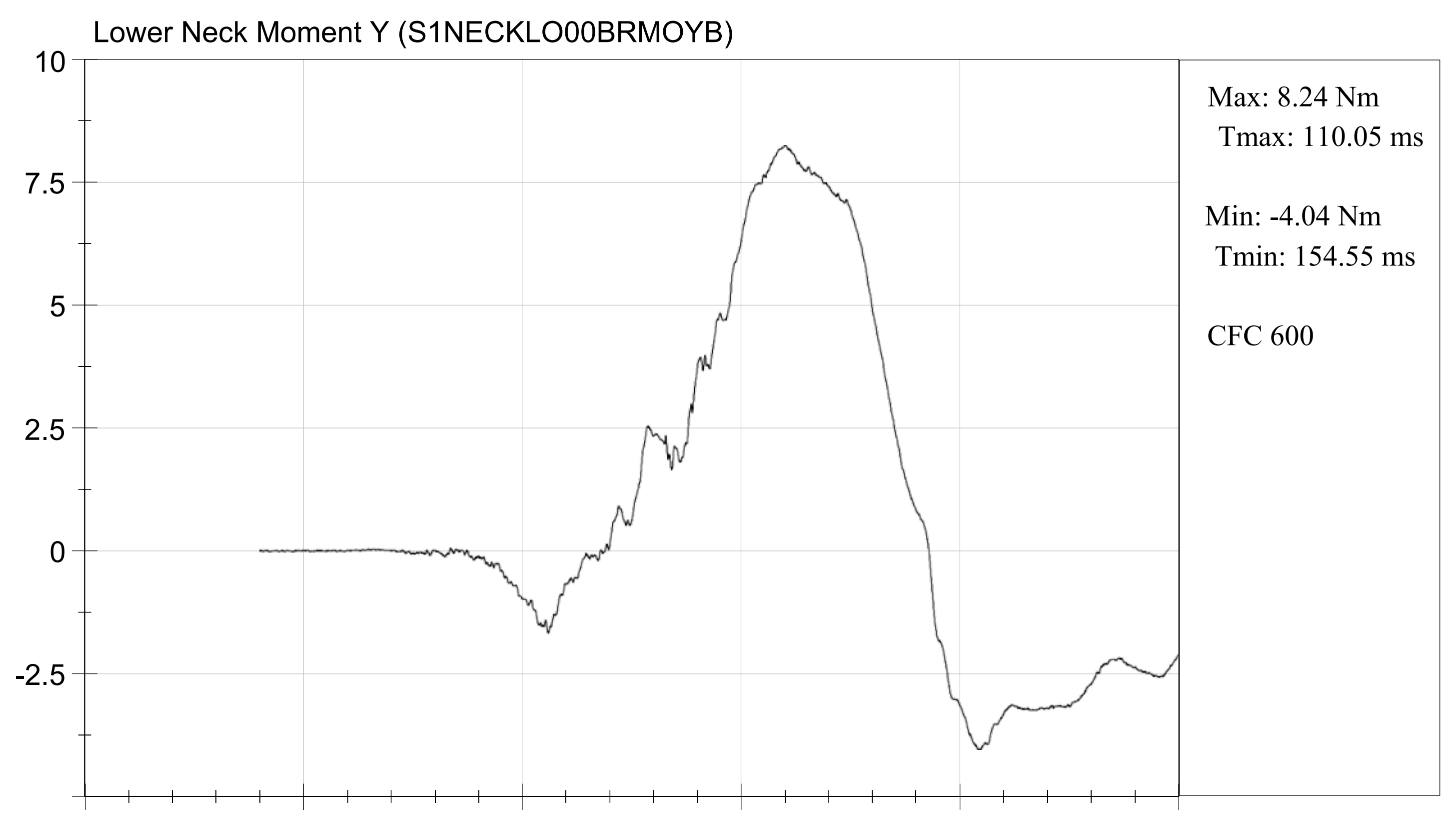
Lower Neck Moment Y (S1NECKLO00BRMOYB)
10
7.5
5
2.5
0
-2.5
Max: 8.24 Nm
Tmax: 110.05 ms
Min: -4.04 Nm
Tmin: 154.55 ms
CFC 600

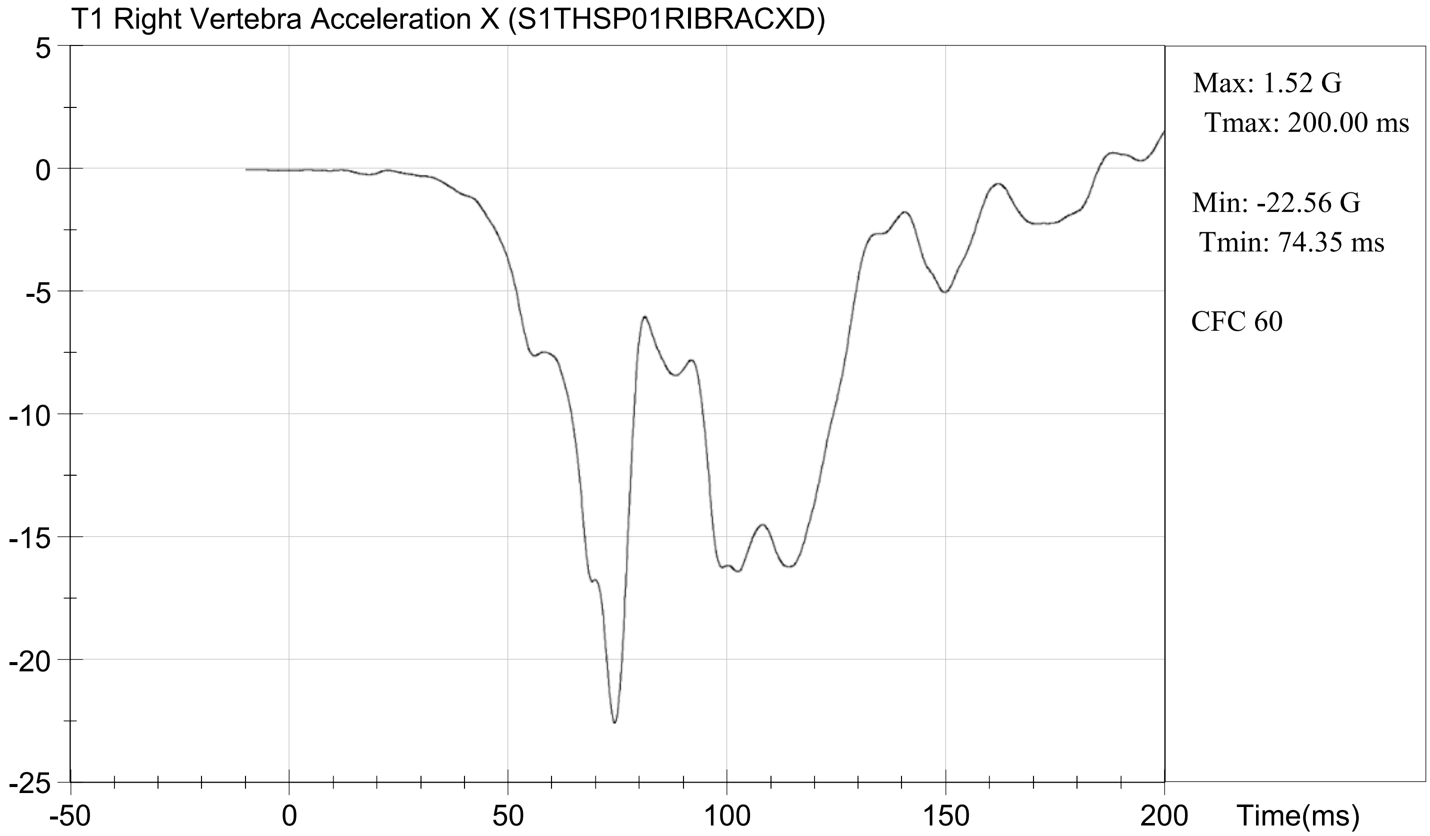
T1 Right Vertebra Acceleration X (S1THSP01RIBRACXD)
5
0
-5
-10
-15
-20
-25
-50
0
50
100
150
200
Time(ms)
Max: 1.52 G
Tmax: 200.00 ms
Min: -22.56 G
Tmin: 74.35 ms
CFC 60

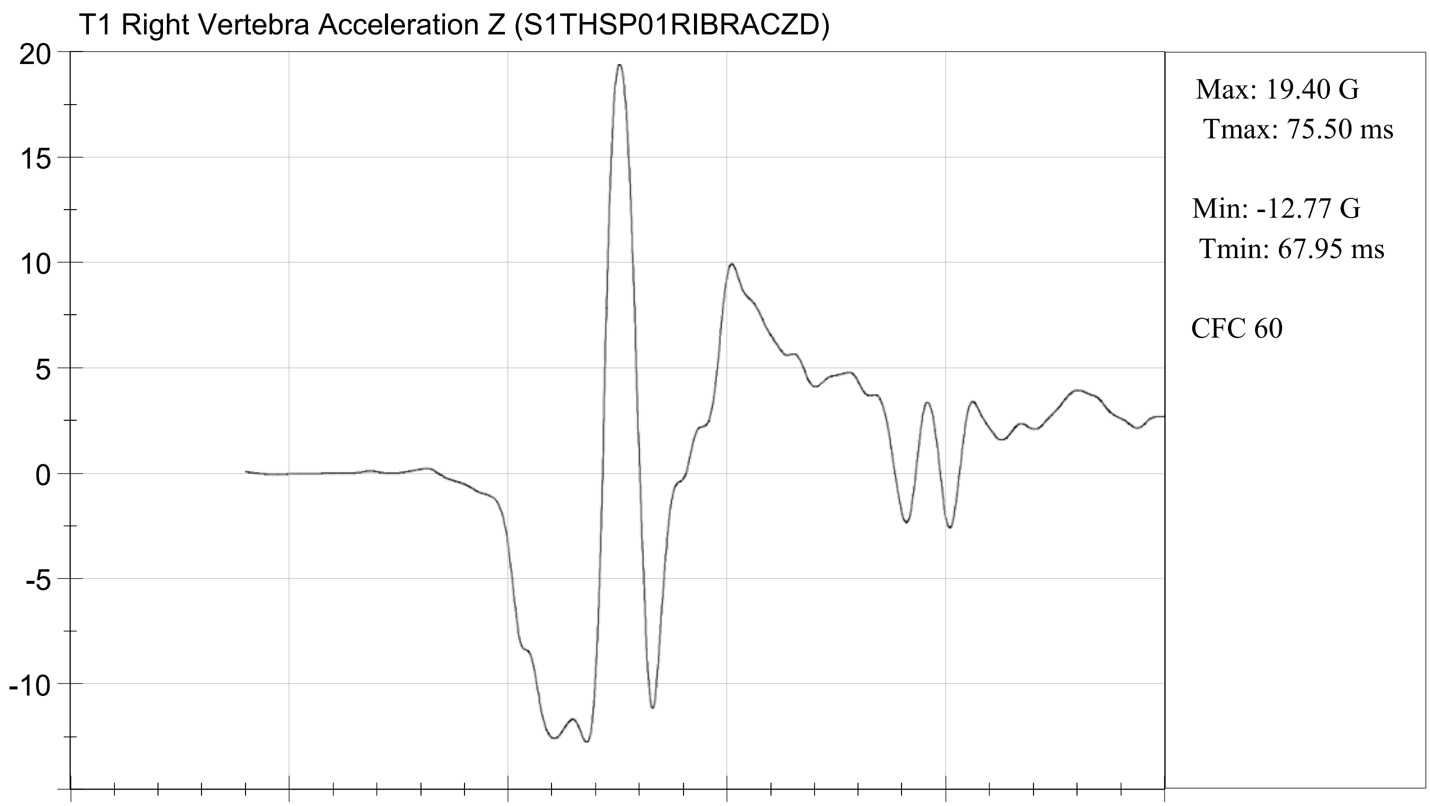
T1 Right Vertebra Acceleration Z (S1THSP01RIBRACZD)
20
15
10
5
0
-5
-10
Max: 19.40 G
Tmax: 75.50 ms
Min: -12.77 G
Tmin: 67.95 ms
CFC 60

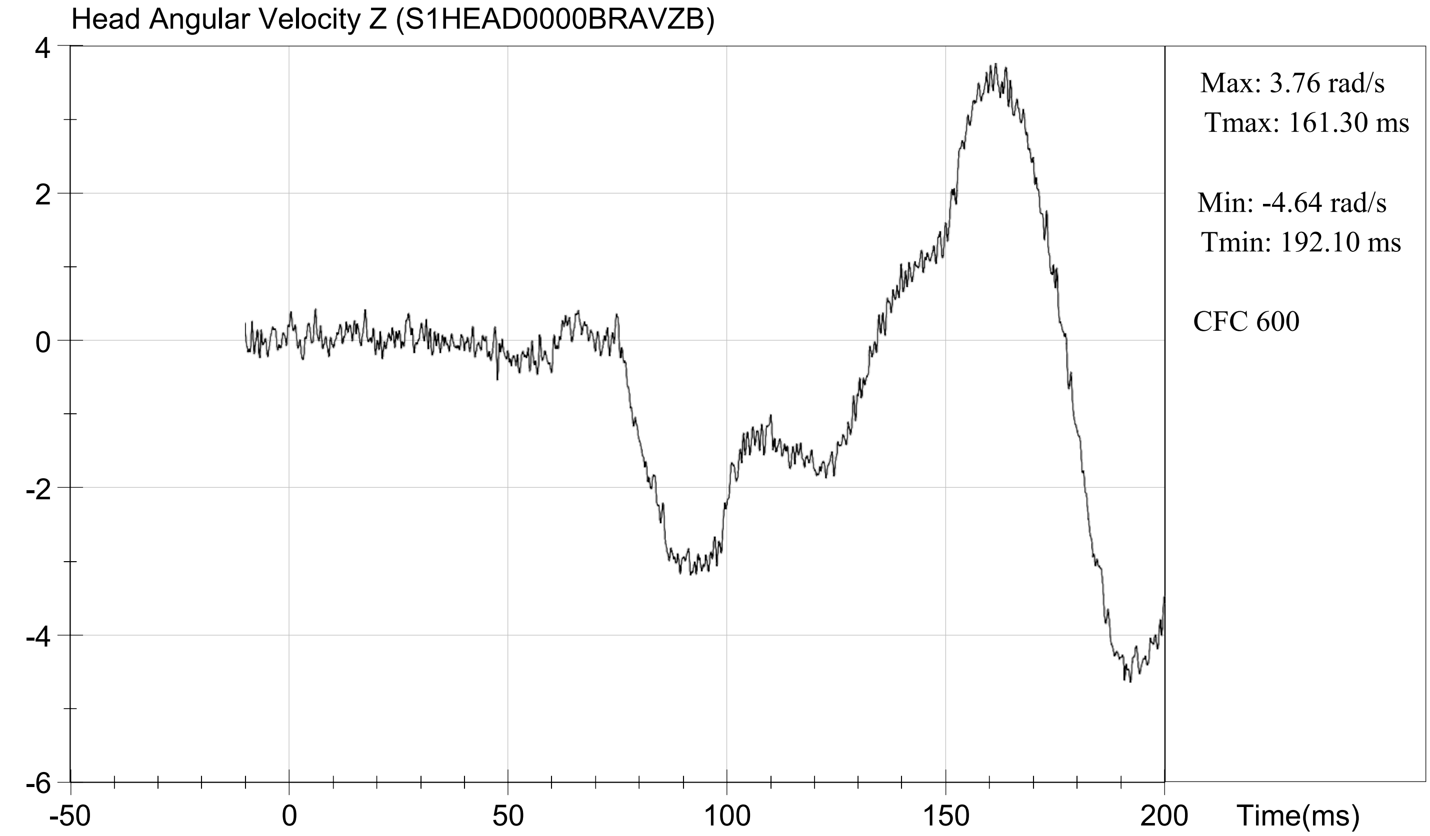
Head Angular Velocity Z (S1HEAD0000BRAVZB)
Max: 3.76 rad/s
Tmax: 161.30 ms
Min: -4.64 rad/s
Tmin: 192.10 ms
CFC 600
4
2
0
-2
-4
-6
-50
0
50
100
150
200
Time(ms)

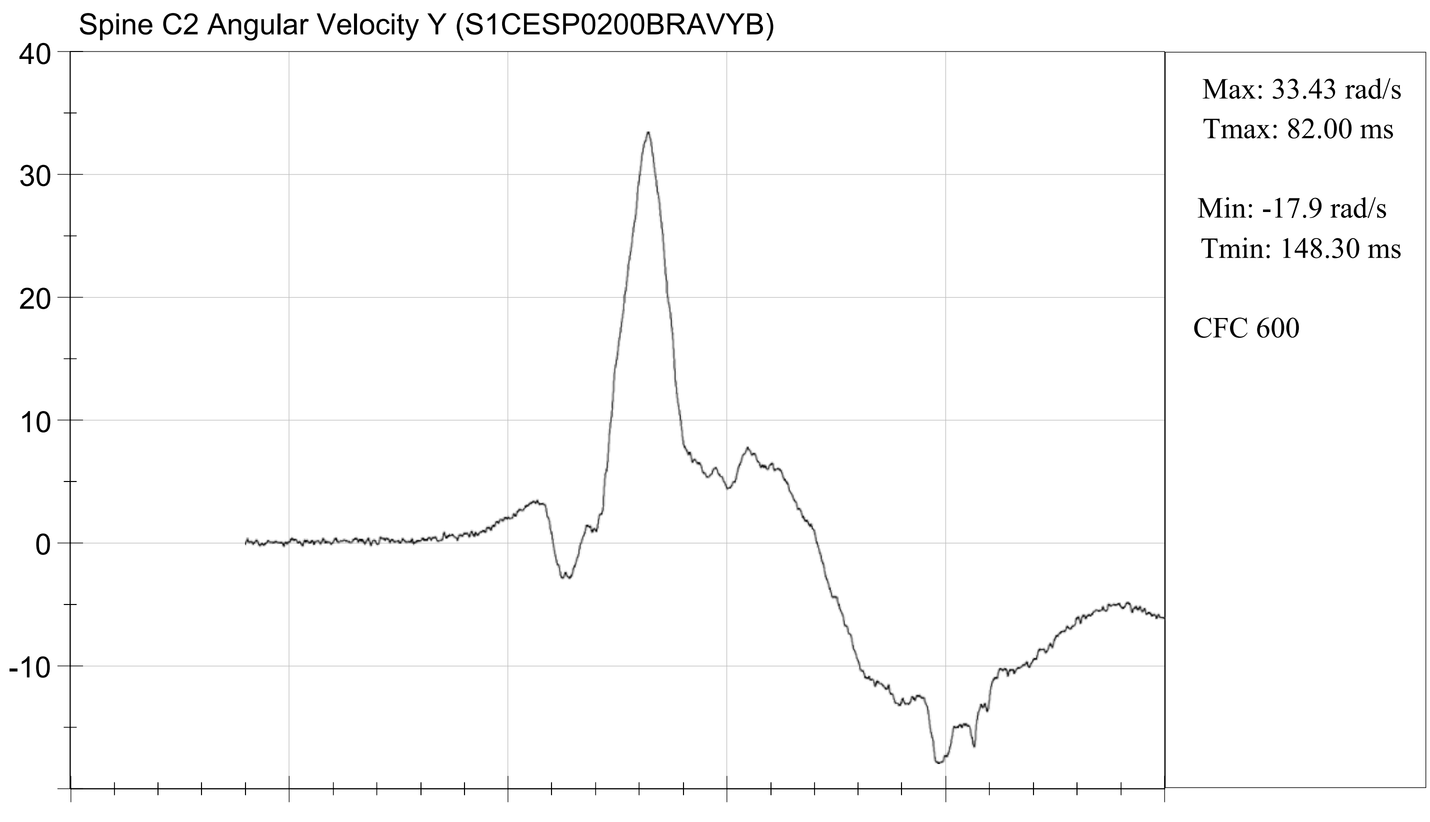
Spine C2 Angular Velocity Y (S1CESP0200BRAVYB)
Max: 33.43 rad/s
Tmax: 82.00 ms
Min: -17.9 rad/s
Tmin: 148.30 ms
CFC 600
40
30
20
10
0
-10

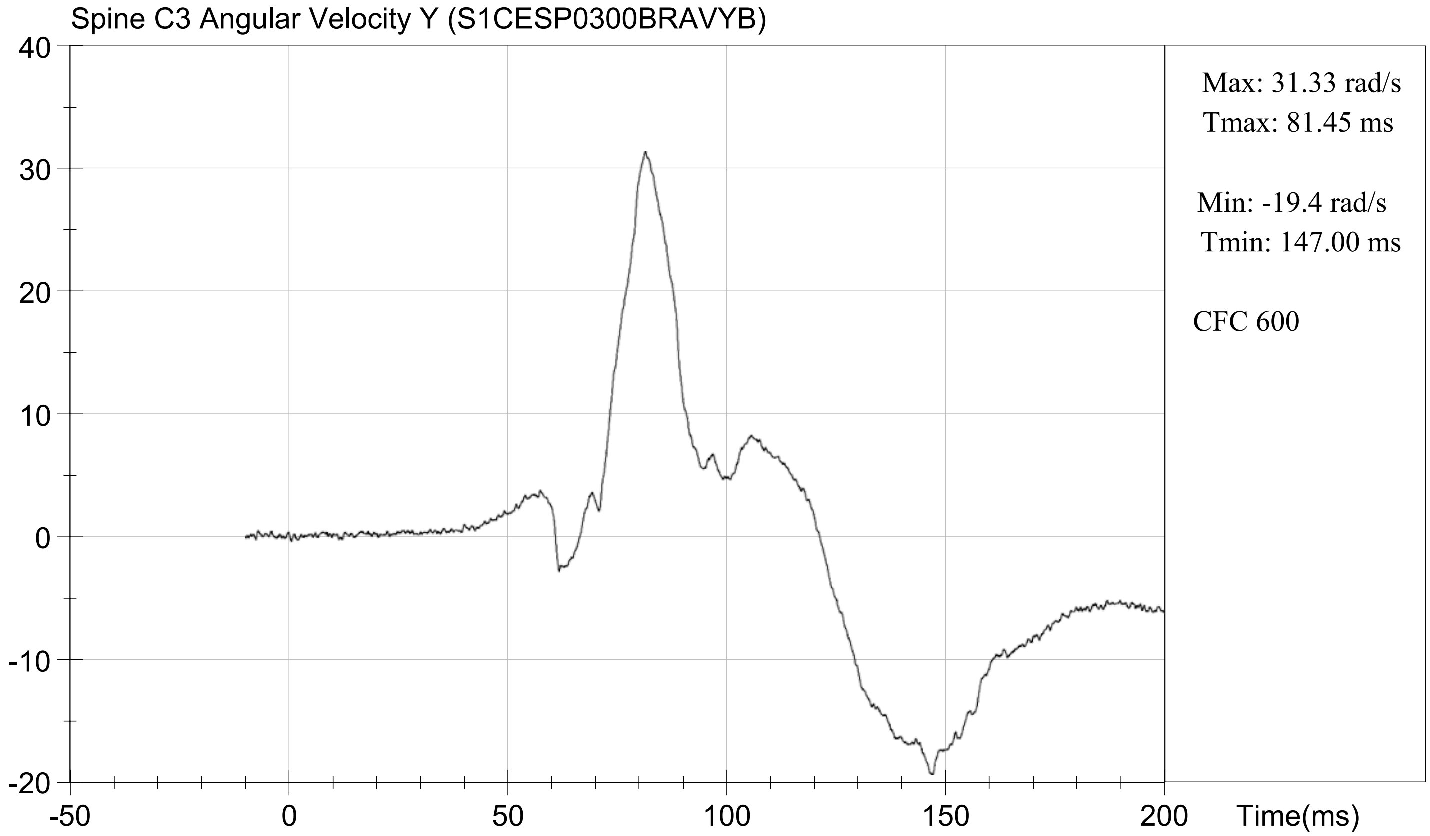
Spine C3 Angular Velocity Y (S1CESP0300BRAVYB)
40
30
20
10
0
-10
-20
-50
0
50
100
150
200
Time(ms)
Max: 31.33 rad/s
Tmax: 81.45 ms
Min: -19.4 rad/s
Tmin: 147.00 ms
CFC 600

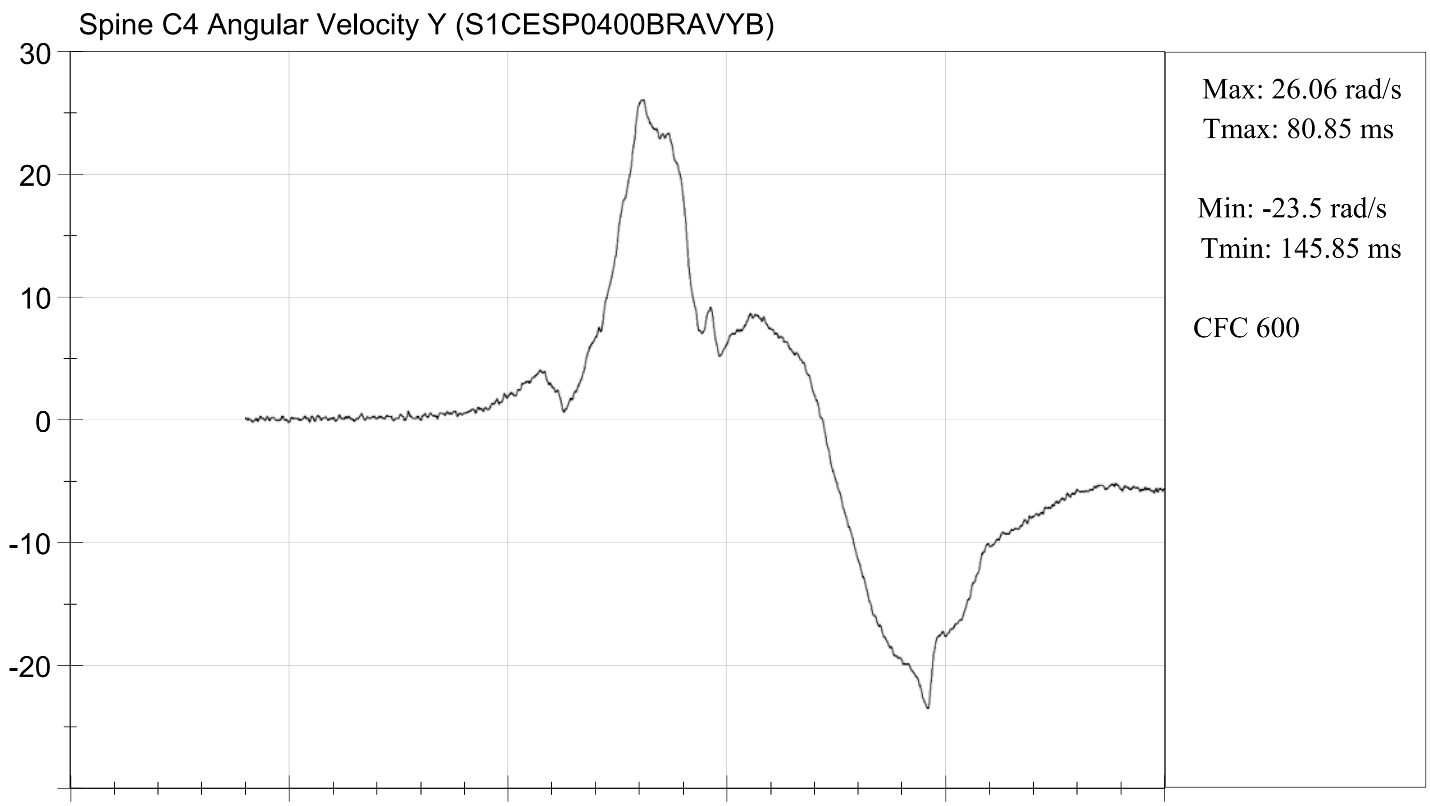
Spine C4 Angular Velocity Y (S1CESP0400BRAVYB)
30
20
10
0
-10
-20
Max: 26.06 rad/s
Tmax: 80.85 ms
Min: -23.5 rad/s
Tmin: 145.85 ms
CFC 600

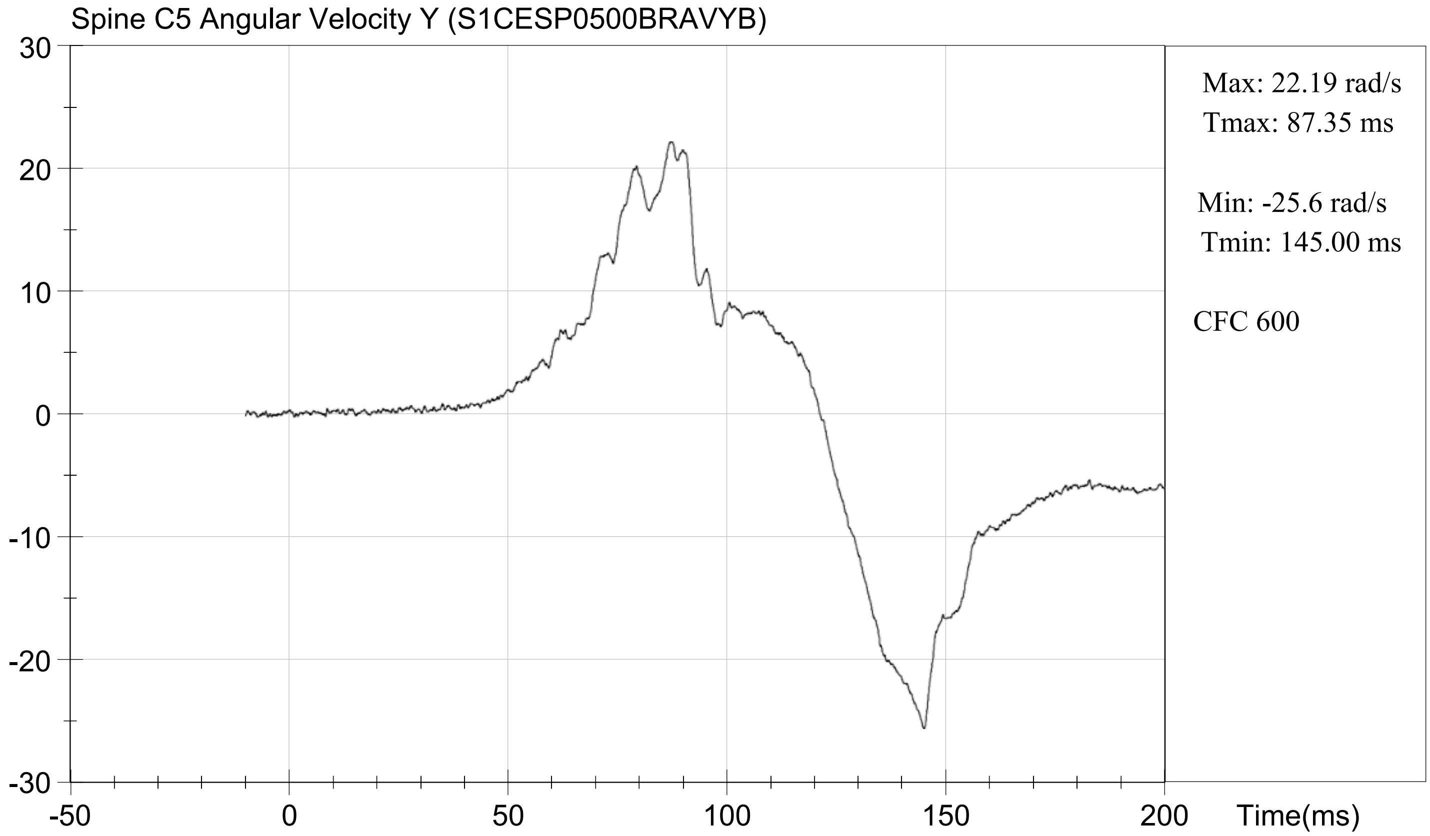

Spine C5 Angular Velocity Y (S1CESP0500BRAVYB)
30
20
10
0
-10
-20
-30
-50
0
50
100
150
200
Time(ms)
Max: 22.19 rad/s
Tmax: 87.35 ms
Min: -25.6 rad/s
Tmin: 145.00 ms
CFC 600

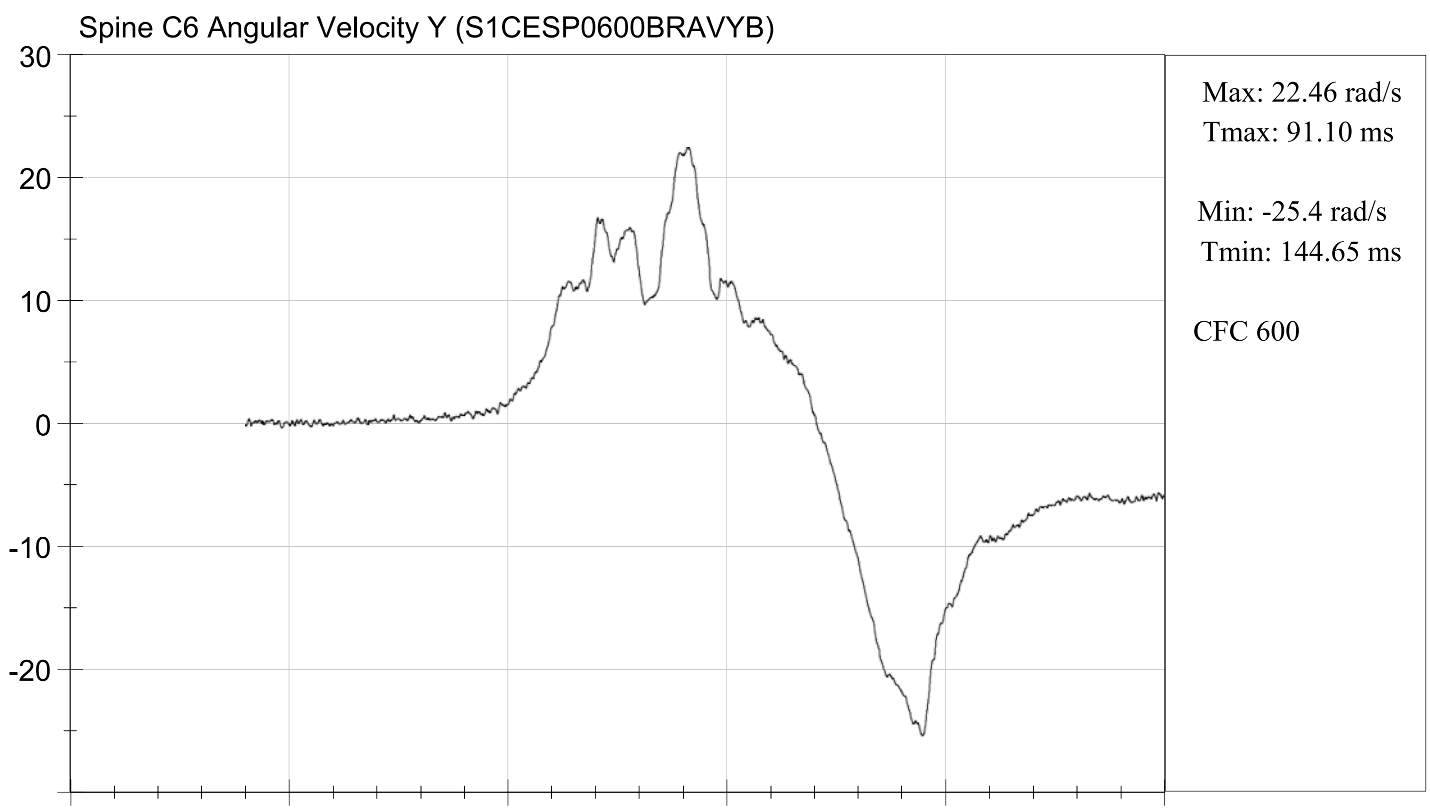

Spine C6 Angular Velocity Y (S1CESP0600BRAVYB)
30
20
10
0
-10
-20
Max: 22.46 rad/s
Tmax: 91.10 ms
Min: -25.4 rad/s
Tmin: 144.65 ms
CFC 600

Spine C7 Angular Velocity Y (S1CESP0700BRAVYB)

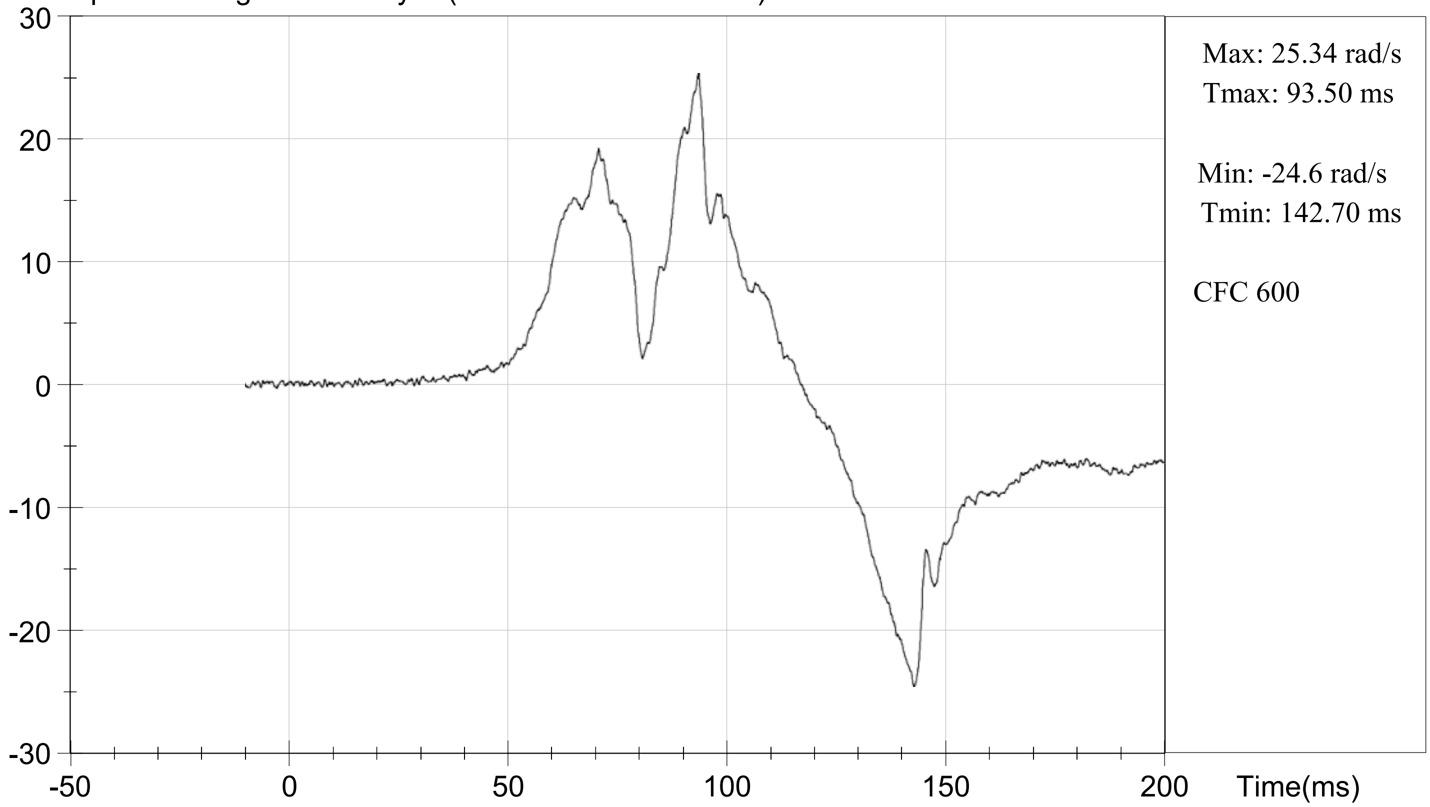

Skull Cap Force X (S1HEADLO00BRFOXA)

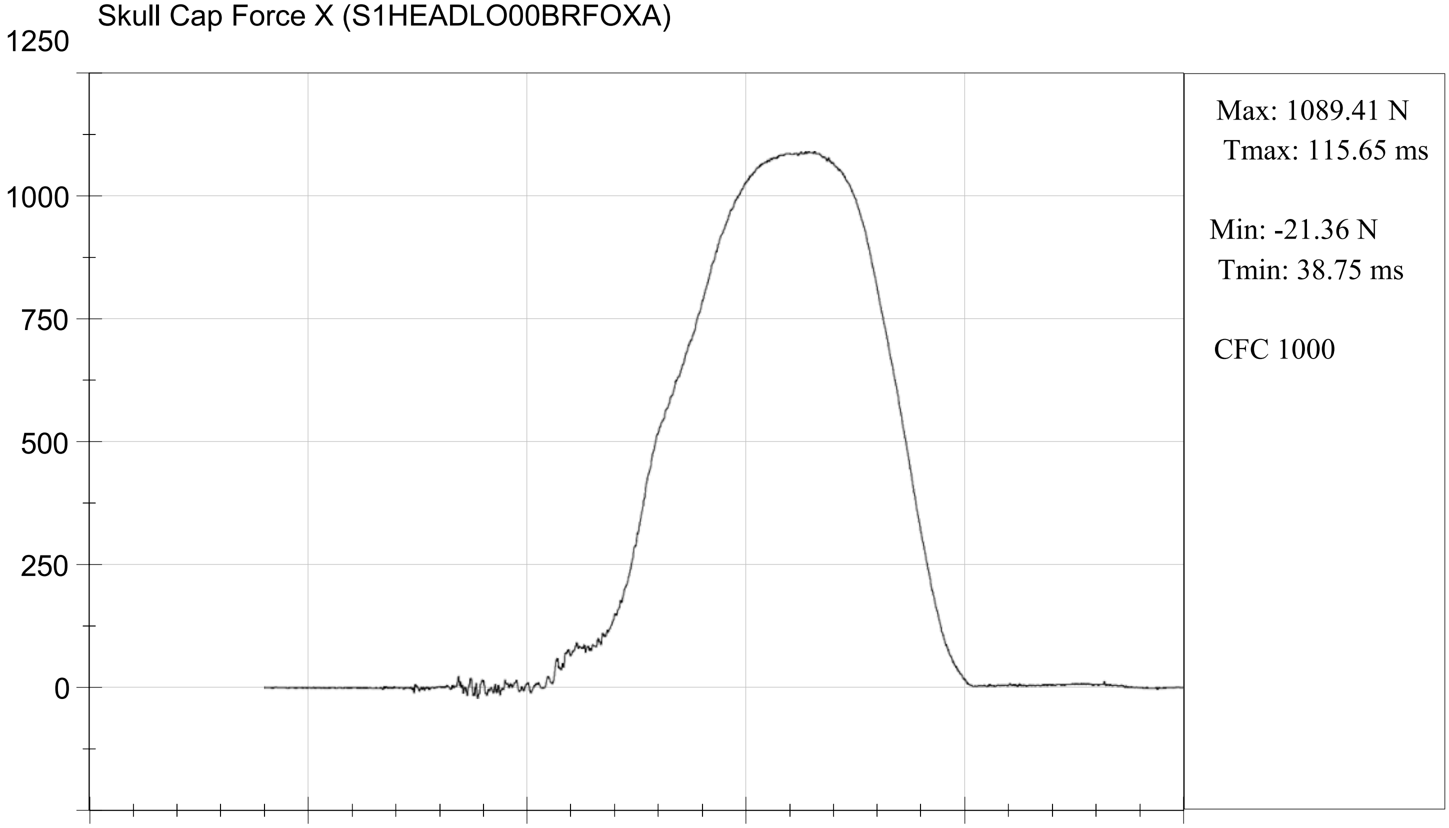

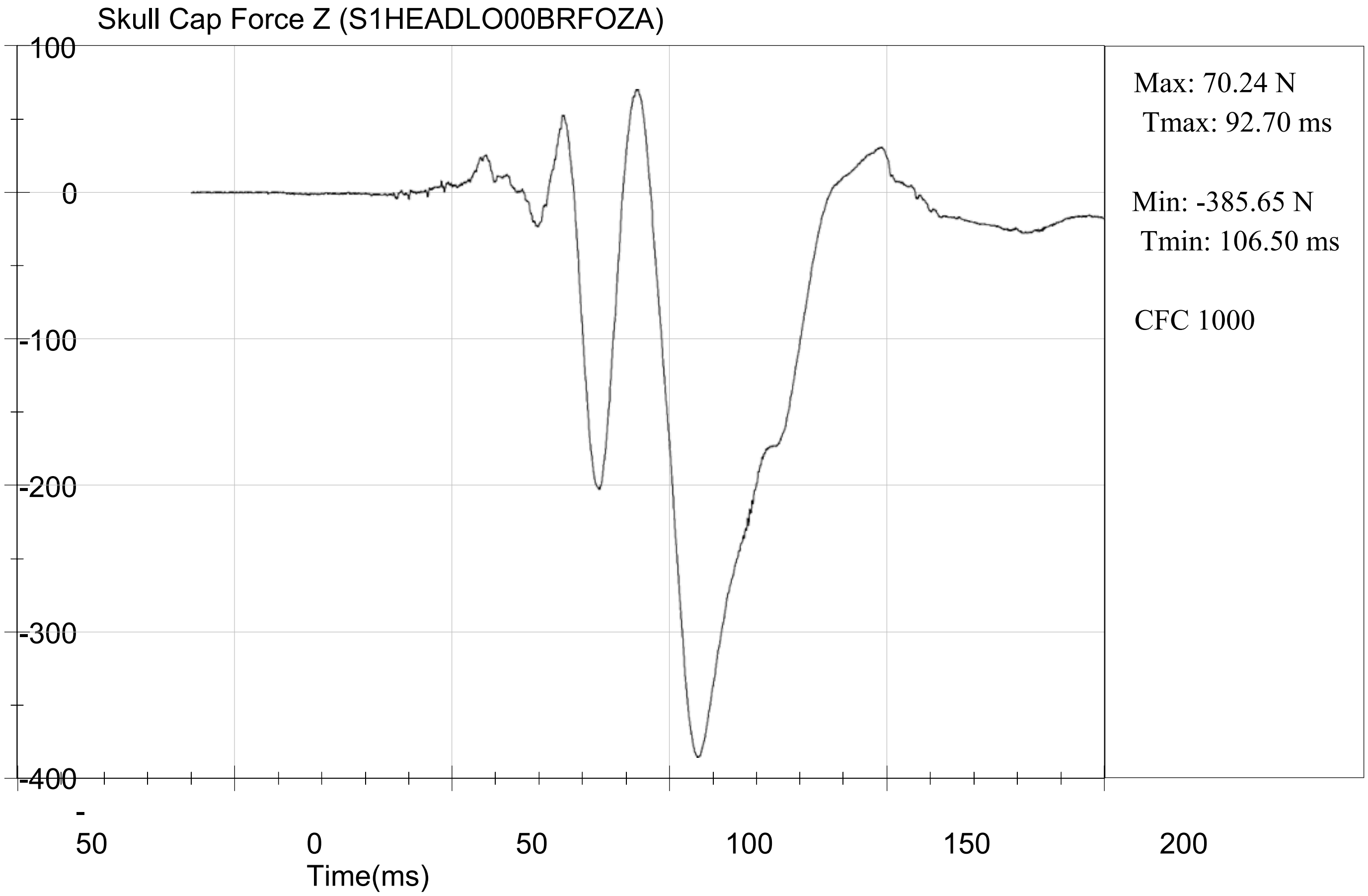
Skull Cap Force Z (S1HEADLO00BRFOZA)
100
0
-100
-200
-300
-400
-50
0
50
100
150
200
Time(ms)
Max: 70.24 N
Tmax: 92.70 ms
Min: -385.65 N
Tmin: 106.50 ms
CFC 1000

Appendix E. Countermeasures

Counter Measu

HSLA 350/450 to HSLA 420/500

Max. Seat Back de-flection=39degrees

Counter Mea

Gauge= 1.6mm to 2mm

Max. Seat Back d flection=39degree

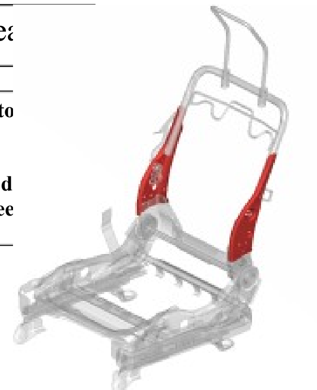

Counter Me

IF 260/410 to DP500/800

Max. Seat Back flection=38degre

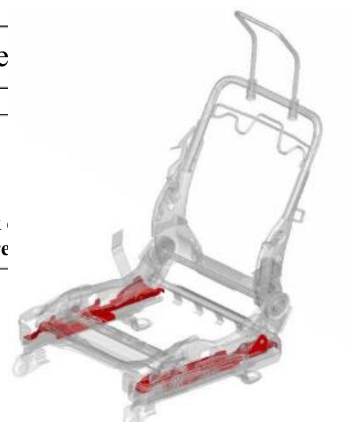

Counter Measu

IF 260/410 to DP500/800

Max. Seat Back de-flection=39degrees

DOT HS 812 737
July 2019

U.S. Department
of Transportation

National Highway
Traffic Safety
Administration

NHTSA

14094-071619-v3